

**A transposon gene delivery system for the
accelerated construction of HEK293S stable cell
lines and its application for the study of rhodopsin
retinitis pigmentosa mutants**

Hannah Rebecca Staggs

A thesis submitted for the degree of Doctor of Philosophy in Biological
Sciences

School of Life Sciences

University of Essex

September 2023

Impact of COVID-19

The COVID-19 pandemic has greatly affected the work of this thesis. PGR access to the School of Life Sciences was stopped on the 23rd March 2020 for 14 weeks, until the 6th July 2020. After this, days in the lab were limited to allow for social distancing, beginning with 2 or 3 half days per week and access remaining by rota only until the 2021 academic year began. This has resulted in over year of 'part-time' style working. Furthermore, during this time delays and restrictions in accessing equipment due to social distancing measures and receiving deliveries of reagents has also impacted my ability to complete this work. Finally due multiple isolation periods due to COVID-19 exposures and testing positive myself, I have missed a further 7 weeks of lab work. This has resulted in the stopping and starting of experiments, which has in itself caused further delays, as the repeating of many steps which would not ordinarily be necessary has been required.

Having only begun my research in October 2019 I was not fully trained in all protocols before the lockdown began and getting training was impeded due to social distancing measures. This work contains places where further repeats would have been included should these time constraints not have occurred, especially in the final results chapter. Further development of the work particularly the use of LMNG in purifying opsin and mutants would have been more fully integrated.

Overall, the work of this thesis, which is almost entirely lab based has been impacted by COVID-19 in a vastly detrimental manner. In total, I have faced problems amounting to the loss of an entire year, with 47 weeks of lost access, and further delays and restrictions caused by COVID-19 preventing completion of this thesis to the standard I desired.

Acknowledgements

My understanding and progress of the work involved in this project has been greatly helped through the support of my supervisor, Dr Philip Reeves. His encouragement throughout has been tremendous. This work benefited through NIH funding to Professor Steven O Smith (Stony Brook University, New York) subcontracted to Dr Reeves. I would like to thank Professor Steven O Smith for his advice and support throughout the work.

I would like to personally thank members of the Reeves and Smith laboratories for their role in the completion of this project. Lynwen James (University of Essex) whose technical support in the lab was invaluable. Dr Sylwia Jencz (University of Essex) who provided many insightful discussions. Lauren Todd (Stony Brook University) whose assistance with the NMR in this project is greatly appreciated.

A special thanks goes to my all my family and friends who have helped me to complete this project and supported me whilst I worked on it. To my parents, Raymond and Julie Staggs, my siblings, Rebecca Staggs and Adam Staggs and my Nan, Jean Hayward this could not have been completed without you. To my husband Joseph Sandy a great thank you for your love and understanding over the years of my work and your support throughout.

Statement of originality

The contents of my thesis presented here are my own original work and where the work of others have been presented this has been clearly acknowledged. This work has not been submitted for any other degree at any University nor has it been submitted previously for publication.

A handwritten signature in black ink, appearing to read 'H. Stagg', is enclosed in a light gray rectangular box.

Abstract

Retinitis pigmentosa (RP) is a degenerative disease of the retina often leading to legal blindness. It is commonly the result of mutations in rhodopsin; a GPCR which initiates the visual signalling cascade. Characterisation of the large volume of such mutations is necessary due to their varied phenotypic outcomes. However, characterisation is often impeded by difficulties and time required to generate sufficient amounts of mutant rhodopsin. Here the PiggyBac transposon system, a rapid and facile method was used to overcome these limitations thus enabling the construction of several HEK293S inducible stable cell lines in under a month. Here, two groups of rhodopsin RP mutants were investigated. Group one comprised enigmatic mutants E122G, R252P, S298D, K311E. E122G had a λ_{\max} shifted to 481 nm and Meta II half-life twice WT. S298D exhibited abnormal photobleaching and a Meta II half-life 4x shorter than WT. R252P and K311E remained enigmatic with photobleaching, Meta II decay and transducin activation unchanged. Group two comprised intradiscal domain mutants: P23A (N-terminus), G101V, V104F and G106W (all EL1). Each of the EL1 mutants were shown to have faster Meta II decay rates (5.96, 10.06, 9.97 mins respectively) than WT (17.68 mins). They also exhibited decreased transducin activation (35%, 64% and 18% relative to WT) and abnormal photobleaching was shown for G101V and V104F. Temperature-sensitivity was demonstrated for P23A, G101V and G106W with time-dependent restricted expression at 37°C which improved at 33°C. Overall, these results have showed the utility of the PiggyBac system for the expression and characterisation of rhodopsin mutants, particularly in high level expression for structural studies. Milligram amounts of E122G, E122Q and Y206F were purified for the collection of NMR data. This system will be valuable for future studies of rhodopsin RP mutants for which structural and functional information is needed for future clinical intervention in RP.

List of abbreviations

ad	autosomal dominant
CMC	critical micelle concentration
CMV	cytomegalovirus
CnBr	Cynagen Bromide
CSNB	congenital stationary night blindness
DDM	dodecyl maltoside
DMEM	Dulbecco's Modified Eagle Medium
DMEM/F12	Dulbecco's Modified Eagle Medium/Ham's F12
EL	extracellular loop
ER	endoplasmic reticulum
ERAD	endoplasmic reticulum associated degradation
ERG	electroretinogram
FBS	Foetal bovine serum
FD	fast digest
FT	flow through
FZD	frizzled
GnTI	N-acetylglucoaminyltransferase
GPCRs	G-protein coupled receptors
HDAC	histone deacetylase
HSE	High Salt Elution
HSR	heat shock response
HSW	High Salt Wash
HTS	high throughput screening
IL	intracellular loop
INL	inner nuclear layer
ITR	inverted terminal repeat
LMNG	lauryl maltose neopentyl glycol
LSE	Low Salt Elution
LSW	Low Salt Wash
Meta	metarhodopsin
Meta I	Metarhodopsin I
Meta II	Metarhodopsin II
Meta III	Metarhodopsin III
OPN1LW	Opsin 3 Long Wave (red cone opsin)
OPN1MW	Opsin 2 Medium Wave (green cone opsin)

OPN1SW	Opsin 1 Short Wave (blue cone opsin)
OPN2	Opsin 2 (rhodopsin)
OPN3	Opsin 3 (encephalopsin)
OPN4	Opsin 4 (melanopsin)
OPN5	Opsin 5 (neuropsin)
pB	piggyBac
pB007	
NCO	piggyBac007 neomycin CMV[Teto] opsin
PDE	phosphodiesterase
PenStrep	Penicillin Streptomycin
PTMs	post-translational modifications
RE	restriction enzyme
<i>RHO</i>	rhodopsin gene
ROS	rod outer segment
RP	retinitis pigmentosa
SMO	smoothened
SS MAS	solid state magic angle spinning nuclear magnetic
NMR	resonance
TM	transmembrane
UPR	unfolded protein response
WT	wild type

Contents

A transposon gene delivery system for the accelerated construction of HEK293S stable cell lines and its application for the study of rhodopsin retinitis pigmentosa mutants	1
Impact of COVID-19.....	2
Acknowledgements.....	3
Statement of originality.....	4
Abstract.....	5
List of abbreviations.....	6
Contents	8
1. Literature Review	1
1.1 G Protein Coupled Receptors.....	1
1.1.1 G Protein Coupled Receptor types.....	1
1.1.2 Opsins.....	2
1.2 Anatomy of the retina.....	3
1.2.1 The retina.....	3
1.2.2 Rod cells	3
1.3 Rhodopsin Protein.....	5
1.3.1 Structure of rhodopsin.....	5
1.3.2 Light transduction.....	7
1.3.3 The role of transducin in signal transduction by rhodopsin	10
1.4 Retinitis Pigmentosa	11
1.4.1 Symptoms and disease progression.....	11
1.4.2 Diagnosis and clinical findings.....	11
1.4.3 Inheritance of genetic mutations associated with RP.....	12
1.4.4 Genetic causes of retinitis pigmentosa	13
1.4.5 Involvement of <i>RHO</i> in RP	14
1.4.6 Potential strategies for the treatment of RP	14
1.5 Classifications of rhodopsin mutants.....	17
1.5.1 Mutant classifications	17
1.5.2 Class One – Defects in outer segment targeting	20
1.5.3 Class Two – Mutations which result in the misfolding of rhodopsin	20
1.5.4 Class Three – Interruption of endocytosis and vesicular trafficking	22
1.5.5 Class Four – Atypical post-translational modifications and instability.....	23
1.5.6 Class Five – Amplification of transducin activation	23
1.5.7 Class Six – Constitutive activation of rhodopsin	23
1.5.8 Class Seven – Defects in dimerisation	24

1.5.9 Effects on other rhodopsin functions	24
1.5.10 Rhodopsin RP mutants under investigation.....	24
1.6 Recombinant protein expression.....	27
1.6.1 Recombinant protein expression hosts.....	27
1.6.2 Transposons and their use in protein expression	28
1.7 PiggyBac transposon for rhodopsin expression	29
1.7.1 PiggyBac transposon	29
1.7.2 The construction of tetracycline inducible stable cell lines using the piggyBac delivery system	32
1.7.3 Mechanisms of insulator function	33
1.8 Solid State Magic Angle Spinning NMR.....	33
1.9 Aims.....	34
2. Methods.....	35
2.1 General materials	35
2.1.1 Materials	35
2.1.2 Buffers and media	36
2.2 General methods	39
2.2.1 Sanger sequencing of DNA.....	39
2.2.2 Agarose gel electrophoresis.....	39
2.2.3 General procedure for restriction enzyme digest	39
2.2.4 <i>Escherichia coli</i> transformation.....	40
2.2.5 Small scale purification of plasmid DNA from <i>E. coli</i> transformants	41
2.3 Generation of mutant rhodopsin in pB007NCO.....	42
2.3.1 QuikChange Mutagenesis	42
2.4 Generation of mutant rhodopsin in pB007NCO by molecular cloning.....	42
2.4.1 Molecular cloning steps.....	42
2.4.2 Mutagenesis of pMT4-rho	42
2.4.3 Agarose gel electrophoresis for the separation of DNA fragments	43
2.4.4 Alkaline Phosphatase treatment of DNA	43
2.4.5 Ligation	44
2.4.6 Transfer of opsin gene expression cassette into piggybac vector.....	44
2.5 Isolation of plasmids from <i>E. coli</i>	45
2.5.1 Small scale production and confirmation of presence of mutant codon	45
2.5.2 Medium scale preparation of plasmid DNA.....	45
2.5.3 Purification of plasmid DNA from medium scale <i>E. coli</i> cultures	45
2.6 General culture and transfections method for the HEK293S cell line	47
2.6.1 General media, reagents and equipment for cell culture.....	47

2.6.2 Thawing of HEK293S cell line from liquid nitrogen stocks	47
2.6.3 Passaging of HEK293S cell line	48
2.6.4 Transfection of HEK293S cell line using the Calcium BES method	48
2.6.5 Transfection of HEK293S cell line using the Turbofect method	49
2.6.6 Making cell line stocks by freezedown.....	50
2.7 Examination of WT rhodopsin and rhodopsin RP mutant expression levels.....	50
2.7.1 Variation of induction time and medium.....	50
2.7.2 Expression of rhodopsin RP mutants by variation of induction medium.....	51
2.7.3 Comparison of expression of opsin and mutants at 33 °C or 37 °C	51
2.7.4 Harvesting of induced cells	51
2.8 Analysis of rhodopsin expression levels by UV-vis absorbance spectroscopy.....	52
2.8.1 Formation of rhodopsin pigment by treatment of harvested cells with either 9- <i>cis</i> -retinal or 11- <i>cis</i> -retinal.....	52
2.8.2 UV-vis Spectroscopy to determine amount of pigment formation	52
2.9 Expression of rhodopsin RP mutants and purification for use in their functional analysis	53
2.9.1 Cell culture and induction for expression rhodopsin RP mutants for functional analysis.....	53
2.9.2 Rho 1D4-sepharose bead preparation for use in purification of rhodopsin	53
2.9.3 Rhodopsin and rhodopsin RP mutant purification.....	54
2.9.4 Stability of purified rhodopsin pigments	56
2.9.5 Rhodopsin and opsin purification in LMNG.....	56
2.10 Spectral and functional analysis of rhodopsin RP mutants.....	57
2.10.1 Formation of rhodopsin pigment from purified opsins	57
2.10.2 Assessment of rhodopsin RP mutant stability at 55 °C	57
2.10.3 Capture of the rhodopsin RP mutant-Schiff base in the dark state	57
2.10.4 Photobleaching of rhodopsin RP mutants.....	57
2.10.5 Examination of the stability of the Meta II (active) state of rhodopsin RP mutants	58
2.10.6 Purification of transducin from bovine retinas	59
2.10.7 Transducin activation assay	61
2.10.12 SDS PAGE.....	62
2.10.12 Coomassie blue staining	62
2.10.12 Western blot.....	63
2.11 Computational methods	64
2.11.1 PyMOL.....	64
2.11.2 SigmaPlot.....	64

3. Development of an inducible piggyBac expression system for rhodopsin and mutant production	65
3.1 Introduction.....	65
3.1.1 Inducible stable cell lines.....	65
3.1.2 PiggyBac transposon vector.....	66
3.1.4 Aims.....	66
3.2 Methods - Construction of mutant rhodopsin in the plasmid pB007NCO.....	67
3.2.1 Construction of mutant rhodopsin in the plasmid pB007NCO by Quikchange mutagenesis	67
3.2.2 Construction of mutant rhodopsin in the plasmid pB007NCO by molecular cloning	68
3.2.2 Transfection to produce stable cell lines and induction of rhodopsin expression .	72
3.2.3 Determination of WT rhodopsin expression levels by UV-vis absorbance spectroscopy.....	72
3.3 Results	73
3.3.1 Construction of mutant rhodopsin – pB007NCO.....	73
3.3.2 Construction of rhodopsin RP mutants using molecular cloning method	75
3.3.2 Medium scale production of pB007NCO plasmids containing rhodopsin mutants	77
3.3.3 Expression of WT rhodopsin	80
3.3.4 Cell line stability	82
3.3.5 Expression of WT rhodopsin, RP mutants and stabilised rhodopsin/ RP mutants	84
3.4 Discussion.....	86
4. Retinitis pigmentosa mutants located in the intradiscal domain of rhodopsin	89
4.1 Introduction.....	89
4.1.1 The intradiscal domain of rhodopsin.....	89
4.1.2 Disruption of rhodopsin pigment formation	89
4.1.3 Improving protein expression levels by lowering the temperature of the host cells	90
4.1.4 Aims.....	92
4.2 Materials and Methods	93
4.2.1 Production of stable cell lines.....	93
4.2.2 Standard expression of the rhodopsin mutants	93
4.2.3 Lowering the growth temperature from 37 to 33 °C in an attempt to improve mutant rhodopsin expression levels	93
4.2.4 Lowering the growth temperature from 37 to 33 °C and 30 °C in an attempt to improve P23A rhodopsin expression levels.....	94
4.2.5 Rhodopsin immunoaffinity purification	94
4.2.6 Functional assessment of rhodopsin and its mutants	94
4.3 Results	95

4.3.1 Production of pB007 NCO mutants	95
4.3.2 Expression of the rhodopsin mutants G101V, V104F, G106W and their N2C D282C background counterparts in HEK293S cells	98
4.3.3 Improvement of expression of rhodopsin mutants by expression at 33°C.....	100
4.3.4 Variation to temperature changes expression levels in P23A	104
4.3.5 Purification of mutant rhodopsin from HEK293S stable cell lines.....	107
4.3.6 Photobleaching and acidification	110
4.3.7 Meta II stability of light activated mutants	112
4.3.8 Transducin activation by light activated mutants	114
4.4 Discussion.....	116
4.4.1 Improving the expression of difficult to express mutants.....	116
4.4.2 Biochemical characteristics of EL1 mutant rhodopsins	117
5. Characterisation of rhodopsin RP mutants: previously unclassified	120
5.1 Introduction	120
5.1.1 Classification of rhodopsin retinitis pigmentosa mutations.....	120
5.1.2 Function of rhodopsin.....	120
5.1.3 Opsin and pigment formation	121
5.1.4 Detergent solubilisation of membrane proteins.....	122
5.1.5 Aims.....	125
5.2 Methods	126
5.2.1 Construction of stable HEK293S cell lines.....	126
5.2.2 Rhodopsin mutant production in HEK293S GnT1 ⁻ cells	126
5.2.3 Purification of rhodopsin mutants in DDM	126
5.2.4 Examination of rhodopsin mutant biochemical and spectral properties.....	126
5.2.5 Solubilisation and purification purification of rhodopsin in detergent DDM or LMNG: a comparative study.....	126
5.2.6 Biochemical property comparison of rhodopsin in DDM and LMNG	128
5.2.7 Purification of opsin in LMNG	128
5.2.8 Pigment formation in LMNG	128
5.3 Results	129
5.3.1 Assessment of the expression of rhodopsin mutants using UV-vis absorption spectroscopy.....	129
5.3.2 Immunoaffinity purification of rhodopsin using the rho-1D4 antibody.....	132
5.3.4 Dark state acidification of rhodopsin.....	135
5.3.5 UV-vis absorption spectroscopy examination of rhodopsin photobleaching followed by acidification	137
5.3.6 Rhodopsin active state (metarhodopsin II) stability.....	139
5.3.7 Ability of rhodopsin and mutants to activate transducin	141

5.3.8 Comparison of rhodopsin purified in DDM or LMNG.....	143
5.3.9 Meta II stability and transducin activation ability of rhodopsin purified in LMNG	144
5.3.10 Purification of opsin and RP mutant opsins in LMNG	146
5.3.11 Pigment formation in LMNG	148
5.4 Discussion.....	150
5.4.1 Use of the detergent LMNG for the purification and biochemical examination of rhodopsin and opsin.....	150
5.4.2 Characteristics of the rhodopsin RP mutants E122G, R252P, S298D and K311E	151
6. The role of residue E122 in the stability of the metarhodopsin II intermediate	154
6.1 Introduction.....	154
6.1.1 The Opsin Family	154
6.1.2 Residue 122 in opsins	156
6.1.3 Aims.....	157
6.2.1 Alignment of opsin sequences.....	158
6.2.2 Construction of the mutant PiggyBac plasmids	158
6.2.3 Construction of stable HEK293S cell lines expressing E122 mutants.....	158
6.2.4 Expression of the E122 mutants in HEK293S cells	159
6.2.5 Analysis of the E122 mutant rhodopsin proteins.....	159
6.2.6 Expression of the E122G and E122Q (N2C D282C) mutants for Solid State NMR	159
6.2.7 Purification of the E122G and E122Q (N2C D282C) mutants for Solid State NMR	160
6.2.8 Solid State Magic Angle Spinning NMR of the E122G and E122Q (N2C D282C) stable isotope labelled rhodopsin mutants.....	162
6.3 Results	163
6.3.1 Alignments of opsins at E122	163
6.3.2 Expression of the rhodopsin residue E122 mutants.....	164
6.3.4 Stability of the Meta II intermediate in E122 rhodopsin mutants	170
6.3.5 Transducin activation by the E122 rhodopsin mutants	172
6.3.6 SS MAS NMR comparison between E122G N2C D282C and E122Q N2C D282C	175
6.4 Discussion.....	179
7. Conclusion	183
7.1 PiggyBac transposon cell line construction and expression optimisation provide a rapid, easy and effective method for rhodopsin mutant expression at high levels.	183
7.2 LMNG provides a suitable alternative to DDM for studies of opsin function.	185
7.3 Rhodopsin RP mutants have vastly different phenotypic properties that hold the key to understanding the structure and activation of rhodopsin.	186

7.4 Concluding remarks.....	192
8. References	193
9. Appendices	220
Appendix 1 Mutagenic primers.....	220
Appendix 2 PCR and sequencing primers	221
Appendix 3 Sequencing results	222
Chapter 4 – N-terminal/EL1 mutants	222
Chapter 5 – RP mutants.....	230
Chapter 6 – E122 mutants	241
Appendix 4 Protein sequences/species used for the alignment of transmembrane helix 3.	255

1. Literature Review

1.1 G Protein Coupled Receptors

1.1.1 G Protein Coupled Receptor types

G Protein Coupled Receptors (GPCRs) are responsible for many processes both in health and disease, and are key targets in drug discovery (Costanzi *et al.*, 2009; Basith *et al.*, 2018). Stimulated through extracellular chemical or physical changes, GPCRs, which are found on the plasma membrane, recognise and begin the signalling response (Costanzi *et al.*, 2009).

Forming a large superfamily GPCRs have been categorised into six classes:

rhodopsin like,

secretin family,

metabotropic glutamate receptors,

fungal mating pheromone receptors,

cAMP receptors,

frizzled (FZD) and smoothened (SMO) receptors (Basith *et al.*, 2018).

Rhodopsin, the name sake of class A GPCRs, can be described as the prototypical GPCR (Costanzi *et al.*, 2009; Basith *et al.*, 2018). From its discovery in the late 19th Century to the elucidation of its structure forming a basis for the study of other GPCRs, it is a key receptor for understanding the structure/ function relationship in GPCRs (Costanzi *et al.*, 2009).

1.1.2 Opsins

There are seven categories into which opsins can be divided. Rhodopsin (OPN2) is the rod cell photoreceptor, responsible for dim-light vision. Cone opsins are those which are responsible for colour vision: OPN1SW or blue cone photopigment, OPN1MW or green cone photopigment and OPN1LW or red cone photopigment. A further three opsins which are not involved in image producing responses are OPN3 (encephalopsin), OPN4 (melanopsin) and OPN5 (neuropsin) (Provencio *et al.*, 1998; Blackshaw and Snyder, 1999; Tarttelin *et al.*, 2003).

Table 1.1 Opsins

Opsin	Name	Chromosome
OPN1SW	blue cone photopigment	7
OPN1MW	green cone photopigment	X
OPN1LW	red cone photopigment	X
OPN2	rhodopsin	3
OPN3	encephalopsin	1
OPN4	melanopsin	10
OPN5	neuropsin	6

1.2 Anatomy of the retina

1.2.1 The retina

The retina, found in the posterior section of the eye, is made up of multiple layers of cells (Hoon *et al.*, 2014; Dias *et al.*, 2018). Beginning from where light strikes the retina, the layers are: the ganglion cell layer, the inner plexiform layer and the inner nuclear layer (Hoon *et al.*, 2014). Following this are: the outer plexiform layer and the outer nuclear layer, the photoreceptor layer and the retinal pigment epithelium (Hoon *et al.*, 2014; Dias *et al.*, 2018). The photoreceptor layer is made up of the inner and outer segments of the rod and cone photoreceptor cells (Dias *et al.*, 2018).

1.2.2 Rod cells

Rod and cone cells are responsible for light reception in the retina; with cones being wavelength specific for colour vision in the central retina and rods in the peripheral retina for vision in dim light conditions (Hoon *et al.*, 2014; Dias *et al.*, 2018). Rod cells can be divided into the inner segment and the outer segment as (Figure 1.1); with the inner segment containing the nucleus and other organelles (Park, 2014). The outer segment is comprised of discs, the membranes of which contain proteins for phototransduction, such as rhodopsin and transducin (Park, 2014; Dias *et al.*, 2018). Rhodopsin accounts for the large majority of the protein found in the outer segment of the rod cells and is the protein responsible for initiating the light transduction pathway (Ferrari *et al.*, 2011).

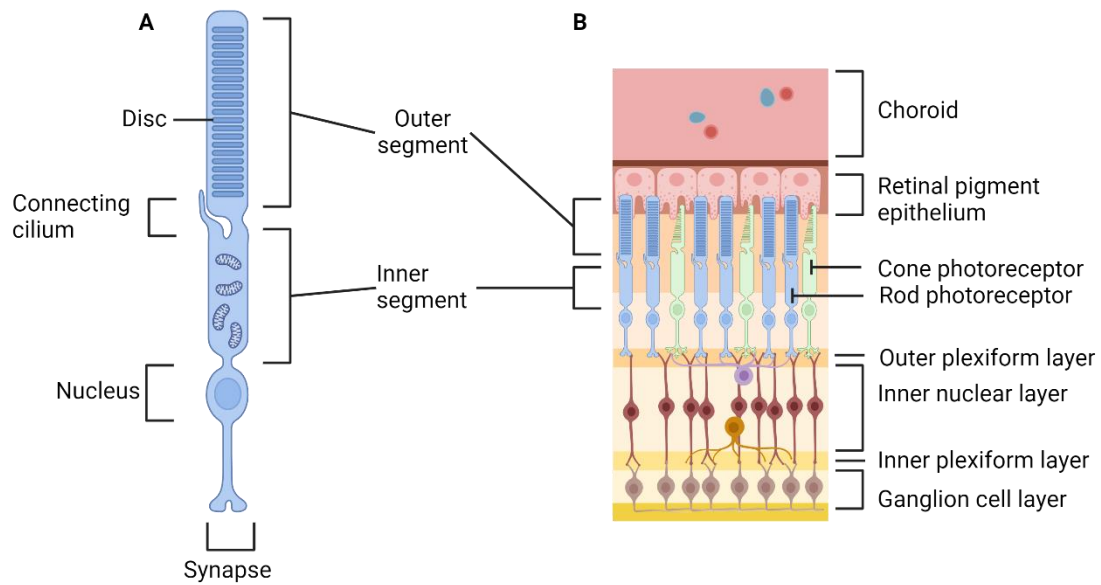


Figure 1.1 The structure of a rod cell and the retina. A: Rod cell showing the inner and outer segments, discs, connecting cilium, nucleus and synapse. B: Layers of the retina. Choroid, Retinal Pigment Epithelium, Photoreceptors, Outer plexiform layer, inner nuclear layer, inner plexiform layer and ganglion cell layer. Created with BioRender.com.

1.3 Rhodopsin Protein

1.3.1 Structure of rhodopsin

The rhodopsin protein (shown as a rainbow ribbon in Figure 1.2) is a highly conserved GPCR of 384 amino acids (Ferrari *et al.*, 2011). It has seven transmembrane helices, N terminal cap, and a C terminal region which contains an eighth helix. Intracellular and extracellular loops link the helices. Rhodopsin is found within the rods outer segment, in the disc and plasma membranes (Ferrari *et al.*, 2011).

11-*cis*-retinal is the rhodopsin ligand and is a derivative of vitamin A (Daruwalla *et al.*, 2018). It binds within the transmembrane segment of rhodopsin (Ferrari *et al.*, 2011). 11-*cis*-retinal is covalently bound to the rhodopsin protein by a Schiff base bond (Figure 1.2, black sticks) (Meng and Bourne, 2001; Ferrari *et al.*, 2011). It is attached to lysine 296, forming what is known as the rhodopsin pigment (Khorana, 1993).

Studies of the rhodopsin crystal structure have shown the importance of the extracellular region (with high organisation and conservation of a disulphide bridge) and 11-*cis*-retinal which has a key role in the maintenance of the transmembrane helix arrangement (Palczewski *et al.*, 2000). However, mutations found throughout the rhodopsin polypeptide sequence can be detrimental rod cells and eventually to the entire retina due to its fundamental function as the receptor at which vision is initiated (Nathans, 1992).

Research here will use bovine rhodopsin to study mutations which occur in retinitis pigmentosa. While there is high sequence similarity between bovine and human rhodopsin, subtle differences might need to be considered when using bovine rhodopsin as a model for human retinitis pigmentosa mutants (Kazmin *et al.*, 2015).

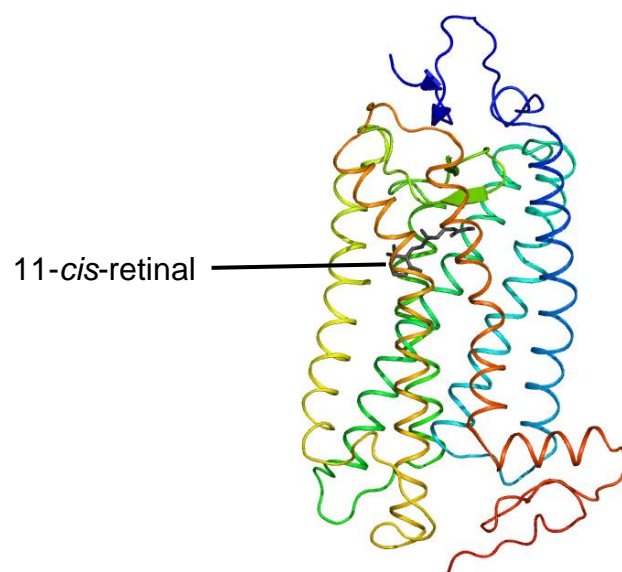


Figure 1.2 The structure of the rhodopsin pigment. The rhodopsin protein is shown as a ribbon and the ligand 11-cis-retinal is shown as black sticks. Helices are coloured as followed: TM1 – dark blue, TM2 – cyan, TM3 – teal, TM4 – green, TM5 – yellow, TM6 – orange, TM7 – dark orange and helix 8 - red. Produced using PyMOL (PDB1U19).

1.3.2 Light transduction

Rod and cone photoreceptor cells are found in the outer retina of the mammalian eye where the eye's lens focusses light, and these cells are where photons are captured (Ferrari *et al.*, 2011; Athanasiou *et al.*, 2018). In vision, the function of the highly conserved visual pigment rhodopsin is to receive photons, and trigger the signalling cascade allowing the brain to form the image (Ferrari *et al.*, 2011). The formation of the visual pigment rhodopsin requires rod opsin to bind with its ligand 11-*cis*-retinal, through the formation of a Schiff base bond at lysine 296 (Wald, 1968; Opefi *et al.*, 2013). Rhodopsin has a peak absorbance (λ max) at 500 nm (Wald, 1968). The intradiscal loop 2 acts as a cover to the retinal binding pocket of rhodopsin, through the ionic link formed between Arg 177 and Asp 190 which are necessary for the dark state stability and folding of opsin (Janz *et al.*, 2003).

The rhodopsin ligand undergoes isomerisation from 11-*cis*-retinal to all-*trans*-retinal upon absorption of a photon, causing a sequence of structural changes resulting in rhodopsin transmembrane helices three and six parting (Meng and Bourne, 2001; Ferrari *et al.*, 2011). The isomerisation of 11-*cis*-retinal was shown through the study of rhodopsin's crystal structure in both its inactive and photoactive forms and HPLC showed the inactive rhodopsin to contain only 11-*cis*-retinal and the active to contain its isomers (Salom *et al.*, 2006). This isomerisation event causes rhodopsin to transition through a series of metastable intermediates eventually arriving at metarhodopsin II form. It is the Meta II intermediate that interacts with transducin (the G protein associated with rhodopsin) thus activating it and initiating a second messenger pathway (Figure 1.3) (Ferrari *et al.*, 2011; Park, 2014). Rhodopsin kinase phosphorylates the metarhodopsin II, leading to arrestin binding. This step leads to its inactivation and the all-*trans*-retinal is released from the binding pocket following its

hydrolysis (Park, 2014). The metarhodopsin II transitions back to rhodopsin and can rebind 11-*cis*-retinal to begin the cycle again (Park, 2014).

The transition of rhodopsin through its intermediates occurs upon this isomerisation of 11-*cis*-retinal (Figure 1.3) (Wald, 1968; Shichida and Morizumi, 2006)(Wald, 1968; Shichida and Morizumi, 2006). From its excited state, rhodopsin transitions through the forms of photo-, batho-, BL-, and Lumi- rhodopsin, before transitioning into the metarhodopsin I (Meta I) conformation (Figure 1.3) (Wald, 1968; Shichida and Morizumi, 2006). Upon reaching the Meta I conformation, it interacts with the G-protein transducin (Shichida and Morizumi, 2006).

An equilibrium shift towards Metarhodopsin II (Meta II) occurs when transducin interacts with Meta I (Hofmann, 1999; Shichida and Morizumi, 2006). Metarhodopsin II (Meta II) is the active conformation of rhodopsin which binds transducin leading to the exchange of GDP for GTP (Figure 1.3) (Shichida and Morizumi, 2006).

This leads to a calcium signalling pathway (Mendes *et al.*, 2005). Calcium ions are imperative to the process of dim light vision, providing signalling following the reception of a single photon (Polans *et al.*, 1996). A network of hydrogen bonds surround the retinal Schiff base which act to control the hydrolysis and subsequent release of all-*trans*-retinal from Meta II (Janz and Farrens, 2004).

Arrestins recognise the phosphorylated rhodopsin and bind, subsequently decreasing the binding of transducin (Gray-Keller *et al.*, 1997; Krupnick *et al.*, 1997; Vishnivetskiy *et al.*, 2007).

Dissociation of the all-*trans*-retinal from the Metarhodopsin III (Meta III) conformation circles the process back to rod opsin, which can then re-associate with the 11-*cis*-retinal ligand to begin the process again (Shichida and Morizumi, 2006).

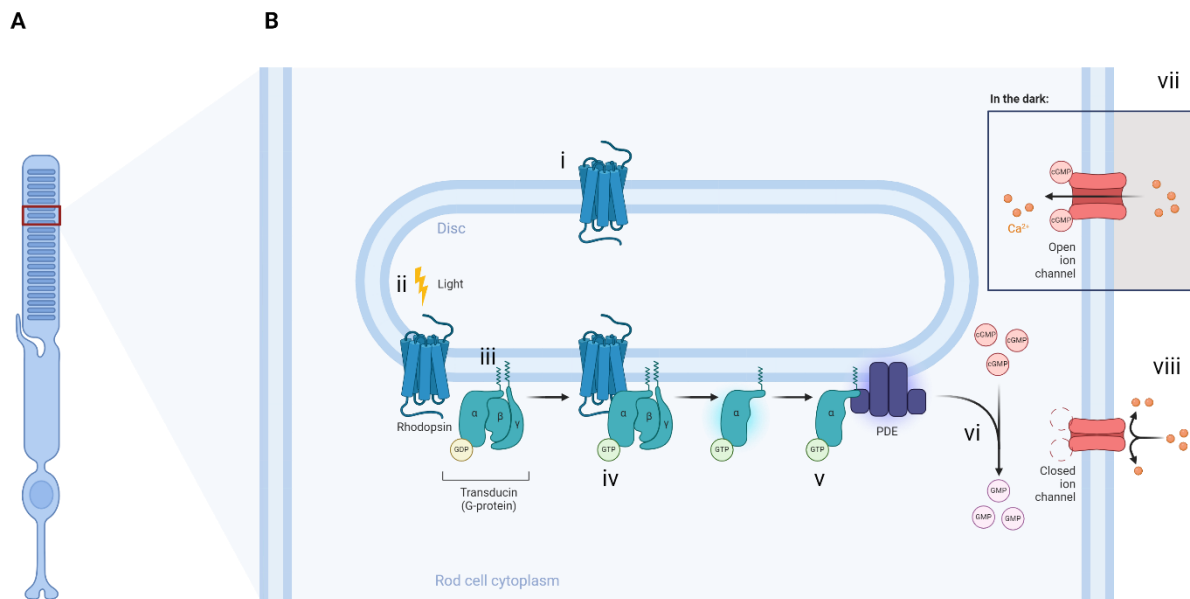


Figure 1.3 The activation pathway of rhodopsin. A: shows the structure of a rod cell, with discs found in the outer segment. B: shows the activation pathway of rhodopsin. i: rhodopsin is located in the disc membranes. ii: Light is absorbed by rhodopsin causing isomerisation of 11-cis-retinal to all-trans-retinal. iii: This results in rhodopsin interacting with transducin (a G-protein). iv: This interaction results in the exchange of GDP for GTP in transducin. v: Activated transducin can then interact with phosphodiesterase (PDE). vi: PDE hydrolyses cGMP to GMP. vii: In the dark cGMP keeps the calcium channels to open resulting in calcium ions entering the cell. viii: However, the reduction of cGMP results in cGMP-gated channels to close, preventing calcium ions from entering the cell. The change in membrane potential results in termination of glutamate release at the rod cell synapse, an event that inhibits ON bipolar cells and excites OFF bipolar cells, thus initiating a nerve impulse. Created with BioRender.com.

1.3.3 The role of transducin in signal transduction by rhodopsin

Transducin is the G protein associated with rhodopsin. Hundreds of transducin molecules were found to be activated by a single rhodopsin, but more recently using intact rods from mouse models it was found that the amount was in the 12-14 range (Yue *et al.*, 2019). Several key sites for transducin activation have been found in rhodopsin. including the cytoplasmic loops 2 and 3 and helix 8 in cytoplasmic loop 4 (Hargrave *et al.*, 1993; Natochin *et al.*, 2003; Gao *et al.*, 2019). Hargrave *et al.* (1993) found that these sites were important in the binding of transducin to rhodopsin via the 5kDa carboxyl terminal region of transducin. Rhodopsin with mutations in the cytoplasmic loops 2 and 3 were unable to activate transducin (Natochin *et al.*, 2003). Rhodopsin-transducin complexes studied using cryo-EM showed interactions between transmembrane helices three, five and six, cytoplasmic loop 2 and helix 8 (cytoplasmic loop 4) and several regions of transducin in light activated rhodopsin (Gao *et al.*, 2019)(Gao *et al.*, 2019). The activation of transducin by the Meta II form of rhodopsin can be exploited to study its interactions. This can be examined through the intrinsic fluorescence change brought about by the exchange of GDP for GTP (Phillips and Cerione, 1988).

1.4 Retinitis Pigmentosa

1.4.1 Symptoms and disease progression

Retinitis pigmentosa (RP) defines a group of retinal diseases characterised by the progressive loss of rod and then cone photoreceptor cells. It is caused by various mutations affecting genes expressed in rod cells (Hartong *et al.*, 2006; Campochiaro and Mir, 2018). RP therefore differs phenotypically from rod-cone dystrophies where rod and cone loss is simultaneous (Campochiaro and Mir, 2018). Characteristic of RP is the deposit of retinal pigment mainly in the peripheral retina, as well as the early symptoms of night blindness and then loss of peripheral vision (Hamel, 2006; Hartong *et al.*, 2006). This is due to the abundance of rod cells in the peripheral retina (Nathans, 1992). Symptoms progress leading to tunnel vision and eventually loss of central vision which is caused by the subsequent loss of cone cells (Hartong *et al.*, 2006). Cone cells are thought to be lost due to oxidative damage once the majority of rod cells have died which leads to increased concentrations of oxygen in the outer retina (Campochiaro and Mir, 2018). The mechanism of cell death has been described to be a results of unfolded protein response (UPR) and heat shock response (HSR) (1.5.3) (Parfitt *et al.*, 2014).

The onset of RP symptoms is highly variable; however, typically the symptoms begin in adolescence (night blindness), progressing throughout early and into late adulthood, with loss of central vision generally occurring by age 60 (Hartong *et al.*, 2006).

1.4.2 Diagnosis and clinical findings

Diagnosis of RP is based upon a number of clinical assessments. Amplitudes on an electroretinogram (ERG) are greatly reduced in patients with RP (Hamel, 2006). ERGs

measure a-waves which show photoreceptor function and b-waves which show bipolar cell function, low intensity flashes are used which can only be detected by b-waves however this ensures the measurement due to the rod cells alone responding and stimulating the bipolar cells (Cakir *et al.*, 2011). Other clinical assessments for RP include: assessing patients visual fields, colour vision, dark adaptation and contrast sensitivity (Hartong *et al.*, 2006). It has been shown that contrast sensitivity is an important parameter when observing photoreceptor deterioration in a rhodopsin deficient mouse model of RP (Xiao *et al.*, 2019). For routine molecular testing to become a possibility a greater understanding of the relationship between genetic and clinical data needs to be achieved (Ferrari *et al.*, 2011).

The clarity of vision at 20 feet is described as visual acuity with the norm being 20/20. At very low visual acuity levels visual acuity is described by an individual's ability to count fingers, perceive hand motion or perceive light which would be the case for patients with advanced RP (Schulze-Bonsel *et al.*, 2006).

1.4.3 Inheritance of genetic mutations associated with RP

1 in 3000 to 1 in 7000 people have RP (Nathans, 1992; Ferrari *et al.*, 2011). There have been a variety of genes linked to RP; for example: *PRPH2/RDS*, *PRPF31*, *RP1* and *RHO* (Ferrari *et al.*, 2011). The inheritance of the mutant genes can be autosomal recessive, autosomal dominant or X-linked and can be common to multiple inherited retinal diseases such as macular degeneration and night blindness (Ferrari *et al.*, 2011; Dias *et al.*, 2018). There are also syndromes associated with RP; Usher syndrome which also involves hearing loss, and Bardet-Biedl syndrome which has many effects (Ferrari *et al.*, 2011). The great numbers of mutations which can cause RP result in varied disease phenotypes making the study of changes in the

histopathology of the retina important (Milam *et al.*, 1998). As part of this research, the characterisation of mutations in the rhodopsin gene (*RHO*) (the most common cause of autosomal dominant RP) will be performed (Athanasίου *et al.*, 2018).

1.4.4 Genetic causes of retinitis pigmentosa

Many mutations have been observed in rhodopsin which can cause autosomal dominant and autosomal recessive inheritance patterns (Ferrari *et al.*, 2011). Missense and nonsense *RHO* mutations inherited in an autosomal dominant manner have been recognised in excess of 150 times. It is variation in the rhodopsin amino acid sequence that leads to toxic effects caused by the mutant rhodopsin to the rod cells (Hartong *et al.*, 2006; Athanasίου *et al.*, 2018). These toxic effects on the rod photoreceptors are a suggested cause of cell death, and a dependent relationship between the rod and cones for viability as a reason for the subsequent death of cone photoreceptors (Hartong *et al.*, 2006). For RP to be better understood, the mechanisms by which the gradual deterioration of the rod cells is caused through the mutations needs to be identified (Milam *et al.*, 1998).

A total of 22 genes are implicated as causes of RP (Ferrari *et al.*, 2011)(Ferrari *et al.*, 2011). These genes are involved in a wide variety of processes. Some examples of the processes the genes may be involved in include: phototransduction (*RHO*, *PDE*), splicing (*PRPF3*, 8, 31), cell structure (*ROM1*), transcription (*CRX*), and tissue development and maintenance (*RP11*) (Phelan and Bok, 2000; Ferrari *et al.*, 2011; Dias *et al.*, 2018).

1.4.5 Involvement of *RHO* in RP

RP inheritance arising from mutation of the *RHO* gene may be either autosomal dominant (ad) or autosomal recessive (Athnasiou et al., 2018)(Athnasiou et al., 2018). Autosomal dominant disease-causing mutations in the rhodopsin gene were identified through the study of RP patients from the US and Canada (Dryja et al., 1990). The first discovered, most common and extensively studied autosomal dominant *RHO* mutation results in the P23H rhodopsin mutant. It is the most prevalent mutation in the North American population of RP cases (Mao et al., 2012). Its high prevalence can be attributed to the founder effect, caused by reduced genetic variability when a small population is cut off from the original population resulting in much higher frequency of the genetics of the founding population. Many other mutations in the N-terminus of rhodopsin have been studied, such as T4K, P23A/L and T17M (Athnasiou et al., 2018) Other mutations have been identified throughout the transmembrane helices, such as L40R, E113K and H211P (Athnasiou et al., 2018). Recently, novel mutations in *RHO* have been identified at amino acid P12NA resulting in a frameshift and stop codon at residue 47 and Q28X, both thought to result in rhodopsin proteins that are not full length (Wang et al., 2019).

1.4.6 Potential strategies for the treatment of RP

With no treatments currently available, ways to lengthen the time in which the disease progresses are the only methods to help RP patients, such as through nutritional changes (Hartong et al., 2006). Previously, for RP patients with a class 2 rhodopsin mutation, increasing vitamin A consumption was thought to be possibly advantageous (Li et al., 1998). However, re-evaluation of the data has shown that vitamin A doesn't have a protective affect and is therefore no longer recommended (Comander et al.,

2023). Prolonging photoreceptor survival may be possible through red tinted glasses which filter light, as was seen in autosomal dominant mouse models; however, greater research into the effect of such filters is required (Orlans *et al.*, 2019).

For patients, along with increasing understanding of the relationship between RP genotypes and the related phenotype, it is also important for research to determine the relationship between rod and cone cells, as cone mediated vision is relied upon by patients as the disease progresses (Milam *et al.*, 1998). There is possibility in prolonging cone functioning by increasing WT rhodopsin and decreasing mutant rhodopsin in autosomal dominant RP, however more research is needed for this to be a treatment option (Lewin *et al.*, 2014).

Stem cell and organoid based therapies are possibilities based on recent advances. For example, recent advances in retinal organoid growth from human pluripotent stem cells show great potential for modelling different retinal diseases and for developing therapies where cells lost through these diseases can be replaced - such as rod cells in retinitis pigmentosa (Zerti *et al.*, 2019). Stem cell based therapy for diseases like RP could be important for personalised medicine to become a reality (Hoshino *et al.*, 2017).

Owing to the different effects on rhodopsin which mutations can have, different therapeutic drugs may be required to treat RP patients. Ascertaining compounds aimed at restoring proteostasis also could have possible advantages in helping rhodopsin RP patients (Parfitt and Cheetham, 2016).

Multiple non-retinoid small molecules have been recently identified as potential therapeutics approaches for the treatment of RP. This has been achieved by high throughput screening (HTS) where a non-retinoid small molecule with low toxicity was

identified to act as a pharmacological chaperone with high efficacy in some misfolding mutants (Chen *et al.*, 2018). YC-001 demonstrated improvements to rhodopsin proteostasis and F5257-0462 showed ability to preserve function and delay death of the photoreceptor cells (Chen *et al.*, 2018; Vats *et al.*, 2022). Therapeutic potential was also seen for small molecule non-retinoids containing chromenone (Ortega *et al.*, 2022).

1.5 Classifications of rhodopsin mutants

1.5.1 Mutant classifications

Rhodopsin mutants were first classified on the basis of those which reached the rod surface and those which didn't (misfolded). This system was then expanded further (first to six and then to seven categories), depending on various properties of the mutant rhodopsin (Kaushal and Khorana, 1994; Mendes *et al.*, 2005; Athanasiou *et al.*, 2018). The wide range of amino acid substitutions which occur in the rhodopsin gene mean a variety of effects on the protein have been identified (Athanasiou *et al.*, 2018). The impact onto the rhodopsin protein which the *RHO* mutation causes allow for their classification (Figure 1.4):

1. the rhodopsin folds correctly, but the mutation has an effect post-golgi trafficking and outer segment is not targeted,
2. the rhodopsin misfolds, resulting in the protein being unstable and retained in the endoplasmic reticulum,
3. endocytosis and vesicular trafficking are interrupted,
4. post-translational modifications are distorted, and the rhodopsin is less stable,
5. activation of the G-protein transducin is amplified,
6. the rhodopsin exhibits constitutive activation,
7. the rhodopsin exhibits defects in dimerization

(Kaushal and Khorana, 1994; Mendes *et al.*, 2005; Athanasiou *et al.*, 2013, 2018).

The classes of rhodopsin mutants are not completely defining; with some mutants having characteristics associated to different classes resulting in the death of rod cells (Figure 1.4) (Athanasiou *et al.*, 2018). The subsequent death of cone cells has been

linked to inflammatory processes, such as the regulation by P2RX7 of pyroptosis (Viringipurampeer *et al.*, 2016).

To understand the mechanisms of RP in more detail, further study of RP causing genes to identify how photoreceptor death and visual symptoms are caused is important and the increased understanding of biochemical pathways involved in RP have potential to bring about ways to treat the disease (Hamel, 2006; Hartong *et al.*, 2006). For rhodopsin RP, classifying mutations based on their effect on the protein will allow for not only better understanding of the molecular mechanisms of the disease but also help in the design of treatments for the disease.

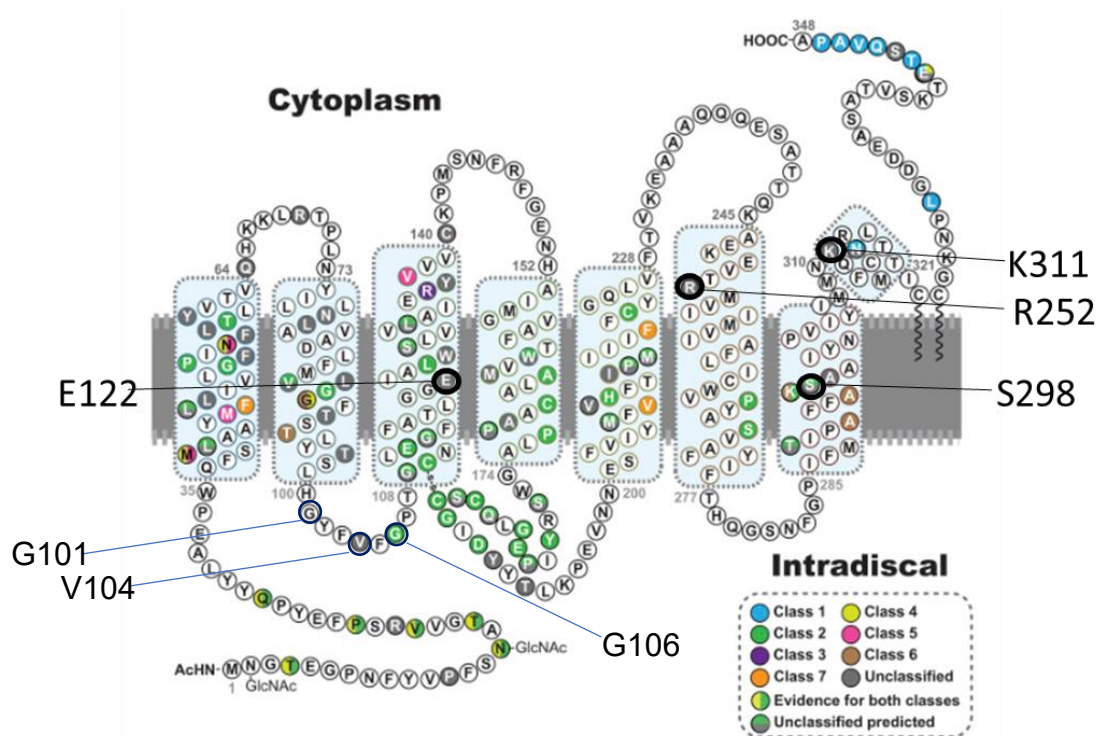


Figure 1.4 Secondary structure of rhodopsin, adapted from Athanasiou et al. (2018). Rhodopsin consists of seven transmembrane helices, and an eighth helix is found on the cytoplasmic side (towards the C-terminus). Mutations have been identified throughout the protein, and the aim in the current study characterisation of these mutants, most of which are unclassified. These are: E122, R252, S298, K311, G101 and V104 (unclassified), and G106 (class 2).

1.5.2 Class One – Defects in outer segment targeting

Post-production in the ER the protein travels to the Golgi after which it is trafficked to the rod outer segment where rhodopsin locates in the discs for use (Dias *et al.*, 2018). Mutations of Class One lead to this not being the case; due to impaired targeting to the rod outer segment (Dias *et al.*, 2018). Pathological effects as a result of mutant rhodopsin mislocalisation in a study of *Xenopus laevis*, were found to be related to the activation of the protein, however still result in the deterioration of the retina (Tam *et al.*, 2006). The study of an autosomal dominant RP mutant which results in the rhodopsin being mislocalised to the rod inner segment in *Xenopus laevis*, showed that the lysosomal pathway is triggered (Ropelewski and Imanishi, 2019). Research identifying Class One mutants has shown the importance of the C-terminus for outer segment targeting, with residues L328, T342, Q344, V345, A346 and P347 all identified as positions where mutations can result in impaired outer segment targeting (Athanasίου *et al.*, 2018; Dias *et al.*, 2018).

1.5.3 Class Two – Mutations which result in the misfolding of rhodopsin

Class Two rhodopsin mutations were one of the first categories established and mutants of this category have been well documented. They result in misfolding of the rhodopsin apo protein 'rod opsin' and are most frequent outcome of rhodopsin mutations (Krebs *et al.*, 2010; Comitato *et al.*, 2019). Class Two mutations have been identified at residues throughout the protein with residues in the N-terminus (e.g. P23), extracellular loops (e.g. G106) and throughout the TM helices (e.g. L125) affected (Athanasίου *et al.*, 2018; Dias *et al.*, 2018). From experiments using recombinant cells

to express such mutants it was found they were misfolded and retained in the endoplasmic reticulum (ER) (Kaushal and Khorana, 1994).

As a result of the retention of the misfolded protein in the ER, ER stress occurs which can lead to the initiation of UPR pathways such as IRE1 (Lin *et al.*, 2007). The activation of the IRE1 pathway was shown to decrease the levels of misfolded protein and in turn promote the survival of photoreceptor cells (Lin *et al.*, 2007). The UPR has also been shown to elicit altered cell signalling resulting in activation of apoptotic pathways (Sizova *et al.*, 2014). ER stress can also cause cells to exhibit autophagy and proteasome overload, both of which have been shown to contribute to cell death (Lobanova *et al.*, 2013; Yao *et al.*, 2018).

A reduction in photoreceptor deterioration was seen using arimoclomol as a treatment in a mouse model (Parfitt *et al.*, 2014). Here the UPR and HSR pathways were upregulated (Parfitt *et al.*, 2014). A further observation was a reduction in the aggregation of the rhodopsin protein (Parfitt *et al.*, 2014). It has also been shown that misfolded protein may form aggregates like entities; however there may be dissimilarities in the aggregates between mutants due to differences in completely or partially misfolded rhodopsin mutants (Saliba *et al.*, 2002; Gragg and Park, 2018).

Krebs *et al.* (2010) found that misfolding mutant rhodopsin displays features of inactive rhodopsin following activation by a photon or break down into possibly cytotoxic products. The resultant death of the photoreceptor cells from a misfolding mutation has been linked to the activation of calpain, by preventing this activation pathway and the subsequent activation of caspase-7 and apoptosis inducing factor, for P23H the breakdown of the retina has been shown to be reduced (Comitato *et al.*, 2019).

However, by just increasing the movement of Class Two mutant rhodopsins to the rod outer segment remains detrimental, as shown in a study using metformin to increase P23H movement to the outer segment which led to cell death and instability of the outer segment, with the P23H rhodopsin remaining unstable also (Athanasidou *et al.*, 2017a).

Rescue of misfolded rhodopsin mutants using pharmacological chaperones, either 9-*cis*-retinal or 11-*cis*-retinal, during biosynthesis has been shown to restore pigment at levels of 50-100% of that of wild type rhodopsin (Opefi *et al.*, 2013). Previously, 9-*cis*-retinal, 11-*cis*-retinal and a variant of 11-*cis*-retinal (containing a 7 membered ring) were shown to behave as pharmacological chaperones (Noorwez *et al.*, 2003, 2004). Due to the high quantity of misfolded protein mutations, where pharmacological rescue has been shown to be effective, there is potential for this strategy to be used in treating RP (Krebs *et al.*, 2010).

1.5.4 Class Three – Interruption of endocytosis and vesicular trafficking

Rhodopsin mutations at R135 (to G, L, P and W) have been reported to be class three mutations (Iannaccone *et al.*, 2006; Athanasidou *et al.*, 2018; Dias *et al.*, 2018). In a study of a family with the R135W mutation, they reported night blindness at 1-2 years, reduced periphery field after 30 years and blindness between 45 and 50 years (Wu *et al.*, 2019). The mutations R135L, R135G and R135W were categorised clinically as Class A (severe, early onset), reporting night blindness in early life (Cideciyan *et al.*, 1998; Iannaccone *et al.*, 2006).

1.5.5 Class Four – Atypical post-translational modifications and instability

Class four mutants are those which result in atypical post-translational modifications (PTMs) and instability of the mutant (Athanasίου *et al.*, 2018). There are multiple types of PTMs which rhodopsin undergoes and these are critical for the structure and function of the protein (Murray *et al.*, 2009). The PTMs which rhodopsin undergoes are: Schiff base formation at K296, C110 to C187 disulfide bond, palmitoylation of C322 and C323, M1 acetylation, phosphorylation of C-terminus residues, cytoplasmic lysine ubiquitination and N-glycosylation at N2 and N15 (Murray *et al.*, 2009). Mutations which have been identified as Class Four include T4K and T17M which have been shown to impair glycosylation (Tam and Moritz, 2009; Athanasίου *et al.*, 2018).

1.5.6 Class Five – Amplification of transducin activation

Mutants which result in the increased activation of transducin, without constitutional activation properties are categorised as class five mutants (Athanasίου *et al.*, 2018). The mutants M44T and V137M were identified to have increased transducin activation rates, while not showing signs of dark activity and were therefore categorised as Class Five mutants (Andrés *et al.*, 2003; Athanasίου *et al.*, 2018).

1.5.7 Class Six – Constitutive activation of rhodopsin

The constitutive activation of rhodopsin has been observed for mutation of residues near the the ligand binding pocket. This class of rhodopsin mutant can activate transducin with and without the 11-*cis*-retinal ligand but it has been difficult to identify the origin of the form responsible for the disease (Park, 2014). The death of photoreceptor cells may also be caused by the build-up of abnormal activated

rhodopsin exhibiting distorted activation pathways such as found in the case of G51V and G89D (Bosch-Presegué *et al.*, 2011). G90D, T94I, A292E, A295V

1.5.8 Class Seven – Defects in dimerisation

The inability of a rhodopsin mutant to dimerise leads to its categorisation as class seven (Athanasίου *et al.*, 2018). The mutations F45L, V209M and F220C have been identified as Class Seven (Athanasίου *et al.*, 2018).

1.5.9 Effects on other rhodopsin functions

Some mutants have been found to have no effect on the light transduction pathway, however do not exhibit the same scramblase activity as in WT rhodopsin, possibly due to the improper functioning as a scramblase causing improper functioning of ABC4, implicated in preventing the build-up of toxic retinoids in rod cells (Ernst and Menon, 2015; Ploier *et al.*, 2016).

1.5.10 Rhodopsin RP mutants under investigation

As described by (Athanasίου *et al.*, 2018), five of the autosomal dominant RP rhodopsin mutants in this study are as yet unclassified, with no biochemical or cellular faults identified (V104F, E122G, R252P, S298D and K311E). G106W was previously classified as class two and G101V still to be classified but likely to be class 2,3 or 4 based studies by other groups (Sung *et al.*, 1991b; Athanasίου *et al.*, 2018; Wan *et al.*, 2019). Owing to their different locations through the rhodopsin protein, we hypothesise that these mutants will have varying effects on the functioning of rhodopsin and therefore are likely to fall into different classifications. Importantly,

E122G, R252P, S298D and K311E mutations appear to not be misfolding, meaning their study may elucidate information about the functional properties of the WT residues in rhodopsin.

In a study of Mexican adRP patients, E122G was identified as a novel mutation, where c.365 A>G was identified in exon 2 of rhodopsin, resulting in a GAA to GGA (Glu to Gly) change (Matias-Florentino *et al.*, 2009). This mutation was identified to have broad variability in clinical presentation but an overall mild retinal phenotype (Matias-Florentino *et al.*, 2009).

V104F is also unclassified (Athanasίου *et al.*, 2018). G101V was determined to be pathogenic with low expression levels in HEK293 cells, with class 2, 3 or 4 being likely as its mechanism of causing RP (Wan *et al.*, 2019). G106W rhodopsin has been previously found to be a class two mutant (Sung *et al.*, 1991b; Athanasίου *et al.*, 2018). The WT residue of these RP positions for each mutant is shown (Figure 1.5).

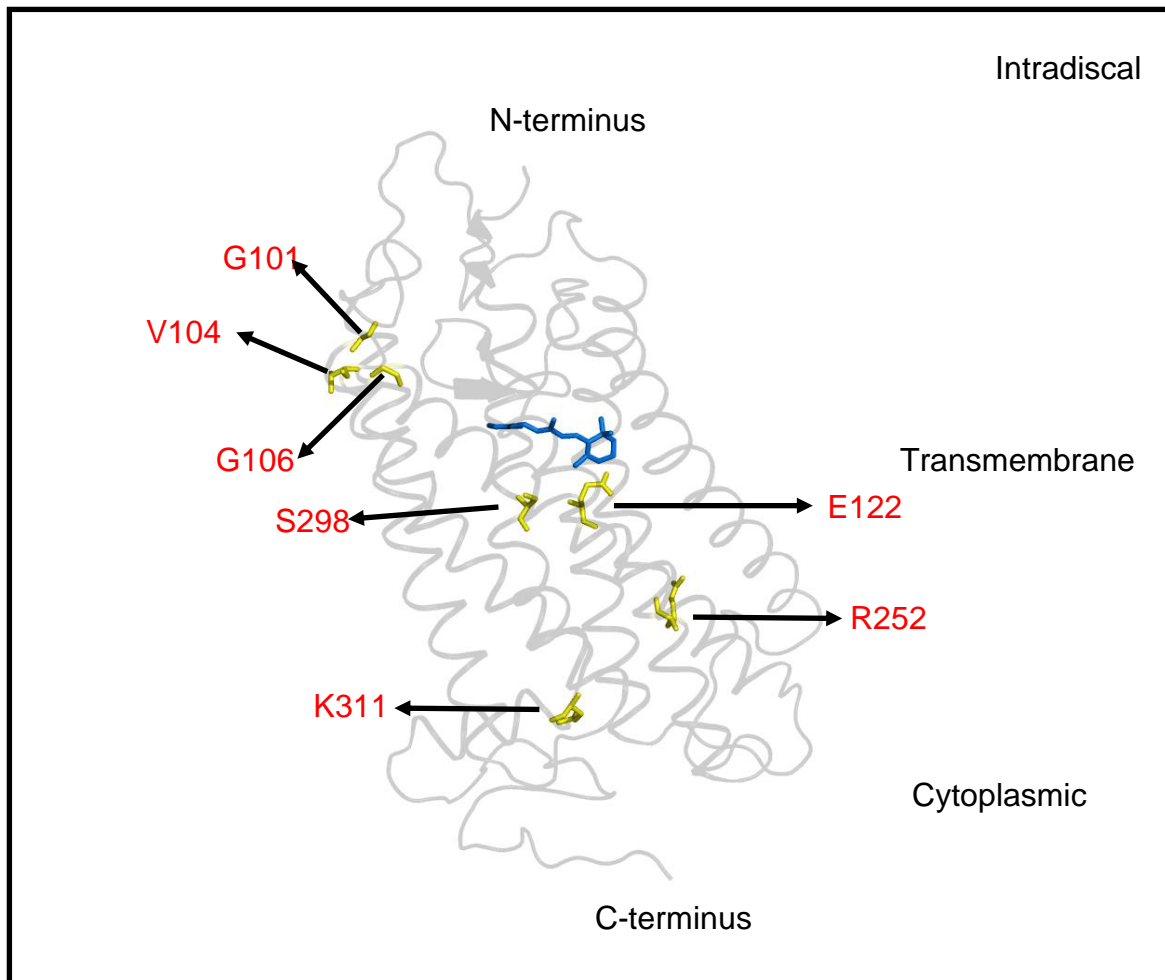


Figure 1.5 Location of the rhodopsin RP positions for the mutations examined in this work. Produced using PyMOL – PDB 1U19. G101, V104 and G106 are all located in extracellular loop one on the intradiscal side of rhodopsin. E122 (transmembrane helix 3) and S298 (transmembrane helix 7) are in close proximity to the 11-cis-retinal binding pocket (blue sticks). R252 is found in the sixth transmembrane helix, towards the cytoplasmic side). K311 is found in helix eight, which is located on the cytoplasmic side, towards the C-terminus).

1.6 Recombinant protein expression

High levels of protein expression at both lab and industry scale are greatly important for both therapeutics and research (Reeves *et al.*, 1996; Tripathi and Shrivastava, 2019). Developments in protein expression methods have been critical for progress in this field (Tripathi and Shrivastava, 2019). The expression hosts for proteins are numerous, with different advantages and disadvantages. The choice of the most suitable host is crucial for successful protein production (Tripathi and Shrivastava, 2019)(Tripathi and Shrivastava, 2019).

1.6.1 Recombinant protein expression hosts

E. coli is suitable option for protein expression due to it being well characterised both at the genetic and physiological level making it an ideal host for the high-level production of many proteins (Baeshen *et al.*, 2015; Tripathi and Shrivastava, 2019). However, there are disadvantages to its use including the absence post-translational modifications such as disulfide bridge formation and glycosylation (Gupta and Shukla, 2016; Tripathi and Shrivastava, 2019). In the case of GPCRs such as rhodopsin, the absence of these post-translational modifications makes *E. coli* unsuitable for functional studies (Wiseman *et al.*, 2020).

P. pastoris and *S. cerevisiae* are regularly used yeasts for protein expression (Tripathi and Shrivastava, 2019). They are fast and cheap to grow with well understood genetics (Tripathi and Shrivastava, 2019). However, the cell stress and effects on the yeast physiology are disadvantageous to their use (Yu *et al.*, 2017). Opsin expression using yeast has been shown to produce rhodopsin which is functionally similar to that produced using mammalian cells but displays differences in its glycosylation (Mollaaghababa *et al.*, 1996).

Transgenic animals and plants offer many benefits. However the ethical drawbacks of transgenic animals and contamination by either zoonotic pathogens or pesticide, herbicide or toxic plant metabolites (Tripathi and Shrivastava, 2019).

Expression using insect cells is also possible using the baculovirus expression system to express the gene of interest (Owczarek *et al.*, 2019; Tripathi and Shrivastava, 2019). The successful application of this for producing GPCRs for crystallisation studies has been shown (White *et al.*, 2012; Xiao *et al.*, 2013).

Widely used hosts for expression of recombinant proteins are mammalian cells (Owczarek *et al.*, 2019). Large and complex proteins are able to be expressed using mammalian cells, however the construction of cell lines capable of this is a time consuming process (Tripathi and Shrivastava, 2019). Mammalian cells are also able to perform post-translational modifications, albeit with a different glycosylation pattern, and there is also risk of contamination with viruses of animal origin (Tripathi and Shrivastava, 2019). Various human cell lines, such as HEK293, are being studied for their gene expression, which allow for post-translational modifications to be similar to those naturally occurring in humans (Tripathi and Shrivastava, 2019).

1.6.2 Transposons and their use in protein expression

A transposon refers to a section of DNA which can move from one site to another, giving rise to its alternate name, the 'jumping gene' (Sandoval-Villegas *et al.*, 2021). The insertion of the transposable element is highly efficient and can be exploited to stably insert DNA for experimental purposes (Sandoval-Villegas *et al.*, 2021). Transposons identified include 'Sleeping Beauty', 'Tol2' and the focus here, 'PiggyBac' (Sandoval-Villegas *et al.*, 2021).

The PiggyBac (PB) transposon was identified in the cabbage looper moth, *Trichoplusia Ni*, and has since been shown as a reliable method for the movement of genetic information in various organisms, including in mammalian and human cells (Ding *et al.*, 2005; Wilson *et al.*, 2007; Zhao *et al.*, 2016; Sandoval-Villegas *et al.*, 2021). The evolution of the PiggyBac transposon has provided it with the ability to efficiently integrate large cargoes of DNA into a host genome making it a valuable asset experimentally for stable DNA introduction (Sandoval-Villegas *et al.*, 2021). As an experimental tool, it is versatile and cost effective, with applications in CAR-T therapy (Kaštánková *et al.*, 2021).

1.7 PiggyBac transposon for rhodopsin expression

1.7.1 PiggyBac transposon

The use of the PB transposon has been previously shown as an effective method to produce rhodopsin in a stable HEK293S cell line (Caro *et al.*, 2015). With the intention to achieve high levels of rhodopsin mutant expression, tetracycline inducible PB systems will be used in this study. Through the inclusion of TetO sequences as part of a CMV promoter upstream of the rhodopsin gene, the addition of tetracycline and sodium butyrate has been shown previously to result in high levels of rhodopsin expression in stable cell lines expressing the TetR repressor (Reeves *et al.*, 2002a). Gene expression can be influenced by the location of its integration, however the use of insulators have been found to shelter against such influences (Sarkar *et al.*, 2006).

Here, the PB transposon cargo will contain rhodopsin under the control of the CMV [TetO] promoter. The neomycin resistance gene is under the control of a H₂L^d promoter. This selection/expression cassette is flanked by insulator and ITR sequences (Figure 1.6). Upon transfection together with a plasmid for transposase

production, this cargo will be inserted into the genome of the cells, to construct the G418 resistant stable cell line pools.

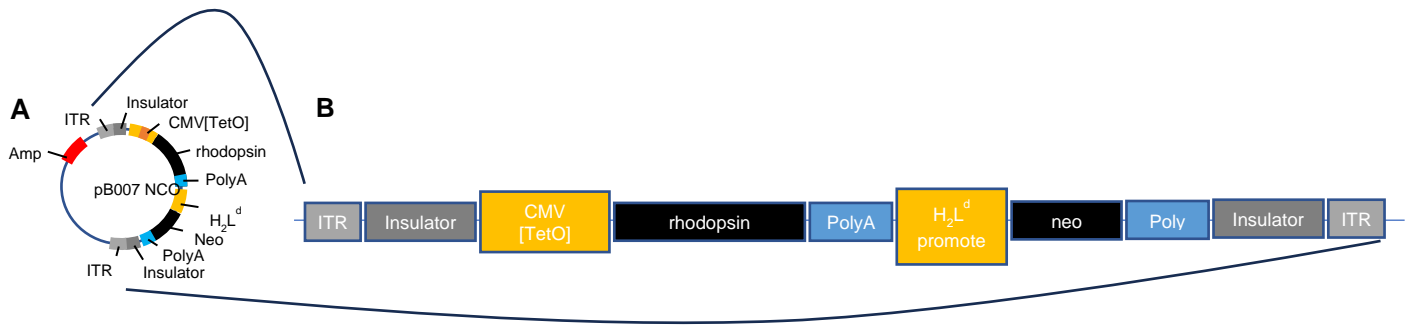


Figure 1.6 pB007 (piggyBac) plasmid and cargo. Length of sequences not to scale. A: The pB007 plasmid is approximately 9000 bp in size when containing the cargo used in this work. B: The transposon cargo from the pB007 plasmid is positioned between two ITR sections (light grey), and insulators (dark grey). A CMV [TetO] (yellow) controls the rhodopsin genes expression (black) and is followed by a polyA tail (blue). The H₂L^d promoter (yellow) is located in front of the neomycin resistance gene (Neo – black), again followed by a polyA tail (blue).

1.7.2 The construction of tetracycline inducible stable cell lines using the piggyBac delivery system

The production of a tetracycline controlled transactivator by the fusion of the virion protein 16 activating domain to the tetracycline repressor showed promise for promoter activating systems in the regulation of gene expression (Gossen and Bujard, 1992). Yao et al. (1998) were first to show that a tetracycline repressor, that directly bound the CMV promoter containing TetO sequences, was able to tightly regulate gene expression. They showed increased regulation of inducible genes compared to other systems in use.

There is a great need to produce high levels of rhodopsin for studies of structure and function (Reeves et al., 2002a). The creation of a stable cell line using a synthetic bovine opsin gene lead to the production of 2 mg/L of rhodopsin (Reeves et al., 1996)(Reeves, Thurmond and Khorana, 1996). Up to 10 mg/L of WT rhodopsin was then produced by the addition of tetracycline and sodium butyrate to a inducible stable cell line through inclusion of a TetO sequences using the system developed by Yao et al. (1998) and Reeves et al. (2002a). This method also counteracts the effects of toxicity of expressed mutants allowing production of rhodopsin at tens of milligrams per litre (Reeves et al., 2002a). Furthermore, by utilising a cell line lacking N-acetylglucoaminyltransferase (GnTI) activity, problems to structure and function studies caused by heterogeneity of N-glycans can be overcome (Reeves et al., 2002b).

Sodium butyrate included in the induction media aids the production of rhodopsin when used alongside tetracycline (Reeves et al., 2002a). Sodium butyrate is a short chain fatty acid histone deacetylase (HDAC) inhibitor. Such inhibitors can be

categorised as hydroxamates, cyclic peptides, benzamides and short chain fatty acids (Shukla and Tekwani, 2020)(Shukla and Tekwani, 2020). Histone deacetylases are the enzymes resulting in the deacetylation of histones, and therefore silencing of genes (Shukla and Tekwani, 2020). Therefore, the sodium butyrate induced over acetylation of histones leads to increased gene expression as the DNA is unwound from the histone and therefore more accessible for transcription factors aiding the increased expression of the gene (Reeves et al., 2002a; Shukla and Tekwani, 2020).

1.7.3 Mechanisms of insulator function

Introduced transgenes can integrate into a transcriptionally repressed region eventually leading to gene silencing and reduced expression levels of the recombinant protein over generations of cell division (Pérez-González and Caro, 2019). Insulators overcome this by acting as a barrier, shielding the transgene from such silencing (Pérez-González and Caro, 2019).

Transgene expression is increased through the utilisation of insulator sequences, and in addition, some insulators may be able to decrease the variability in expression between lines/ individuals (Pérez-González and Caro, 2019).

1.8 Solid State Magic Angle Spinning NMR

Solid State Magic Angle Spinning (SS MAS) NMR provides an adaptive method for the analysis of structure, dynamics and intermolecular interactions (Kraus *et al.*, 2021). This method is able to examine structure and dynamics both at specific locations and across the entirety of GPCRs through the use of the 'magic angle' (54.7°) to analyse chemical shifts and dipolar interactions (Chandler *et al.*, 2021). Samples used can be in a variety of states; such as in detergents or liposomes and can be examined under

low temperature conditions allowing for conditions to be determined by needs of the GPCR in question (Chandler *et al.*, 2021).

In the case of rhodopsin, the use of low temperature can be used to capture its active state and through this method the movement of extracellular loops, transmembrane regions and retinal have all been discovered during rhodopsin activation (Ahuja *et al.*, 2009a; Kimata *et al.*, 2015; Kimata *et al.*, 2016a; Kimata *et al.*, 2016b). ^{13}C , ^{15}N and ^{19}F are commonly used probes for studies of GPCR's (Chandler *et al.*, 2021).

1.9 Aims

The overall aim is to apply the use of the piggyBac transposon to produce rhodopsin and its mutants at suitably high levels for biochemical, spectral and structural analysis.

2. Methods

2.1 General materials

2.1.1 Materials

Table 2.1 List of materials used and suppliers.

9- <i>cis</i> -retinal	Sigma	kit for gel extraction and PCR clean up	
9mer elution peptide	Seq: TETSQVAPA	Penicillin	
Acetic acid		Streptomycin (PenStrep)	Lonza
Agar	Melford	PMSF	Fluka analytical
Agarose	Sigma	Restriction enzymes	ThermoScientific
Ammonium persulfate	Melford	Skim powdered milk	Marvel
BES	Sigma	Sodium azide	Sigma
BTP	Melford Biolaboratories Ltd	TC grade DMSO	Sigma-Aldrich
CaCl ₂	Sigma-Aldrich	Triton X-100	Sigma
CnBr activated sepharose		Trypsin	Lonza
DDM	Anatrace	Tryptone	Melford
DMEM	Lonza	Turbo buffer	ThermoScientific
DMEM/F12	Lonza	Turbofect	ThermoScientific
DMSO	Sigma	Yeast extract	Melford
DNA ladder	Thermo Scientific	Sodium Dodecyl Sulfate	Melford
EDTA	Melford		
Ethanolamine	Aldrich		
FBS	Thermo Scientific		
GeneJET Plasmid Mini-prep kit	ThermoScientific		
Geneticin	Melford		
Glycerol	Fisher		
KCl	Sigma		
KH ₂ PO ₄	Melford		
L-Glutamine	Lonza		
Na ₂ HPO ₄	Sigma		
NaCl	Fisher		
NucleoSnap Plasmid Midi kit	Machery-Nagel		
NucleoSpin Gel and PCR Clean-up, Mini	Machery-Nagel		

2.1.2 Buffers and media

Table 2.2 Buffers and media composition. Organised by method.

Buffer/ Media	Components
Molecular biology	
50X TAE	48.4 g Tris base, 0.5 M (pH 8) EDTA, 11.4 ml glacial acetic acid in 200 ml distilled water
Agarose gel	0.8% agarose, 1X TAE buffer
6x loading dye	10 mM Tris-HCl (pH 7.6), 0.03% w/v bromophenol blue, 0.03% w/v xylene cyanol FF, 60% glycerol, 60 mM EDTA in RO H ₂ O
<i>E. coli</i> culture	
2xYT broth	16 g tryptone, 10 g yeast extract, 5 g NaCl in 1 L distilled water
2xYT agar/ ampicillin	2xYT broth, 1.5% agar, 100 µg/ml ampicillin
Cell culture	
complete DMEM F12	DMEM F12, 10% heat-inactivated FBS, 2 mM L-Glutamine, 1% Penicillin/Streptomycin
complete DMEM	DMEM, 10% heat-inactivated FBS, 2 mM L-Glutamine, 1% Penicillin/Streptomycin
Tetracycline induction media	complete DMEM, 2 µg/ml tetracycline
Sodium butyrate induction media	complete DMEM, 5 mM sodium butyrate
Tetracycline/sodium butyrate induction media	complete DMEM, 2 µg/ml tetracycline, 5 mM sodium butyrate
10X PBS	NaCl 64.05 g, KCl 1.61 g, 1.63 g KH ₂ PO ₄ , 9.09 g Na ₂ HPO ₄ made up to 800 ml in MilliQ H ₂ O
SDS-PAGE/Western blot	
4x Resolving/running buffer	0.025 M Tris, 0.192 M Glycine, 0.1% SDS
4x Stacking buffer	3g Tris (0.5M), 40 ml RO H ₂ O, adjust pH to 6.8 with HCl, made up to 50 ml with RO H ₂ O, filter sterilize
Running/resolving gel (12.5%, 0.75 mm)	3.36 ml 30% acrylamide/bisacrylamide, 2 ml 4x running buffer, 80 µl 10% SDS, 2.48 ml MilliQ water, 80 µl 10% ammonium persulfate, 4 µl TEMED
Stacking gel	0.7 ml 30% acrylamide/bisacrylamide, 1.13 ml stacking gel buffer, 0.06 ml 10% SDS, 2.7 ml MilliQ water, 0.06 ml 10% ammonium persulfate, 0.004 ml TEMED
Tank buffer	0.025M Tris, 0.192M Glycine, 0.1% SDS
4x loading buffer	0.25M Tris HCl, 8% SDS, 40% Glycerol, 0.4M DTT, 0.04% Bromophenol Blue
1x transfer buffer	25mM Tris, 192mM Glycine, 20% Methanol, 0.1% SDS

Wash buffer	1 X PBS, 0.1% Tween 20 or Triton X100 Detergent, 0.5% Dry skimmed milk powder
1D4 primary antibody buffer	0.5% Gelatin, 0.25% BSA, 0.2% Sodium Azide, 100mM Potassium, Phosphate Buffer pH 7.4, 10 µg/ml 1D4 Antibody
Secondary antibody buffer	1x PBS, 0.1% Triton X-100, 0.5% Milk Powder (Marvel), Secondary Antibody (1:10,000)
Blocking buffer	10% Dry skimmed milk powder, 0.1% Sodium Azide (NaN ₃), 0.1% Tween-20, 1x PBS to volume
ECL buffer	10 ml 100 mM tris-HCl, 50 µl 250 mM luminol, 22 µl 90 mM Courmaric acid, 3 µl 30% H ₂ O ₂

Biochemistry

Low Salt Wash (LSW) buffer	10 mM BTP (pH 7.2), 0.1% DDM
Low Salt Elution (LSE) buffer	LSW buffer, 100 µM 9mer elution peptide
High Salt Wash (HSW) buffer	1xPBS, 0.1% DDM
High Salt Elution (HSE) buffer	HSW buffer, 100 µM 9mer elution peptide
1D4-sepharose slurry	50% 1XPBS, 50% 1D4-sepharose, 0.1% sodium azide 100 mM purified transducin, 5 nM rhodopsin/mutant rhodopsin,
Transducin assay buffer	10 mM BTP (pH 7.2), 1 µM DTT, 100 mM NaCl, 0.01%, DDM, 2 mM MgCl ₂ in MilliQ H ₂ O
Solubilisation buffer	1xPBS, 1% DDM, 0.1 mM PMSF
Meta II assay buffer	4 µg rhodopsin/mutant rhodopsin, 10 mM BTP (pH 6.0), 0.1% DDM in MilliQ H ₂ O
Low Salt Wash (LSW) buffer LMNG	10 mM BTP (pH 7.2), 0.02% LMNG
Low Salt Elution (LSE) buffer LMNG	LSW buffer (LMNG), 100 µM 9mer elution peptide
High Salt Wash (HSW) buffer LMNG	1xPBS, 0.02% LMNG
High Salt Elution (HSE) buffer LMNG	HSW buffer (LMNG), 100 µM 9mer elution peptide
Solubilisation buffer LMNG	1xPBS, 0.36% LMNG, 0.1 mM PMSF

Table 2.3 Buffers used for purification of transducin from bovine retinas.

Name	Buffer	Additions just before use
Buffer A	1x potassium phosphate buffer 10x stock: 700 mM KPi (pH 6.8) 30 mM MgCl ₂	1 µl/ml PMSF 5 mM β-mercaptoethanol
Buffer B/C/D/E/F/G	Sucrose at concentrations of: 30%, 15%, 0.64 M, 0.78 M, 1.0 M and 1.2 M All in 1x KPi buffer (pH 6.8)	1 µl/ml PMSF 5 mM β-mercaptoethanol
Buffer H	1x hypotonic buffer 10x stock: 50 mM Tris (pH 7.5) 60 mM MgCl ₂	1 µl/ml PMSF 5 mM β-mercaptoethanol
Buffer I	GTP buffer 1x hypotonic buffer, 100 µM GTP	1 µl/ml PMSF 5 mM β-mercaptoethanol
Buffer J	Column wash buffer 1x hypotonic buffer, 100 mM NaCl	5 mM β-mercaptoethanol
Buffer K	Column elution buffer 1x hypotonic buffer, 300 mM NaCl	5 mM β-mercaptoethanol
Buffer L	Transducin storage buffer 50% glycerol, 100 mM NaCl, 20 mM Tris (pH 7.5), 6 mM MgCl ₂	10 mM β-mercaptoethanol

2.2 General methods

2.2.1 Sanger sequencing of DNA

Plasmid DNA produced by *E. coli* transformation or mutagenesis was sequenced to confirm the sequence integrity before moving onto the next step throughout. Sanger sequencing was performed by Eurofins Genomics and separate primer and DNA samples were prepared and sent as according to their guidelines for their TubeSeq service. Plasmid DNA concentration was determined by nanodrop and diluted in sterile MilliQ water to a concentration of 100 ng/μl. The necessary primers were prepared by dilution in sterile MilliQ to 10 pmol/ μl. Sequencing results were analysed using Chromas and the Needle Pairwise alignment tool where the sequencing data was aligned to the known sequence of rhodopsin DNA to ensure the correct sequence was present, and that any required mutations following mutagenesis were correct (Madeira *et al.*, 2019).

2.2.2 Agarose gel electrophoresis

Agarose was added to 1x TAE buffer to produce a 0.8% agarose gel. DNA samples were loaded as appropriate and run at 100 V. Where GelRed was used as the nucleic acid stain the BIORAD UV transilluminator was used for visualisation. Details of the buffers used for agarose gel electrophoresis can be found in Table 2.2 Molecular Biology.

2.2.3 General procedure for restriction enzyme digest

The restriction enzyme (RE) digestion mix contained 1 μl of RE (fast digest), 0.5 μg of DNA, 2 μl 10X FD Green buffer, 5 μl of GelRed (1:10000 dilution of stock) and was made up to 20 μl in sterile MilliQ H₂O. Where two REs were used 1 μl of each was

added to the mix. The RE digestion mix was then pulse centrifuged before incubation for 20 minutes at 37 °C. The samples were then kept on ice to be separated on an agarose gel (2.2.2).

2.2.4 *Escherichia coli* transformation

Table 2.4 DNA types and volumes used in the transformation of *E. coli*.

Preceding experimental step	Volume added (µl)	Positive control
DpnI digestion of mutagenesis product	3	Either pB007 NCO-rho WT (Section 2.3) or pMT4-rho (Section 2.4.2)
Ligation of DNA (pACMV TetO or pB007 NCO)	2.5	pACMV TetO-rho (Section 2.4.3) pB007NCO-rho WT (Section 2.4.4)

For transformation, XL1 blue competent cells were used and kept on ice throughout unless otherwise stated. The relevant DNA (see **Table 2.4**) was added to 40 µl of *E. coli* competent cells in a sterile 1.5 ml microcentrifuge tube. A negative control had no DNA added to the *E. coli* and a positive control had 0.5 µl of the original plasmid (without mutations) added (see **Table 2.4**). The transformation mixtures were incubated on ice for 30 minutes, followed by a 45 second heat shock at 42°C. Tubes were then put back onto ice for 5 mins before 500 µl of 2XYT broth (see **2.1.1**) was added and the mixtures placed on a shaker for 30 mins at 37°C, 250 rpm. The tubes were then centrifuged for 2 mins at 10,000 rpm and 450 µl of the supernatant was removed. The pellets were resuspended in the remaining 50 µl and spread onto 2XYT Agar/Ampicillin (see **2.1.1**) plates under followed by incubation at 37°C for 16 hours. Single colonies were picked and inoculated into 3 ml of 2 XYT broth/Ampicillin (100 µg/ml) (see **2.1.1**) and incubated on a shaker at 37°C, 250 rpm for 16 hours.

After 16 hours the culture was split 500 μ l of culture added to 500 μ l of sterile glycerol in a cryovial, stored at -70°C , 1.5 ml for small scale plasmid purification (**2.2.5**),

Alternatively 1.5 ml of culture could be centrifuged at 14, 000 rpm for 5 minutes, the supernatant removed and the cell pellet frozen at -20°C .

2.2.5 Small scale purification of plasmid DNA from *E. coli* transformants

1.5 ml of the culture after the 16 hour incubation (**2.2.4**) was centrifuged at 14,000 rpm for 5 minutes. The supernatant was removed, and the cell pellet was purified using the ThermoScientific GeneJET Plasmid Miniprep Kit as according to the instructions (Revision 10). The pellets were resuspended in 250 μ l of resuspension buffer, and 250 μ l lysis solution was added and mixed four times by inversion. 350 μ l of neutralisation solution was immediately added and mixed again by inverting four times. Cell debris and chromosomal DNA were then pelleted by centrifugation at 10, 000 rpm and the supernatant transferred to the GeneJET spin column, centrifuged for 1 minute and the flow through discarded. 500 μ l wash solution was added to the spin column followed by 1 minute of centrifugation and discarding of the flow through. The wash step was repeated, and after discarding the flow through a further 1 minute of centrifugation was performed, removing any remaining wash solution. The spin column was transferred into a sterile 1.5 ml microcentrifuge tube. For plasmid DNA elution, 50 μ l of MilliQ water heated to 65°C was applied to the GeneJET column (differing from the kit instructions) and left to incubate at room temperature for 2 minutes. GeneJET spin column in the sterile microcentrifuge tube was centrifuged for 2 minutes at 10, 000 rpm, the spin column discarded and the flow through kept on ice and the concentration determined by nanodrop. The purified plasmid was then kept on ice for use the same day or stored at -20°C .

2.3 Generation of mutant rhodopsin in pB007NCO

2.3.1 QuikChange Mutagenesis

A description of the methods used for Quikchange mutagenesis, and the relevant mutants produced is described in Chapter 3, **section 3.2.1**.

2.4 Generation of mutant rhodopsin in pB007NCO by molecular cloning

2.4.1 Molecular cloning steps

pMT4 containing the synthetic bovine opsin gene and an ampicillin resistance gene was used as the starting point for molecular cloning. pMT4 Opsin-stabilised mutants (where N2C D282C mutations had been already incorporated, which cause stabilisation of rhodopsin through cysteine bridge formation) were digested using *KpnI* and *NotI* as was pACMV TetO Opsin, again with the N2C D282C mutations already incorporated. Both were run on methylene blue agarose gels (see 2.3.2) and the pACMV vector was treated with alkaline phosphatase before ligation to form the mutants in the pACMV TetO O-stabilised background. PCR was used to replicate the transposable element. *NheI* digestion of this allowed for it to be ligated into pB007 NCO (*NheI* digested and alkaline phosphatase treated). pB007 NCO-mutants ligation mixtures were then used for *E. coli* transformation.

2.4.2 Mutagenesis of pMT4-rho

Mutagenesis was carried out as described in **2.3.1** using pMT4-rho instead of pB007 NCO. The plasmids were expressed using transformation of *E. coli* **2.2.4**. The

plasmids were then purified as described in **2.2.5** and the purified product sequenced and then used for the following cloning steps.

2.4.3 Agarose gel electrophoresis for the separation of DNA fragments

Full details of the buffers used for agarose gel electrophoresis can be found in Table 2.2 Molecular Biology. Plasmid DNA was RE digested using *KpnI* and *NotI*, following the same protocol as in **2.2.3** but without including GelRed in the digestion mix. The digested samples were then mixed with 6x loading buffer. Methylene blue was made to a 0.01% solution in 0.5 X TAE buffer. The agarose gel was stained using the methylene blue solution for 40 minutes on the Bibby Stuart Scientific Gyro-Rocker. The agarose gel was then destained using 0.5 X TAE buffer for 30 minutes. The correct sized band was identified using a white light box and excised from the gel using a scalpel and the DNA purified as according to the 'Macherey-Nagel NucleoSpin Gel and PCR Clean-up, Mini kit for gel extraction and PCR clean up' as according to the instructions, except from the elution step. The steps were as follows. The excised band was solubilised using 200 μ l of buffer NT1 per 100 mg of gel by heating to 50 °C for 5-10 minutes. The solubilised sample was then applied to the column in a collection tube and centrifuged for 30 seconds at 11, 000 x *g*. The membrane was then washed through the addition of 700 μ l of buffer NT3 and centrifugation at 11, 000 x *g* for 30 seconds, the membrane wash was performed twice. The membrane was then dried by centrifugation at 11, 000 x *g* for 1 minute. The DNA was then eluted with 25 μ l sterile MilliQ water heated to 65°C, differing from the kit instructions.

2.4.4 Alkaline Phosphatase treatment of DNA

Following purification, vector DNA was treated with alkaline phosphatase. 2 μ l of Thermo Scientific FastAP Thermosensitive Alkaline Phosphatase was added before

incubation at 37°C for 15 minutes, and then heating to 80°C for 10 minutes to denature the enzyme.

2.4.5 Ligation

0.5 µl of the vector was added to 25-30 ng of the mutant rhodopsin DNA, along with 2 µl of ligation buffer (ligation buffer stock was freshly prepared with 20 µl 20X ligation buffer and an added 1 µl of 5X ATP), 1 µl of T4 DNA ligase and made up to 10 µl with sterile MilliQ water. The reactions were incubated at room temperature for 15 minutes and used for *E. coli* transformation as according to **section 2.5**.

2.4.6 Transfer of opsin gene expression cassette into piggybac vector

The opsin gene expression cassette in pACMV TetO opsin contains the rhodopsin gene under the control of the TetO promoter and a neomycin resistance gene under the control of the weak H₂D^L promoter. Following plasmid generation in *E. coli*, PCR using NEO CMV primers (see appendix) of the pACMV TetO O-stabilised mutants was performed and the presence and size of the plasmid DNA confirmed by agarose gel electrophoresis. The DNA was then digested using NheI, (20 µl of the DNA was added to 4 µl of Fast Digest buffer, 24 µl MilliQ water and 2 µl of Fast Digest NheI. This was incubated for 15 mins at 37°C). The digestion product was then separated on an agarose gel and stained with methylene blue as in **section 2.4.5**, before ligation into NheI digested, alkaline phosphatase treated pB007 NCO. Sequencing (see **2.2.1**) was used to determine if the correct sequence in the rhodopsin gene and the required mutations were present.

2.5 Isolation of plasmids from *E. coli*

2.5.1 Small scale production and confirmation of presence of mutant codon

The mutagenic product from 2.3.1 or cloning product from 2.4.5 was then used to transform XL1 blue competent *E. coli* as described in section 2.2.4 and then a small-scale production as described in section 2.2.5. Sequencing was used to confirm the presence of the mutant codon that was incorporated during Quikchange mutagenesis as described in section 2.2.1.

2.5.2 Medium scale preparation of plasmid DNA

Streak plates were made from frozen glycerol stocks of *E. coli* carrying mutant pMT4 plasmids. mutant. These were incubated (GallenHamp Economy incubator with fan) overnight at 37°C. Single colonies were picked from the plate and inoculated into 3 ml 2XYT broth/ampicillin (100 mg/ml) and incubated at 37°C on a shaker (IKA KS 400 I control) at 250 rpm for 6 hours. 100 µl of these cultures were added to 100 ml of 2XYT broth/ampicillin (100 mg/ml) and incubated overnight at 37°C at 200 rpm.

2.5.3 Purification of plasmid DNA from medium scale *E. coli* cultures

50 ml of the culture was centrifuged at 4000 rpm for 15 mins and the supernatant removed completely. The DNA was then purified from the *E. coli* pellet as according to the Machery-Nagel Plasmid DNA purification user manual, NucleoSnap Plasmid Midi February 2016/Rev.01, NucleoSnap Plasmid Midi Protocol. Bacterial cells were harvested and centrifuged at 6000 x *g* for 10 minutes and the supernatant completely removed. The bacterial cells were then resuspended in 5 ml SN1 buffer, lysed with 5 ml SN2 buffer (gently inverted 5 times followed by incubation for 2 mins, room temperature) and then neutralised using 5 ml SN3 buffer (gently inverted until blue

colour disappeared). The lysate was then clarified by centrifuging at 3000 x *g* for 2 minutes using the NucleoSpin® Plasmid Filter Column. DNA was then precipitated using SN4 buffer added to the flow through from the filter column (SN4 buffer used was half the volume of the flow through). The NucleoSnap® Plasmid Column was then attached to a vacuum manifold and the precipitated DNA added. -0.3 bar vacuum was applied until all solution had passed through the filter. The membrane was then washed using 2 ml SN5 buffer followed by 4 ml SN6 buffer (-0.3 bar vacuum applied). The mini spin column was then added to a collection tube and centrifuged for 1 min at 10000 x *g*. The spin column was then placed into a clean elution tube, here differing from the protocol for the final elution step through the use of 500 µl of sterile MilliQ water heated to 65°C for 1 minute followed by centrifugation for 1 min at 10000 x *g*.

2.6 General culture and transfections method for the HEK293S cell line

2.6.1 General media, reagents and equipment for cell culture

Complete DMEM or DMEM F12 was made by supplementing the media with 10% Heat Inactivated Foetal Bovine Serum, 2 mM L-Glutamine and 1% Penicillin/Streptomycin. Media was stored at 4 °C. All cell culture work was performed under Class 2 Microbiological Safety cabinets (Labgard Class II Biological Safety Cabinet). Cells were kept in incubators for growth at 37 °C, with 5% CO₂.

2.6.2 Thawing of HEK293S cell line from liquid nitrogen stocks

After removal from liquid nitrogen cell stocks were thawed immediately in a 37°C waterbath. Then under aseptic conditions in a Labgard Class II Biological Safety Cabinet, 9 ml of complete DMEM F12 was added slowly and dropwise. The cells were then centrifuged at 1000 rpm for 5 minutes before aspiration of the supernatant (avoiding the cell pellet). The cell pellet was then carefully resuspended in 10 ml of complete DMEM F12 and spread evenly onto a 10 cm cell culture plate. The cells were incubated at 37°C, 5% CO₂. Cells were monitored using (microscope) and fed with fresh media and passaged as required – typically every 3-4 days. 1% blasticidin was added the day after thawing for non-transfected cells. For HEK293S GnTI- TetR3 rhodopsin cell lines 250 µg/ml G418 was used and for HEK293S TetR9 rhodopsin cell lines 500 µg/ml was used.

2.6.3 Passaging of HEK293S cell line

Confluent cells were split under aseptic conditions in a Labgard Class II Biological Safety Cabinet. Cell monolayers on cell culture dishes were rinsed in 1x PBS before treating with 1 ml 1x trypsin. Cells were incubated for up to 2 minutes at 37 °C, 5% CO₂ to detach the cells. Trypsin was then neutralized by the addition of 9 ml of complete DMEM F12. Cells were split (usually at a ratio of 1:4) onto sterile cell culture dishes. For 10 cm dishes, the total volume was made up to 10 ml using complete DMEM F12. For 15 cm dishes the total volume was 25 ml and for 6 well plates the total volume per well was 2 ml.

In preparation for transfection, expansion was performed to give the required number of dishes/wells for the number of transfections to be performed. In these cases they would be split the day before transfection into complete DMEM and at a ratio to give the required confluence for transfection the following day.

2.6.4 Transfection of HEK293S cell line using the Calcium BES method

HEK293S cells were grown to a confluence of 40-50%. 22.5 µg of the mutant plasmid and 7.5 µg of pMT4 pBase were mixed and the solution made up to 450 µl in sterile MilliQ water. 50 µl of CaCl₂ followed by 500 µl of 2x BES was added slowly dropwise over 1 min under constant vortex mixing. The transfection cocktail was added carefully to the HEK293S cell monolayer. Dishes were then incubated for 16-24 hours at 37°C, 1% CO₂.

The following day cells were then rinsed in serum free DMEM before adding 10 ml of complete DMEM F12 followed by further incubation for 48 hours at 37°C, 5% CO₂.

At this stage the medium was removed and replaced with fresh medium containing Geneticin (250 $\mu\text{g}/\mu\text{l}$). Incubation was for a minimum of 10 days, replacing spent medium with fresh every 3-4 days, until 90-95% confluency was reached. Cells were then fed and passaged as required using complete DMEM F12 and geneticin (250 $\mu\text{g}/\mu\text{l}$). Freeze downs were made as described in **2.6.6**.

The cells were cultured in complete DMEM containing geneticin (250 $\mu\text{g}/\mu\text{l}$) for 24 hours before induction of gene expression (see 2.7).

2.6.5 Transfection of HEK293S cell line using the Turbofect method

In order to further reduce the time required to produce stable cell line pools the Turbofect method was utilised. It requires fewer cells initially and less DNA removing the need for medium-scale DNA preparation. It also utilised pB transposase.

Confluent non-transfected cells were split (**section 2.6.3**) and diluted at a 1:3 ratio of cells in DMEM in a sterile 50 ml tube. 2 ml of cell suspension was added into each well of 6 well cell culture dishes with the aim of having approximately 80% confluence the following day for transfection after overnight incubation in a 37 °C, 5% CO₂ incubator.

A transfection mastermix was prepared containing 200 μl unsupplemented DMEM and 0.5 μg pB transposase per transfection. The mastermix was then aliquoted into 200 μl portions and 2.5 μg of the required DNA (the pB007 NCO \pm mutants made by cloning and small scale expressed) was added. 6 μl Turbofect transfection reagent was then added before brief vortexing and then incubation at room temperature for 20 minutes.

The transfection mixture for the mutants and the WT rhodopsin were then added dropwise each to one well of cells (80% confluence) and mixed by gentle swirling. The transfected cells were then incubated at 37 °C, 5% CO₂ for 24 hours.

The following day transfected cells were washed in 2 ml of unsupplemented DMEM and then split using 200 μ l of trypsin using the same method as described in **section 2.6.3** onto two 10 cm cell culture dishes. 96 hours after transfection selection using 250 μ g/ml geneticin was started. Cells were then observed for selection effects, fed and split as necessary. Following the selection, the stably transfected cell line pools could then be made into freezedowns and stored in liquid nitrogen and split for induction and protein production experiments as required.

2.6.6 Making cell line stocks by freezedown

Cell line stocks were prepared from 10 cm cell culture dishes of 60-90% confluence (2-4 freezedowns, depending on confluence). Cells were washed, trypsinised and neutralised as in **2.6.3**. Following neutralisation the suspended cells were transferred into a 15 ml tube and centrifuged for 5 mins at 1000 rpm. The supernatant was then aspirated. Cells were then resuspended in freezing media (90% complete DMEM F12, 10% DMSO Hybri-Max, sterile filtered/cell culture grade), 1 ml per freezedown. 1 ml aliquots were then placed into cryovials before freezing at -70 °C and then transfer to liquid nitrogen.

2.7 Examination of WT rhodopsin and rhodopsin RP mutant expression levels

2.7.1 Variation of induction time and medium

Experiments were set up to examine expression levels of WT rhodopsin under different conditions.

Confluent cells on 10 cm tissue culture dishes were treated with either:

2 µg /ml tetracycline in complete DMEM.

5 mM sodium butyrate in complete DMEM.

2 µg /ml tetracycline and 5 mM sodium butyrate in complete DMEM.

complete DMEM alone.

The stable cell line for WT rhodopsin was induced (in triplicate) with each medium with dishes incubated in each induction medium for 24, 48 and 72 hours at 37°C 5% CO₂ before harvesting in 1x PBS (see **2.7.4**).

2.7.2 Expression of rhodopsin RP mutants by variation of induction medium

Confluent cells on 10 cm tissue culture dishes for each mutant stable cell line underwent gene expression induction as described in **2.7.1** under conditions i, iii and iv. They were incubated for 60-65 hours and harvested in 1x PBS (see **2.7.4**).

2.7.3 Comparison of expression of opsin and mutants at 33 °C or 37 °C

Confluent cells on 10 cm tissue culture dishes for the mutants P23A, G101V and G106W alongside a WT control underwent gene expression induction using 2 µg /ml tetracycline and 5 mM sodium butyrate in complete DMEM (condition iii in **2.7.1**). Cells were harvested as described in **2.7.4** after incubation at 33 °C or 37 °C for 12, 24, 36 or 48 hours.

2.7.4 Harvesting of induced cells

Cells were harvested using a 10 ml pipette to detach to cells in their induction media from the cell culture dish before centrifuging for 2 minutes at 2000 rpm. The spent induction medium was aspirated and the cells resuspended in 10 ml 1x PBS, before

repeating the centrifugation and aspiration of the supernatant. Cells were then resuspended in 500 μ l 1x PBS per 10 cm dish or 1000 μ l 1x PBS per 15 cm dish.

2.8 Analysis of rhodopsin expression levels by UV-vis absorbance spectroscopy

2.8.1 Formation of rhodopsin pigment by treatment of harvested cells with either 9-*cis*-retinal or 11-*cis*-retinal

5 μ M 9-*cis*-retinal or 11-*cis*-retinal was added to each cell suspension and mixed for 4-5 hours (11-*cis*-retinal) or overnight (9-*cis*-retinal) on a nutator at 4 °C. This, and all subsequent steps were carried out in the dark room under dim red light fitted with Kodak filters.

2.8.2 UV-vis Spectroscopy to determine amount of pigment formation

For solubilisation, retinal treated samples in 1x PBS were made to final concentrations of 1% DDM and 0.1 mM PMSF by addition to each cell suspension under dark conditions and mixed by nutation for 1 hour at 4 °C. The solubilised cell samples were then centrifuged using the Sovrall ® Discovery™ 90SE by Hitachi for 20 mins, 15000 rpm, 4 °C.

The Perkin Elmer Lambda 35 UV/vis spectrophotometer was used for generation of spectral data. A baseline was established using 1x PBS containing 1% DDM in sample and reference cuvettes. The supernatant of the solubilised cell samples was loaded into the sample cuvette and a spectrum was obtained between 650 to 250 nm. The sample was then photobleached for 60 seconds using the KL 1500 compact SCHOTT

light source fitted with a >495 nm long-pass filter and the spectra again obtained between 650-250 nm.

The dark and illuminated spectra for each sample could then be used to generate a difference spectrum. This was calculated by the dark spectrum values minus the corresponding illuminated spectrum values.

2.9 Expression of rhodopsin RP mutants and purification for use in their functional analysis

2.9.1 Cell culture and induction for expression rhodopsin RP mutants for functional analysis

Cells were grown, induced and harvested as described in **2.6/2.7** using 15 cm cell culture plates. Harvested cells were treated with 11-*cis*-retinal as described in **2.8.1**, differing only in mixing overnight (16 hours). 11-*cis*-retinal treatment and all subsequent steps were carried out in the dark room under dim red light.

2.9.2 Rho 1D4-sepharose bead preparation for use in purification of rhodopsin

Rho 1D4-sepharose beads were prepared using 5 mg of 1D4 antibody per 1 ml of sepharose slurry required. First, Cynagen Bromide (CnBr) sepharose was activated by washing with 1 mM HCl using a sintered glass filter and mixing with a glass rod. The volume of HCl required is 200 ml per 1 g of dry beads to be activated.

The activated beads were then added to a plastic bottle containing the 1D4 antibody and nutated at room temperature for 2 hours before overnight nutation at 4 °C. The bead/antibody mixture was divided into 50 ml tubes and centrifuged at 1000 x *g* for 2 minutes. The supernatant was removed and checked for remaining antibody. 1 M

ethanolamine (pH 8.0) was then added to the beads at an equivalent volume to the removed supernatant and incubated at room temperature for 2 to 3 hours. The beads were then washed using the sintered glass filter and using a glass rod for mixing alternating between the buffers i) 0.25 M NaHCO₃, 0.5M HCl (pH 8.3) and ii) 0.1 M NaOAc, 0.5 M NaCl (pH 4.0). 100 ml of buffer was used for each wash and the washes repeated 4 times for each buffer. The beads were then stored in a 50% mixture with 1x PBS with 0.1% NaN₃ at 4°C.

2.9.3 Rhodopsin and rhodopsin RP mutant purification

Details of buffers used for purification are described in Table 2.2 Biochemistry. Rhodopsin purification was performed using immunoaffinity chromatography utilising Rho-1D4 antibody Sepharose as previously described (Reeves *et al.*, 1999). The method for preparation of the 1D4-sepharose is described in **2.9.2**. 11-cis-retinal treated induced cell samples were solubilised (final concentrations of 1% DDM and 0.1 mM PMSF) by mixing for 1 hour at 4 °C. The samples were then centrifuged using the Sovrall ® Discovery™ 90SE by Hitachi for 30 mins, 10000 rpm, 4 °C. The overall pigment content of the sample was assessed using a 10% sample of the supernatant diluted in solubilisation buffer (1xPBS, 1% DDM and 0.1 mM PMSF) which was then analysed by UV-vis spectroscopy difference as described in **2.8.2**. This gave an estimated amount of rhodopsin (or mutant rhodopsin) in the total sample, to which the total yield following purification could be compared.

50% 1xPBS, Rho 1D4 Sepharose slurry (200 µl for 100 µg of rhodopsin yield expected, where the binding capacity of the beads was found to be approximately 0.5 mg/ml) was added to the remaining supernatant which was removed from the cell pellet without disruption. This was mixed end over end at 4°C for 3 hours. 2 ml purification

columns were prepared by filling with RO water and the addition of a frit which had been pre-soaked in RO water to prevent air bubbles. The frit was pushed to the base of the column, and the water flowed until it was approximately 1 mm above the frit.

The binding mix was then placed into the column, and the buffer was allowed to flow, collected as a flow through sample, the beads remained above the frit with the rhodopsin bound. The column was then washed with 20 ml high salt wash buffer followed by 10 ml low salt wash buffer (see Table 2.2, Biochemistry). A sample of the flow through and each wash buffer was saved. The column was then equilibrated with low salt elution buffer, which was flowed immediately, prior to the elution step.

The elution step consisted of 3 low salt elution's followed by 3 high salt elution's. 550 μ l low salt elution buffer was used for three consecutive elution's to obtain correctly folded protein followed by 550 μ l high salt elution (three times) to obtain incorrectly folded protein (Opefi *et al.*, 2013). Each time, the elution buffer was added carefully to the column to not disturb the beads, and then the column kept at room temperature in the dark before the elution buffer was flowed and collected in a microcentrifuge tube. The next aliquot of the elution buffer was added and the 1 hour incubation at room temperature followed by collection of the elution fraction was completed, and these steps repeated until all 6 elution fractions were complete (3 low salt, 3 high salt). Where necessary, the addition of any elution buffer step could be performed at 4°C, with the incubation time increased to overnight before elution. All eluates were stored at 4°C in the dark.

To assess the rhodopsin/ mutant yield in the eluates, the eluates were first centrifuged for 30 mins, 10,000 rpm at 4°C, using a dark secure rotor. The UV-vis dark spectrum was collected for each eluate using the same settings and protocol as described in

2.8.2, but no photobleaching step was performed and the spectrophotometer was baselined using low salt wash or high salt wash as relevant for the samples to be examined. Data was normalised at 650 nm for an absorbance of 0.

Samples were stored in the dark at 4 °C prior to use for function analysis either in Fisherbrand™ Black Microcentrifuge Tubes (1.5 ml) or in clear microcentrifuge tubes wrapped in 3 layers of aluminium foil to prevent exposure to light.

2.9.4 Stability of purified rhodopsin pigments

The stability of purified protein stored at 4°C was assessed by repeating the UV-vis dark spectrum for each, which was compared to the initial dark spectra readings for each pigment to ensure there was no loss of pigment during storage time prior to use for functional analysis.

2.9.5 Rhodopsin and opsin purification in LMNG

Protein was purified in LMNG following the same procedure as described for purification in DDM described in **2.9.3**, with the differing solubilisation, wash and elution buffers as described in Table 2.2 (Biochemistry). Further details of the use of this method are described in Chapter 5.

2.10 Spectral and functional analysis of rhodopsin RP mutants

2.10.1 Formation of rhodopsin pigment from purified opsins

A UV-vis spectrum was recorded for purified N2C/D282C opsin in DDM and WT opsin and RP mutants in LMNG. 5 μ M 11-*cis*-retinal was added and a spectrum from 250 to 650 nm (slit width = 2 nm, scan speed 480nm/min) was then recorded at 90 second intervals for a minimum of 30 minutes. The sample was kept at 20 °C throughout using a circulating waterbath connected to the cuvette holder.

2.10.2 Assessment of rhodopsin RP mutant stability at 55 °C

Purified rhodopsin in low salt elution buffer was kept at either 55 °C using a circulating waterbath connected to the cuvette holder for 2 minutes in a quartz cuvette. UV-vis spectra were obtained from 250-650 nm every 2 minutes over the course of 30 minutes, followed by every 20 minutes for up to 24 hours. Data was normalised at 650 nm. The thermal decay was assessed through recording the decrease absorbance at λ max and the increase of absorbance at 380 nm and curve fitting the resulting data.

2.10.3 Capture of the rhodopsin RP mutant-Schiff base in the dark state

A UV-vis dark spectrum was recorded for low salt wash buffer containing 20 μ g/ml of purified rhodopsin. 6 μ l 2 N H₂SO₄ was added to both the sample and the reference cuvette, and a UV-vis dark state spectrum was recorded after 2 minutes. Data was normalised at 650 nm.

2.10.4 Photobleaching of rhodopsin RP mutants

Low salt elution fractions with absorbance at λ max > 0.02 in low salt wash buffer were used. The UV-vis dark spectrum was then obtained as described in **2.10.3**. The

sample was then manually photobleached for 30 seconds using the KL 1500 compact SCHOTT light source equipped with a >495 nm long pass filter, following which a UV-vis spectrum was obtained (250 to 650 nm). The photobleaching and spectrum collecting process was then repeated a further 3 times (total photobleaching time 120 seconds).

After the fourth photobleach spectrum was collected, 3 μ l 2 N H₂SO₄ was added to both the sample and the reference cuvette, and a final spectrum was collected after 2 minutes (250 to 650 nm). Data was normalised at 650 nm = 0 absorbance.

2.10.5 Examination of the stability of the Meta II (active) state of rhodopsin RP mutants

Upon absorption of a photon, 11-*cis*-retinal isomerises and leads to conformational changes in the rhodopsin protein to form its active state known as Meta II (Meng and Bourne, 2001; Ferrari *et al.*, 2011). This leads to an increase in fluorescence caused by the retinal no longer quenching tryptophan fluorescence which is analogous to the decay of Meta II (Farrens and Khorana, 1995). Rhodopsin protein (or mutant rhodopsin) was diluted in Meta II buffer (details in Table 2.2 Biochemistry). The sample was then loaded into the Perkin Elmer Luminescence Spectrometer LS50B and kept at 20°C using a circulating waterbath connected to the cuvette holder (temperatures before and after were recorded using the Omega HH800A thermocouple). The spectrophotometer 'timedrive' function was used with the following parameters: excitation wavelength 280 nm (5 nm slit width) emission wavelength 330 nm (10 nm slit width), measurements taken at 30 second intervals (2 second measurement time) for a minimum of 2 hours. The lamp was set to off to avoid interference with the measurement. The measurement was begun and after 5 minutes the sample was

illuminated using the KL 1500 compact SCHOTT light source equipped with a >495 nm long pass filter for 30 seconds and the measurements continued for the remaining time. Data was normalised to start at an absorbance of 0 immediately after photobleaching. Meta II buffer was changed to contain 0.02% LMNG where the protein was purified in LMNG.

2.10.6 Purification of transducin from bovine retinas

Transducin was prepared from bovine retinas, using a modified version of the methods described previously (Opefi, 2011). Frozen bovine retinas stored at -70°C were thawed overnight on ice at 4°C before purification of transducin. Full details of the buffers used in this method can be found in section **2.1.2**, Table 2.3.

Retinas were divided into centrifuge tubes before thorough mixing with 30% sucrose buffer. Centrifugation was carried out at 6000 rpm for 6 minutes, 4°C, using the JA-25.50 rotor in the Beckman Coulter Avanti JXN-26 centrifuge. The supernatant kept on ice. The pellet was again thoroughly mixed with 30% sucrose buffer and centrifuged. The supernatant was then combined with that from the first centrifugation step and mixed at a 1:1 volume of supernatant to 70 mM potassium phosphate buffer.

The crude ROS (rod outer segments) were pelleted using the above centrifuge and rotor, this time at 20,000 rpm for 30 mins, 4°C and the supernatant removed carefully. The crude ROS pellets were then resuspended in 20 ml of 15% sucrose buffer followed by manual homogenisation using a pestle and homogeniser. The homogenised mixture was divided into 10 ml fractions in centrifugation tubes and underlayered using a needle with 10 ml 0.64 M sucrose buffer. These were then centrifuged again as per the previous step and the supernatant discarded.

The crude ROS were then resuspended to a total volume of 7 ml per tube to be used in the next step (e.g. 21 ml total volume for 3 tubes to use in the next step) in 0.64 M sucrose buffer and manually homogenised. Beckman-Coulter Ultraclear centrifuge tubes were prepared with 9 ml 0.78 M sucrose buffer, underlaid with 9 ml 1.0 M sucrose buffer and that underlaid with 9 ml 1.2 M sucrose buffer. The crude ROS in 0.64 M sucrose buffer was then overlaid carefully at the top of the tube. The tubes were carefully loaded into the JS 24.38 swing bucket rotor and centrifuged using the Beckman Coulter Avanti JXN-30 centrifuge at 103, 860 x g for 60 minutes at 4°C with no deceleration (for this centrifuge, it was set to '11' 'coast' setting for deceleration).

Following centrifugation ROS membranes should have separated and gathered at the 0.78 M/ 1.0 M sucrose buffer interface. The interface was collected by piercing the side of the tube using a needle attached to a syringe to collect the ROS membranes. The ROS membranes were then mixed to a total of 50 ml in 70 mM potassium phosphate buffer and kept on ice at 4°C overnight.

The ROS membranes were split into Beckman Coulter centrifuge tubes (approximately 25 ml per tube) and centrifuged using the Beckman Coulter Avanti JXN-30 centrifuge using the JA.30.50 fixed angle rotor at 100, 000 x g for 30 minutes at 4°C. The supernatant was discarded, and the pellet resuspended in 30 ml 1x hypotonic buffer followed by manual homogenisation and passing through a needle. The centrifugation and pellet washing steps were repeated a further 2 times.

The supernatant was discarded, and the pellet resuspended in 30 ml GTP buffer followed by manual homogenisation and passing through a needle. The pellet resuspended in buffer was centrifuged using the Beckman Coulter Avanti JXN-30 centrifuge using the JA.30.50 fixed angle rotor at 100, 000 x g for 30 minutes at 4°C,

resulting in the extraction of the G protein transducin. The supernatant was kept on ice whilst the extraction step was repeated a further two times.

The supernatants from the extraction step were combined and ran through a column (following its equilibration with 15 ml hypotonic buffer) overnight at 4°C, with a flow rate of approximately 0.5 ml/min.

The next day, a white band was visible in the column which is the bound transducin. Any remaining buffer was flowed, following which 1 ml of wash buffer was added and the flow through collected. This was repeated so a total of 10 ml of wash buffer had been passed through the column and collected separately. 1 ml of elution buffer was then added and the flow through collected, again repeated to a total of 10 ml and collected separately. The elution fractions containing transducin as determined by their protein concentration were combined and dialysed overnight using 8000 MWCO BioDesign Dialysis tubing in 1 L of dialysis buffer with stirring at 4°C. The purified G protein was then stored at -20°C for use in the transducin activation assay.

2.10.7 Transducin activation assay

Transducin was purified from bovine retina outer segments as described in **2.10.6** for use in the transducin activation assay. Purified transducin (100 nM) was added to the transducin assay buffer (see Table 2.2 Biochemistry) in a cuvette containing a stirrer, on ice. Under dark conditions by red lights, 5 nM rhodopsin (or mutant rhodopsin) was added, and the sample inverted 5 times before being photobleached for 30 seconds using the KL 1500 compact SCHOTT light source equipped with a >495 nm long pass filter. The sample was then loaded into the Shimadzu fluorometer with electronic stirring and circulating waterbath set to 20 °C. A timecourse started, set to take readings every 2 seconds for 2000 seconds, with wavelength set to 295 nm, emission wavelength to

340 nm. After approximately 500 seconds, 5 μ M GTP γ S was added and the timecourse continued to take readings for approximately another 1500 seconds, measuring the relative fluorescence increase caused by intrinsic fluorescence when GDP is exchanged for GTP (Phillips and Cerione, 1988).

Transducin assay buffer was changed to contain 0.02% LMNG instead of DDM where the protein was purified in LMNG, all other buffer components remained the same and the assay was performed in the same manner.

2.10.12 SDS PAGE

A running gel was prepared (see Table 2.2) and left to polymerise for 30 minutes and then stacking gel was added and left to polymerise for 15 minutes. Alternatively, using the pre-cast gels GenScript SurePAGE™ Bis-Tris, 10x8 10% 15 well gels, were run using 1 sachet of GenScript Tris-MOPS-SDS Running Buffer Powder prepared in 1L RO water (as instructed by the packaging) for 1x MOPS tank buffer. Rhodopsin samples were prepared in 4x SDS PAGE loading buffer. The gel was loaded into the tank along with SDS PAGE tank buffer or MOPS tank buffer as appropriate, following which the samples were loaded and then run at 80 V for 10 mins and the 200 V for 60 – 90 mins.

2.10.12 Coomassie blue staining

The gel was added to a container holding Coomassie stain, for 1 hour at room temperature with rocking. The gel was then rinsed with and stored overnight in RO water before photographic imaging on a light box after 16 hours.

2.10.12 Western blot

Details for the buffers used for Western blot can be found in Table 2.2. Equipment for transfer was equilibrated in chilled transfer buffer. The gel and nitrocellulose membrane were then loaded into the transfer cassette. The cassette was prepared with sponges on each side, 2 layers of blotting paper, a nitrocellulose membrane, and the gel. The tank was then filled with transfer buffer and electrophoresis was run at 100 V for 60 mins. The nitrocellulose membrane was removed from the cassette and placed in a container for blocking with 50 ml blocking buffer at 4°C overnight.

The nitrocellulose membrane was washed 3 times in 1x PBS and then incubated for 5 hours at room temperature in 1D4-primary antibody buffer. 50 ml Western blot wash buffer was added for 5 mins with gentle rocking, 5 times. The nitrocellulose membrane was incubated in 10 ml ECL buffer, 1 min room temperature. For all steps, details of the buffers used can be found in Table 2.2. After incubation in ECL buffer the membrane was wrapped in cling film and loaded into the imager. Fusion software was used for imaging, using the chemiluminescence protocol on auto. Manual marker exposure was then carried out, with 1 second exposure time. The images were then merged in the Fusion software using the processing tab.

2.11 Computational methods

2.11.1 PyMOL

PyMOL version 0.99 was used to generate all PyMOL images, and the mutagenesis wizard was used to introduce the studied mutations into the rhodopsin structure (PDB 1U19).

2.11.2 SigmaPlot

Curve fitting and statistics were performed using SigmaPlot as appropriate for the data collected, the type of curve fitted or statistical test performed is stated where this has been used.

3. Development of an inducible piggyBac expression system for rhodopsin and mutant production

3.1 Introduction

3.1.1 Inducible stable cell lines

Expression of rhodopsin and other GPCR's for biophysical structure and function experiments demands many milligrams of protein (Reeves et al., 2002a). Previously it was shown that through exploiting a synthetic bovine opsin gene, stable mammalian cell lines could be produced expressing opsin at a minimum of 2 mg/L (Reeves *et al.*, 1996). This approach has been used extensively for preparation of samples for magic angle spinning (MAS) NMR investigations (Eilers *et al.*, 1999; Klein-Seetharaman *et al.*, 1999).

Toxicity of the certain expressed proteins required the development of an inducible system for rhodopsin expression, with the opsin gene being under control of a CMV promoter containing TetO sequences (Reeves et al., 2002a). This system allowed for further improvements in the expression levels of WT rhodopsin (up to 10 mg/L) by the addition of tetracycline and sodium butyrate to the growth media of high cell density cultures (Reeves et al., 2002a).

A further issue when obtaining rhodopsin for studies such as crystallisation, is the heterogeneity of the complex glycans (Reeves et al., 2002b). To overcome this, a HEK293S cell line deficient for N-acetylglucosaminyltransferase (GNTI) activity was developed, this restriction on the formation of N-glycan led to homogeneous expression of the N-glycan Man₅GlcAc₂ (Reeves et al., 2002b).

When studying a wide variety of rhodopsin mutants, there is a need to produce large amounts of each sample; however, the process of developing inducible, stable cell lines for this purpose is time consuming and laborious. Here, the aim was to produce inducible, stable cell lines, without the usual requirement to isolate individual colonies expressing the retinitis pigmentosa (RP) mutants of interest.

3.1.2 PiggyBac transposon vector

The use of the 'piggyBac' transposon vector for the expression of rhodopsin in HEK293S GNTI⁻ cell lines was investigated in an attempt to reduce the time taken to produce inducible, stable cell lines expressing high levels of rhodopsin.

The piggyBac transposon vector is thought to target integration sites in the host chromosomal DNA that favour high level expression (Yusa, 2015). Also, the design of a transposon containing the use of 'insulators' to shield the transgene were found to be effective (Sarkar *et al.*, 2006). Furthermore, the transposon is capable of multiple insertions and of multiple distinct transgenes thus effectively increasing the copy number of the transgene (Kahlig *et al.*, 2010). Copy number of the transgene can vary significantly, ranging from several to several hundred (Adelman *et al.*, 2004).

3.1.4 Aims

Here, the aim was to make a piggyBac transposon vectors containing *RHO* or *RHO* RP mutants for construction of stable cell lines for inducible expression of opsin at high levels.

3.2 Methods - Construction of mutant rhodopsin in the plasmid

pB007NCO

3.2.1 Construction of mutant rhodopsin in the plasmid pB007NCO by Quikchange mutagenesis

QuikChange reactions were utilised to incorporate the rhodopsin RP mutants into a plasmid where a site-directed mutagenesis primer is used to cause DNA mutations in a gene to incorporate a mutant codon for a specific amino acid. The DNA template was diluted to a concentration of 20 ng/ μ l. The primers were diluted in MilliQ H₂O to a concentration of 75 ng/ μ l, and frozen at -20°C post dilution. Forward and reverse primers for the E122G, R252P and S298D bovine rhodopsin mutations were used as appropriate (see Appendix 1).

The reaction was set up in PCR tubes as follows. 3 μ l 10X PFU Turbo buffer (Agilent), 6% DMSO, 0.2 mM dNTP mix, 0.66 ng/ μ l pB007NCO-rho, 1.25 units of PFU Turbo Hot-Start DNA polymerase, and 2.5 ng/ μ l of both forward and reverse mutagenic primers made up to a total volume of 30 μ l. Then using the Applied Biosystems 2720 Thermal Cycler the mutagenesis was performed with the conditions set as described in Table 3.1.

Table 3.1 PCR conditions for Quikchange mutagenesis of pB007NCO-rho

Step	Temperature	Time (minutes)	Cycles
1 Initial denaturation	95 °C	2:00	1
2 Denaturation	95 °C	0:50	Steps 2-4 were repeated to have each cycled 15 times in total.
3 Anneal	55 °C	1:00	
4 Extension	68 °C	13:00	
5 Hold	12 °C	∞	1

This method was also employed for the production of the K311E rhodopsin mutant, which didn't work. The method worked for the mutants E122G, R252P and S298D, however its unreliability meant that a cloning method was used going forward to produce further rhodopsin mutants.

25 µl of the mutagenesis product plus 1 µl of DpnI was mixed and incubated for 2 hours at 37°C. 5 µl of each mutagenesis product, or 5µl DpnI digested product was added to the following: 5 µl of gel red dye, 1 µl of 6X loading dye and 9 µl of 1X loading buffer. These were run on an agarose gel as according to **Section 2.2.2**.

3.2.2 Construction of mutant rhodopsin in the plasmid pB007NCO by molecular cloning

As an alternative to Quikchange mutagenesis which was not found to be a reliable method for construction of rhodopsin mutants, a molecular cloning method was used. Throughout the following process *E. coli* was used for small scale expression of the plasmids at each stage. Quikchange mutagenesis was first performed on pMT4-rho to incorporate mutations as required (G101V, V104F, G106W and K311E). Each of the mutant sequences were then cut from the plasmid backbone by *KpnI/NotI* digestion and a methylene blue agarose gel (see Chapter 2) was used to separate the fragments. The fragment containing the rhodopsin/mutant rhodopsin gene was excised from the gel and the DNA purified (see Chapter 2). The purified fragments were then ligated into pACMV TetO which had also been digested with *KpnI/NotI* to form pACMV TetO-rhodopsin(mutant). Following expression in *E. coli* PCR using NEOCMV primers (sequence shown in Appendix 2) were used for PCR of the WT rhodopsin pACMV TetO plasmid as well as for each mutant. The PCR fragment

contains the rhodopsin gene under the control of the CMV[TetO] promoter and followed by the neomycin resistance gene which is under the weak control of the H₂L^d promoter (Reeves et al., 2002a). The PCR fragment was then digested using the *NheI* restriction enzyme and again using a methylene blue agarose gel separated from the waste fragments before excision and purification from the gel. The plasmid pB007 was also digested with *NheI*, and the fragments separated on and purified from a methylene blue agarose gel. In this case the backbone fragment of pB007 was excised and purified. The digested PCR fragment was ligated into the pB007 backbone. The pB007-**Neo**CMV[TetO]**Opsin** (NCO) (\pm mutants) was then expressed on a small scale by *E. coli* and then expressed on a medium scale for those used in the Calcium/BES transfection method (see Chapter 2). Figure 3.1 shows the steps of the cloning protocol.

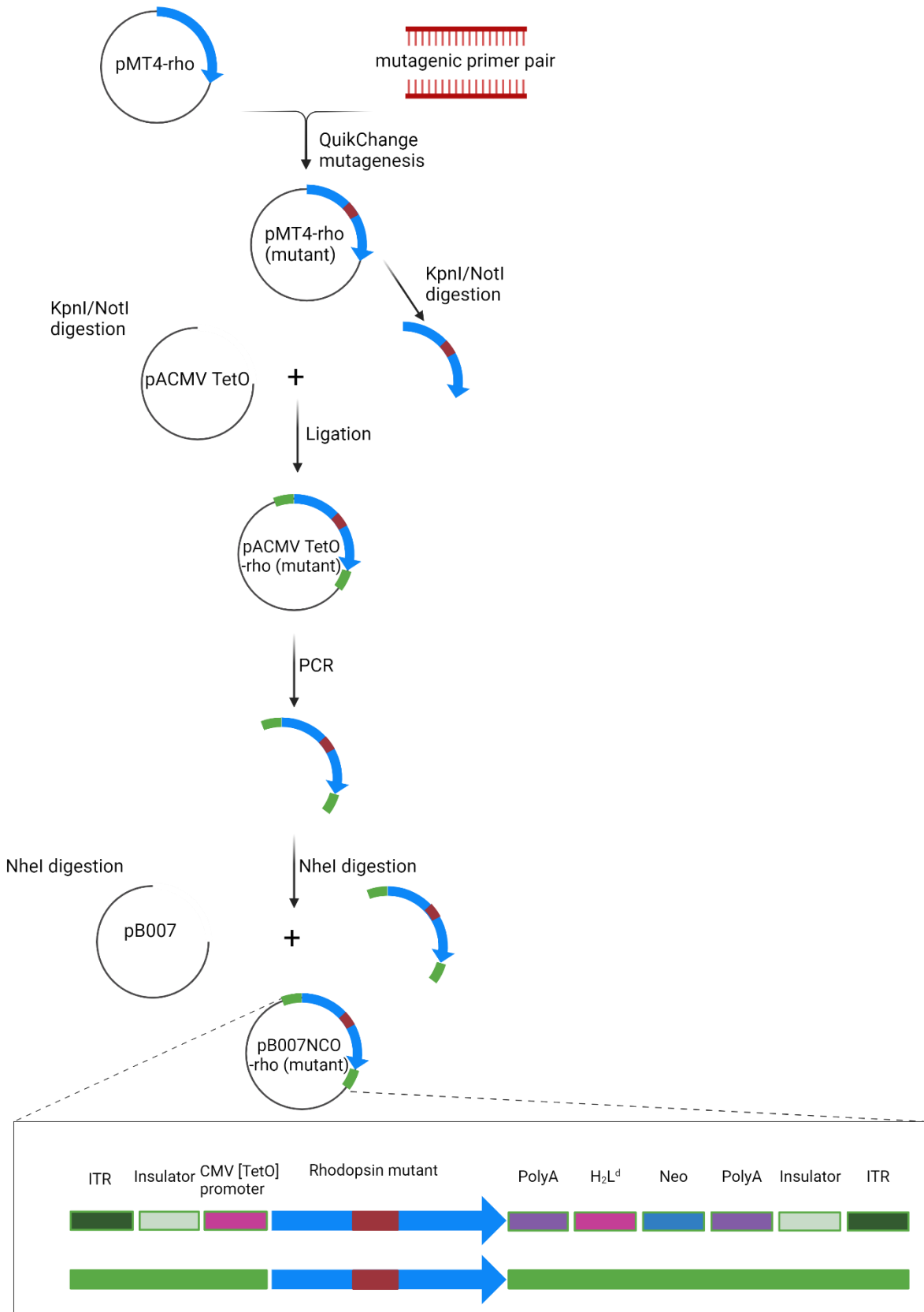


Figure 3.1 Cloning scheme for the production of rhodopsin mutant genes in the pB007 plasmid. A mutagenic primer pair are used to perform QuikChange mutagenesis on the pMT4-rho plasmid. The mutant pMT4-rho plasmid was then digested with *KpnI* and *NotI*, and the pACMV-TetO-rho plasmid was also digested with these restriction enzymes. These were then ligated to form pACMV-TetO-rho (mutants). PCR was then performed with the NeoCMV primers, following which a *NheI* restriction enzyme digestion was performed on the PCR fragment and the pB007NCO plasmid. Ligation of the fragment and plasmid formed the pB007-NCO-rho (mutant). The piggyBac transposon cargo will insert into the genome of the cells into which it is transfected. At each end of the piggyBac transposon cargo are inverted terminal repeat sections (ITR), insulator sequences. The rhodopsin mutant is under control of the CMV [TetO] promoter and followed by a polyA tail, and also contains the neomycin resistance gene which is under the control of the H₂L^d promoter and followed by a polyA tail. Created with BioRender.com

3.2.2 Transfection to produce stable cell lines and induction of rhodopsin expression

Materials and methods for the culture, transfection and induction of the stable cell lines is described in Chapter 2.6-2.7. For the E122G, R252P and S298D the Quikchange/calcium/BES-pBase method was used for transfection (**Chapter 2.6.4**). For all other mutants the cloning/ turbofect method was used (**Chapter 2.6.5**).

3.2.3 Determination of WT rhodopsin expression levels by UV-vis absorbance spectroscopy

Method of UV-vis spectroscopy for determination of rhodopsin expression is described in Chapter 2.8. Expression levels experiments for the rhodopsin mutants can be found in Chapter 4 (EL1 mutants) and Chapter 5 (E122G, R252P, S298D and K311E).

3.3 Results

3.3.1 Construction of mutant rhodopsin – pB007NCO

The RP mutants E122G, R252P and S298D seen in rhodopsin were constructed due to their unknown phenotype which did not appear to be obvious misfolding. Construction of the E122G, R252P and S298D rhodopsin mutants was achieved through Quikchange mutagenesis of the pB007 NCO plasmid. Following mutagenesis and DpnI digestion, an agarose gel was run (Figure 3.2A) which determined that in the case of E122G, R252P and S298D that mutagenic product had been formed. These were used for the transformation of *E. coli*, and a small-scale production was used to produce the plasmids for purification. Following *NheI* digestion and agarose gel electrophoresis (Figure 3.2B) the E122G, R252P and S298D mutant plasmids were found to be of the correct overall size. Sequencing of the rhodopsin gene within the plasmid showed the presence of the required mutations.

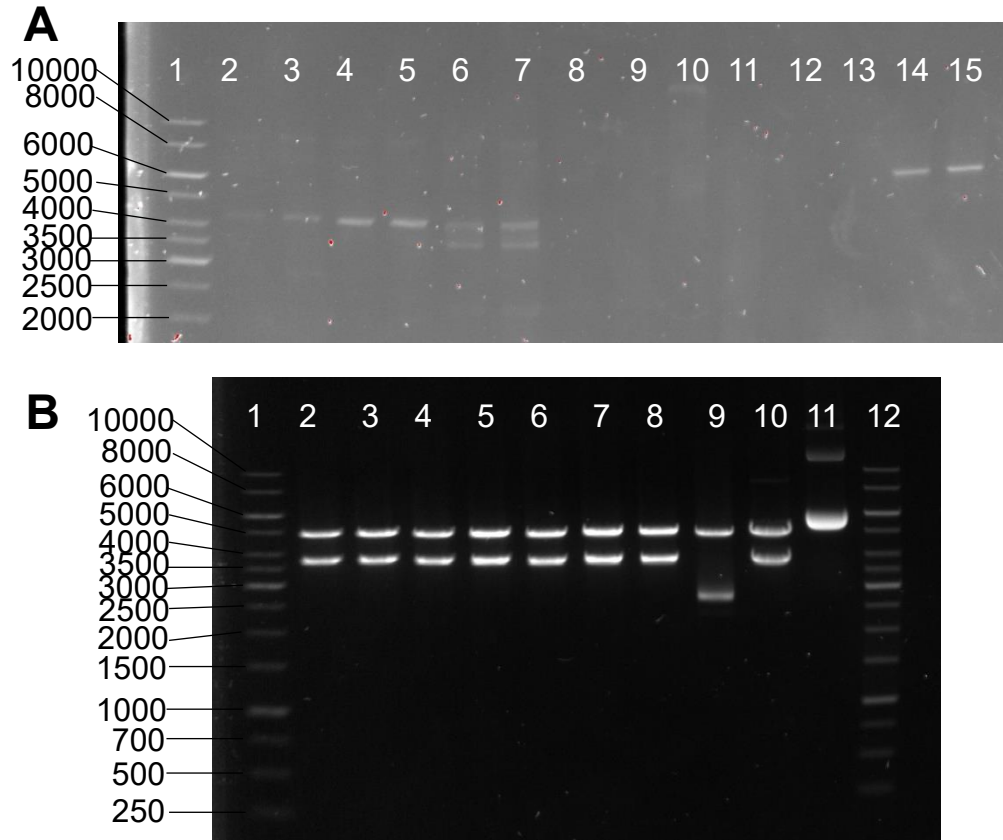


Figure 3.2 Agarose gel electrophoresis of A) mutagenesis products and B) Mini-prep products. A) Mutagenesis products, pre and post DpnI digestion. Lane 1 Thermoscientific GeneRuler 1kb DNA ladder. 2/3 E122G, 4/5 R252P, 6/7 S298D, 8/9 K311E, 10/11 no primer, 12/13 no polymerase, 14/15 pMT4 control. B) Mini-prep products after *NheI* digestion. Lane 1 and 12 Thermoscientific GeneRuler 1kb DNA ladder. 2-4 E122G, 5-6 R252P, 7-8 S298D, 9 K311E, 10 WT, 11, undigested WT.

3.3.2 Construction of rhodopsin RP mutants using molecular cloning method

For the production of K311E, and N2C D282C WT rhodopsin/mutant genes, a molecular cloning method was employed (Figure 3.3). The mutations were produced by quikchange mutagenesis of the pMT4-rho or pMT4-rho(N2C/D282C) plasmids as appropriate and replicated in/mini-prepped from *E. coli*. Digestion of the plasmids using *KpnI* and *NotI* allowed for cloning into the pACMV TetO background, which again was replicated in and mini-prepped from *E. coli*. PCR of the pACMV TetO Opsin (mutants) produced a section containing the transposon cargo. Finally digestion using *NheI* removed the transposon cargo which could then be cloned into pB007NCO. Sequencing was used to confirm the presence of the correct mutations throughout and results of this can be found in Appendix 3.

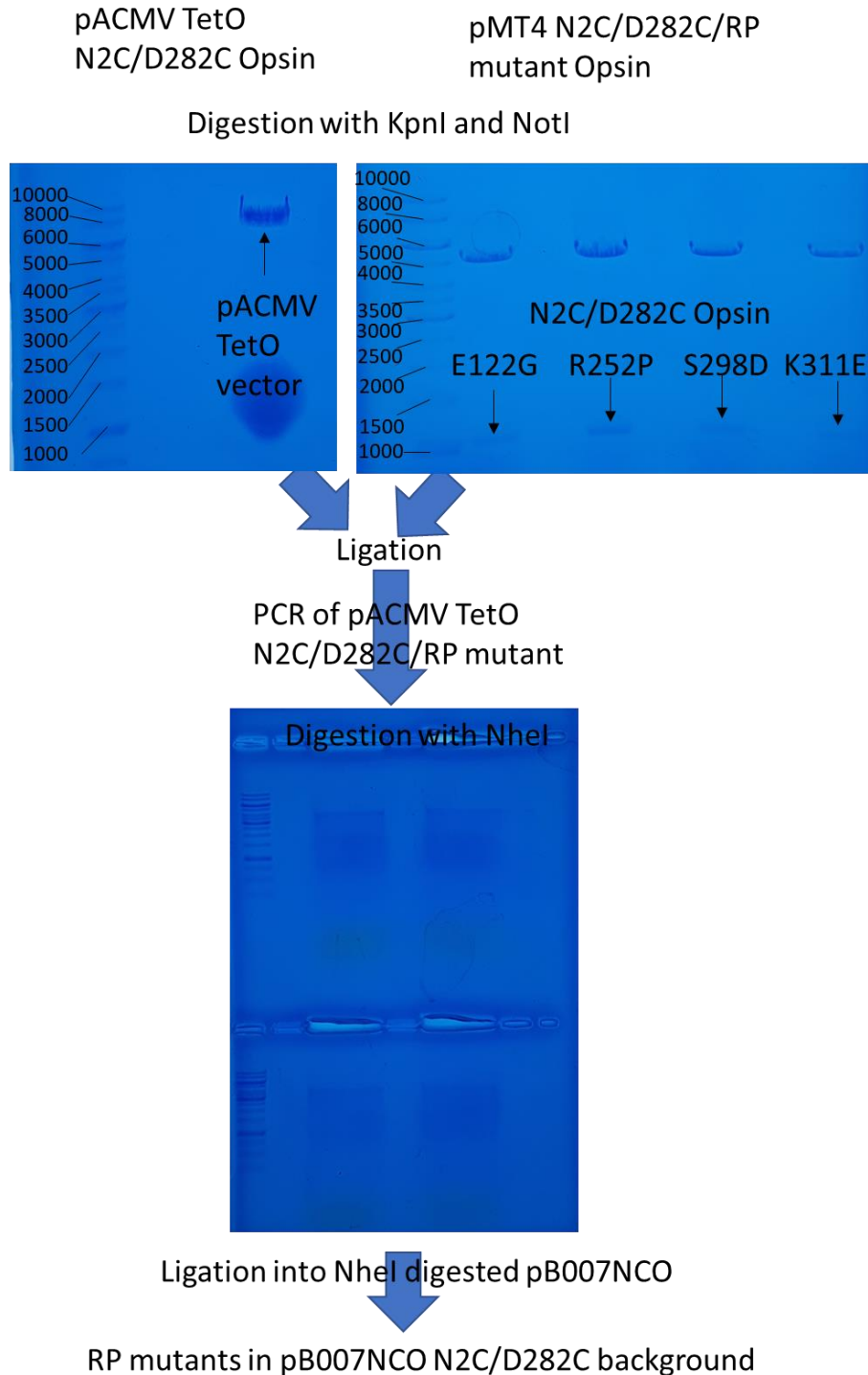


Figure 3.3 Cloning steps for the construction of the rhodopsin RP mutants. Methylene blue stained agarose gels for the construction of pB007 NCO. pACMV TetO Opsin and pMT4 RP mutant opsin (both N2/D282C) were digested with *KpnI* and *NotI*. The pACMV TetO vector fragment and RP mutant rhodopsin fragments were purified from the gel and ligated. Then PCR of the transposon element was performed. *NheI*

digestion of this and ligation of the approximately 4000 bp fragment into the pB007 vector produced the RP mutants in the N2C/D282C background in the piggyBac vector.

3.3.2 Medium scale production of pB007NCO plasmids containing rhodopsin mutants

Confirmed mutants made through both mutagenesis and cloning methods were used for medium scale plasmid DNA production. After medium scale plasmid production was complete, confirmation of the transposon inserts presence, rhodopsin genes presence and relevant mutation presence was achieved using *NheI* digests, *KpnI/NotI* digests and sequencing respectively (Figure 3.4). By using *NheI* to digest the midi-prep products, the presence of the transposon insert in each mutant (bands at approximately 4000 bp) was shown. The bands at approximately 5000 bp is the rest of the pB007 NCO vector and bands at approximately 9000 bp are linearised vector. Digestion with *KpnI* and *NotI* showed a band at approximately 1000 bp for all mutants (rhodopsin gene), with variation in the vector size bands.

Sequencing of the midi-prep products showed the presence of the relevant mutations in the pB007 NCO background (Figure 3.5). The opsin gene with each of the RP mutants both with and without the N2C and D282C mutations was seen. These were then used for the transfection of the HEK293S Ric15 TetR9 GnTI⁻ rhodopsin cell line.

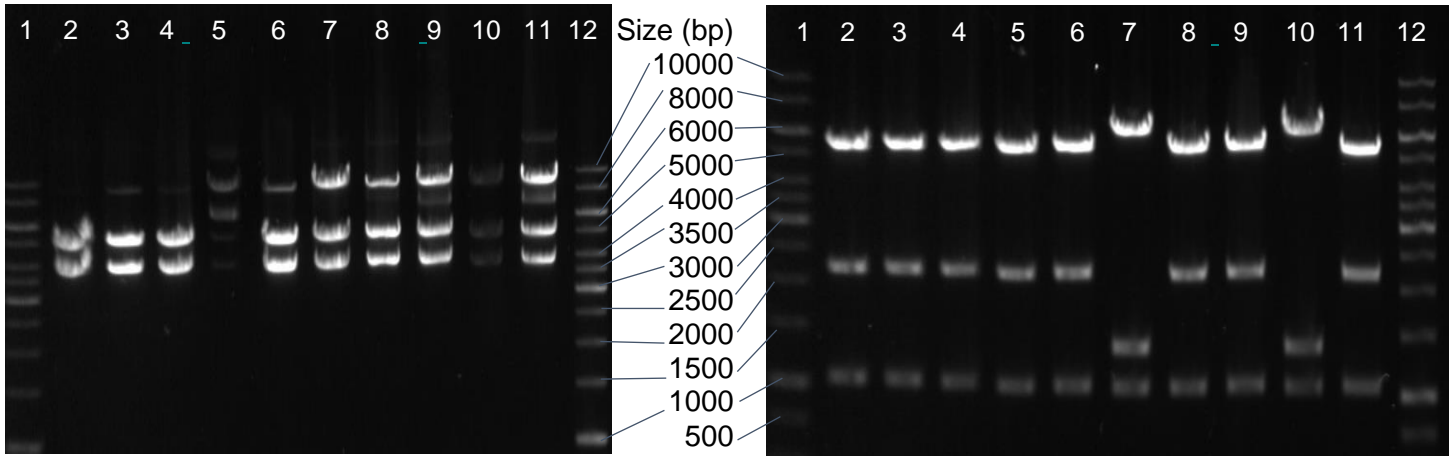


Figure 3.4 Construction of mutant rhodopsin genes in pB007NCO. KpnI/NotI (A) and NheI digestion (B) of the midi prep plasmids. Midi-prep restriction enzyme digests and sequencing. A shows a digest with NheI and B shows a digest using KpnI and NotI. In both A and B, lanes 1 and 12 shows the ThermoScientific GeneRuler. A and B lane 2 and C show E122. Lane 3 and G show E122G stabilised. Lane 4 and D show R252P. Lane 5 and H show R252P stabilised. Lane 6 and E show S298D. Lane 7 and I show S298D stabilised. Lane 8 and F show K311E. Lane 9 and J show K311E stabilised. WT and WT stabilised are shown in lanes 10 and 11 respectively.

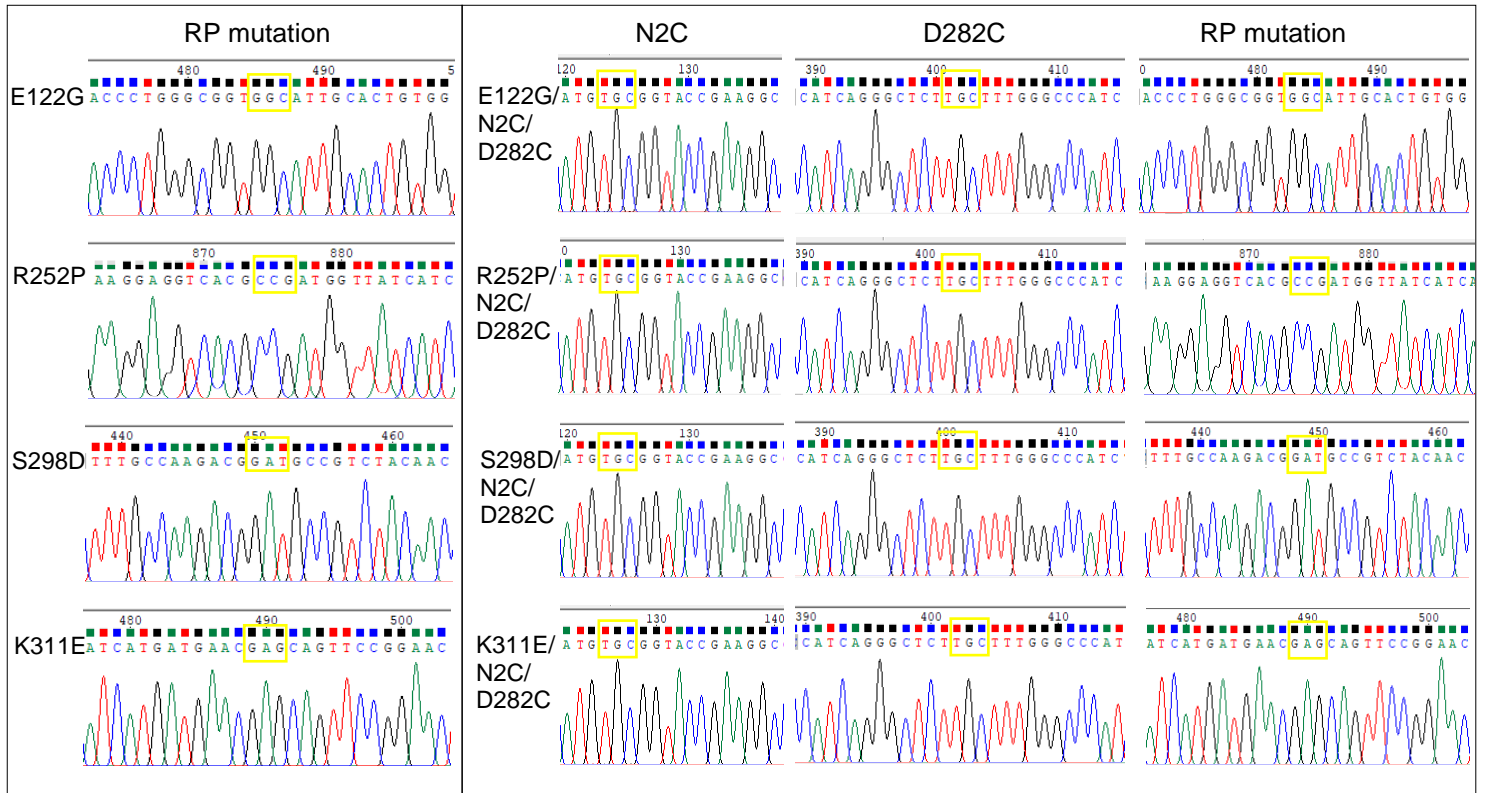


Figure 3.5 Sequence mutation confirmation. Sequencing shows the presence of the mutations for each of the retinitis pigmentosa (RP) mutants and the N2C D282C mutations where relevant. Yellow boxes highlight the mutated codon. The WT codons at each position are: aac (N2), gac (D282), gaa (E122), cgt (R252), tct (S298) and aag (K311).

3.3.3 Expression of WT rhodopsin

The HEK2923S RTG pB Opsin WT cell line was grown on 10 cm cell culture dishes in DMEM/F12 supplemented with 10% FBS, 2 mM L-Glutamine and 1% PenStrep. Cells were passaged by trypsinisation to expand to the necessary number of 10 cm cell culture dishes. The cells were grown to confluence ($1e^7$ cells), fed with DMEM (supplemented as above) and then the following day were induced with tetracycline (2 $\mu\text{g}/\text{ml}$), sodium butyrate (5 mM) or both in DMEM (supplemented as above) and harvested in 1x PBS after 24, 48 and 72 hours. Following 5 hours treatment with 11-*cis*-retinal, UV-vis spectroscopy in dark and photobleached states was performed and Beer-Lambert Law used to calculate the yield of rhodopsin pigment based upon the absorbance difference (Figure 3.6). Non-induced cells and cells induced with sodium butyrate alone produced very small amounts of rhodopsin pigment at all time points. When induced with tetracycline alone, after 24 hours an average of 8.3 μg of rhodopsin pigment was produced. This increased to 21.9 μg and 23.1 μg after 48 and 72 hours respectively. The greatest mass of rhodopsin pigment produced at each time point, was in the cells induced with both tetracycline and sodium butyrate. 70.3 μg , 76.9 μg and 80.4 μg were produced at 24, 48 and 72 hours respectively.

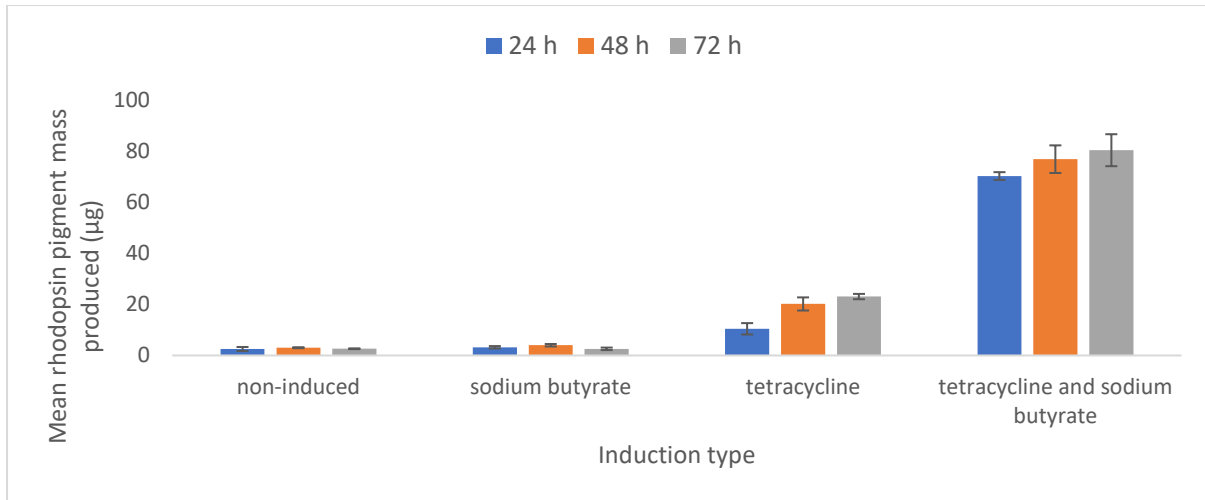


Figure 3.6 Induction condition variations for the expression of the opsin gene in stable cell lines. Cells were grown on 10 cm cell culture dishes to confluence before induction in DMEM with either 2 µg/ml tetracycline, 5 mM sodium butyrate or both. The average mass of rhodopsin produced by triplicate cell culture dishes following treatment with 11-cis-retinal as determined by UV-vis spectroscopy was calculated. Error bars show one standard deviation between the three replicates.

3.3.4 Cell line stability

The stability of the cell line HEK293S Ric15 TetR9 GnTI⁻ rhodopsin was determined through continuous culture, with inductions taking place on every second passage of the cells. The cells (mixed pools following transfection) were either kept in complete DMEM media containing the selection antibiotic G418 at 250 µg/ml or complete DMEM with no selection antibiotic.

In Figure 3.7, the yield of rhodopsin pigment over the course of 16 passages (2 per week for 8 weeks) is shown. For the cells in the selection antibiotic, the yield of pigment remained fairly stable throughout the passages, with an average yield across all weeks of 57.7 µg. The cells kept in culture without the selection antibiotic showed higher yields in the first two passages however this then dropped down to similar levels to that of the cell line with selection, giving an overall average yield of 63.1 µg.

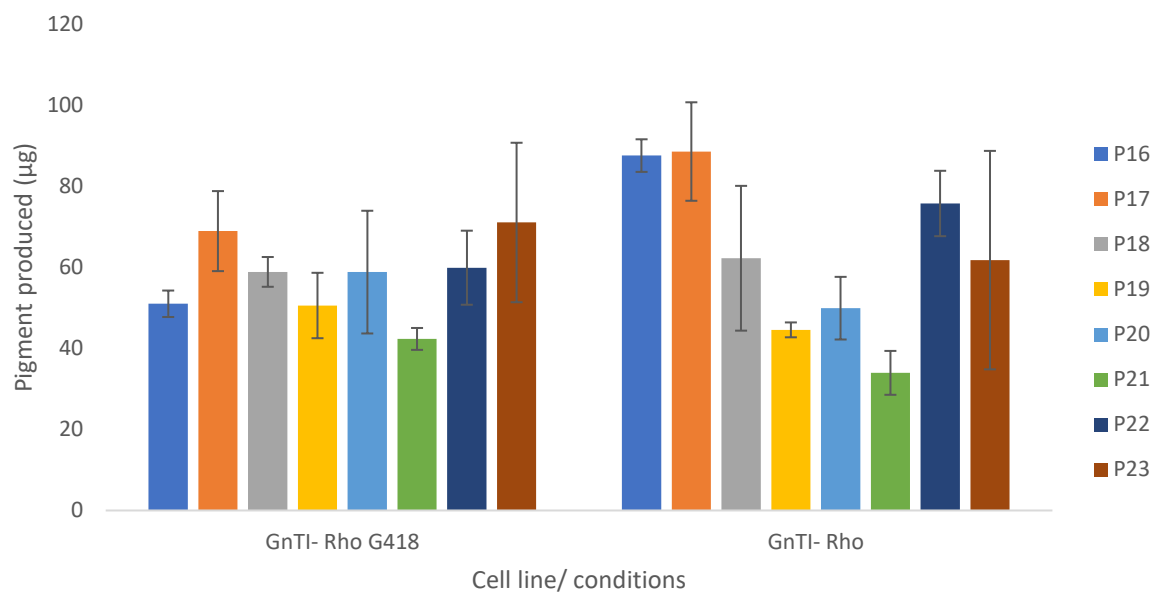


Figure 3.7 Yield of rhodopsin pigment obtained across 16 passages (twice weekly for 4 weeks). HEK293S Ric15 TetR9 GnTI⁻ rhodopsin cells were kept in continuous culture over the course of 4 weeks, with twice weekly passaging. The cells were either kept in complete DMEM media or complete DMEM with the selection antibiotic G418 at 250 µg/ml whilst in growth and expansion stages each week. The cells were split onto 3x 10 cm cell culture dishes for induction of protein production every passage, with a further 10 cm dish kept for growth and the next expansion. For induction, the media was replaced to complete DMEM with 2 µg/ml tetracycline and 5 mM sodium butyrate for 65 hours. Harvested cell suspensions were treated with 9-cis-retinal overnight, the rhodopsin solubilised and then UV-vis difference spectra between 250 and 650 nm (pre and post photobleaching) were obtained. The difference in absorbance at 500 nm was then used to determine the yield through Beer-Lambert law assuming ϵ 42700 M⁻¹ cm⁻¹ and molecular weight of 43200 Da. Average yields across the passages are shown with error bars representing the standard deviation. The average yield across all dishes throughout all 4 weeks was 57.7 µg and 63.1 µg for the selected and unselected cells respectively.

3.3.5 Expression of WT rhodopsin, RP mutants and stabilised rhodopsin/ RP mutants

After production of inducible, stable cell lines for WT opsin, the opsin RP mutants, stabilised WT opsin and stabilised opsin RP mutants induction of 10 cm confluent dishes was performed to assess expression levels. These plates were induced using sodium butyrate and tetracycline, or tetracycline, in complete DMEM. Non-induced samples were produced from cells grown in complete DMEM only, alongside GnTI⁻ cells isolated from a single colony stable cell line expressing WT rhodopsin through pACMV TetO WT Opsin.

After treatment of the harvested cells with 11-*cis*-retinal for 5 hours, the cells were solubilised as before and UV-vis absorbance spectra were obtained for each. The peak difference between dark and photobleached spectra was used in Beer-Lambert Law to calculate the amount of rhodopsin pigment produced (Figure 3.7).

In all cases, induction with tetracycline and sodium butyrate expressed the highest yields in comparison to their tetracycline and non-induced counterparts. Tetracycline induced cells expressed a moderate amount in comparison to the tetracycline and sodium butyrate induced counterparts. Little to no expression was yielded by non-induced samples. The level of expression varied greatly between mutants, with V104F and K311E expressing at WT like levels. G101V and G106W expressed at very low levels or had no detectable pigment. All other mutants expressed at levels between approximately 12.5% and 60% of WT rhodopsin.

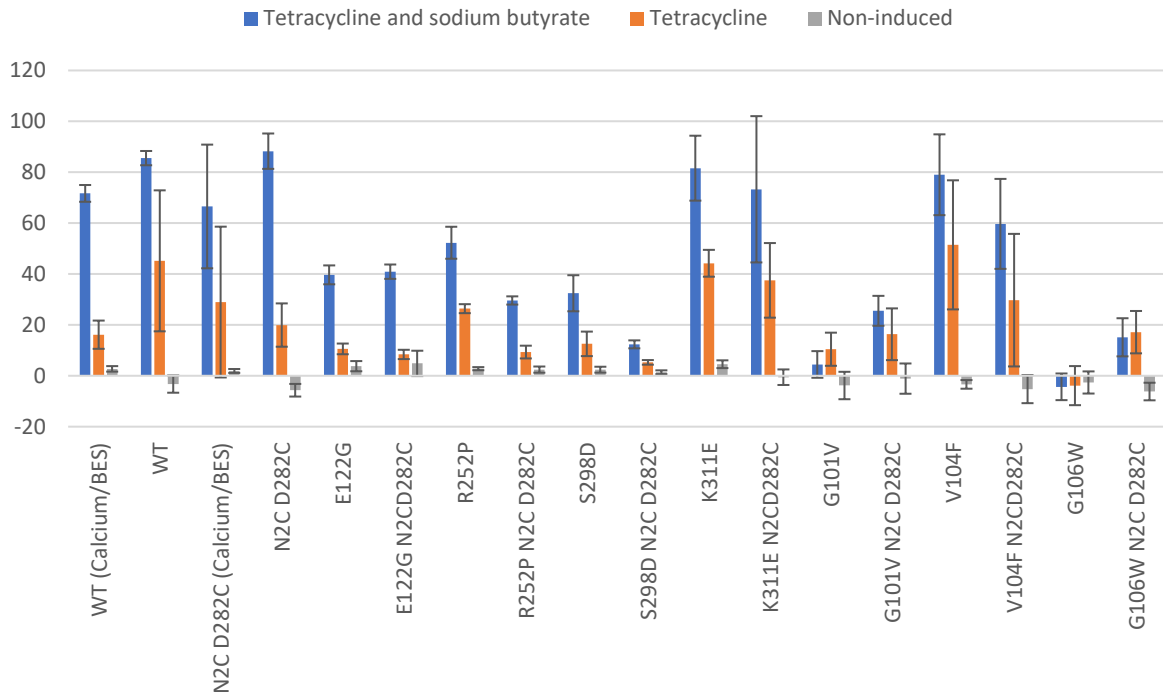


Figure 3.8 Expression of WT rhodopsin, rhodopsin RP mutants and their stabilised counterparts. Stable cell line pools were used for expression of rhodopsin and its mutants using tetracycline \pm sodium butyrate in the induction media. UV-vis absorbance spectroscopy was used to determine the rhodopsin pigment yield. The mean yield for each mutant is shown (blue bars = tetracycline and sodium butyrate induced, orange bars = tetracycline induced and grey bars = non-induced control). Error bars represent 1 standard deviation.

3.4 Discussion

The use of QuikChange mutagenesis on the pB007 NCO plasmid was attempted but found to be inefficient, likely due to the plasmids large size (Yang *et al.*, 2022). Progression to a cloning based method was therefore attempted which yielded better results and was therefore favoured going forwards. This is particularly important for cases where multiple mutations are being introduced, for example mutations needed in the stabilised rhodopsin background. Other methods for introducing multiple mutations in larger plasmids include a ligation of fragment ends after PCR method and use of primers with non-overlapping sequences (Liu and Naismith, 2008; Zeng *et al.*, 2018). The cloning method provided a sequential method for the production of mutant plasmids for transfection.

It was previously found that the pACMV TetO Opsin WT could be expressed in HEK293S cells when induced with tetracycline and sodium butyrate at 75 µg in 10 cm dishes after 72 h, with 25 µg and 55 µg after 24 and 48 hours respectively (Reeves *et al.*, 2002a). Here, with the piggyBac expression system a similar yield of pigment was seen after 72 hours, approximately 80 µg. However, higher amounts were also seen at 24 h and 48 h, with approximately 70 µg and 77 µg produced. This has shown that the use this method to produce inducible stable cell line pools is as effective if not more than the previous method used to express rhodopsin. Use of the tetracycline inducible system helps to counter toxic effects caused by rhodopsin mutants (Reeves *et al.*, 2002a). The piggyBac system itself has a number of advantages. The presence of the insulator sequences protect the cargo from gene silencing effects if inserted into transcriptionally inactive regions (Pérez-González and Caro, 2019). It also provides a high copy number of the transposon cargo being inserted, however variation in copy number has been noted previously between cell lines (Adelman *et al.*, 2004). The

method used here to produce a stably transfected cell line pool is much faster (approximately 3 weeks) compared to previous methods requiring colony isolation and growth as well as removing the need for multiple transient transfections to produce high levels of rhodopsin transiently (Reeves *et al.*, 1996).

Cell line stability when in continuous culture was also probed here which was important due to the pooled cell nature of the cell lines produced. Results of this experiment were not fully conclusive particularly in the case of the cells grown without selection where the expression level dropped and then increased again following the final 2 passages however this could be explained by the differences in the piggyBac cargo copy number which was previously shown to range from several to several thousand and instability of the inserted genes (Adelman *et al.*, 2004). For the cells grown in the medium with G418 selection, less variation in the expression was seen across the weeks however variation was still present.

The N2C D282C mutant forms a disulfide bond thought to aid the folding of opsin and stabilise the folded structure (Opefi, 2011; Opefi *et al.*, 2013). Use of this stabilisation feature here yielded varied results, with increased expression of some RP mutants (e.g. G101V and G106W) but decreased expression of others (R252P, S298D). The use of these mutations was previously shown to restore folding in some cases, therefore suggesting that some of the mutants expressed here may be misfolded, however this isn't always the case and detrimental outcomes are also possible (Opefi *et al.*, 2013).

Overall, here it has been shown that the use of the piggyBac method for stable cell line pool construction for rhodopsin expression is fast, effective and produces cells with the ability for high level rhodopsin production. This will be of great use for the

study of rhodopsin RP mutations, of which many have been discovered but not characterised. Its application throughout this work to generate rhodopsin RP cell lines for the mutants characterised throughout Chapters 4 to 6 will further define its utility in these kind of studies as well as for the study of other GPCRs.

4. Retinitis pigmentosa mutants located in the intradiscal domain of rhodopsin

4.1 Introduction

4.1.1 The intradiscal domain of rhodopsin

Located on the intradiscal side of the rhodopsin are the N-terminus and extracellular loop (EL) one to three (see Chapter One, Figure 1.4). EL1 joins TM helices 2 and 3, EL2 joins TM helices 4 and 5, and EL3 joins TM helices 6 and 7. In this work rhodopsin RP mutations located in the EL1 region are studied. Starting from G101 at the end of TM helix 2 and ending with G106 found at the start of TM helix 3. Residues G101, V104 and G106 are shown in Figure 4.1 (A, C, E) and the RP mutants studied in Figure 4.1 B: G101V, D: V104F and F: G106W. The motivation for this work on EL1 is based on previous work showing the N-terminus of rhodopsin folds into a compact structure and docks onto the ELs (Opefi *et al.*, 2013).

4.1.2 Disruption of rhodopsin pigment formation

The rhodopsin pigment is formed when its ligand, 11-*cis*-retinal forms a Schiff base bond to lysine 296 located in the opsin binding pocket. The 11-*cis*-retinal ligand is now primed to isomerise following the absorption of a photon, leading to conformational changes in rhodopsin to begin the signalling process. As such formation of correctly folded rhodopsin is imperative for its function as a photoreceptor (Athanasίου *et al.*, 2018).

Rhodopsin pigment formation can be disrupted by mutations in rhodopsin which can lead to retinitis pigmentosa. The pigment formation capabilities of rhodopsin RP mutants can be impeded, and the misfolded opsin remains trapped in the ER prior to its degradation by the Endoplasmic Reticulum Associated Degradation (ERAD)

system (Parfitt and Cheetham, 2016). Mutants of EL1 have been shown previously to fail to form the pigment as well as lead to abnormal glycosylation (Doi *et al.*, 1990).

G101V was identified as low surface expressing and likely pathogenic (Wan *et al.*, 2019). V104F was previously an unclassified mutant, but at the same residue position the V104I variant was found to be asymptomatic when expressed in yeast (Athanasίου *et al.*, 2018; Scott *et al.*, 2019). Residue G106 is the most extensively studied previously in this group. It is highly conserved with 95.5% conservation in the rhodopsin subfamily (Smith, 2010). G106W was identified in a patient group in 1991 and subsequent studies have led to its classification as a Class 2 mutant (Sung *et al.*, 1991a; Sung *et al.*, 1991b; Scott *et al.*, 2019).

4.1.3 Improving protein expression levels by lowering the temperature of the host cells

Improvements to expression methods to increase protein yield is of great interest for the study of proteins biochemically and structurally. However, the effects on mutant proteins can be varied due to the properties of the mutation. For example, in a study of mutations in HERG, a human potassium channel mutation involved in congenital long QT syndrome, lowering expression temperature when using stably transfected HEK293 cells to 27 °C rather than the standard 37 °C enabled protein trafficking and function to be improved (Zhou *et al.*, 1999). In another study of transiently transfected HEK293 cells, lowering the temperature to 33 °C 24 hours after transfection were found to increase expression of GFP/AMPA receptor 1.5 times (Lin *et al.*, 2015). A study looking at rhodopsin expression at 27 °C comparatively to 37 °C showed that plasma membrane expression is increased for some mutants found in TM2 (Mckee *et al.*, 2021).

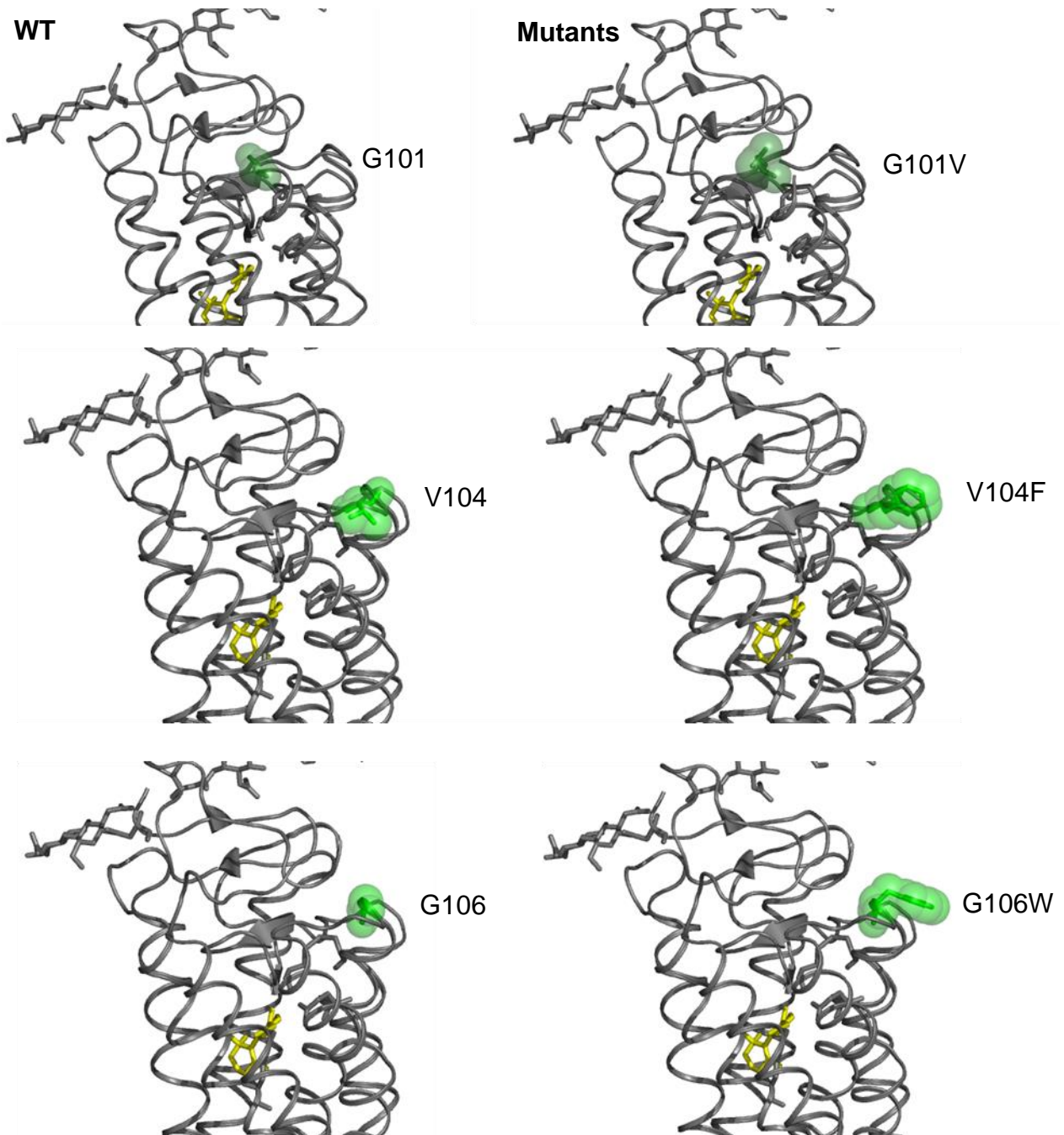


Figure 4.1 Comparison of rhodopsin residue 101, 104 and 106 in WT (G, V, G respectively) and as the EL1 mutants studied (V, F, W respectively). PyMOL mutagenesis wizard was used to show the mutations studied in the bovine rhodopsin structure (PDB 1U19).

4.1.4 Aims

Here the aim was to improve the expression of the 'difficult' to express mutants G101C, V104F and G106W and to attempt to determine the biochemical and spectral properties of said rhodopsin RP mutants, to evaluate to their active state stability and G-protein activation capabilities.

4.2 Materials and Methods

4.2.1 Production of stable cell lines

The cloning/ Turbofect method (see Chapter 2/Chapter 3) was utilised for generation of plasmids for stable cell line transfection. Sequences were checked using the Eurofins TubeSeq service. HEK293S stable cell line pools for G101V, V104F and G106W, along with their stabilised (N2C/D282C) counterparts were established.

4.2.2 Standard expression of the rhodopsin mutants

Cells were induced for to test their expression and harvested as described in Chapter 2. UV-vis difference spectroscopy was used to determine protein expression as described in Chapter 2.

4.2.3 Lowering the growth temperature from 37 to 33 °C in an attempt to improve mutant rhodopsin expression levels

Cells were grown on dishes in duplicate and induced using tetracycline and sodium butyrate as in 4.2.2; however, 1 hour after induction cells were either transferred to a 33 °C incubator or left at 37 °C as appropriate. Cells were then harvested at 12-hour intervals from 12 to 48 hours using the same method as in 4.2.2. Immediately after harvest the cell suspensions were treated with 9-*cis* retinal overnight. UV-vis absorbance spectroscopy was performed on non-illuminated samples followed by 1-minute photobleaching. The spectrum was recorded again and the difference in absorbance at the λ_{\max} was used to calculate the amount of rhodopsin pigment expressed. $\epsilon = 42700$ at the λ_{\max} and a molecular weight of 42300 Da were used to determine rhodopsin amounts.

4.2.4 Lowering the growth temperature from 37 to 33 °C and 30 °C in an attempt to improve P23A rhodopsin expression levels

Cells were grown to confluence on 10 cm cell culture dishes in complete DMEM/F12. At near confluence the media was replaced to be complete DMEM. 24 hours after media exchange, induction was started (2 µg/ml tetracycline and 5 mM sodium butyrate added to the dishes). Cells were then incubated for the required time at either 30, 33 and 37°C. The cells were then harvested in 1x PBS at 12-, 24- and 48-hour timepoints. Images were recorded using the EVOS at 28- and 48-hour timepoints to illustrate observational differences in cell density, lifting and morphology. The cell suspensions were then treated with 9-cis-retinal overnight and solubilised in DDM. A UV-vis dark spectrum was first recorded before photobleaching for 60 seconds and a recording of an illuminated spectrum. These were used to produce a difference spectrum and the difference at the λ_{max} was used in Beer-Lambert Law to calculate the yield of rhodopsin pigment.

4.2.5 Rhodopsin immunoaffinity purification

Stable cell lines were induced to enable rhodopsin production and harvested as described in Chapter 2. UV-vis spectroscopy was used to determine protein yields as described in Chapter 2. Rhodopsin and its mutants were purified, UV-vis spectral profiles were collected, and an SDS/ PAGE Western Blot experiment was conducted as described in Chapter 2.

4.2.6 Functional assessment of rhodopsin and its mutants

Meta II stability and transducin activation assays of the G101V, V104F and G106W mutants were performed as described in Chapter 2. Photobleaching profiles were obtained for G101V and V104F

4.3 Results

4.3.1 Production of pB007 NCO mutants

Following the cloning protocol described in Chapter 2, the G101V, V104F and G106W and their stabilised versions (N2C D282C) were produced. Restriction enzyme digestion, agarose gel (Figure 4.2) and sequencing (Figure 4.3) were used to confirm the correct construction of these mutants in the pB007 NCO plasmid. Sequencing results showed the DNA mutations G101V, V104F and G106W mutations were present (Figure 4.3 B, C and D, mutations highlighted by yellow boxes). The WT sequence is shown in Figure 4.3 A.

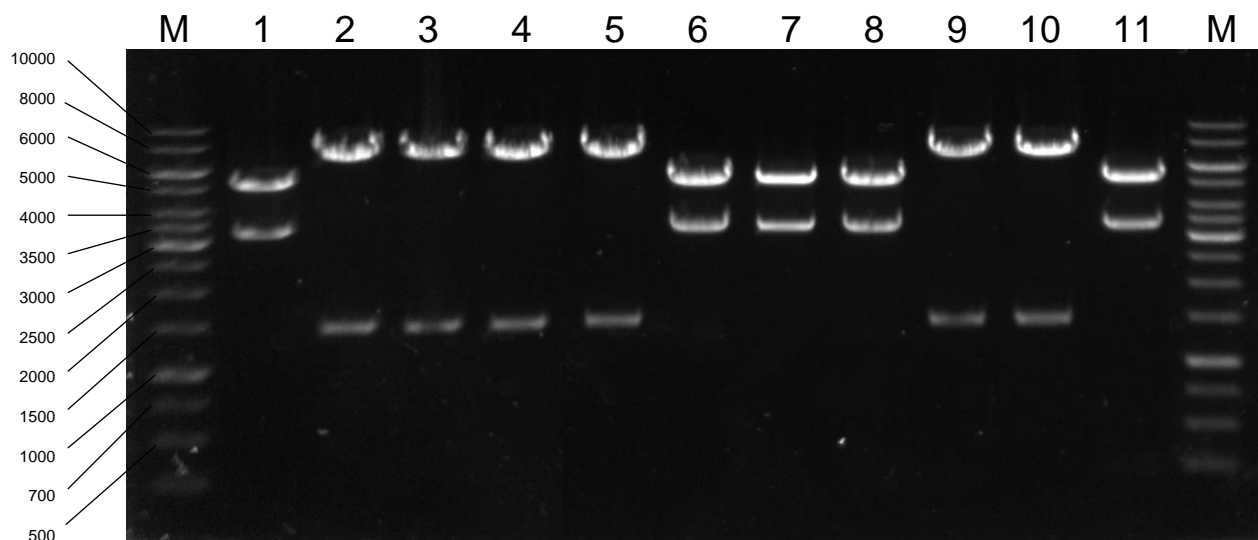


Figure 4.2 Agarose gel electrophoresis of medium-scale prepared pB007 NCO (\pm mutants) digested using *NheI*. Lanes marked M contain the ThermoScientific GeneRuler™ 1 kb DNA ladder. 1: WT rhodopsin, 2: N2C D28C, 3: P23A, 4: P23A N2C D282C, 5: G101V, 6: G101V N2C D282C, 7: V104F, 8: V104F N2C D282C, 9: G106W, 10: G106W N2C D282C, 11: K311E. Gel has been cropped to remove unnecessary lanes for clarity purposes.

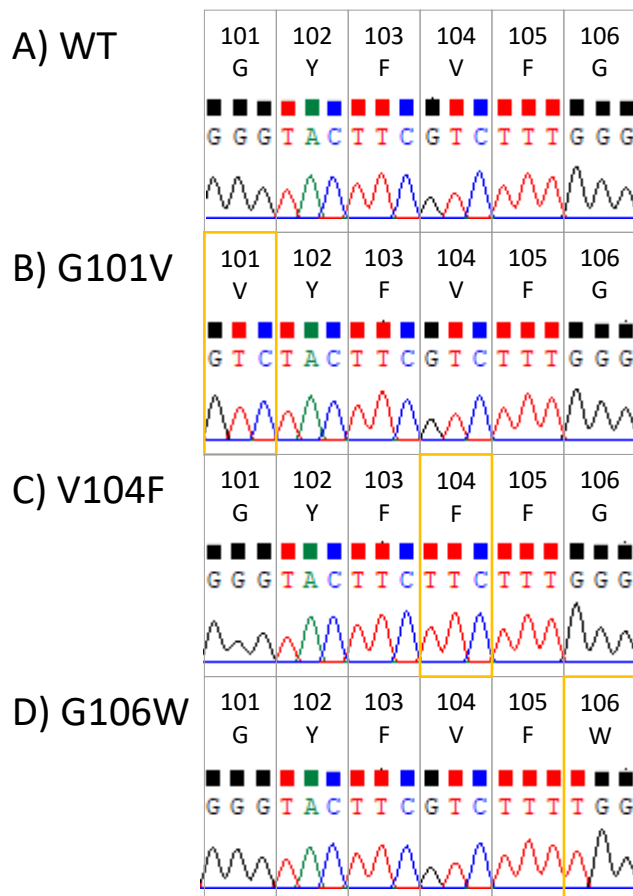


Figure 4.3 Sequencing of rhodopsin EL1 mutants. Following the medium scale preparation of each mutant plasmid, DNA sequencing was performed using the RhoSeqF1 primer. The numbers show the amino acid residue number, and the corresponding amino acid is shown below as a one letter code. Below this sequencing results are presented, with the DNA bases and sequencing trace shown for WT bovine rhodopsin and each mutant from those encoding residue 101 to residue 106. A) shows the WT bovine rhodopsin sequence. B) shows the mutated sequence for G101V where GGG becomes GTC. C) shows the mutated sequence for V104F where GTC becomes TTC. D) shows the mutated sequence for G106W where GGG becomes TGG.

4.3.2 Expression of the rhodopsin mutants G101V, V104F, G106W and their N2C D282C background counterparts in HEK293S cells

Transfection using transposon expression cassette plasmids performed to produce a stable HEK293S Ric15 TetR9 GnTI⁻ cell line pools for each rhodopsin mutant. By utilising the cell lines inducible properties, each of the mutant proteins was produced on 10 cm cell culture dishes and harvested after 65 hours. These were then treated with 9-*cis*-retinal and solubilised for UV-vis spectroscopy to determine the yield of rhodopsin pigment produced (Figure 4.4).

V104F and V104F/N2C/D282C were produced at comparable levels when induced with tetracycline and tetracycline/sodium butyrate, and at about half the yield of WT and N2C/D282C cell lines. However, very low levels of pigment were produced by the G101V and G106W cell lines, with less produced by the tetracycline/sodium butyrate induction for each. N2C D282C stabilised versions of both G101V and G106W had improved production when induced with tetracycline/sodium butyrate.

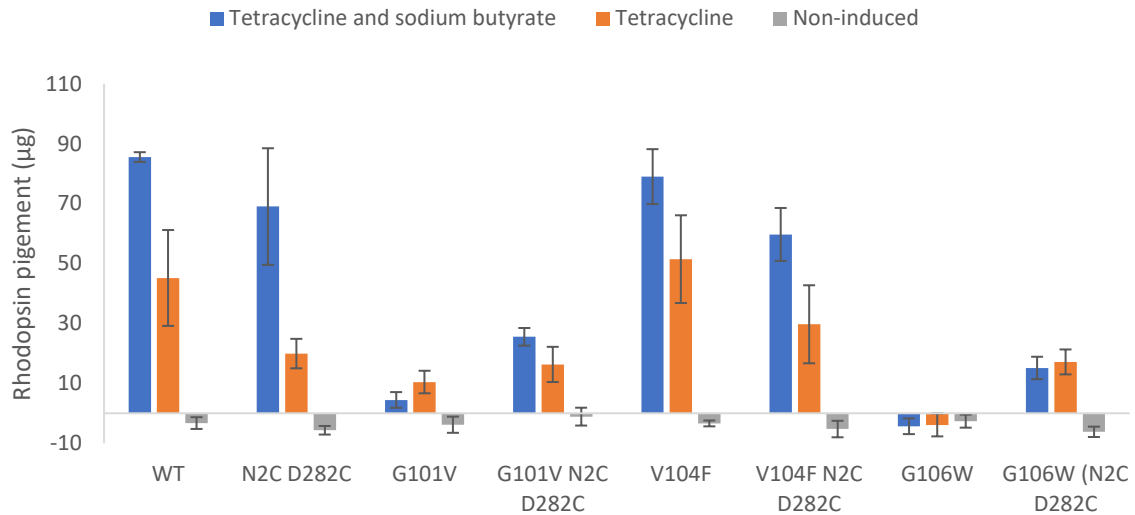


Figure 4.4 Expression of mutants in the EL1 region of rhodopsin using tetracycline and sodium butyrate for 65 hours at 37°C. Mutants in the EL1 region and their stabilised counterparts (N2C D282C) were produced using stable cell lines generated using the piggyback expression system. Expression of V104F and V104F N2C D282C was similar to that of WT and N2C D282C rhodopsin. G101V and G106W were both poorly expressed, and the stabilising mutations (N2C D282C) partially increased their expression.

4.3.3 Improvement of expression of rhodopsin mutants by expression at 33°C

Rhodopsin WT, P23A, G101V and G106W cell lines were expressed on confluent 10 cm dishes using tetracycline and sodium butyrate at 12-hour intervals up to 48 hours before harvesting in 1x PBS. 9-*cis*-retinal was then added to form the pigment before solubilisation of the samples. UV-vis difference spectra were calculated after collection of dark and light-irradiated UV-vis absorbance spectra as described previously. The Beer-Lambert law was then used to calculate the pigment produced. The same samples used for spectroscopy were then separated on an SDS-PAGE gel and a Western blot was performed using the rho-1D4 antibody.

Expression levels of WT rhodopsin increased throughout the timepoints, both at 33°C and 37°C. The difference between expression at each temperature relative to the timepoint was minimal from 12 to 36 hours, and only a small increase was seen at 48 hours when cells were induced at 33°C. This was observed both by UV-vis difference spectra and Western blot (Figure 4.5).

When expressed at 37 °C the mutant P23A showed a low level of expression which peaked at 12 hours (17.5 µg) and decreased thereon. At 33 °C the expression levels improved. The maximum expression level was reached at 36 hours with a calculated yield of 57.9 µg.

Expression of G101V at 37 °C peaked at 24 hours with a calculated yield of 69.8 µg. At 37 °C, an improved calculated yield of 100.5 µg was achieved at 24 hours and levels remained high at 48 hours with 99.7 µg.

At 37°C expression of G106W reached a maximum at 12 hours of 7.7 µg was seen followed by a decrease to no detectable pigment. When expressed at 33°C an improvement was observed, peaking at 24 hours with a calculated yield of 30.7 µg.

The calculated expression levels of WT rhodopsin and the mutants at each timepoints was echoed when the same samples were analysed by Western blot (Figure 4.5).

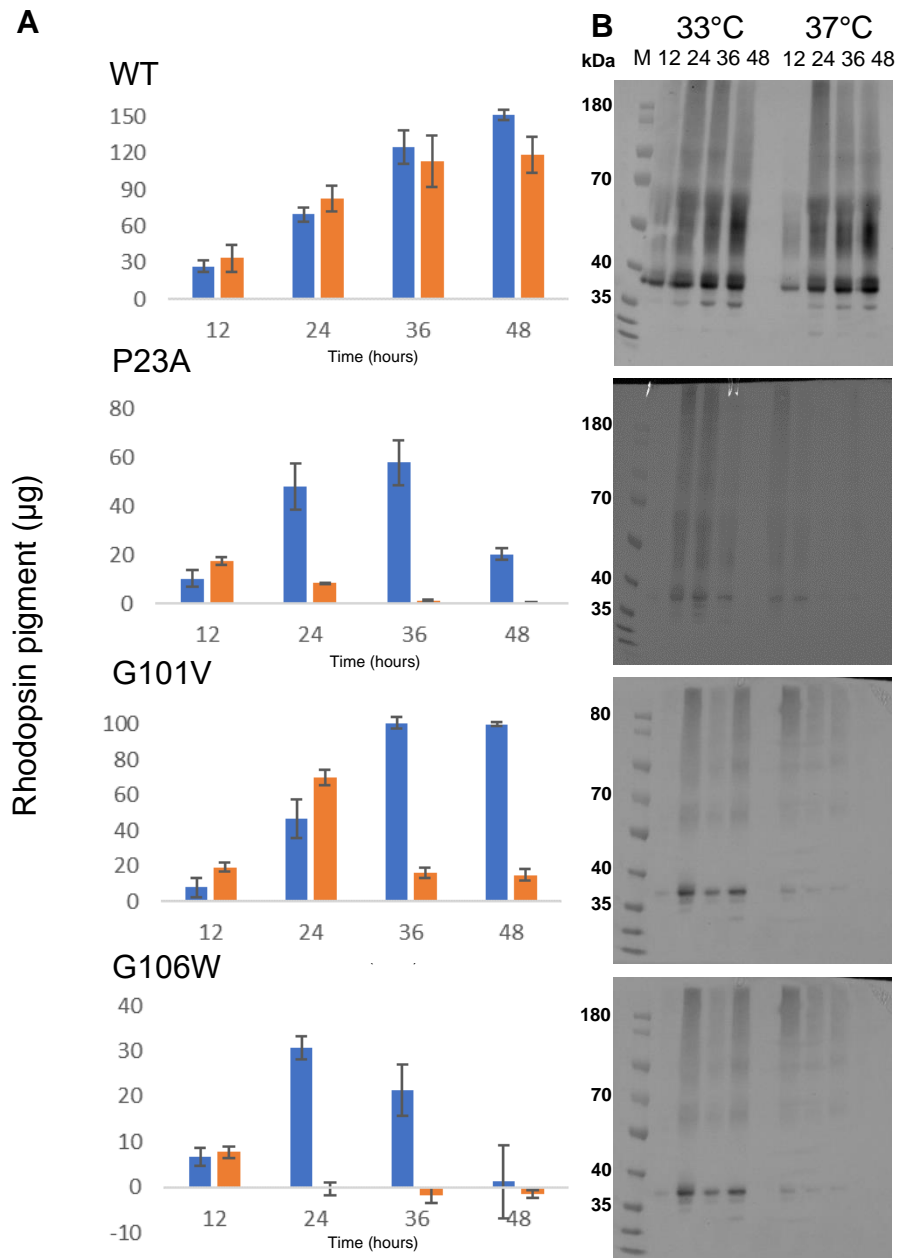


Figure 4.5 Expression of the rhodopsin mutants P23A, G101V and G106W at 33°C versus 37°C when induced with tetracycline and sodium butyrate. HEK293S RTG cells with either WT, P23A, G101V or G106W rho gene on 10 cm cell culture dishes were prepared, and complete DMEM containing 2 µg/ml tetracycline and 5 mM sodium butyrate was added for the relevant induction length (either 12, 24, 36 or 48 hours) and then incubated at either 33°C (blue bars) or 37°C (orange bars). The cells were then harvested in 1x PBS before overnight treatment with 5 µM 9-cis-retinal. UV-vis absorbance difference spectra were used to determine rhodopsin yields, followed by

separation by SDS-PAGE and a Western blot using the Rho-1D4 antibody. The marker (M) contains the ThermoScientific PageRuler™ Prestained 10-180kDa Protein Ladder.

4.3.4 Variation to temperature changes expression levels in P23A

Following induction of rhodopsin expression of P23A and WT at the temperatures 30, 33 and 37 °C, at 12-, 24- and 48-hour timepoints cells were observed and harvested for expression level determination by UV-vis difference spectroscopy. WT rhodopsin expression increased across all timepoints (Figure 4.6). P23A also increased, expressing best at 33 °C after 24 hours and 30 °C induction yielding the highest expression after 48 hours. 37 °C expression was highest after 12 hours.

Additionally, cells were imaged at 28- and 48-hour timepoints. Observationally, WT cells appeared normal after 12 hours, with some detaching from the dish at each temperature after 24 hours. At 48 hours WT at 30 °C remained having a few floating cells, with more lifted cells observed at 33 °C and the most detached cells observed at 37 °C. For P23A, at 12 hours a few cells had begun to appear rounded. After 24 hours this increased, with more rounded cells appearing and more lifting of cells as temperature increased. This remained the similar for the images taken at 28 hours. Finally, after 48 hours, the cells appeared rounded with the levels of lifting increasing with increased expression temperature.

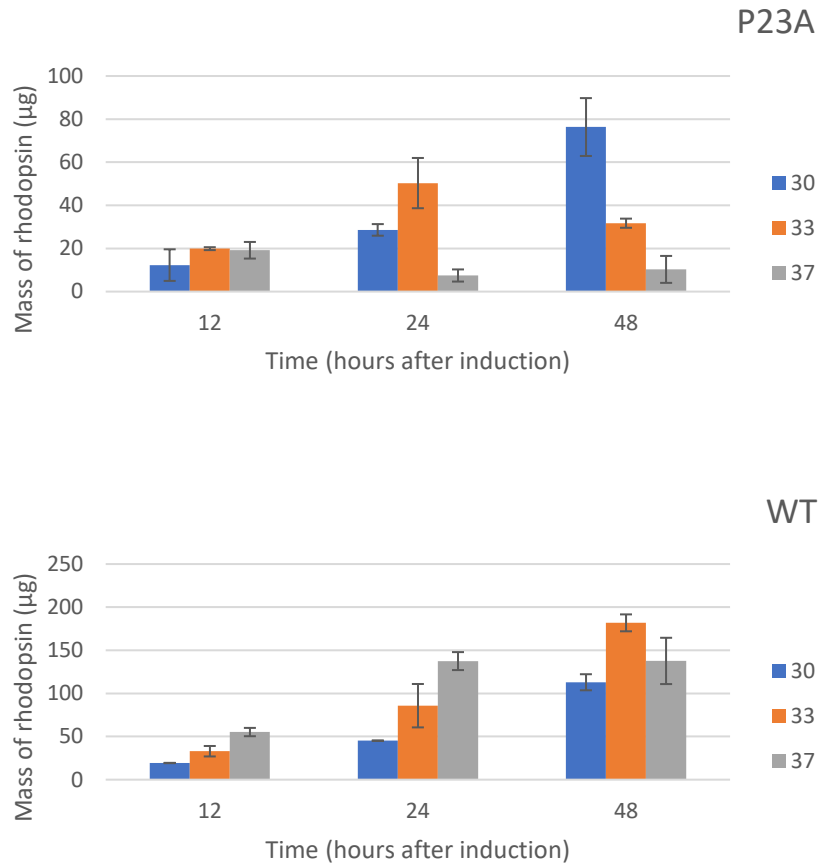


Figure 4.6 Expression of P23A and WT rhodopsin at 12-, 24- and 48-hour timepoints after expression was induced at 30, 33 and 37 °C. Cells were induced using tetracycline and sodium butyrate and then incubated for either 12, 24 or 48 hours at 30, 33 and 37 °C. Cells were harvested and treated with 9-*cis*-retinal to form rhodopsin pigment. UV-vis absorption spectra were recorded for each first in the dark and then following 60 seconds of illumination. The difference in absorption at the λ_{\max} was then used in Beer-Lambert Law to calculate the rhodopsin pigment produced.

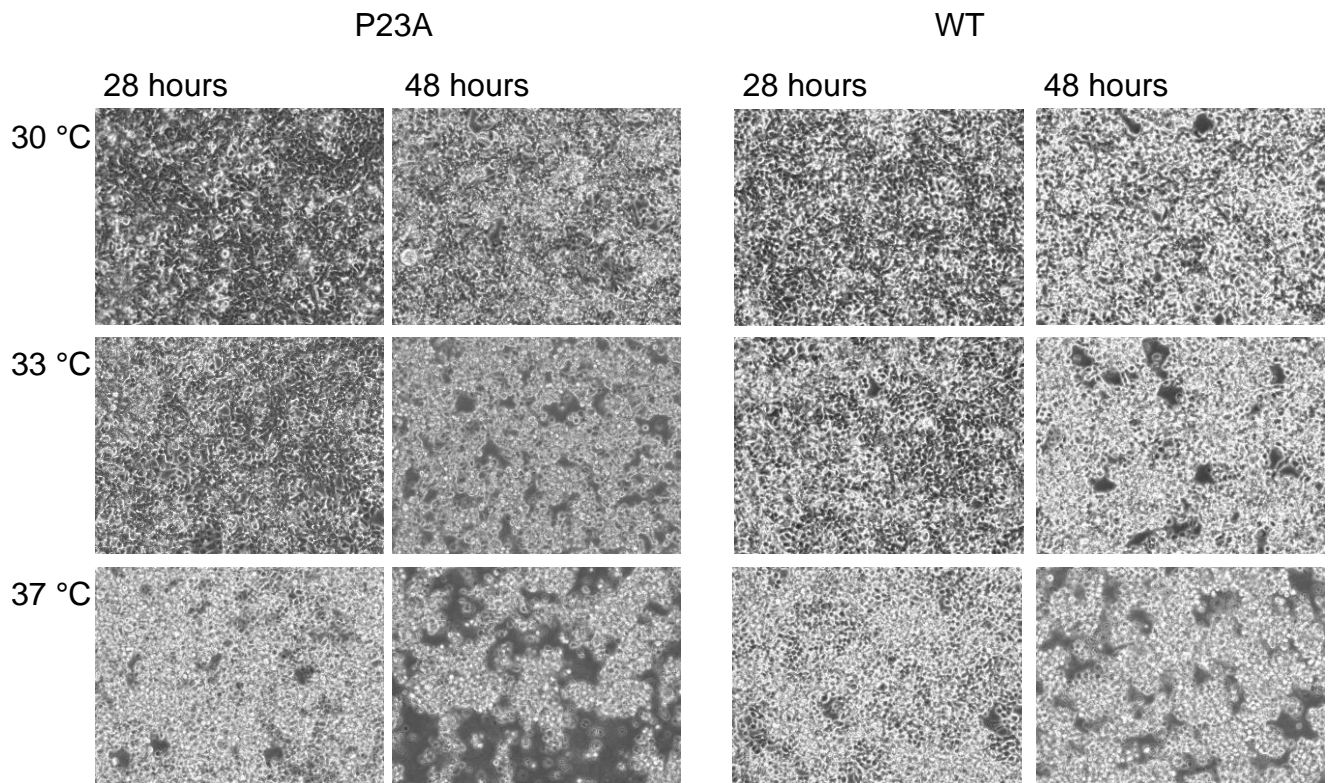


Figure 4.7 P23A and WT rhodopsin were expressed at 30, 33 and 37 °C. At 28 hours and 48 hours the cells were imaged using the EVOS microscope. Images show that with increased temperature and increased time, both cell lines became more rounded, and more lifting of the cells was present, with P23A showing more rounding and lifting earlier than its WT equivalent.

4.3.5 Purification of mutant rhodopsin from HEK293S stable cell lines

Stable cell lines processed by tetracycline and sodium butyrate induction at the appropriate timepoint, and temperature based on (4.3.2 and 4.3.3) using 15 cm dishes confluent with each cell line was harvested in 1 ml of 1x PBS. Harvested cell suspensions were then treated with 11-*cis*-retinal and solubilised before purification using 6 elutions. The yield of rhodopsin in each elution was then assessed by UV-vis spectroscopy, and then a Western blot was performed (Figure 4.8).

The WT rhodopsin, P23A, G101V, V104F and G106W mutant rhodopsin spectra (Figure 4.8) showed varying amounts of rhodopsin pigment. WT rhodopsin was expressed at the highest level (104.1 μg), with G101V and V104F producing slightly less (75.5 and 66.3 μg respectively). G106W produced the least (7.3 μg). For all the mutants, the highest amount of rhodopsin was purified in the first low salt elution (LSE1, blue lines spectral traces in Figure 4.8). The purified samples, along with a sample of the flow through following binding, high salt and low salt washes were then examined by SDS-PAGE after which a Western blot was performed using the rho-1D4 antibody (Figure 4.8).

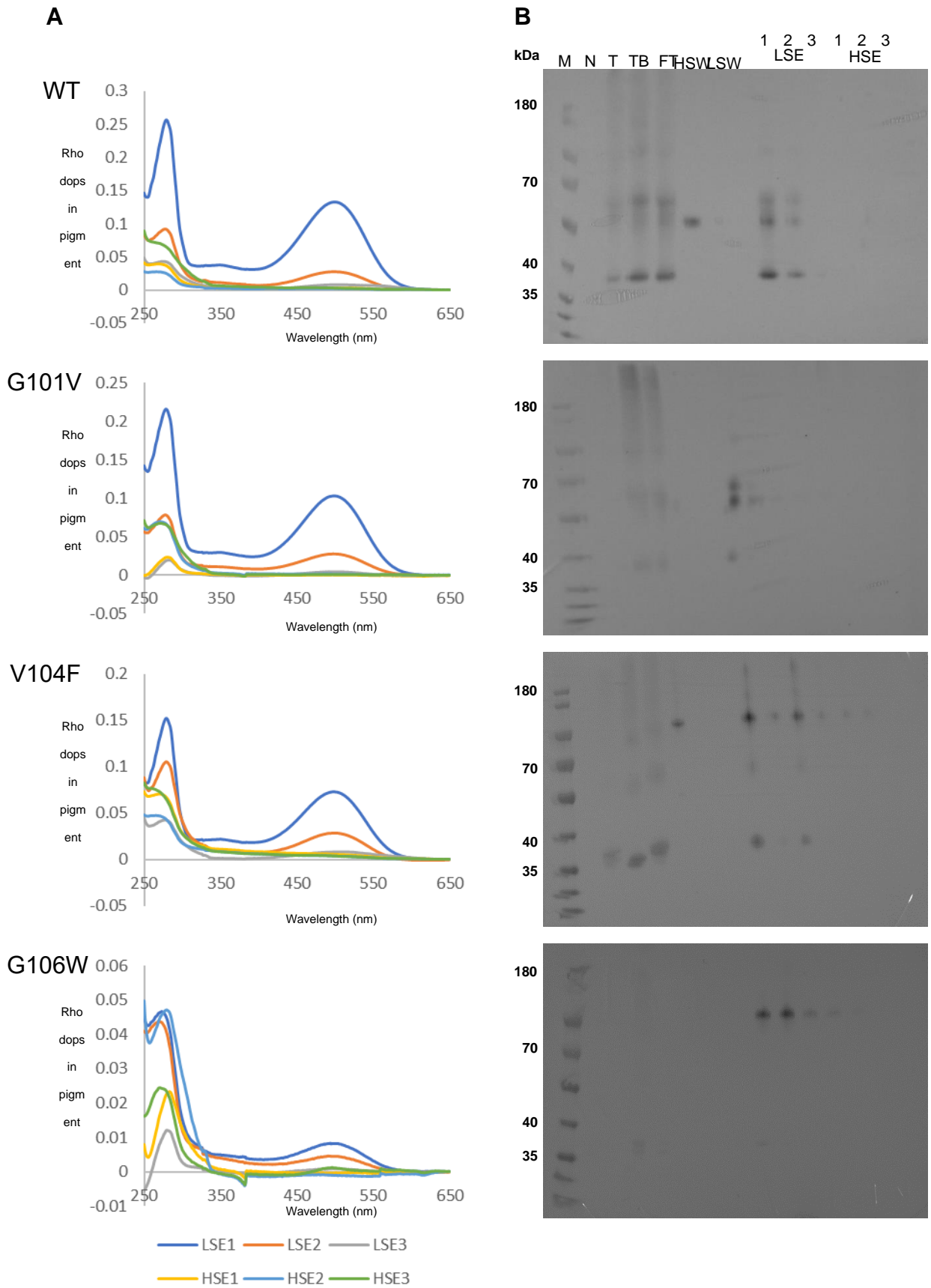


Figure 4.8 UV-vis absorbance spectra of elutions (A) and Western blot (B) for WT rhodopsin and the mutants P23A, G101V, V104F, G106W. Confluent 15 cm cell culture dishes were induced using 2 µg/ml tetracycline and 5 mM sodium butyrate in complete DMEM for differing lengths of time, and at 33°C or 37°C depending on the optimal time/temperature for expression of that mutant. After induction, the cells were harvested in 1x PBS before treatment with 5 µM 11-cis-retinal overnight. The treated cell suspensions were then purified using 1D4-immunoaffinity purification following which the elution samples (LSE1-3 and HSE1-3), alongside flow through (FT) and high and low salt wash samples (HSW/LSW) were used for SDS-PAGE and Western blot by rho-1D4 antibody. The marker (M) is ThermoScientific PageRuler™ Prestained 10-180kDa Protein Ladder. Non-induced (N), tetracycline only (T) and tetracycline and sodium butyrate (TB) unpurified samples were used as controls.

4.3.6 Photobleaching and acidification

Upon activation by light, WT rhodopsin is converted from its inactive form which has a λ_{\max} of 500 nm (dark blue line, Figure 4.9) to its active (Meta II) state which has a λ_{\max} of 380 nm (orange, grey, yellow and light blue lines, measured after repeated 30 second photobleaches). The covalent Schiff base that forms between Lys296 of rhodopsin and 11-*cis*-retinal can be captured by acidification of the protein causing its denaturation and is observed as a 430 nm peak (green line).

G101V and V104F rhodopsin mutants had slightly different photobleaching patterns in comparison to WT rhodopsin, this difference is highlighted by the black arrow on the G101V and V104F panels (Figure 4.9). V104F did not fully convert after 30 seconds photobleaching with a peak at both 500 nm and 380 nm present (orange line), from 60 seconds onwards photobleaching appeared complete. G101V was slower in converting to the 380 nm species, taking 90 seconds of photobleaching before it appeared complete. Upon acidification, a peak at 430 nm was seen for G101V and a peak at 423 nm was seen for V104F.

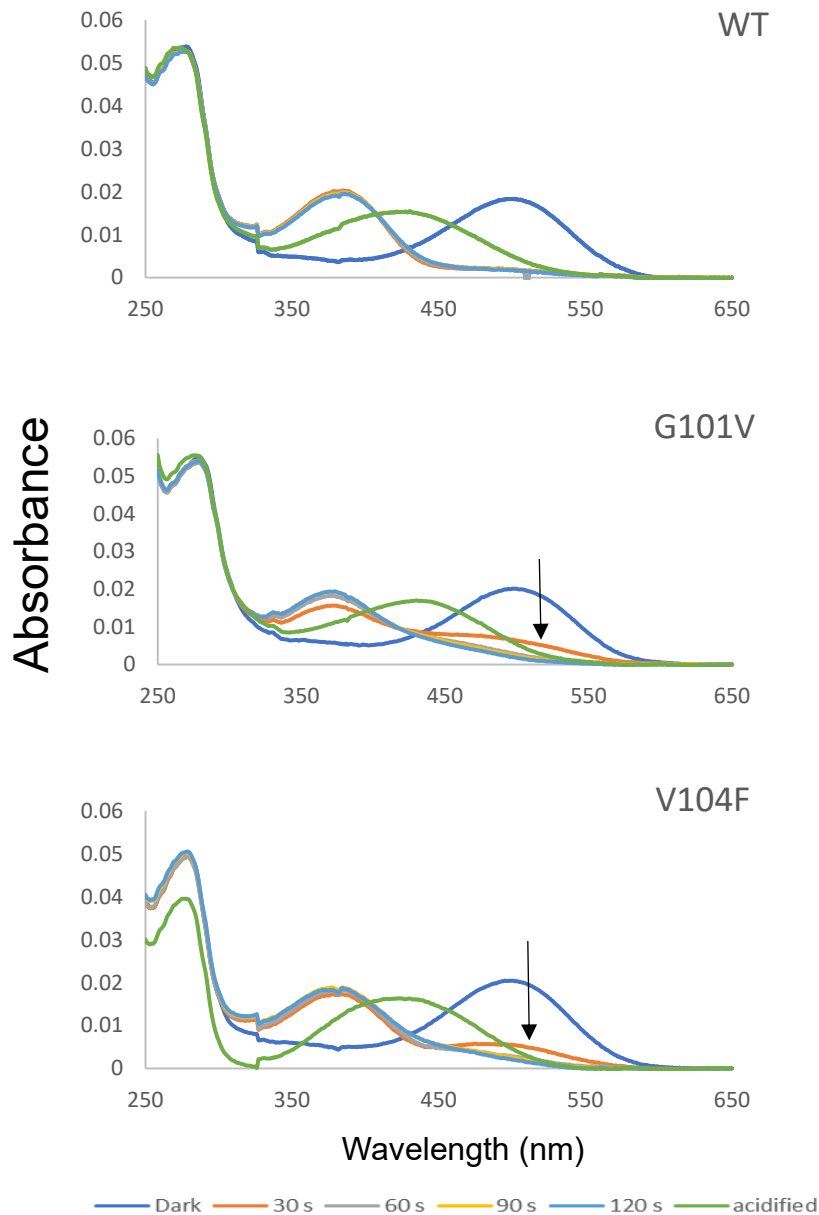


Figure 4.9 Photobleaching and acidification profiles of WT, G101V and V104F rhodopsin. A spectrum was first recorded for the dark state between 650 and 250 nm (dark blue line spectral trace for each purified pigment). Then four 30 second photobleaches were performed with spectra recorded for each (orange, grey, yellow and light blue line spectral traces). Finally 2N H₂SO₄ was added and a final spectrum was recorded (green line spectral trace). Black arrows show the abnormal spectra.

4.3.7 Meta II stability of light activated mutants

Upon activation by light, rhodopsin converts to its active state known as Meta II. Purified rhodopsin was activated by photobleaching at $t = 0$ for 30 seconds and then the stability of the Meta II conformation was determined by fluorescence spectroscopy. WT rhodopsin Meta II intermediate has a half-life of 17.67 minutes. The Meta II half-life of G101V was 5.96 minutes, V104F was 10.06 minutes and G106W was 9.97 minutes. Figure 4.10 shows representative fluorescence spectra for each of the EL1 mutants and WT rhodopsin, and their calculated half-lives and standard deviation are presented in Table 4.1.

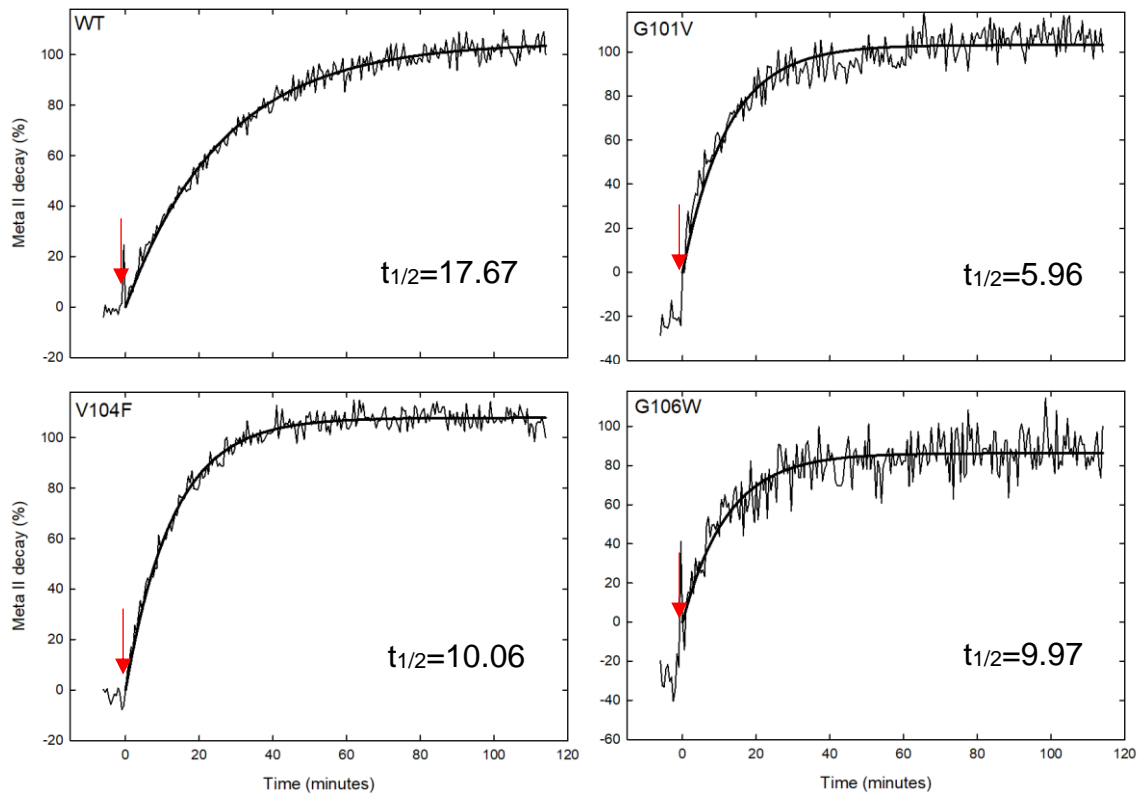


Figure 4.10 Meta II decay of the EL1 mutants. Measurement of Meta II decay was achieved by recording the inherent increase in tryptophan fluorescence that occurs as retinal is released from the rhodopsin binding pocket after illumination. Samples were illuminated at time = 0 for 30 seconds (red arrow), and fluorescence measured for 2 hours. All data best fitted to single, 2 parameter curves using SigmaPlot. $t_{1/2}$ is shown for each mutant.

4.3.8 Transducin activation by light activated mutants

Photobleached rhodopsin activates transducin which is the first key biochemical event in signal transduction. The ability of the purified rhodopsin mutants to activate transducin was assessed by measuring the increase in tryptophan fluorescence that occurs when GTP γ S displaces GDP in transducin.

The ability of the EL1 mutants to activate transducin varied from 18.3% to 63.6% compared to WT rhodopsin. The relative activation rate of G101V in comparison to WT was 35.1%. V104F was able to activate transducin relative to WT at a rate of 63.6%. G106W had a relative activation rate of 18.3%. For V104F the curve when activated followed a similar shape to the WT with a rapidly increasing linear line followed by a plateau, however for both G101V and G106W a slowly increasing linear line was observed for the first 60 seconds and the trend remained linear after. In Figure 4.11 representative curves for G101V, V104F and G106W rhodopsin mutants and WT rhodopsin are presented and the calculated relative initial rate activity and standard deviation for each is shown in Table 4.1.

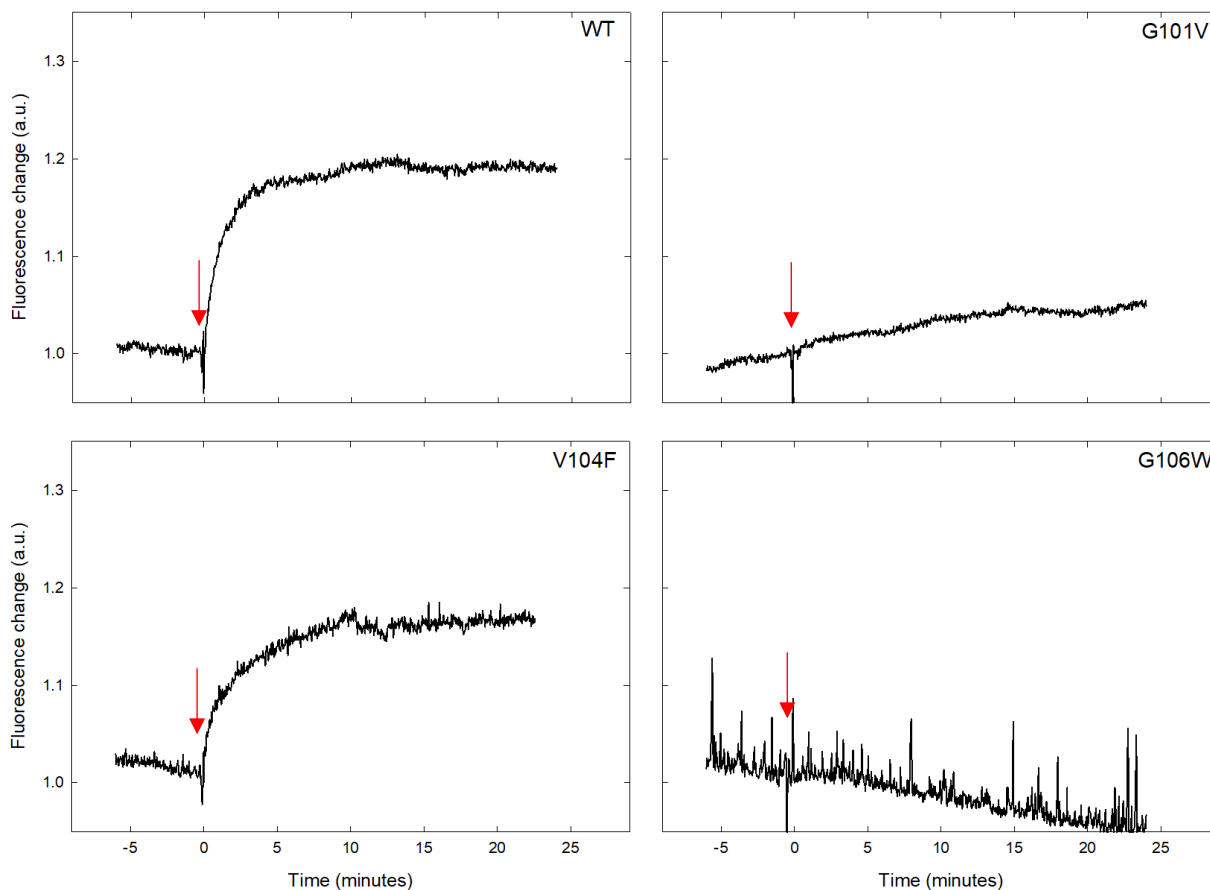


Figure 4.11 Transducin activation of EL1 mutants G101V, V104F and G106W. The change in fluorescence following the addition of GTP γ S (arrow) to an illuminated sample containing a rhodopsin mutant and transducin was measured. The first 60 seconds following GTP γ S addition was used to calculate the initial rate kinetics of transducin activation.

Table 4.1 Purification, Meta II decay and transducin activation characteristics of the EL1 mutants G101V, V104F and G106W

	λ_{\max} (nm)	Yield (μ g)	Ratio $A_{280}/A_{\lambda_{\max}}$	Meta II stability Half-life (mins)	S.D.	Transducin activation Relative rate (%)	S.D.
WT	500	104.08	1.80	12	17.67 1.77	11	100 0.000693
G101V	499	75.46	2.08	2	5.96 2.96	6	35.1 0.000216
V104F	499	66.25	2.08	5	10.06 1.78	8	63.6 0.000585
G106W	494	7.27	5.40	2	9.97 0.78	2	18.3 0.000226

4.4 Discussion

4.4.1 Improving the expression of difficult to express mutants.

While V104F expressed reasonably well following induction of the piggyBac generated cell line, very little G101V and almost no G106W rhodopsin was expressed at 37 °C. G106W and G101V have been previously found to express at very low levels and performing 9-*cis* retinal rescue whilst the proteins were being expressed was required for expression to be improved (Neaves, 2020).

In an attempt to improve expression of these mutants different conditions were explored. Changes were made to both the temperature used for expression and the time allowed for expression. These experiments were motivated by finding that the most common CFTR mutant (d508) could fold at lower (permissive) temperatures (Sharma *et al.*, 2000; Wang *et al.*, 2008). The outcome of these studies was that G101V and G106W rhodopsin could be prepared in sufficient quantities for purification and biochemistry experiments. The increase in mutant rhodopsin expression using HEK293 cells is in agreement with previous studies of the GFP/AMPA receptor and HERG by both transient and stable transfection methods (Zhou *et al.*, 1999; Lin *et al.*, 2015). Interestingly while expression was improved for both at 33 °C, the timepoint at which maximum expression was observed was different. For G101V expression level peaked at 36 hours while for G106W expression levels peaked after 24 hours. G101V was previously identified as a low surface expressing mutation and therefore further work to look at differences in surface expression between the two temperatures is necessary (Zhou *et al.*, 1999; Wan *et al.*, 2019). Likewise, G106W has also previously been found to not be effectively transported to the cell surface membrane and

therefore further work to establish whether the lowered temperature improves this is also needed (Sung et al., 1991b).

4.4.2 Biochemical characteristics of EL1 mutant rhodopsins

G101V rhodopsin exhibited a range of different biochemical properties when compared to the WT rhodopsin protein. G101V rhodopsin had a short Meta II half-life (5.96 minutes compared to 17.68 minutes for WT) and was only able to activate transducin at 35% the relative rate compared to WT rhodopsin. It also exhibited abnormal photobleaching properties requiring 90 seconds to fully convert to the 380 nm species (WT readily converts after 30 seconds).

V104F rhodopsin also exhibited some differences in its biochemical properties in comparison to WT rhodopsin, with a nearly 2x shorter Meta II half-life, a relative transducin activation rate of 64% and an abnormal photobleaching pattern (60 seconds to convert to 380 nm species) with a slight shift to its acidification profile.

G106W rhodopsin exhibits very low expression levels compared to WT rhodopsin and the other mutants in the EL1 region, despite lowered temperature and shorter induction length improving this. Despite this, usable amounts of protein for biochemistry were able to be harvested when using the optimum conditions established in the expression at 33 °C experiments. The slightly shifted λ_{\max} (494 nm), faster Meta II half-life (9.97 minutes) and 18% transducin activation ability compared to WT rhodopsin showed that the G106W mutation also affects the biochemical properties of the protein.

In the rhodopsin subfamily G106 is highly conserved (Smith, 2010). The G106W mutation has been previously established to be a class 2 rhodopsin RP mutation with misfolding and instability characteristics (Sung et al., 1991b; Athanasiou et al., 2018;

Scott et al., 2019). Here we have established that the protein is unstable as illustrated by its rapid decrease in abundance when expressed after 12 hours at 37 °C and 24 hours at 33 °C. Its short Meta II half-life is also often an indicator of general instability of pigments which is in agreement with the previous findings.

The shortened Meta II half-life seen in each of the mutants is often indicative of protein instability, which echoes previous work where G101V and G106W have been labelled as likely class 2 mutants, suggesting a necessary role of the EL1 loop in the stability of rhodopsin (Sung et al., 1991b; Scott et al., 2019; Wan et al., 2019) as well as light activation. The variation in the degree of detriment to the transducin activation capability of 64% for V104F down to 18% for G106W despite their similar Meta II half-lives suggest that it is not the shortening of the Meta II half-lives which explains this. EL1 links helix 2 to helix 3, and these mutations may affect the folding of rhodopsin to varying degrees. The movements in helix 3 which normally occur upon activation and eventually to lead to formation of the rhodopsin:transducin complex may be affected by mutations in this region leading to variation to the transducin activation capabilities (Patel *et al.*, 2005; Gleim *et al.*, 2009).

These results highlight the nature of rhodopsin mutations in the EL1 region to not solely be due to misfolding and instability but to have functional effects in addition. To understand their mechanisms further work using human rhodopsin and *in vivo* models would be necessary. Parallels can be drawn with the observations described here and those for CFTR misfolding mutants in that, for both, the rescue of misfolding can be achieved by either reducing temperature of expression or by including correctors or pharmacological chaperones during expression. While lowering the temperature of expression is not applicable for therapeutic intervention, it could indicate which mutations might be amenable to pharmacological chaperone therapy. Overall, the

results have shown that EL1 has not only a role in the folding stability of rhodopsin but can affect the signalling properties as well.

In summary, experiments exploring the role of time and temperature on the expression of rhodopsin RP mutants have identified conditions that in certain cases enable the conditional formation of pigments. This outcome is important for two reasons. First, it might now be possible to obtain sufficient quantities of these mutants for use in biophysical experiments to probe their effects on structure, function, and unfolding. Second, examination of the way these mutants interact with molecular chaperones and co-chaperones under these different conditions could provide further insight into their folding and misfolding/unfolding, and degradation pathways.

5. Characterisation of rhodopsin RP mutants: previously unclassified

5.1 Introduction

5.1.1 Classification of rhodopsin retinitis pigmentosa mutations

Classification of rhodopsin retinitis pigmentosa (RP) mutations aims to group the mutations by their biochemical and biophysical properties. Most RP mutations are class 2 which are defined by misfolding of the protein. Other mutation classes have effects on rhodopsin function and cellular processes which in turn can indicate functional properties of the residue in the WT protein (see Chapter 1.5). The mutants E122G, R252P, S298D and K311E were identified as unclassified rhodopsin mutations and have been linked to RP (Athanasidou *et al.*, 2018). Preliminary investigations in the Reeves' laboratory demonstrated they did not misfold thus ruling out class two classification. These enigmatic mutations were chosen for further study because of their potential to have defects other than folding, potentially providing insight into rhodopsin function. In order to assess the effects of each of these mutations on rhodopsin, their pigment formation and biochemical functioning will be examined.

5.1.2 Function of rhodopsin

An array of spectroscopic and functional studies are available to probe rhodopsin structure and function. Rhodopsin pigment is formed when the opsin protein forms a Schiff base bond with the 11-*cis*-retinal ligand, and by assessing the pigment formation

extent kinetics the folding of these mutants can be examined. The Schiff base bond can be captured by acidification. When the rhodopsin receives a photon 11-*cis*-retinal isomerises into all-*trans*-retinal and photobleaching occurs, which can be observed through the reduction in the 500 nm species and the increase of the 380 nm species. Isomerisation of the ligand results in conformational changes in rhodopsin to the metarhodopsin (Meta) II state, from which the all-*trans*-retinal is released, the rate of which determines the half-life of the Meta II active state in turn determining the potential to activate transducin. Activated rhodopsin interacts with the G-protein transducin which *in vivo* would then initiate the biochemical stage of the signalling process. The steps of rhodopsin activation and signalling are shown in Chapter 1, Figure 1.3.

5.1.3 Opsin and pigment formation

While methods to study the Meta II stability and transducin activation of rhodopsin have been well established, studies using the apoprotein rod opsin present a greater challenge. The rod opsin apoprotein when bound to the ligand 11-*cis*-retinal forms the pigment rhodopsin. While many biochemistry studies require rhodopsin in its native state, the stable opsin purified in detergent itself is often essential for studies of pigment formation and regeneration steps which are key for the recycling of rhodopsin in the eye. However, opsin is very unstable when solubilised in detergent compared to its rhodopsin counterpart.

Previously, it was shown that rod opsin and its mutants could be purified in a stable form using lipid/detergent mixed micelles (Reeves *et al.*, 1999). Later it was discovered that a disulfide bond formed by engineering in cysteines residues at positions N2 and D282 could also stabilize the apo protein rod opsin. (Xie *et al.*, 2003). This method has

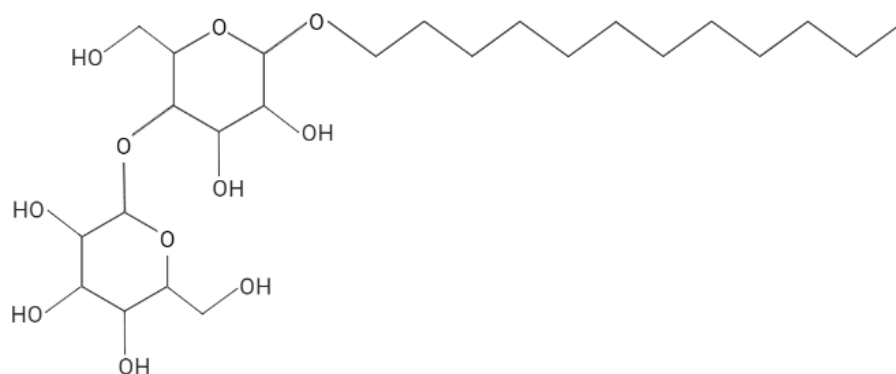
since been used to aid the study of mutant rhodopsins/opsins as well (Opefi *et al.*, 2013). The introduction of these mutations has been shown to not greatly impact activation properties of rhodopsin as demonstrated by studies of Meta II stability and transducin activation (Xie *et al.*, 2003; Opefi *et al.*, 2013). However, it means that study of pigment formation cannot be achieved using WT opsin apoprotein due to its need for these stabilising mutations to be purified in DDM. This mutation also changes the overall thermostability of opsin thus interfering with studies of opsin mutant stability, unless the 2C-282C bond is first reduced (Xie *et al.*, 2003).

5.1.4 Detergent solubilisation of membrane proteins

Membrane proteins such as rhodopsin need to be extracted and purified from the cell membrane by using a detergent before they can be examined. After which the detergent stabilises the extracted protein (Singh and Sigworth, 2015). Recent advances using SMALPs represents an alternative strategy, but this procedure is not yet well established (Grime *et al.*, 2021). The formation of detergent-protein complexes is possible due to detergent ability to separate membrane proteins from their membranes within a micelle when the detergent concentration is above its critical micelle concentration (CMC) (Le Maire *et al.*, 2000; Breyton *et al.*, 2019). Previously, Dodecyl Maltoside (DDM, also known as lauryl maltoside) has been used for the isolation of rhodopsin from cell membranes. This detergent allows full light activation of rhodopsin enabling spectroscopic analysis and signal transduction experimentation. However, DDM solubilisation for many proteins (opsin included) especially in the absence of the cognate ligand, results in their instability preventing purification and study of some GPCRs (Lee *et al.*, 2020).

Lauryl Maltose Neopentyl Glycol (LMNG) is an amphiphilic detergent which can stabilise membrane proteins previously found to be difficult to study biochemically in conventional detergents such as DDM or OG. This has made it of great interest in the field (Breyton *et al.*, 2019). LMNG has potential advantages for purifying GPCRs over DDM due to its ability to retain receptor stability (Lee *et al.*, 2020). In LMNG two hydrophilic maltoside groups are joined via a quaternary central carbon to an equal length pair of hydrophobic n-dodecyl chains, which form much larger micelles than DDM (Chaptal *et al.*, 2017; Breyton *et al.*, 2019; Lee *et al.*, 2020). The LMNG micelle encapsulates the receptor tightly, covering the hydrophobic TM portion of receptors with LMNG tail groups (Lee *et al.*, 2020).

The nature of the LMNG micellular environment potentially results in differences in the receptor properties compared to the receptor in DDM. The linkage of the tail chains results in more hydrogen bonds between both head groups on the LMNG molecule and to the receptor itself, reducing movement in comparison to DDM but likely to be responsible for the increased stability and decreased activity of receptors tA₂AR and WT-β₂AR (Lee *et al.*, 2020). LMNG has been shown to increase thermal stability whilst also increasing activity in some membrane proteins (bacteriorhodopsin, *E. coli* outer membrane ferrichrome iron transporter, *S. pneumoniae* Nox protein and Bacillus multidrug resistance ATP) when compared to DDM (Breyton *et al.*, 2019). In the study of cone opsin, LMNG has also been found to increase stability which holds promise for structural and other studies (Owen *et al.*, 2018). Chemical structures for both DDM and LMNG are shown in Figure 5.1.

Dodecyl- β -D-maltoside (DDM)

Lauryl-maltose-neopentyl-glycol (LMNG)

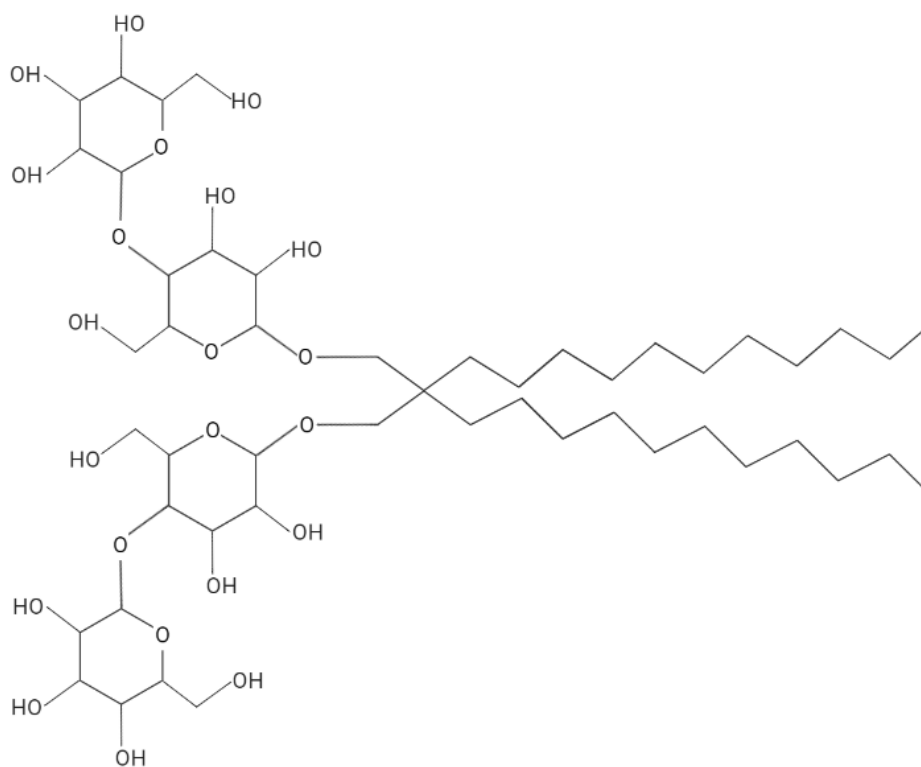


Figure 5.1 Chemical structure of DDM and LMNG

5.1.5 Aims

Here the aim was to assess functional properties of the rhodopsin and opsin mutant E122G, R252P, S298D and K311E alongside examining the use of LMNG for opsin purification and analysis.

5.2 Methods

5.2.1 Construction of stable HEK293S cell lines

The E122G, R252P and S298D cell lines were produced as described in Chapter 3 using Quikchange mutagenesis with pB007 NCO as the template. K311E was produced by the molecular cloning method described in Chapter 3, cloning the mutated rhodopsin from pMT4 into pACMV TetO and then into pB007. Mutagenic primers and sequencing are listed in Appendix 1 and 2.

5.2.2 Rhodopsin mutant production in HEK293S GnTI⁻ cells

This procedure is described in Chapter 2, section 2.6.

5.2.3 Purification of rhodopsin mutants in DDM

Rho-1D4-sepharose immunoaffinity purification was used for purification as described in Chapter 2.

5.2.4 Examination of rhodopsin mutant biochemical and spectral properties

Dark state acidification, photobleaching, Meta II stability and transducin activation for each of the mutants were performed and analysed. The methods used in this section are described in Chapter 2.

5.2.5 Solubilisation and purification purification of rhodopsin in detergent DDM or LMNG: a comparative study

A description of the methods for purification of rhodopsin can be found in Chapter 2, and buffer composition for LMNG based purification is shown in Table 5.1. Opsin and

rhodopsin with and without N2C D282C mutations was purified in DDM/LMNG (see Table 5.2). The biochemical properties of the opsin purified were then assessed.

LMNG concentrations were based on previous work for solubilisation and elution concentrations (green cone pigment) (Owen *et al.*, 2018). For transducin and Meta II stability assays CMC concentration was taken into account to give the equivalent to that used in DDM based assays.

Table 5.1 LMNG buffer compositions for purification and biochemistry.

Buffer	Composition
LMNG solubilisation	0.36% LMNG, 2 μ l PMSF made up to 1 ml total (including sample) with 1xPBS
LMNG low salt wash	10 mM BTP pH 7.2, 0.02% LMNG made up to required volume in MilliQ H ₂ O
LMNG low salt elution	10 mM BTP pH 7.2, 0.02% LMNG, 100 μ M 9mer elution peptide
LMNG high salt wash	10 mM BTP pH 7.2, 140 mM NaCl, 0.02% LMNG made up to required volume in MilliQ H ₂ O
LMNG high salt elution	10 mM BTP pH 7.2, 140 mM NaCl, 0.02% LMNG, 100 μ M 9mer elution peptide

Table 5.2 Rhodopsin and opsins purified in DDM and LMNG for use in comparative studies.

	DDM	LMNG
WT rhodopsin	✓	✓
N2C D282C rhodopsin	✓	-
WT opsin	-	✓
N2C D282C opsin	✓	-
E122G opsin	-	✓
R252P opsin	-	✓
S298D opsin	-	✓
K311E opsin	-	✓

5.2.6 Biochemical property comparison of rhodopsin in DDM and LMNG

A description of the methods for biochemistry can be found in Chapter 2, along with buffer composition for DDM based samples. For LMNG based samples, see Table 5.1.

5.2.7 Purification of opsin in LMNG

A description of the methods for purification can be found in Chapter 2. As described in 6.2.1, opsin and mutant opsins were purified in LMNG. The purified samples were then used to assess their pigment formation and pigment stability properties.

5.2.8 Pigment formation in LMNG

A description of the methods for pigment formation can be found in Chapter 2.

5.3 Results

5.3.1 Assessment of the expression of rhodopsin mutants using UV-vis absorption spectroscopy

Expression of rhodopsin mutant pigments was assessed using UV-vis difference spectra. The absorbance at λ_{\max} for each pigment was used in Beer-Lambert Law to determine the amount of rhodopsin pigment produced after induction of corresponding stable cell lines with tetracycline and sodium butyrate or with tetracycline alone in comparison to a non-induced control. For Beer-Lambert Law calculations, an assumed $\epsilon = 42700 \text{ M}^{-1} \text{ cm}^{-1}$ at the λ_{\max} and a molecular weight of 42300 Da was used. UV-vis difference spectra (Figure 5.2) and λ_{\max} values and mass of rhodopsin pigment produced were calculated (Table 5.3).

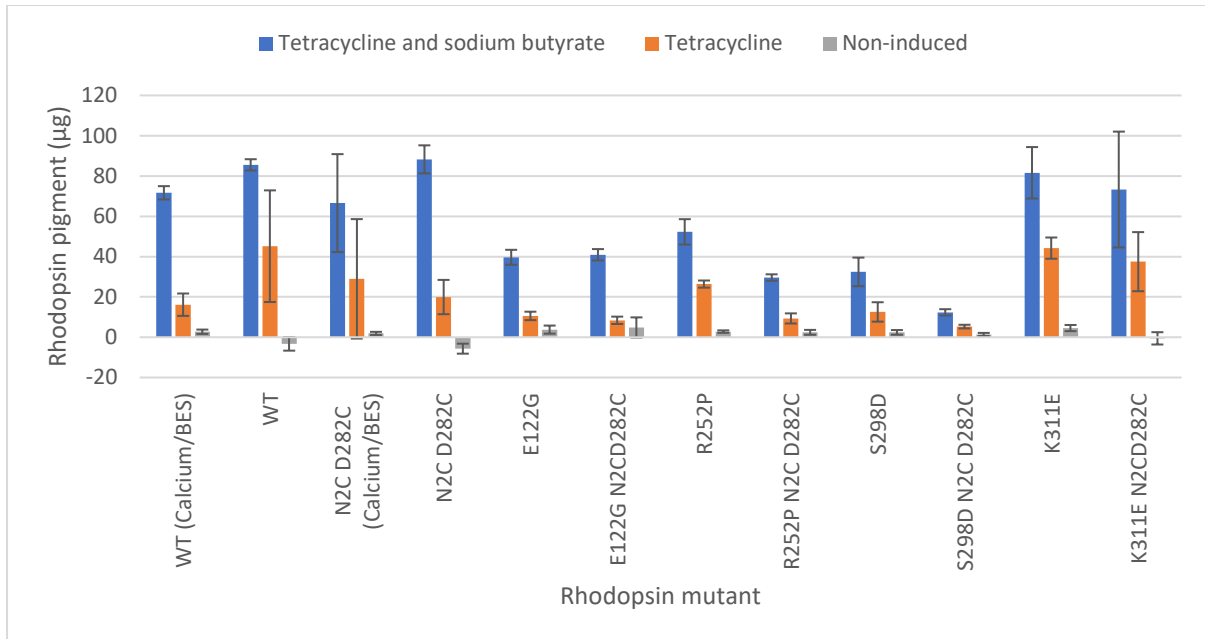


Figure 5.2 Rhodopsin pigment produced by induction of expression for the unclassified RP mutants. Induction of expression was carried out for 65 hours, using either tetracycline, tetracycline and sodium butyrate in complete DMEM. A non-induced control was carried out where only complete DMEM was added to the cells. Rhodopsin pigment was determined by UV-vis absorbance spectroscopy for each of the 10 cm cell culture dishes.

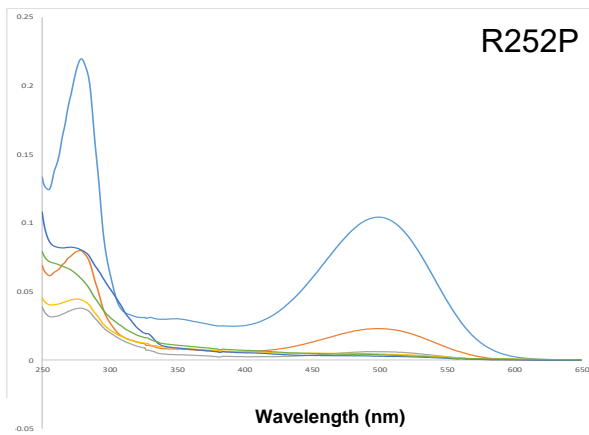
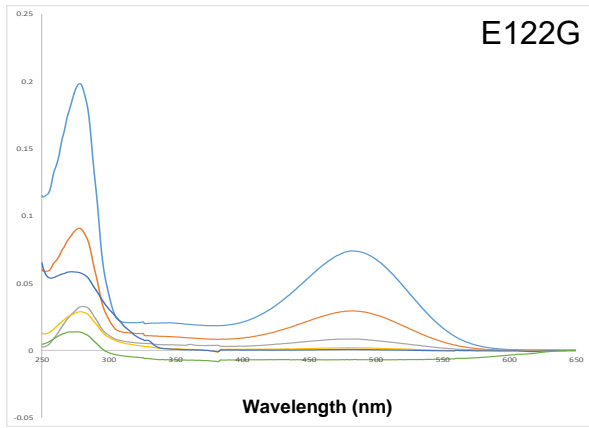
Table 5.3 Rhodopsin pigment expression when induced with varying conditions. Mean mass was calculated from their UV-vis absorbance difference spectra. Standard deviation is shown in columns S.D. and *n* for each is shown in the final column.

	Rhodopsin pigment when expressed using							<i>n</i> =
	Tetracycline and sodium butyrate		Tetracycline		Non-induced control			
	Mean mass (µg)	S.D.	Mean mass (µg)	S.D.	Mean mass (µg)	S.D.		
WT (Calcium/BES)	71.67	3.30	16.14	5.56	2.71	1.08	2, 3, 3	
WT	85.54	2.80	45.17	27.71	-3.27	3.39	3, 3, 3	
N2C D282C (Calcium/BES)	66.55	24.31	28.97	29.63	1.90	0.76	3, 3, 3	
N2C D282C	88.27	6.95	19.93	8.51	-5.68	2.48	2, 3, 3	
E122G	39.66	3.71	10.56	2.10	3.77	2.00	3, 3, 3	
E122G N2CD282C	40.91	2.82	8.39	1.83	4.86	4.99	3, 3, 3	
R252P	52.28	6.29	26.38	1.77	2.78	0.61	3, 3, 3	
R252P N2C D282C	29.60	1.61	9.32	2.51	2.43	1.21	3, 3, 3	
S298D	32.43	7.09	12.54	4.82	2.40	1.16	3, 3, 3	
S298D N2C D282C	12.35	1.56	5.27	0.91	1.40	0.74	3, 3, 3	
K311E	81.59	12.76	44.21	5.27	4.54	1.53	4, 4, 4	
K311E N2CD282C	73.29	28.74	37.50	14.66	-0.56	3.06	3, 3, 3	

5.3.2 Immunoaffinity purification of rhodopsin using the rho-1D4 antibody

Confluent cells on 15 cm cell culture dishes were induced with tetracycline and sodium butyrate for rhodopsin protein production. These were harvested and the cell suspensions treated with 11-*cis*-retinal. The cell suspensions were then solubilised, and the cell lysate used for 1D4-sepharose immunoaffinity purification of the rhodopsin and rhodopsin mutant pigments. Rhodopsin 1D4 immunoaffinity purification of the samples obtained most rhodopsin in low salt eluates 1-3. The maximum absorbance of WT rhodopsin and the mutants R252P, S298D and K311E was 500 nm; however, following purification E122G had a shifted maximum absorbance of 481 nm (Figure 5.3).

5. Characterisation of rhodopsin RP mutants: previously unclassified



Absorbance

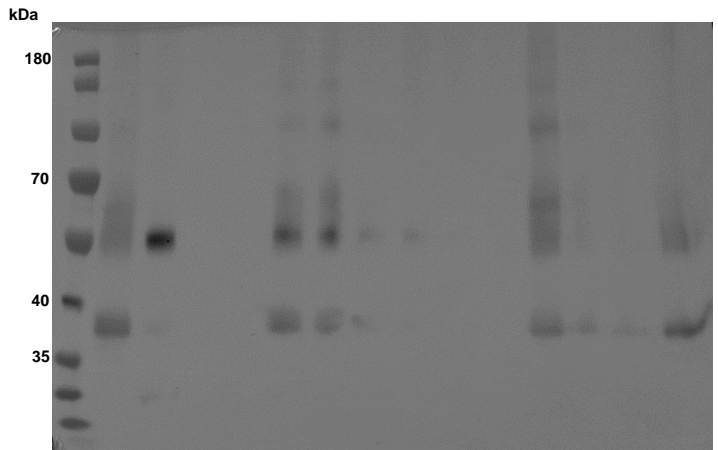
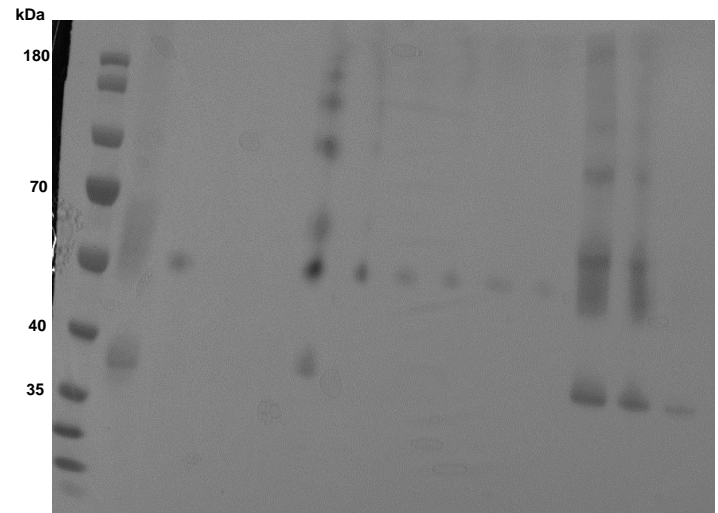
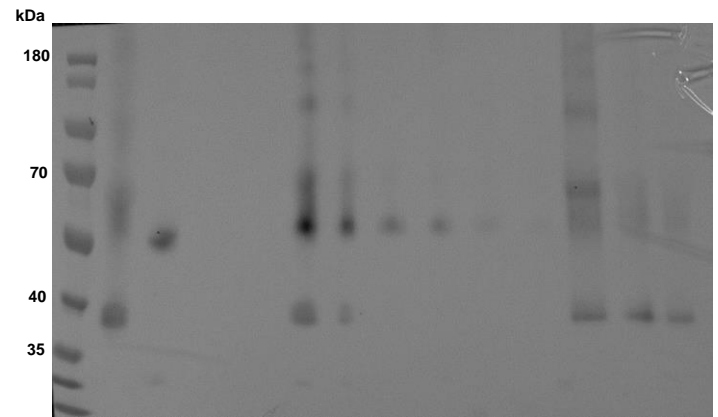
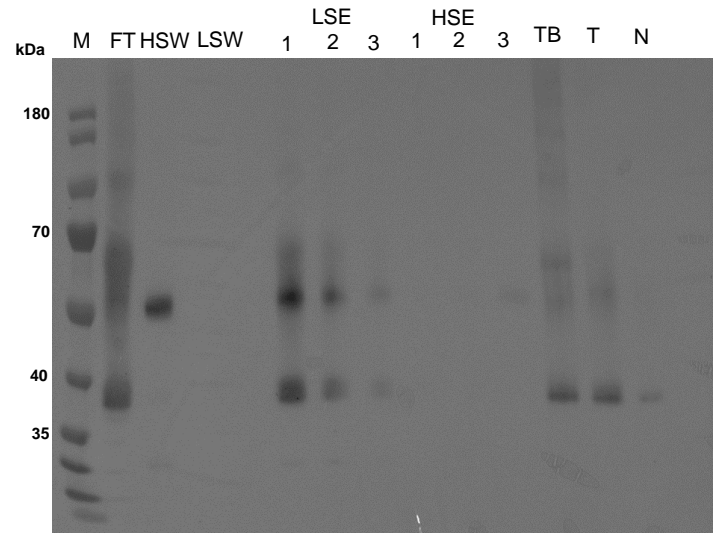
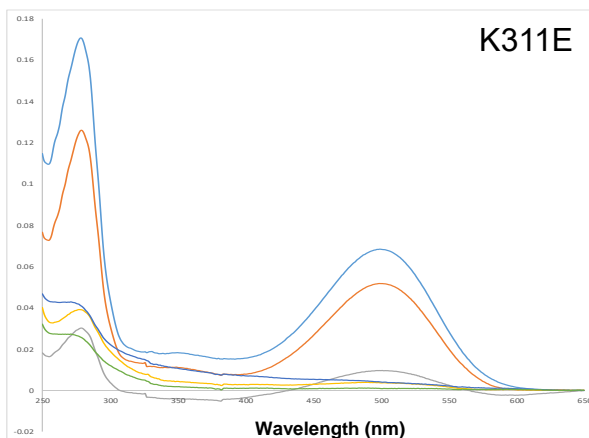
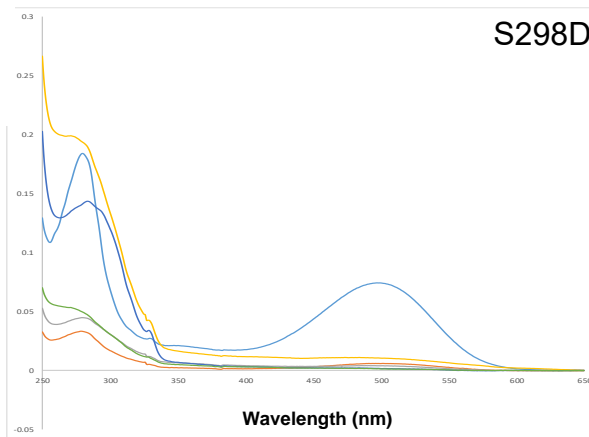


Figure 5.3 UV-vis absorbance spectra of elutions (A) and Western blot (B) for WT rhodopsin and the mutants E122G, R252P, S298D and K311E. Confluent 15 cm cell culture dishes were induced using 2 µg/ml tetracycline and 5 mM sodium butyrate in complete DMEM for differing lengths of time, and at 33°C or 37°C depending on the optimal time/temperature for expression of that mutant. After induction, the cells were harvested in 1x PBS before treatment with 5 µM 11-cis-retinal overnight. The treated cell suspensions were then purified using 1D4-immunoaffinity purification following which the elution samples LSE1-3 (1- blue, 2- orange, 3- grey) and HSE1-3 (1- yellow, 2- dark blue, 3- green), alongside flow through (FT) and high and low salt wash samples (HSW/LSW) were used for SDS-PAGE and Western blot by rho-1D4 antibody. The marker (M) is ThermoScientific PageRuler™ Prestained 10-180kDa Protein Ladder. Non-induced (N), tetracycline only (T) and tetracycline and sodium butyrate (TB) unpurified samples were used as controls.

5.3.4 Dark state acidification of rhodopsin

Acidification of the rhodopsin mutants in the dark state should reveal a shift from the 500 nm peak (rhodopsin) to 440 nm revealing the covalent Schiff base bond between the ligand 11-*cis*-retinal and lysine 296 of the protein (Opefi *et al.*, 2013). Upon acidification, this shift was observed in the WT and each mutant (Figure 5.4), showing that there is a Schiff base bond formed by each of these mutants and the 11-*cis*-retinal ligand.

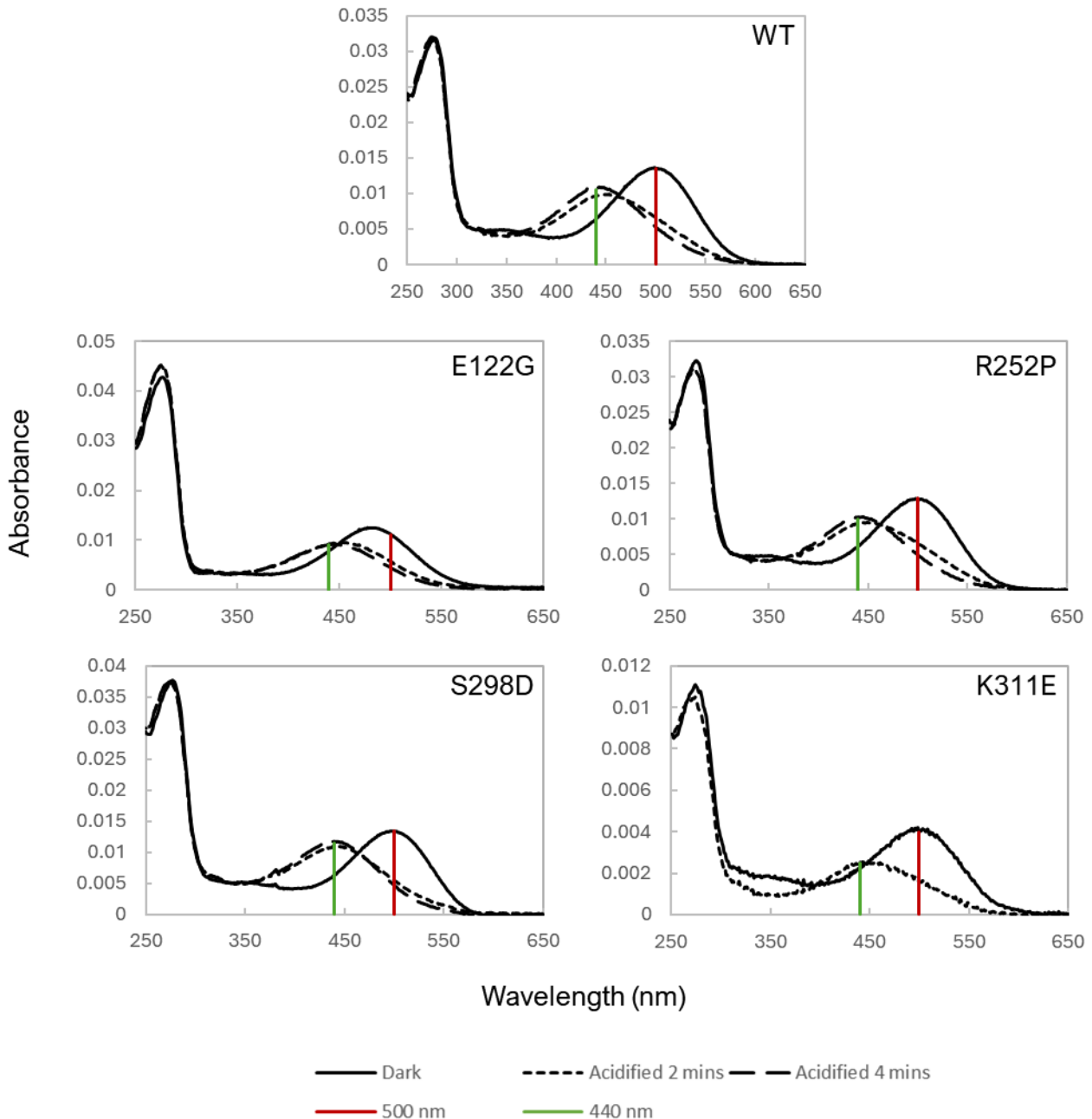


Figure 5.4 Acidification of rhodopsin RP mutants in their dark state. Purified rhodopsin was kept under dark conditions and a UV-vis spectrum was taken, following which 6 μ l 2N H_2SO_4 was added, and another UV-vis spectrum was taken. The dark state spectrum had a λ_{max} of 500 nm for the WT and all mutants except E122G, which has a shifted λ_{max} of 482 nm. Following the addition of 6 μ l 2N H_2SO_4 the λ_{max} shifted to 440 nm for WT and all mutants which shows the protonated Schiff base linkage between the opsin apo protein and 11-cis-retinal was present in each.

5.3.5 UV-vis absorption spectroscopy examination of rhodopsin photobleaching followed by acidification

When activated by light the receptor changes from a species which can be seen at 500 nm by UV-vis spectroscopy, to a species at 380 nm (Opefi *et al.*, 2013). The WT rhodopsin protein demonstrated this transition, as did each of E122G, R252P and K311E, with the majority of the 500 nm species (480 nm in the case of E122G which has a shifted max absorption) converting to 380 nm after 30 seconds of photobleaching (Figure 5.5). However, the mutant S298D showed abnormal photobleaching properties with a more gradual conversion to the 380 nm species over the course of four 30 second photobleach steps, where a UV-vis absorption spectrum was obtained between each. After photobleaching, acidification should cause a shift from the 380 nm species to 440 nm as described in the dark state acidification (Opefi *et al.*, 2013).

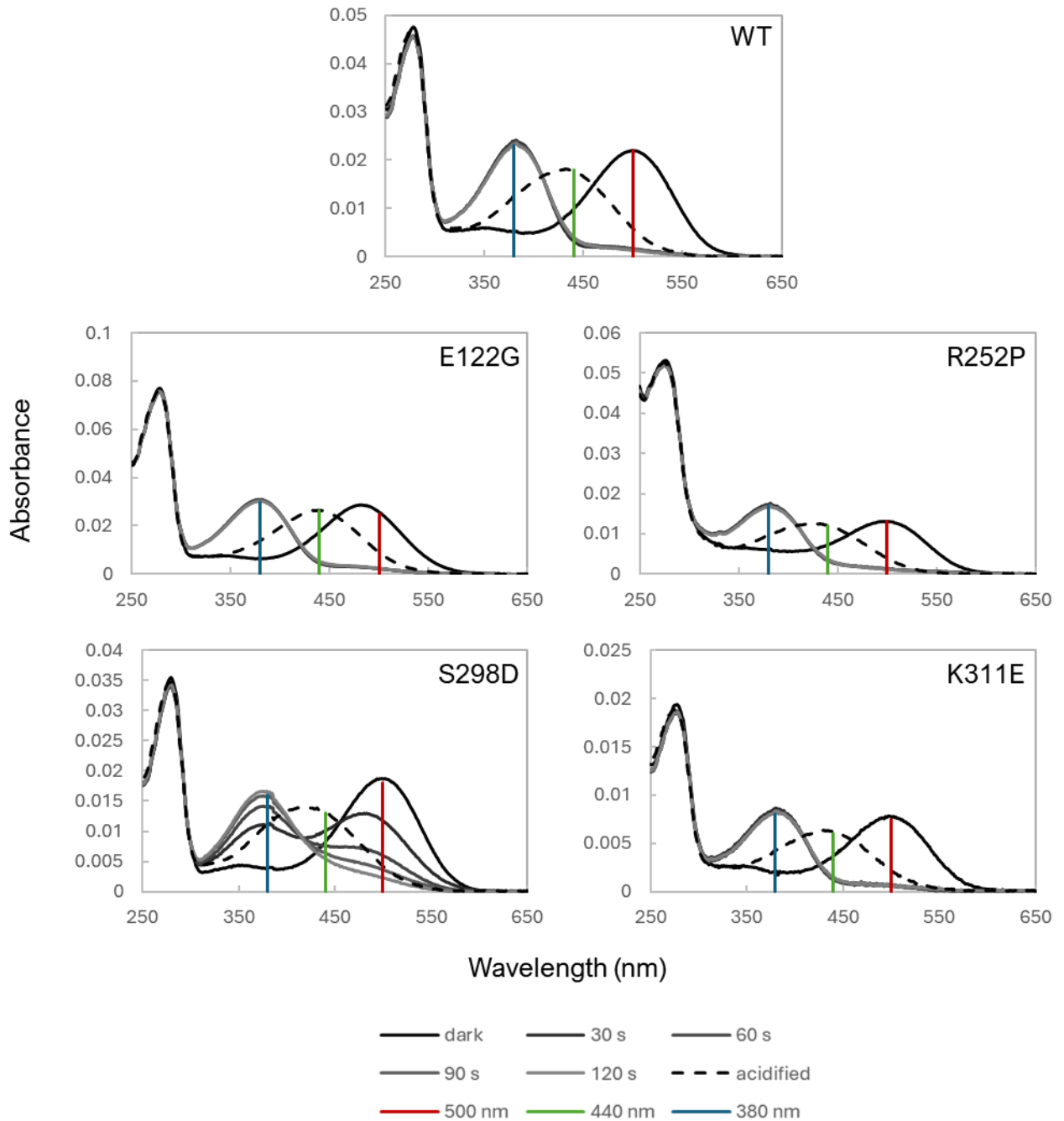


Figure 5.5 Acidification of rhodopsin RP mutants after photobleaching. Purified rhodopsin was kept under dark conditions and a UV-vis spectrum was obtained. Photobleaching for 30 seconds was then performed 4 times, with a UV-vis spectrum taken immediately after each. Finally of 6 μ l 2N H_2SO_4 was added, and a final UV-vis spectrum was recorded.

5.3.6 Rhodopsin active state (metarhodopsin II) stability

Upon activation by light, rhodopsin is converted to the Meta II conformation (Shichida and Morizumi, 2006). The process of Meta II decay, where all-*trans*-retinal is released from Meta II, can be followed by measuring the increase in fluorescence after rhodopsin has been photobleached (Farrens and Khorana, 1995; Opefi *et al.*, 2013). The stability of Meta II was assessed by monitoring the fluorescence increase caused by the release of all-*trans*-retinal, which can be measured by following the increase in tryptophan fluorescence (Farrens and Khorana, 1995).

Data was analysed using SigmaPlot and the parameters from curve fitting used to calculate the half-lives. WT rhodopsin had an average Meta II half-life of 17.67 minutes, R252P and K311E showed similar half-lives of approximately 13.87 and 18.69 minutes respectively. S298D was found to have a half-life of approximately 4.00 minutes, which is more than 4 times faster than WT rhodopsin. Whereas E122G showed Meta II stability more than twice as long as WT rhodopsin with a half-life of approximately 42.45 minutes. Representative curves are shown in Figure 5.6 and Table 5.4 shows the average half-lives and standard deviation.

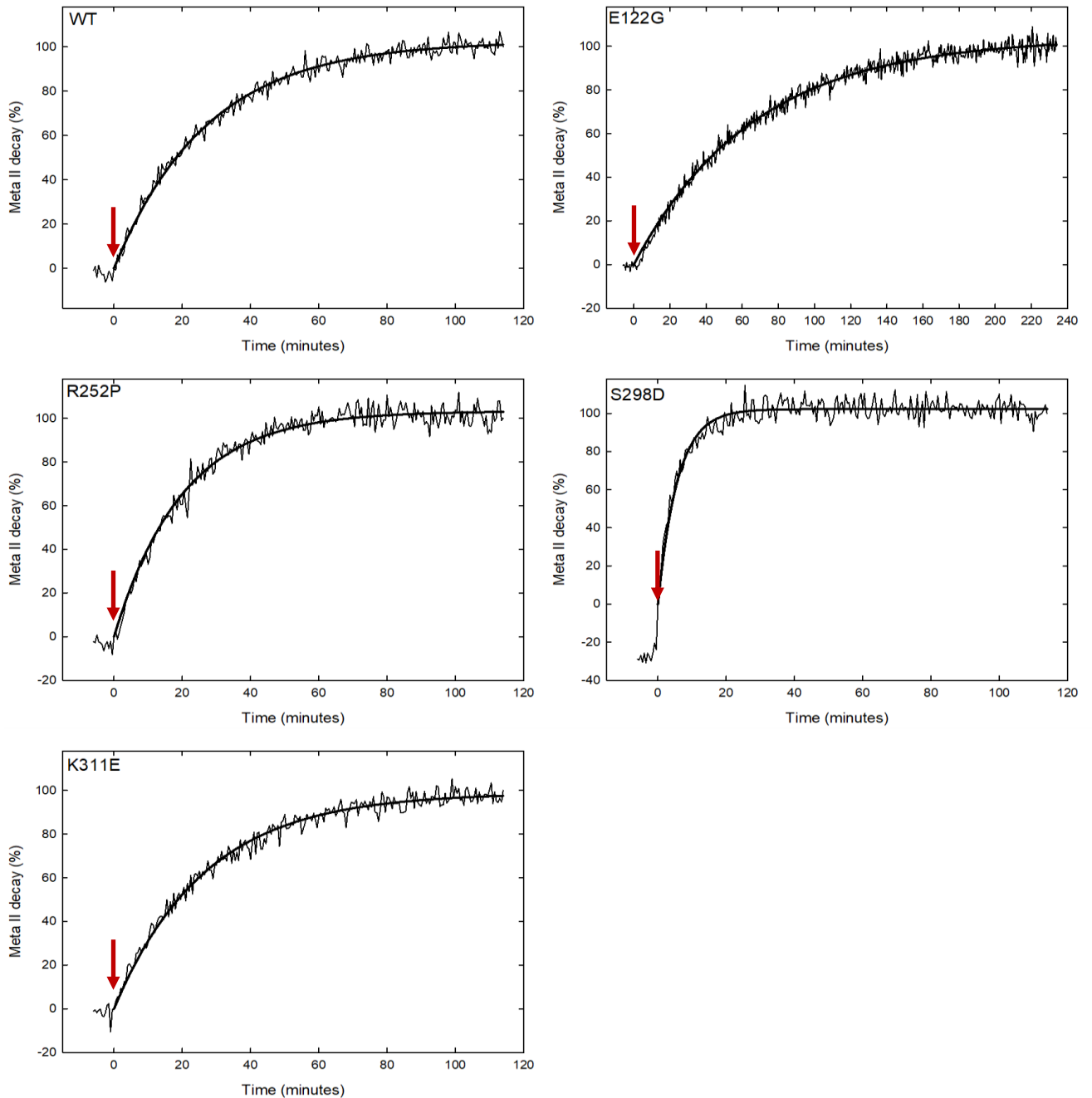


Figure 5.6 Meta II stability (active state) of rhodopsin RP mutants. Meta II stability was measured by photobleaching rhodopsin and measuring the increase in fluorescence. The rhodopsin and mutants were subjected to illumination for 30 seconds at time = 0, indicated by the red arrows. WT rhodopsin has a half-life of approximately 17.67 minutes. R252P and K311E have similar half-lives to that of the WT (13.87 and 18.69 minutes respectively). S298D has a shorter half-life of 4.00 minutes. E122G has a greatly extended half-life of 42.45 minutes.

5.3.7 Ability of rhodopsin and mutants to activate transducin

Fluorescence observed when transducin activation occurs is a consequence of the change in position of tryptophan 207 in the alpha subunit. This transition which is trapped by the bound non-hydrolysable GTP γ S allows the activation of transducin by rhodopsin to be measured (Phillips and Cerione, 1988; Faurobert *et al.*, 1993). The assay demonstrates the ability of rhodopsin to activate transducin which initiates signal transduction pathway resulting in vision (Opefi *et al.*, 2013).

The initial rate of transducin activation was similar for the WT and R252P rhodopsin. E122G rhodopsin did show a change in the fluorescence, albeit at a slow rate. The S298D rhodopsin resulted in a minimal fluorescence change. Transducin activation traces are shown in Figure 5.7 and their relative initial rate and standard deviation are shown in Table 5.4.

Table 5.4 Meta II decay and transducin activation characteristics of WT and rhodopsin RP mutants.

	Meta II			Transducin activation		
	Half-Life (mins)	S.D.	<i>n</i> =	Relative rate	S.D.	<i>n</i> =
WT	17.67	1.76	11	1.00	0.0007	14
E122G	42.45	3.07	7	0.45	0.0002	8
R252P	13.87	0.53	8	0.85	0.0005	9
S298D	4.00	0.38	7	0.30	0.0002	8
K311E	18.69		1	0.76	0.0003	3

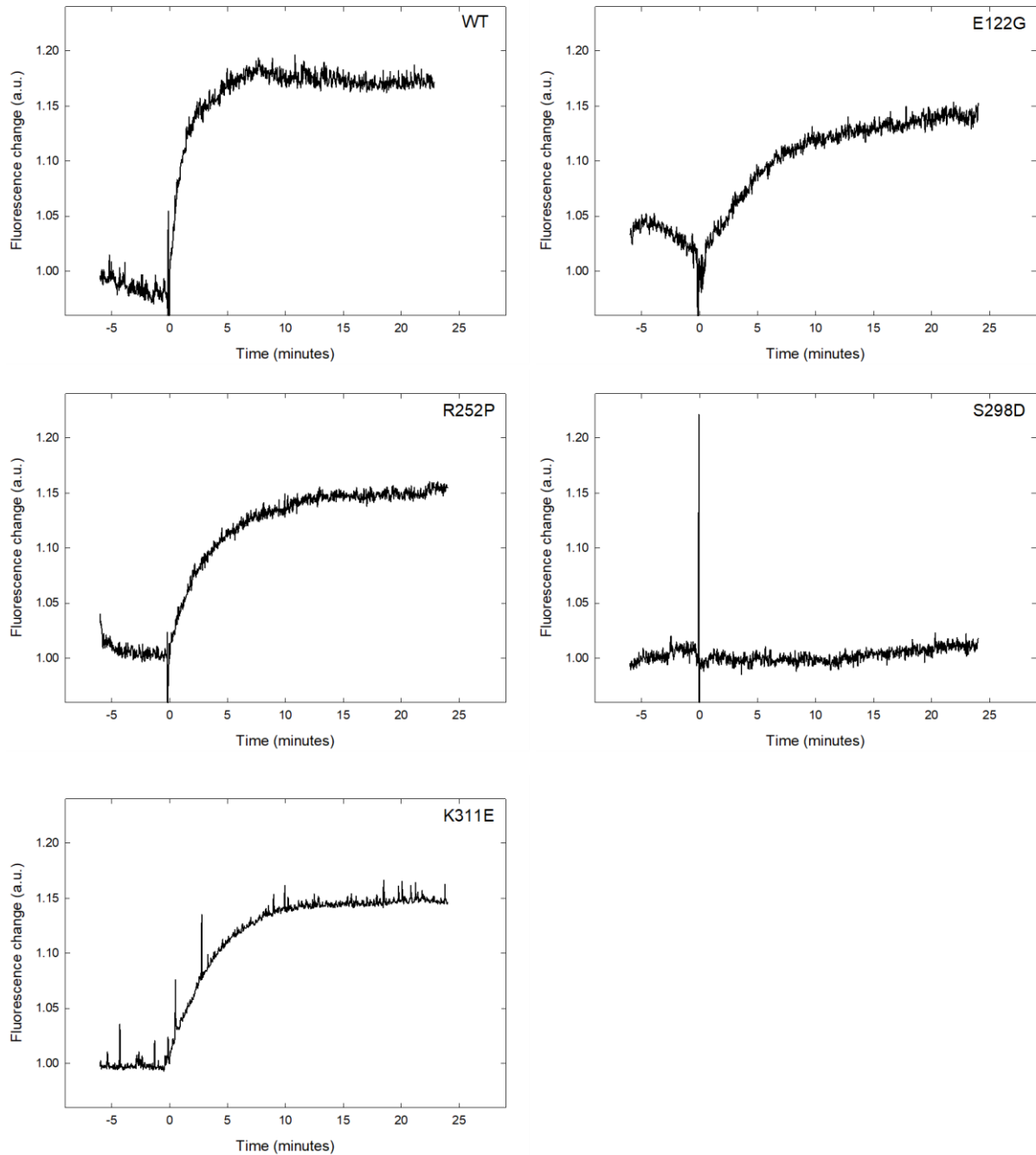


Figure 5.7 Transducin activation of rhodopsin RP mutants. Activation of transducin was determined by photobleaching of rhodopsin in buffer containing transducin, followed by the addition of GTP γ S at time = 0.

5.3.8 Comparison of rhodopsin purified in DDM or LMNG

Rhodopsin was purified in LMNG, and its properties were compared to rhodopsin or N2C D282C rhodopsin purified in DDM. Upon purification of rhodopsin in buffer containing either DDM or LMNG the majority of the rhodopsin pigment was eluted in the first low salt eluate (LSE1) (Figure 5.8). Yields were calculated using Beer-Lambert Law using absorbance value at 500 nm. Further correctly folded rhodopsin pigment was eluted in LSE2 and LSE3, albeit at much lower amounts.

Following low salt elutions further high salt elutions were performed to recover misfolded rhodopsin. The absorbance at 500 nm was very low, signifying that minimal misfolded rhodopsin pigment was present.

The total rhodopsin pigment yield was calculated, and based on a difference spectrum of an aliquot of the sample pre-purification a percentage yield of rhodopsin pigment was then calculated. Overall, as shown in Table 6.3, on average 58% of the rhodopsin pigment in DDM purified from the clarified lysate, and the rhodopsin pigment in LMNG was on average 83% purified.

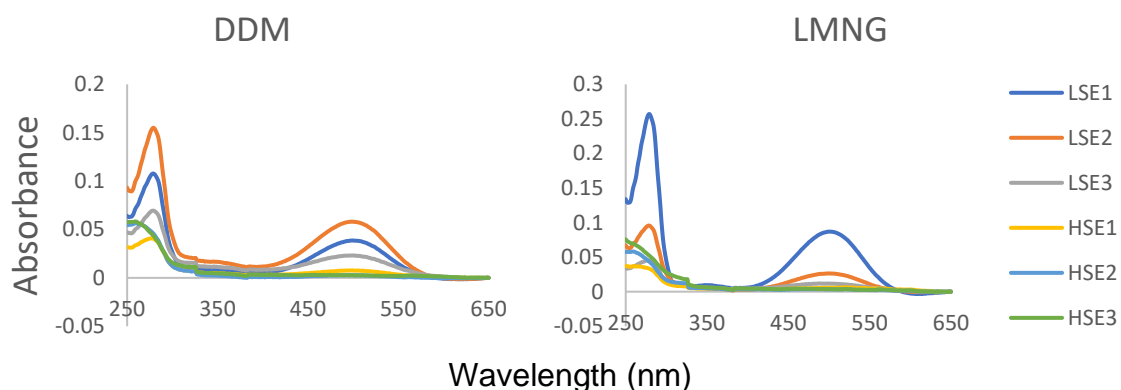


Figure 5.8 WT rhodopsin expressed by HEK293S purification in DDM or LMNG

5.3.9 Meta II stability and transducin activation ability of rhodopsin purified in LMNG

Meta II stability and transducin activation ability of rhodopsin can be affected by the buffer composition in which these assays are performed, with both being highly sensitive to changes in concentration. Therefore, determining the meta II stability and transducin activation ability of rhodopsin purified in LMNG was required. Figure 5.9 shows meta II stability traces of rhodopsin in DDM or LMNG and transducin activation ability of rhodopsin in DDM and LMNG. The activity of rhodopsin in LMNG is given as a percentage of its activity in DDM.

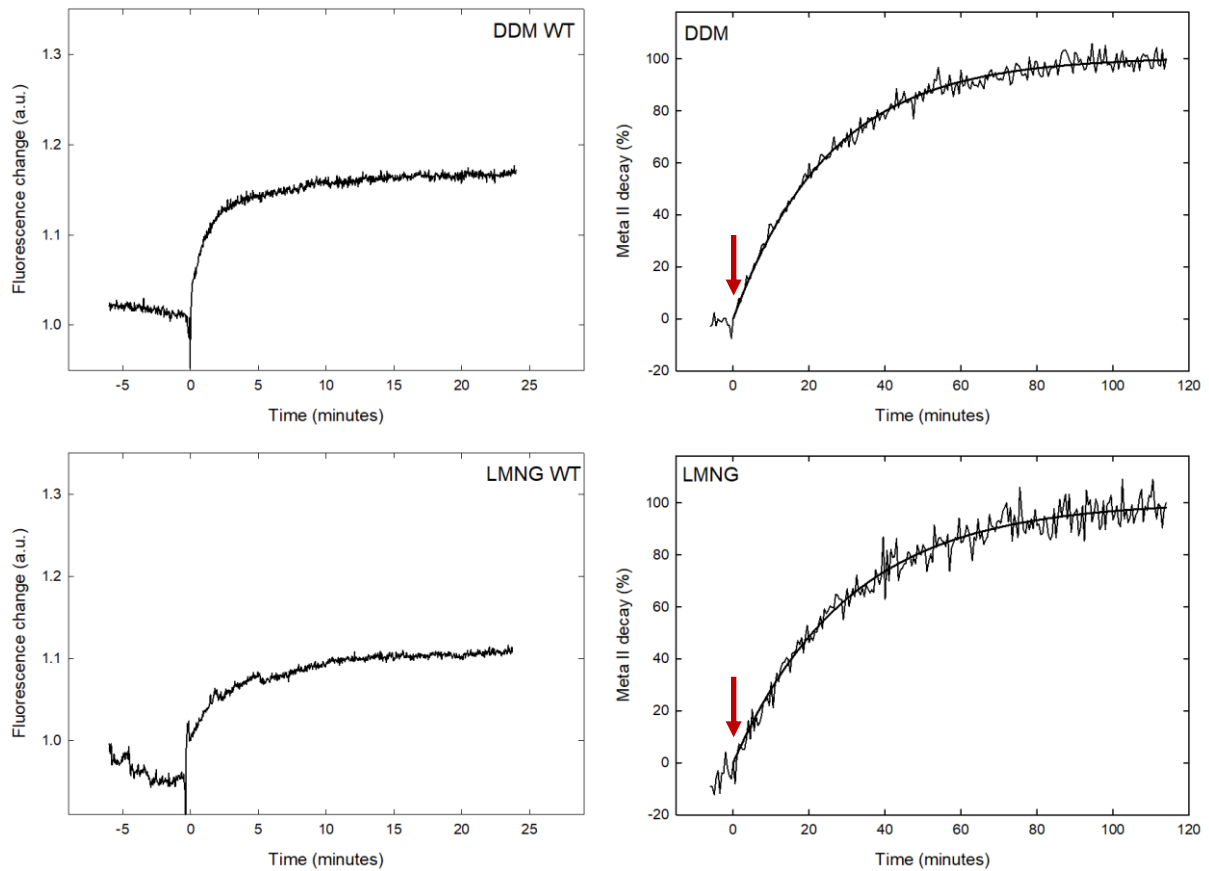


Figure 5.9 Meta II and transducin activation in LMNG and DDM. Meta II stability was measured by photobleaching rhodopsin and measuring the increase in fluorescence. The rhodopsin and mutants were subjected to illumination for 30 seconds at time = 0, indicated by the red arrows. Activation of transducin was determined by photobleaching of rhodopsin in buffer containing transducin, followed by the addition of GTP γ S at time = 0.

5.3.10 Purification of opsin and RP mutant opsins in LMNG

Opsin and mutant opsins were purified in LMNG. The opsin protein content in each was determined using the A_{280} value and Beer-Lambert Law. Stable and regeneration competent N2C D282C opsin can be purified in DDM, however WT opsin is unable to be purified in stable form in this buffer. In LMNG, WT opsin demonstrates a good purification profile. For both N2C D282C opsin in DDM and WT opsin in LMNG, immunoaffinity purification was performed and the majority of protein being rod opsin was eluted in LSE1, followed by LSE2 (Figure 5.10). LSE3 contained low levels of opsin in each, and similarly low levels were seen in all HSEs. Likewise, N2C D282C rhodopsin immunoaffinity purification resulted in a similar pattern in elutions.

As purification of WT opsin was found to be effective when using LMNG as a solubilisation detergent, and in the LMNG containing elution buffers, pigment formation properties and stability of opsin could be measured.

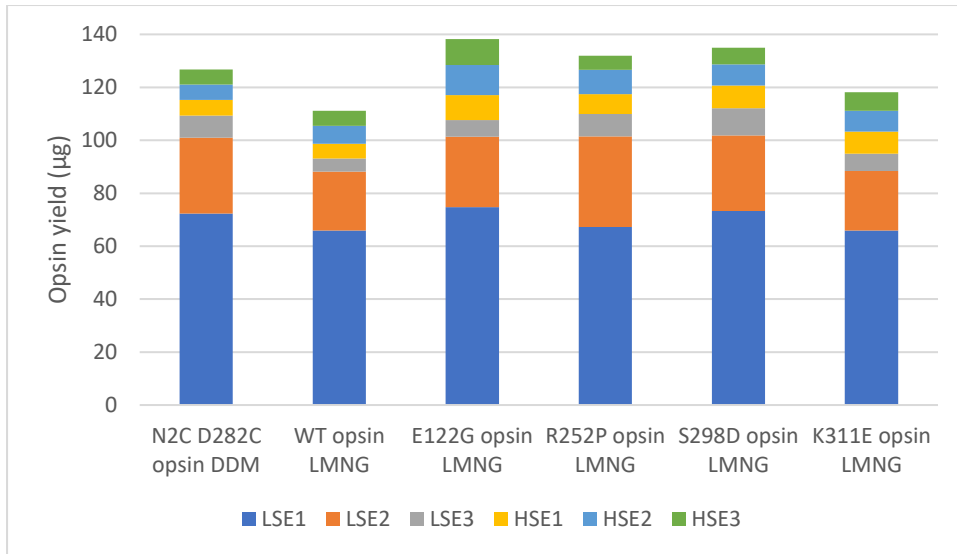


Figure 5.10 Recovery of opsin and RP mutant opsins purified in LMNG. Opsin and mutant opsins were solubilised, washed and eluted using LMNG based buffers. Alongside, N2C D282C opsin was purified in the equivalent DDM based buffers. UV-vis spectroscopy was used to estimate the protein present and Beer-Lambert law was used to calculate the yield of opsin.

5.3.11 Pigment formation in LMNG

Upon addition of 11-*cis*-retinal to opsin, the formation of the rhodopsin pigment can be monitored by the increase in absorbance at 500 nm. N2C D282C opsin in both DDM and LMNG was compared, along with the inclusion of WT opsin, and the opsin mutants E122G, R252P, S298D and K311E all in LMNG. The initial rate of pigment formation was calculated (Figure 5.11).

The initial rate of pigment formation of N2C D282C opsin formed in either DDM or LMNG based buffers were very similar (0.030 and 0.0362 $\mu\text{g sec}^{-1}$ respectively). The mutant K311E also had a similar rate of pigment formation (0.0379 $\mu\text{g sec}^{-1}$).

The WT opsin and R252P opsin mutant generated the rhodopsin pigment slightly slower, with initial rates of 0.0214 and 0.0237 $\mu\text{g sec}^{-1}$ respectively. The mutant S298D had an initial rate for pigment generation of 0.0166 $\mu\text{g sec}^{-1}$ and E122G had the slowest initial rate of the mutants in this experiment, with an initial rate of 0.0104 $\mu\text{g sec}^{-1}$, which is about half that of WT opsin.

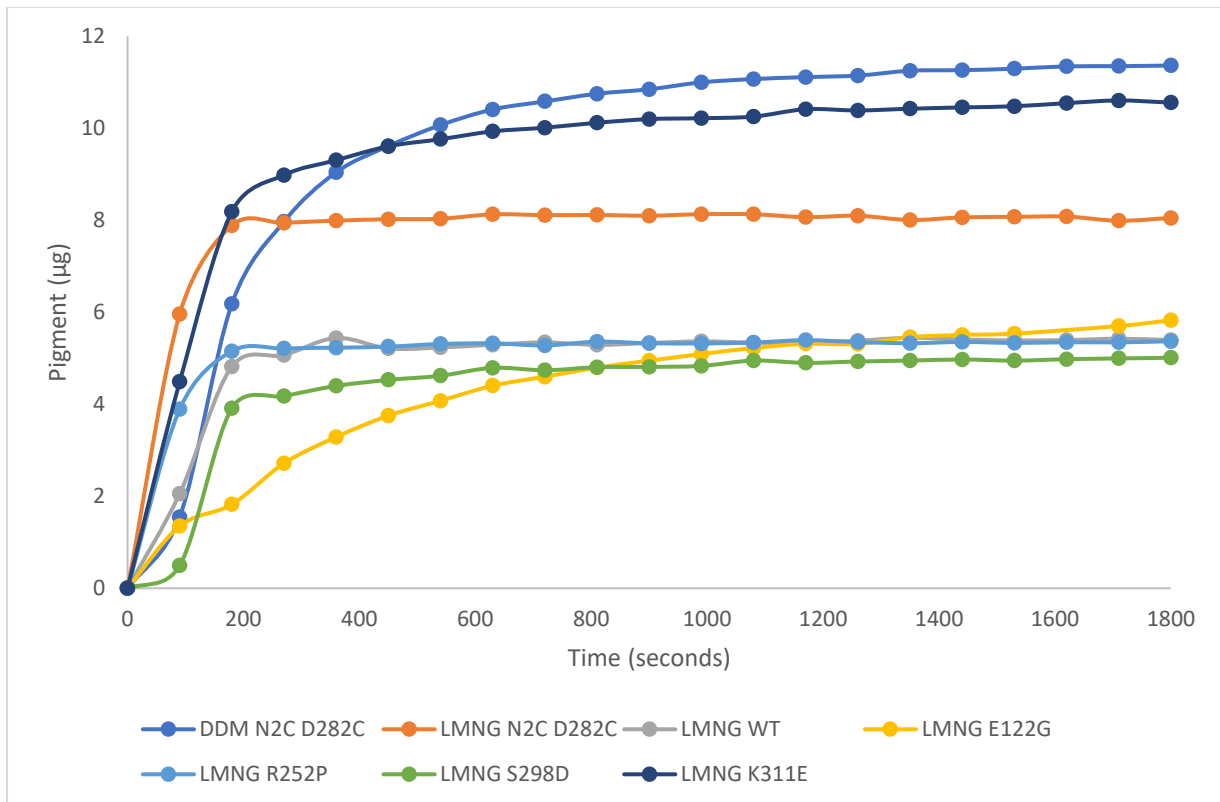


Figure 5.11 Rates of pigment formation by opsin and opsin mutants over 30 minutes in LMNG. The N2C D282C mutant in DDM or LMNG was able to form pigment faster than WT opsin in LMNG. The K311E opsin RP mutant was able to form pigment faster than the WT and N2C D282C mutants. R252P formed pigment at a similar rate to that of WT. S298D had a slightly slower rate of pigment formation and E122G had the lowest rate of pigment formation approximately half that of WT opsin.

5.4 Discussion

5.4.1 Use of the detergent LMNG for the purification and biochemical examination of rhodopsin and opsin.

The detergent DDM has previously been used for purification of GPCRs including rhodopsin (Xie *et al.*, 2003; Opefi *et al.*, 2013). The instability of rod opsin in this detergent meant that it was not previously possible to purify opsin in its stable form capable of combining with its 11-*cis*-retinal ligand to form pigment (Opefi *et al.*, 2013). The increased density of alkyl chains around the TM region of GPCRs shown by Lee *et al.* (2020), and increased interactions between head groups and head group to protein provides an explanation for the increased stability of GPCRs in LMNG compared to DDM. Here, it was shown that rod opsin could be purified in LMNG.

As WT opsins are too unstable to be purified in DDM in a stable form, studies of pigment formation had to be performed using either CHAPS/DMPC mixed micelles or N2C D282C stabilisation mutations in order for purification to be possible. However, as opsins in LMNG remain stable and are able to be purified, WT opsin pigment formation kinetics and WT opsin stability were able to be determined.

Transducin activation initial rates by rhodopsin in LMNG was lower than DDM, but activity was still enough to be measured and compared. The large number of hydrogen bonds found both between pairs head groups and between head groups and the protein was suggested to be responsible for the reduced flexibility of receptors, explaining why GPCRs may be more active in DDM (Lee *et al.*, 2020). This is echoed through the data presented here, showing that the ability for rhodopsin to activate transducin is reduced in WT rhodopsin.

5.4.2 Characteristics of the rhodopsin RP mutants E122G, R252P, S298D and K311E

The extended half-life of Meta II of the E122G mutant, might suggest the path of pathogenicity is through its extended activation of transducin. As previously found in the mutants G90D (CSNB) and G90V (RP) (Rao *et al.*, 1994; Sieving *et al.*, 1995; Dizhoor *et al.*, 2008; Toledo *et al.*, 2011). The extended meta II half-life of E122G suggests that E122 is a crucial position with regards to the stability of rhodopsin following its activation with light. Coupling these results with previous work which showed E122 to be a functional determinant between rod and cone pigments it further infers the importance of this residue in rhodopsin specific function (Imai *et al.*, 1997). E122G was also found to have a reduced ability to activate transducin suggesting the mutation may result in incorrect signalling. These results show similarities to that of mutations found at R135 (G/L/P/W) which are clinically severe, and the residue was suggested to have an important role in G-protein signalling (Cideciyan *et al.*, 1998; Iannaccone *et al.*, 2006; Athanasiou *et al.*, 2018). Together the results suggest that E122G may be a class three mutation and further work to establish whether it results in signalling other G-proteins, RK, GRK or arrestin, if it has constitutive activity and whether its subcellular localisation is altered would be necessary. The exact mechanism by which E122G causes RP remains elusive however NMR analysis may uncover differences in the activation pathway and this line of thought was further probed and is discussed in Chapter 6.

The half-life of Meta II in S298D mutant rhodopsin was greatly decreased, to 4 minutes. S298D also displayed abnormal photobleaching properties, taking 120 seconds of photobleaching to convert to the 380 nm species. After photobleaching, this mutant converted to the 440 nm species upon acidification, and in the dark state

it converted to the 440 nm species more readily than the WT following acidification. The work on S298D suggests it potentially being a class four mutation due to it appearing to fold but exhibiting instability echoing mutants of the N-terminus (Opefi *et al.*, 2013).

Meta II stability, photobleaching and acidification properties of R252P and K311E were similar to that of WT rhodopsin. These RP mutants remain enigmatic with no clear differences to WT rhodopsin were observed. R252P also exhibited similar transducin activation capabilities (93%) compared to WT, and K311E was able to activate transducin at approximately 75% the relative rate compared to WT. These mutations will therefore need further studies to determine the mechanism by which they cause RP. Further work using LMNG to determine their pigment formation and regeneration capabilities and determining their thermal stability may help with their classification. Furthermore, by studying their subcellular localisation and trafficking Class 1 characterisation could be possible. Finally, by establishing if these mutations are constitutively active or have altered interactions with cytoplasmic proteins could direct their classification to Class 5 or 6 due to both their locations being on or in close proximity to the cytoplasmic side of rhodopsin (Deupi, 2013; Athanasiou *et al.*, 2018).

Overall, the use of LMNG for the purification and analysis of opsin RP mutants has been shown to have promise for their further characterisation. In addition, the characterisation of 2 rhodopsin RP mutants has resulted in likely classifications being established. E122G appears to have similar characteristics to the Class 3 mutants which occur at R135, however determining if this mutant is constitutively active is also required as it may be a Class 6 mutant. S298D shows similarities in its characteristics to mutants in the N-terminal domain, which are characterised as Class 2/4 mutants. Characterisation of mutants through these methods will continue to help build

understanding of the mechanisms which cause RP and how rhodopsin structure and function is affected, which may impact future methods of treatment of the disease.

6. The role of residue E122 in the stability of the metarhodopsin II intermediate

6.1 Introduction

6.1.1 The Opsin Family

Rhodopsin is part of the opsin family of proteins, GPCR's which share many common structural features (Tarttelin *et al.*, 2003). GPCR's are receptors with 7 transmembrane (TM) helices and in the seventh TM helix of opsins residue 296 (based on rhodopsin) lysine forms a bond to its cognate ligand 11-*cis*-retinal (Ebrey and Koutalos, 2001). Other conserved features include the DRY motif in helix 3 and E113 counterion to K296 (Ebrey and Koutalos, 2001; Tarttelin *et al.*, 2003). Aside from rhodopsin there are several other opsins with varied functions as light sensors in different tissues of the body. These include the blue, green and red photoreceptors as well as panopsin, melanopsin and neuropsin (Provencio *et al.*, 1998; Blackshaw and Snyder, 1999; Tarttelin *et al.*, 2003; Duda *et al.*, 2020; Suh *et al.*, 2020).

Opsins can be categorised into groups. Ciliary opsins are characterised by a cyclic signalling cascade and include the different opsins found in vertebrate photoreceptors (Suh *et al.*, 2020). Rhabdomeric opsins utilise a phosphoinositol signalling cascade and include melanopsin and invertebrate visual opsins (Suh *et al.*, 2020). Tetraopsins are the least studied group with poor characterisation; they include peropsin, neuropsin and retinal G-protein coupled receptor opsins (Suh *et al.*, 2020). It has been suggested that tetraopsins may be involved in the conversion of retinal from *trans* to *cis* forms (Leung and Montell, 2017; Morshedien *et al.*, 2019; Zhang *et al.*, 2019; Suh *et al.*, 2020).

The ciliary opsins include rhodopsin, and blue, green and red cone opsins (Suh *et al.*, 2020). Rhodopsin is the major photoreceptor located in the rod cells of the retina. In the cone cells, colour specific cone opsins are present which mediate response to different wavelengths of light. Rhodopsin absorption λ_{\max} is in the visible region between 495-500 nm (Nathans *et al.*, 1986). In humans, OPN1SW (short wave) is the blue cone photoreceptor, OPN1MW (medium wave) is the green cone photoreceptor and OPN1LW (long wave) is the red cone photoreceptor (Nathans *et al.*, 1986). The wavelength of the cone opsin λ maximum is dependent on the cone type, with blue at 420 nm, green at 530 nm and red at 560 nm (Nathans *et al.*, 1986).

OPN3 is also part of the ciliary opsin group (Suh *et al.*, 2020). It was the first opsin type to be found outside of the retina and was initially discovered at high abundance in the mouse brain (Blackshaw and Snyder, 1999) It was referred to originally as encephalopsin and then panopsin following its detection in a wider range of tissues including the liver and retina in addition to the brain where it was first found (Blackshaw and Snyder, 1999; Halford *et al.*, 2001). In the skin, OPN3 has been found to be the receptor involved in blue-light induced melanogenesis (Espósito *et al.*, 2021).

OPN4, known as melanopsin was discovered in *X. laevis*, in photosensitive dermal melanophores (Provencio *et al.*, 1998). It is also present in the brain, iris, and cells of the Inner Nuclear Layer (INL) of the retina (Provencio *et al.*, 1998). Melanopsin is part of the rhabdomeric opsin group (Suh *et al.*, 2020). It has multiple known functions, aside from a role in vision it also is involved in the pupillary light reflex, sleep circadian rhythms and cognitive functions (Duda *et al.*, 2020). Neuropsin (OPN5) was discovered in 2003 in the eye, brain, testis and spinal cord in mice and humans and is one of the tetraopsins (Tarttelin *et al.*, 2003; Suh *et al.*, 2020). Vertebrate neuropsins may be involved in the inhibition of adenylyl cyclase (Leung and Montell, 2017). Other

tetraopsins may be isomerise retinal from *trans* to *cis* forms (Morshedian *et al.*, 2019; Zhang *et al.*, 2019).

6.1.2 Residue 122 in opsins

Located in transmembrane (TM) helix 3 of rhodopsin, residue 122 is the amino acid glutamic acid in both human and bovine rhodopsin (Kazmin *et al.*, 2015). It is highly conserved in rhodopsin, having been set as E122 350 million years ago; however, the residue at position 122 varies between the different opsin types where isoleucine, leucine and cysteine are the next most common (Castiglione and Chang, 2018).

Rhodopsin E122 is in close proximity to the 11-*cis*-retinal ligand (Figure 6.1) (Ahuja *et al.*, 2009b). It forms a hydrogen bond to H211 on TM helix 5 in the inactive state (Bhattacharya *et al.*, 2008). Activation of rhodopsin occurs due to light mediated isomerisation of the 11-*cis*-retinal ligand, displacement of EL2 and consequential movement of helix 5 where H211 is located (Ahuja *et al.*, 2009a; Hornak *et al.*, 2009). This leads to breakage of the E122-H211 hydrogen bond (side chain to backbone) and allows H211-W265 hydrogen bond formation (Bhattacharya *et al.*, 2008; Hornak *et al.*, 2009). In addition to the H211-W265 bond, H211 also forms a hydrogen bond between its indole group and the E122 sidechain helping stabilise the active form of rhodopsin (Pope *et al.*, 2013).

In other opsins different residues are found at the equivalent position to E122 in rhodopsin. In chicken cone pigments glutamine and isoleucine are found (green and red pigments respectively) (Imai *et al.*, 1997). Studies of the mutation E122Q in rhodopsin revealed a shift in rhodopsin properties to that of cone pigments, with a 10x shortened Meta II lifetime observed alongside 70% photosensitivity and 80% single photon response in comparison to WT rhodopsin (Imai *et al.*, 1997). Visual pigment

regeneration was also faster in E122Q and E122I (Imai *et al.*, 1997). Therefore residue 122 determines many properties of the visual pigments (Imai *et al.*, 1997).

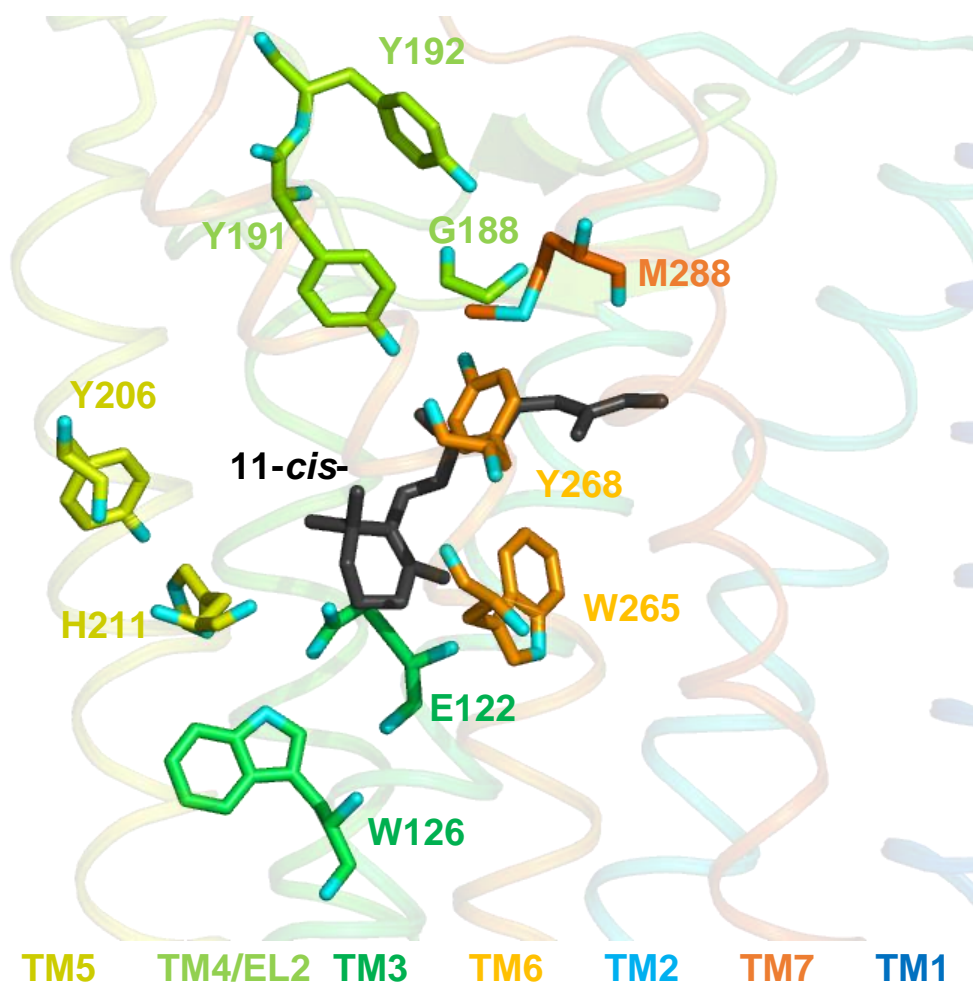


Figure 6.1 Key residues around the retinal binding pocket. E122 (green, TM3) is located close to the retinal as is H211 (dark yellow, TM5) between which a hydrogen bond is formed. Image created using PyMOL and PDB 1U19.

6.1.3 Aims

Here the aim was to determine the functional effects of incorporating other opsin residues into the E122 position of rhodopsin in an attempt to understand at a molecular level the pathogenesis of the rhodopsin RP mutant E122G.

6.2 Methods

6.2.1 Alignment of opsin sequences

Alignment of opsin sequences was performed using the sequence alignment tool from the GPCRdb (Isberg *et al.*, 2016; Kooistra *et al.*, 2021). The TM3 sequences of rhodopsins, OPN3, OPN4, OPN5, OPN1SW, OPN1MW and OPN1LW were aligned and position 3.37 was analysed by residues present.

6.2.2 Construction of the mutant PiggyBac plasmids

Mutagenic primers were designed for E122G, E122C, E122I, E122L, E122M and E122Q (see Appendix 1). Quikchange mutagenesis of pMT4-rho was performed, using a pMT4 plasmid where a *KpnI* had replaced *EcoRI* meaning that rhodopsin was flanked by *KpnI* and *NotI*.

In the cases of E122G and E122Q the mutagenesis was also performed in pMT4-rho with N2C D282C mutations already incorporated. Molecular cloning was then used to incorporate the mutant rhodopsin first into pACMV-TetO and then into pB007. Further details of the cloning steps can be found in Chapter 2.

6.2.3 Construction of stable HEK293S cell lines expressing E122 mutants

The mutants E122C, E122G, E122I, E122L, E122M and E122Q in pB007-NCO was replicated in using *E. coli* and a small-scale preparation was purified and the sequences confirmed (see Chapter 2). The purified plasmids were then used to stably transfect HEK293S cells (see Chapter 2). Cells were grown on 10 cm cell culture dishes in DMEM/F12 supplemented with 10% heat inactivated FBS, 1% PenStrep and 2 mM L-Glutamine for 7 days to allow for transposon insertion into the genome of the cells. Geneticin was then used for selection at 2 mg/ml and then maintenance at 500

µg/ml 7 days after transfection. Cell line stocks were made by freezedown and stored in liquid nitrogen (see Chapter 2).

6.2.4 Expression of the E122 mutants in HEK293S cells

Two 10 cm cell culture dishes were used to determine expression. Each cell line was grown to confluence, and then induced using 2 µg/ml tetracycline and 5 mM sodium butyrate. Induction was carried out for 65 hours, after which the cells were harvested in 1x PBS (see Chapter 2).

6.2.5 Analysis of the E122 mutant rhodopsin proteins

The 2 cell suspensions for each cell line were then treated, one with 20 µM 9-*cis* retinal and the other with 11-*cis*-retinal. 9-*cis* retinal treated samples were used for difference spectra to assess the amount of rhodopsin pigment produced. 11-*cis*-retinal treated samples were used for rhodopsin immunoaffinity purification to determine the Meta II stability of each mutant and their ability to activate transducin. Further details of these procedures can be found in Chapter 2.

6.2.6 Expression of the E122G and E122Q (N2C D282C) mutants for Solid State NMR

For Solid State Magic Angle Spinning NMR (SS MAS NMR), 3 to 6 mg of the rhodopsin pigments is necessary. Cells were brought up from frozen stocks (see Chapter 2) and expanded to the required number of 15 cm cell culture dishes estimated by their expression determined in 6.2.4. Once the cell culture dishes had reached near confluence, the media was exchanged to one containing the necessary labelled amino acids (see Table 6.1). 24 hours after media exchange (or once the dishes were confluent) the induction mix was added (final concentration 2 µg/ml tetracycline and 5 mM sodium butyrate). The cells were induced for 40 to 50 hours, and harvested when

they were observed to be completely rounded and just beginning to lift from the cell culture dishes. For the cell line expressing E122G N2C D282C this was at approximately 40 hours and for the cell line expressing E122Q N2C D282C this was at approximately 50 hours.

The cells were then harvested from the dishes by pipetting up and down in the media using a 10 ml pipette. The cell suspensions were then centrifuged at 4°C, 6000 rpm for 20 mins using the SORVALL RC 5B Plus centrifuge with the rotor SORVALL SLA-3000. The supernatant was poured off carefully to ensure cell pellet was not disturbed. 500 ml of 1x PBS was added to the cell pellet for each mutant and the pellet resuspended. The cell suspensions were centrifuged again as above. The supernatant was again carefully poured off before resuspension of the pellets in 60 ml 1x PBS. The cell suspension was split into two 50 ml tubes and treated with 2 µl of 11-*cis*-retinal (final concentration 20 µM) per harvested 15 cm dish, in the dark overnight at 4°C with mixing by nutation.

A 100 µl sample was then taken and solubilised in DDM/PMSF and used to assess the amount of rhodopsin pigment formed by UV-vis difference spectroscopy. Complete incorporation of 11-*cis*-retinal was observed as no 380 nm peak was seen, therefore an additional 11-*cis*-retinal treatment was performed (1 µl per harvested 15 cm dish). Following completion of pigment formation, the cell suspensions were snap frozen using liquid nitrogen.

6.2.7 Purification of the E122G and E122Q (N2C D282C) mutants for Solid State NMR

Rho-1D4 sepharose slurry was made fresh for the purification of the samples (see Chapter 2). The binding capacity of the beads was found to be approximately 373

µg/ml of slurry (per 0.5 ml of settled beads). All the following steps were performed in the dark under dim red light. The cell suspensions were thawed and then solubilised in 10% DDM, PMSF and using one Pierce™ Protease Inhibitor tablet (EDTA free) per 50 ml of cell suspension used for 1 hour at 4 °C with end over end mixing. They were then centrifuged in a light-safe rotor at 15000 rpm for 30 minutes. Rho-1D4 sepharose was then prepared for use by removal of the PBS containing sodium azide. Based on the UV-vis difference spectra of a sample for each pigment (see 6.2.5) a slight excess amount of beads were used based on the estimated pigment yield and the binding capacity. The supernatant from the centrifugation step and the Rho-1D4 slurry was mixed end over end, for approximately 16 hours at 4 °C.

The beads containing immunocaptured rhodopsin pigment were then added to a 10 ml column prepared with a porous frit. The beads were allowed to settle and the flow through was then collected (and analysed by UV-vis dark spectra to ensure near complete binding had occurred). A second frit was then placed above the beads to prevent drying out while the subsequent steps were performed. The column was then washed with a high salt, PBS based buffer containing 0.02% DDM (50 column volumes) at 4 °C. Then low salt buffer (0.02 % DDM, 2 mM Na phosphate, pH 6(10 column volumes) at 4 °C was passed through the column.

The stable isotope labelled rhodopsin pigment was then eluted by incubating for 1 hour at room temperature using 5 ml (four times) 100 µM rhodopsin C-terminal 9-mer in low salt buffer (2 mM Na P pH6, 0.02%DDM). The sample was then concentrated using Milipore® Centrifugal filter units (Sigma Aldrich) at 4000 rpm for 6 minutes (repeated as necessary until all sample had been added and the sample volume is 0.5-1 ml) and snap frozen.

6.2.8 Solid State Magic Angle Spinning NMR of the E122G and E122Q (N2C D282C) stable isotope labelled rhodopsin mutants

The E122G N2C D282C and E122Q N2C D282C stable isotope labelled rhodopsin samples were used for Solid State Magic Angle Spinning (SSMAS) NMR. These experiments were performed at Stony Brook University, New York by Lauren Todd from Professor Steven Smith's group. The experiments were performed using a 500 MHz Bruker NMR spectrometer with a 2 channel 4 mm MAS probe (7.9 kHz spinning rate). Rhodopsin samples were converted to Meta II in the rotor by illumination for 60 seconds.

6.3 Results

6.3.1 Alignments of opsins at E122

The GPCRdb was utilised for alignments of rhodopsin, OPN3, OPN4, OPN5, OPN1SW, OPN1MW and OPN1LW (Isberg *et al.*, 2016; Kooistra *et al.*, 2021). Their alignment allowed for the conservation of residues at this position to be examined and the results are shown in Table 6.2. A list of the protein sequences/species aligned can be found in Appendix 4.

Out of all the opsin types aligned, at position 3.37 (rhodopsin residue 122) the most frequently occurring amino acid was glutamic acid (711 occurrences), of which all were in the rhodopsin group except one seen in OPN1SW. Isoleucine was next most frequently aligned at this position (459 occurrences) with it being the most frequent amino acid in OPN3, OPN4, OPN1MW and OPN1LW. Leucine occurred 255 times being the most frequent amino acid at this position in OPN1SW. In OPN5 the most frequent amino acid was cysteine with 137 occurrences.

While varied amino acids were seen at this position across the different types of opsins within groups the amino acids seen were highly conserved. In rhodopsin 94.41% of the sequences aligned contained glutamic acid at position 3.37 (residue 122). Across the other opsin types isoleucine was aligned at this position for 89.9% of OPN3 sequences, 98.82% of OPN4 sequences, 88.89% of OPN1MW sequences and 100% of OPN1LW sequences. In OPN5, 95.8% of the sequences contained cysteine at this position and in OPN1SW 82.79% of the sequences contained leucine at this position.

Table 6.2 Alignment of position 3.37 (rhodopsin residue 122) of rhodopsin, OPN3, OPN4, OPN5, OPN1SW, OPN1MW and OPN1LW. Sequence alignments were performed using GPCRdb. Amino acids are sorted by the most frequently occurring over all the opsin types aligned. X represents no residue at this position.

		All	Rho	OPN3	OPN4	OPN5	OPN1SW	OPN1MW	OPN1LW	
Glu	E	711	710	0	0	0	1	0	0	
Iso	I	459	5	89	168	2	2	16	177	
Leu	L	259	3	0	0	1	255	0	0	
Cys	C	152	14	0	1	137	0	0	0	
Met	M	55	11	0	0	0	44	0	0	
Phe	F	11	6	4	1	0	0	0	0	
Glu	Q	5	1	0	0	0	2	2	0	
Val	V	5	0	2	0	3	0	0	0	
Ser	S	3	1	0	0	0	2	0	0	
Thr	T	4	0	4	0	0	0	0	0	
Asp	D	1	1	0	0	0	0	0	0	
Ala	A	0	0	0	0	0	0	0	0	
Gly	G	0	0	0	0	0	0	0	0	
His	H	0	0	0	0	0	0	0	0	
Lys	K	0	0	0	0	0	0	0	0	
Asp	N	0	0	0	0	0	0	0	0	
Pro	P	0	0	0	0	0	0	0	0	
Arg	R	0	0	0	0	0	0	0	0	
Try	W	0	0	0	0	0	0	0	0	
Tyr	Y	0	0	0	0	0	0	0	0	
	X	2	0	0	0	0	2	0	0	
Consensus	E	Total	1667	752	99	170	143	308	18	177
		% most frequent residue (green)	42.65%	94.41%	89.90%	98.82%	95.80%	82.79%	88.89%	100.00%

6.3.2 Expression of the rhodopsin residue E122 mutants

The expression level of E122 mutant rhodopsin mutant pigment produced on 10 cm cell culture dishes following induction with tetracycline and sodium butyrate and treatment with 9-*cis*-retinal was assessed by UV-vis difference spectra. Spectra were recorded between 650 and 250 nm with a spectrum was obtained first in the dark, and then another after 60 seconds of photobleaching using the SCHOTT KL1500 Compact fitted with a >495 nm long-pass filter. Difference spectra for each rhodopsin mutant

were calculated (Figure 6.2). The difference at the λ max was then used in Beer-Lambert Law to calculate the yield of rhodopsin pigment, using an assumed $\epsilon = 42700$ at the λ max and a molecular weight of 42300 Da.

The λ max for WT rhodopsin is 500 nm. For the E122 mutants, this varies by about 20 nm ranging from 501 nm to 482 nm in solubilised cell samples. The expression levels also varied even though all of the cell lines were induced under the same conditions. The resulting yields and the λ max for each mutant is described in Table 6.2.

Table 6.2 λ_{\max} values and yields of each E122 mutant. λ max was determined by difference spectra between 250 nm and 650 nm (n=1). Yields were determined by Beer-Lambert Law using the absorbance difference at the λ_{\max} value, $\epsilon = 42700$ and M.W. 42300.

Mutant	λ max (nm)	Yield (μg) per 10 cm dish (1×10^7 cells)
E122C	491	30.4
E122G	482	26.9
E122I	501	19.0
E122L	494	48.6
E122M	495	20.5
E122Q	488	19.6

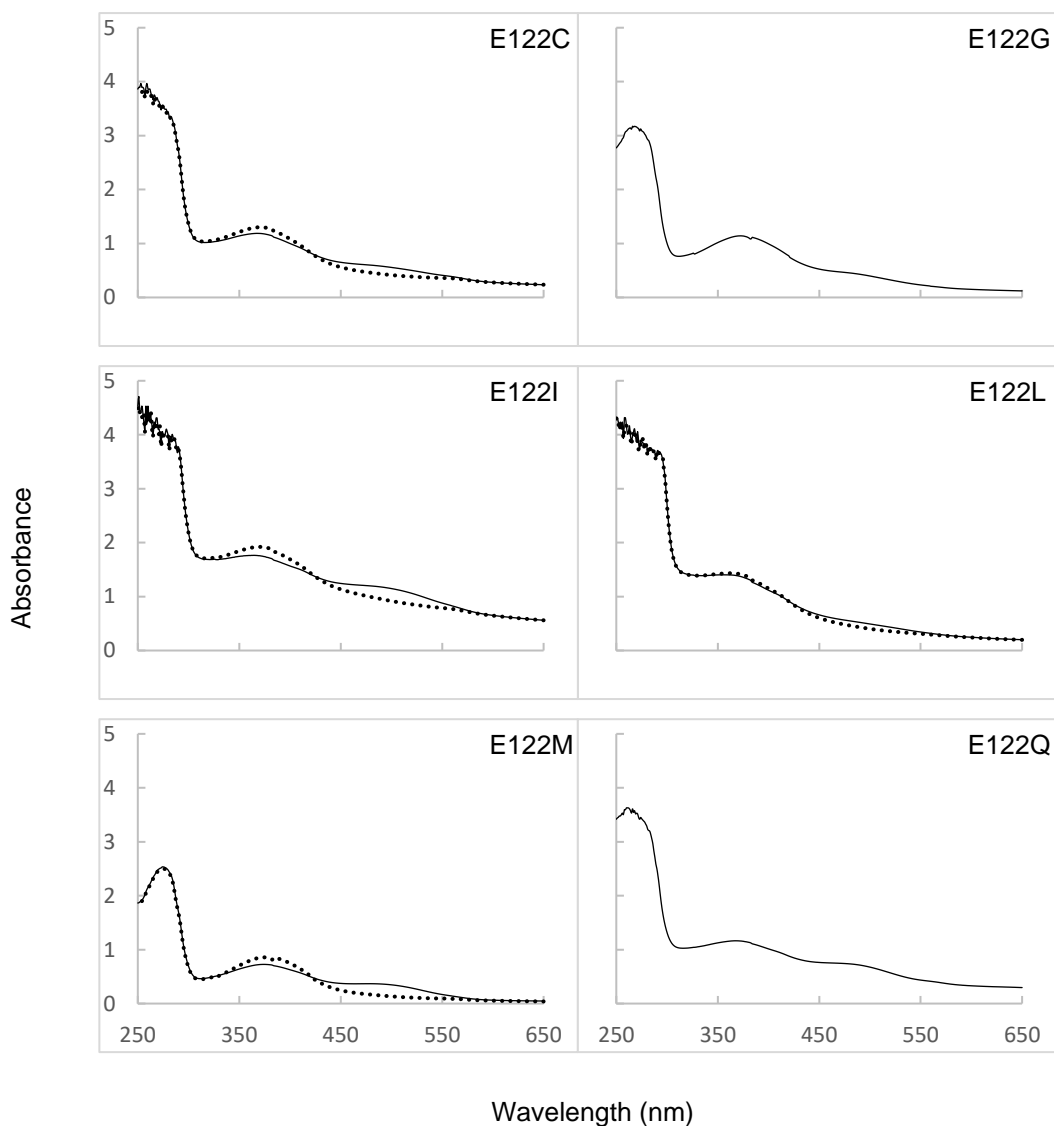


Figure 6.2 UV-vis spectra of the E122 mutants before and after photobleaching for 1 minute ($h\nu < 495$). 10 cm cell culture dishes were grown to confluence, each with a stable E122 mutant HEK293S cell line. Cells were induced with tetracycline and sodium butyrate for 65 hours before harvesting in 1x PBS. The resulting cell suspensions were treated with 9-*cis*-retinal. UV-vis absorption was measured between 250 and 650 nm, first under dark conditions (solid line) and then following 60 seconds illumination (dashed line).

6.3.3 Immunoaffinity purification of the E122 rhodopsin mutants

The E122 mutant rhodopsin proteins were purified from cells harvested from 10 cm cell culture dishes following induction with tetracycline and sodium butyrate. Following treatment with 11-*cis*-retinal and solubilisation of the cell lysates, 50 μ l was kept as a pre-purification sample which was then used to determine the amount of each mutant rhodopsin in the samples. The remaining lysate was then subjected to 1D4-sepharose immunoaffinity purification. Figure 6.3 shows the UV-vis absorption spectral profiles of each, and Table 6.3 shows the yields and purity of the first low salt elution (as judged by the $A_{280} : A_{\lambda_{\max}}$ ratio) of the E122 mutant rhodopsins.

For all the E122 mutants, the majority of the rhodopsin pigment was eluted in the first low salt elution. The $A_{280} : A_{\lambda_{\max}}$ ratio for each purified pigment was between 2.00 and 2.84, indicating a reasonable level of purity. The yield of E122 mutant rhodopsin proteins was varied with total yields across 3 low salt and 3 high salt elution's ranging from 18.3 μ g to 69.5 μ g.

The purified rhodopsin mutants also showed variation in their λ_{\max} values. WT rhodopsin λ_{\max} is at 500 nm. This was seen to shift slightly in the mutants E122I, E122L and E122M where shifts to 496, 496 and 492.5 nm were observed. E122C had a blue shifted λ_{\max} to 488 nm. E122G and E122Q showed the biggest shifts in their λ_{\max} values with 482 and 480 nm being observed respectively.

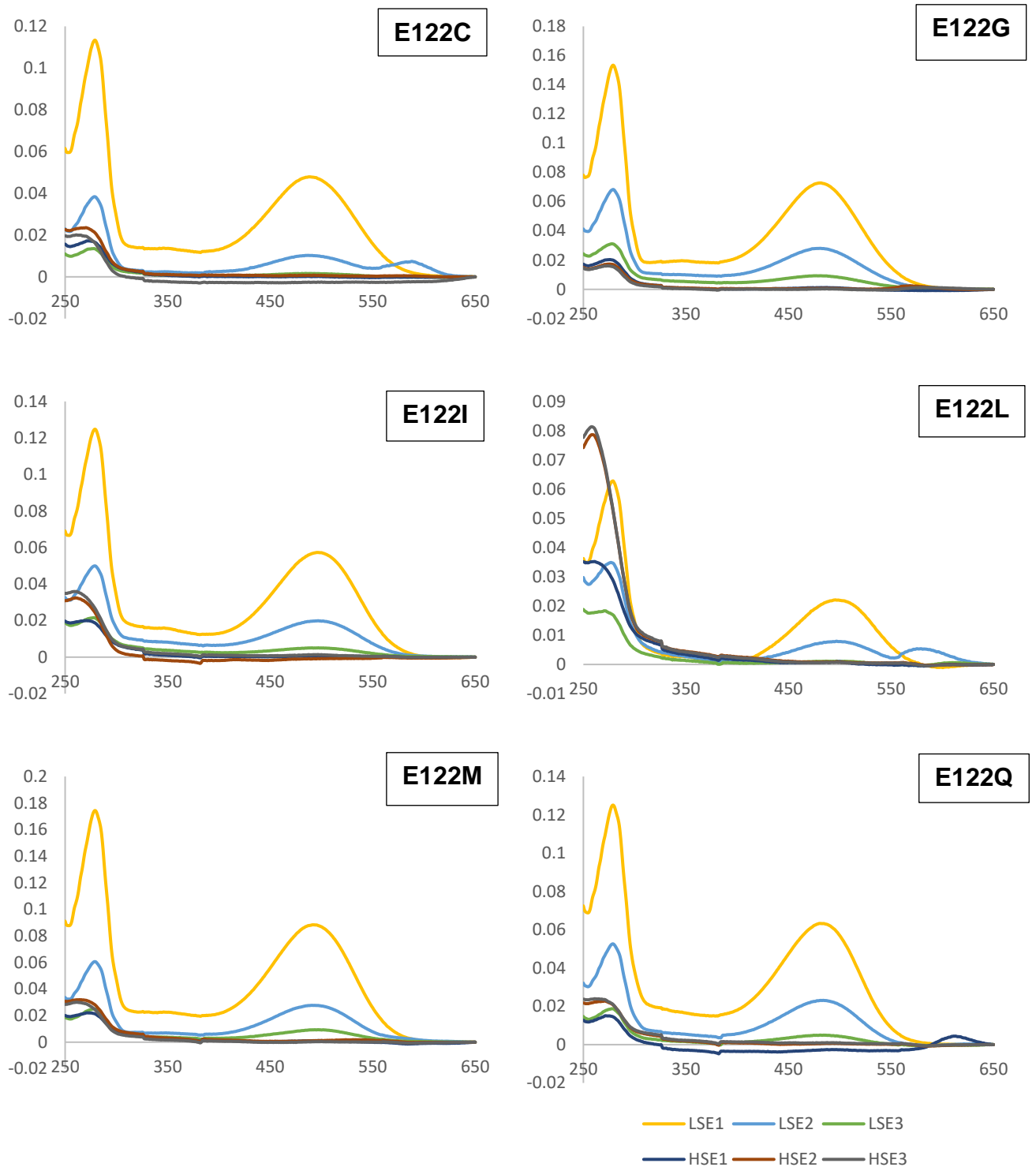


Figure 6.3 UV-vis absorption spectra of low and high salt elution purified E122 rhodopsin mutants. 10 cm cell culture dishes were grown to confluence, each with a stable E122 mutant HEK293S cell line. Cells were induced with tetracycline and sodium butyrate for 65 hours before harvesting in 1x PBS. The resulting cell suspensions were treated with 11-*cis*-retinal. Rho-1D4 immunoaffinity purification was

performed, using 3 low salt elution steps followed by 3 high salt elution steps. The majority of the rhodopsin mutant pigments were eluted in the first low salt elution (LSE1 – yellow). Some pigment was then eluted in LSE2 (light blue), and LSE3 (green). Very low levels of the rhodopsin mutant pigments were eluted in the high salt elution (HSE1-HSE3 – dark blue, dark orange and grey).

6.3.4 Stability of the Meta II intermediate in E122 rhodopsin mutants

Metarhodopsin II (Meta II) is the activated form of rhodopsin. In Chapter 5, it was seen that E122G rhodopsin had a greatly extended Meta II half-life of approximately 42 minutes when expressed using HEK293S cells which lack GnTI activity. Previously E122Q was described to have a much shorter (10-fold) Meta II half-life than in WT rhodopsin in rod outer segment membranes (E122Q 7.7 seconds and WT rhodopsin 95 seconds) (Imai *et al.*, 2007). For this reason, we decided to investigate the effect of varying the residue found at 122 to that found in different opsin types. This was of interest in determining the effect of varying residue 122 in the rhodopsin background.

Meta II stability assays were performed and the half-life for each protein was determined by curve fitting data using SigmaPlot. WT rhodopsin which contains glutamic acid at residue 122, had a Meta II half-life of 15.7 minutes. Across various opsin types and from different species, the next 4 most common residues at 122 are isoleucine, leucine, cysteine, and methionine, which were also examined alongside E122G and E122Q.

Mutation of rhodopsin to E122Q led to the shortest half-life being observed (3.5 minutes). E122I and E122M closely followed in being the next fastest 3.8 and 5.3 minutes respectively. E122L had a faster Meta II half-life compared to WT rhodopsin, but not as fast as Q, I and M mutants with a half-life calculated to be 7.6 minutes. The Meta II half-life of E122C was 16.7 minutes which was slightly slower than that of WT rhodopsin. In contrast, the RP mutation E122G (which was not found to be present naturally in any of the opsin types) had a Meta II half-life of 38.4 minutes, which is more than twice as slow as WT. Representative graphs for each experiment can be seen in Figure 6.4, and the calculated half-life and standard deviation for each is presented in Table 6.3.

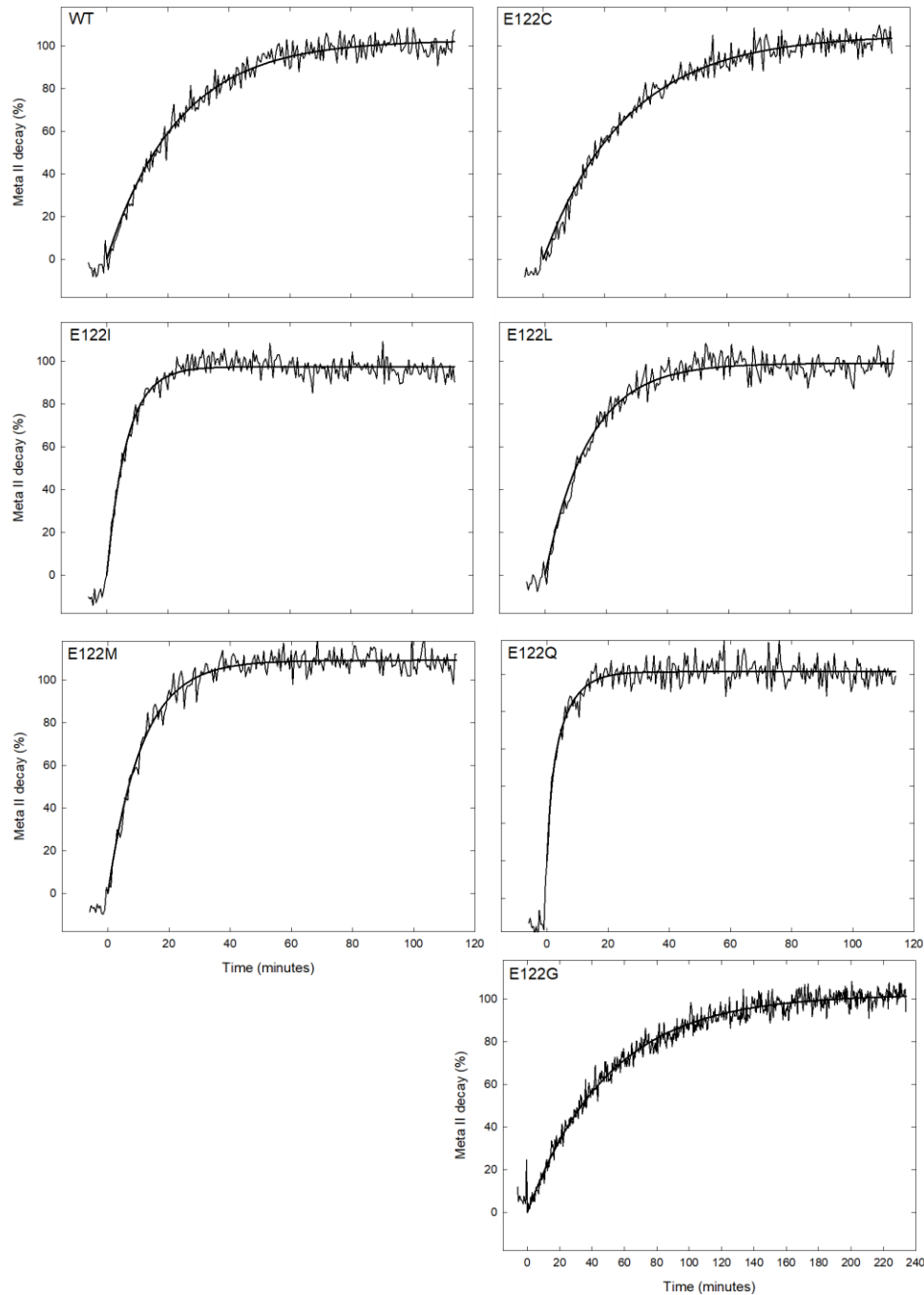


Figure 6.4 Meta II decay of the E122 mutants. Meta II decay was measured by recording the increase in tryptophan fluorescence that occurs as retinal is released from the binding pocket after illumination. Samples were illuminated at time = 0 for 30 seconds, and fluorescence measured for 2 hours for all but E122G which was measured for 4 hours. All data best fitted to single, 2 parameter curves using SigmaPlot.

6.3.5 Transducin activation by the E122 rhodopsin mutants

Upon absorption of a photon rhodopsin is converted to the Meta II intermediate and activates transducin. The signal transduction capability of rhodopsin and its mutants can be measured by measuring this step of signal transduction. The use of GTP γ S which cannot be hydrolysed leads to the accumulation of transducin in its active state bound to this form of GTP. This brings about an increase in the tryptophan fluorescence of transducin brought about by a conformational change in the G-protein upon binding of GTP γ S. The initial rate of activation was determined by measuring the ability of the rhodopsin or rhodopsin mutant to catalytically convert transducin to transducin: GTP γ S. Relative initial rates, measured over the first 60 seconds of the reaction, were calculated relative to WT rhodopsin.

The E122 mutants had varied abilities to activate transducin ranging from 89.5% to 1.8% relative to WT opsin. Compared to WT rhodopsin, E122C was 89.5% active. E122M was able to activate at 67.0% of the rate of WT rhodopsin. The relative rate of E122Q was 51.9%, with an abnormal curve observed where a rapid linear increase was observed during the first 60 seconds following GTP γ S addition, followed by a very slowly increasing linear line for the rest of the data points. This contrasts with the usual quick linear increase followed by a curve increasing which was observed in WT. E122M had a higher relative activation rate and E122L which had a lower rate of 37.1% compared to WT. E122G activated transducin at a relative rate of 10.1% in comparison to WT rhodopsin. The lowest relative activation rate was generated by E122I which was 1.8% of WT rhodopsin. In Figure 6.5 representative curves for each E122 mutant and WT rhodopsin are presented and the calculated relative activity and standard deviation for each is shown in Table 6.3.

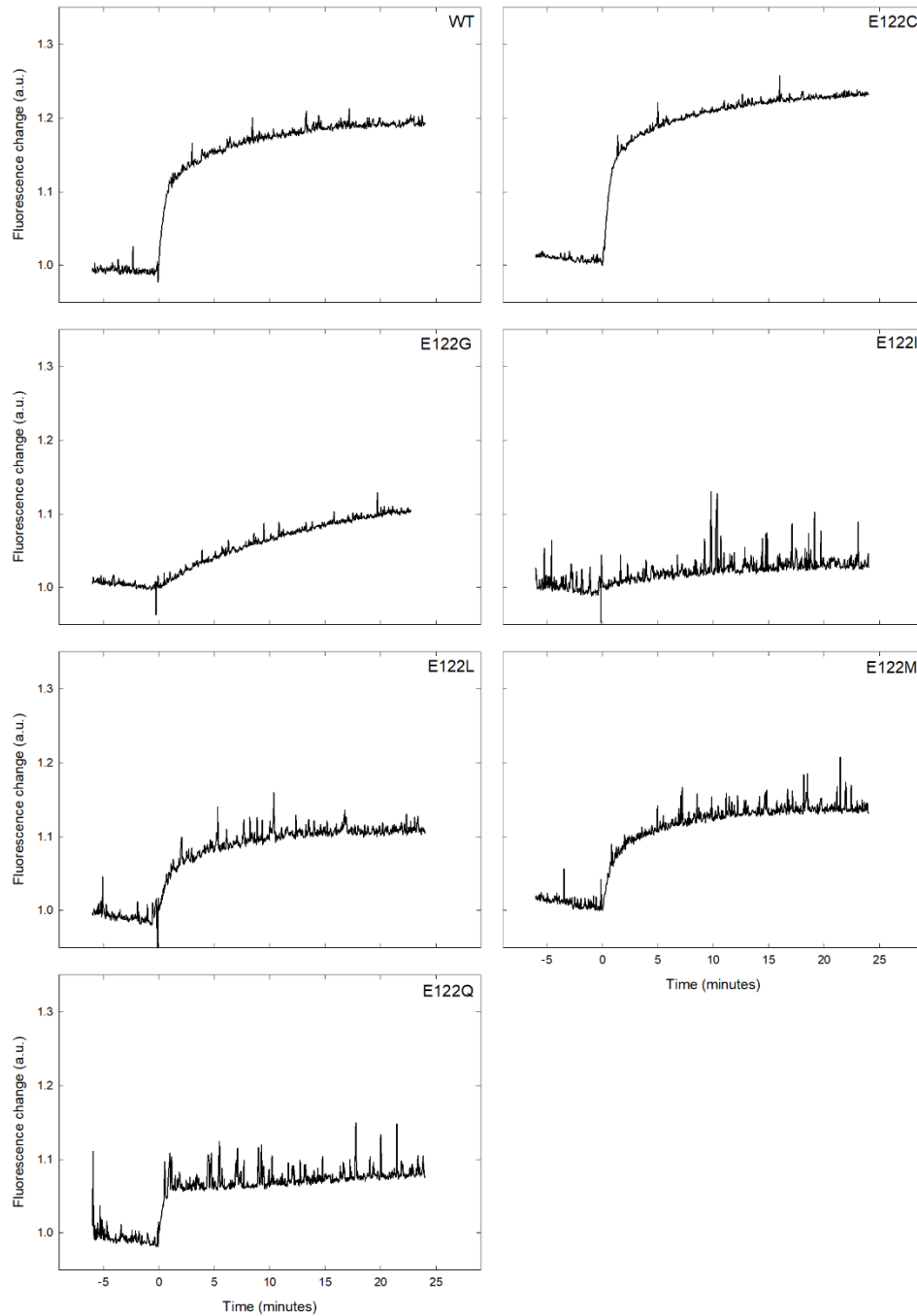


Figure 6.5 Transducin activation by rhodopsin E122 mutants. The change in fluorescence following the addition of GTP γ S to an illuminated sample containing an E122 mutant and transducin was measured. The first 60 seconds following GTP γ S addition was used to calculate the initial rate kinetics of transducin activation.

Table 6.3 Purification, Meta II decay and transducin activation characteristics of WT and E122 mutants.

	Purification			Meta II (n=2)		Transducin activation (n=2)	
	λ max	Yield	280/500	Half-Life	S.D.	Relative	S.D.
	(nm)	(μ g)	Ratio	(mins)		rate	
WT	501	55.6	1.88	15.65	0.14	100.00	0.00
E122C	488	31.7	2.44	16.75	1.19	89.48	4.40
E122G	482	58.5	2.38	38.41	6.76	10.10	1.43
E122I	496	45.5	2.18	3.83	1.18	1.83	2.12
E122L	496	18.3	2.84	7.56	3.50	37.12	5.36
E122M	492.5	69.5	2.00	5.30	2.08	67.00	4.76
E122Q	480	47.6	2.18	3.49	1.03	51.85	10.48

6.3.6 SS MAS NMR comparison between E122G N2C D282C and E122Q N2C D282C

Stabilised (N2C D282C) mutants E122G and E122Q which had the longest and shortest Meta II half-lives were prepared for Solid State Magic Angle Spinning (SS MAS) NMR. The mutants were expressed using inducible HEK293S stable cell lines for each and the protein purified as described in Chapter 6.2.5 and 6.2.6. The protein was then purified (6.2.7) and SS MAS NMR was then performed (6.2.8) to producing ^{13}C and ^{15}N spectra. All NMR was performed in the N2C D282C background.

Figure 6.6 shows the ^{13}C and ^{15}N spectra for E122G rhodopsin and Meta II. Panel a. displays a WT (N2C D282C) rhodopsin and Meta II labelled with ^{15}N tryptophan comparison for reference. The main points of difference between the two are the upfield shifts of Trp126 and Trp265 NH indole resonances caused by the transition from rhodopsin to Meta II. Panel b. (Figure 6.6) compares the rhodopsin and Meta II ^{15}N spectra of E122G. These both appear to look similar to the spectra of the WT Meta II conformation, with no upfield shifts seen and appear as small shoulders in Meta II. To further illustrate this panel c. overlays the ^{15}N spectra of WT rhodopsin and E122G rhodopsin and panel d. overlays the spectra of E122G rhodopsin and WT Meta II. These illustrate that the E122G rhodopsin spectra is more similar to that of WT Meta II than WT rhodopsin.

Figure 6.6 panels e.-h. show the ^{13}C NMR difference spectra of E122G rhodopsin and its Meta II counterpart overlaid onto the WT rhodopsin/Meta II difference spectra. These were labelled with the amino acids 1- ^{13}C -histidine, 4- ^{13}C -tyrosine, 2- ^{13}C -glycine and 5- ^{13}C -methionine (e.-h. respectively). Tyr191, Gly188 and Met288 resonances for E122G are alike those seen in the WT. Differences are seen however in regards to Tyr206 where a shift seen in the WT is not present in the E122G and in the ^{13}C

methionine spectra where a strong band appears for E122G which is not observed in the WT.

Figure 6.7 shows the ^{13}C and ^{15}N spectra for E122Q rhodopsin and Meta II. Panel a. displays a WT (N2C D282C) rhodopsin and Meta II labelled with ^{15}N tryptophan comparison for reference. Panel b. shows E122Q rhodopsin and E122Q Meta II spectra, c. E122Q rhodopsin and WT rhodopsin and d. E122Q Meta II and WT Meta II. These show a distinct difference compared to E122G. The ^{15}N spectrum of E122Q shows a downfield shift in comparison to E122G of the Trp126 indole NH resonance. In addition when comparing E122Q rhodopsin and E122Q Meta II only one clear difference is observed, the Trp265 indole resonance in Meta II. No differences in the Trp126 resonances are observed.

Figure 6.7 e.-h. show the ^{13}C NMR difference spectra of E122Q rhodopsin/Meta II overlaid onto the WT rhodopsin/Meta II difference spectra. These were labelled with the amino acids 1- ^{13}C -histidine, 4- ^{13}C -tyrosine, 2- ^{13}C -glycine and 5- ^{13}C -methionine (e.-h. respectively). The E122Q Tyr, Gly and Met ^{13}C spectra are similar to the WT (f.-h.). However the His spectra (e.) shows a difference in the His211 region.

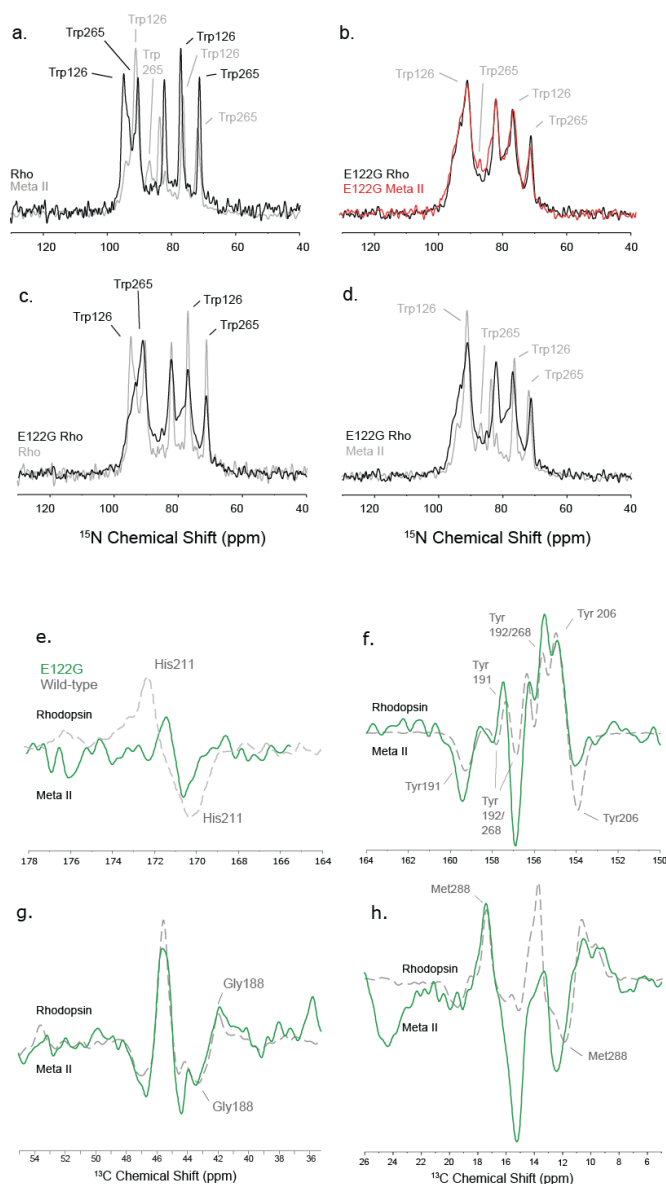


Figure 6.6 ^{15}N and ^{13}C spectra of NMR E122G rhodopsin. Spectra were recorded using solid state magic angle spinning NMR of purified E122G rhodopsin labelled with ^{15}N tryptophan and ^{13}C histidine, tyrosine, glycine and methionine. Panels a-h contain the following spectrum comparisons. a. WT rhodopsin and WT Metarhodopsin II (Meta II). b. E122G rhodopsin and E122G Meta II. c. E122G rhodopsin and WT rhodopsin. d. E122G rhodopsin and WT Meta II. e. 1- ^{13}C -histidine labelled E122G and WT rhodopsin. f. 4- ^{13}C -tyrosine labelled E122G and WT rhodopsin. g. 2- ^{13}C -glycine labelled E122G and WT rhodopsin. h. 5- ^{13}C -methionine labelled E122G and WT rhodopsin. Panels e.-h. show the difference spectra of rho/Meta II.

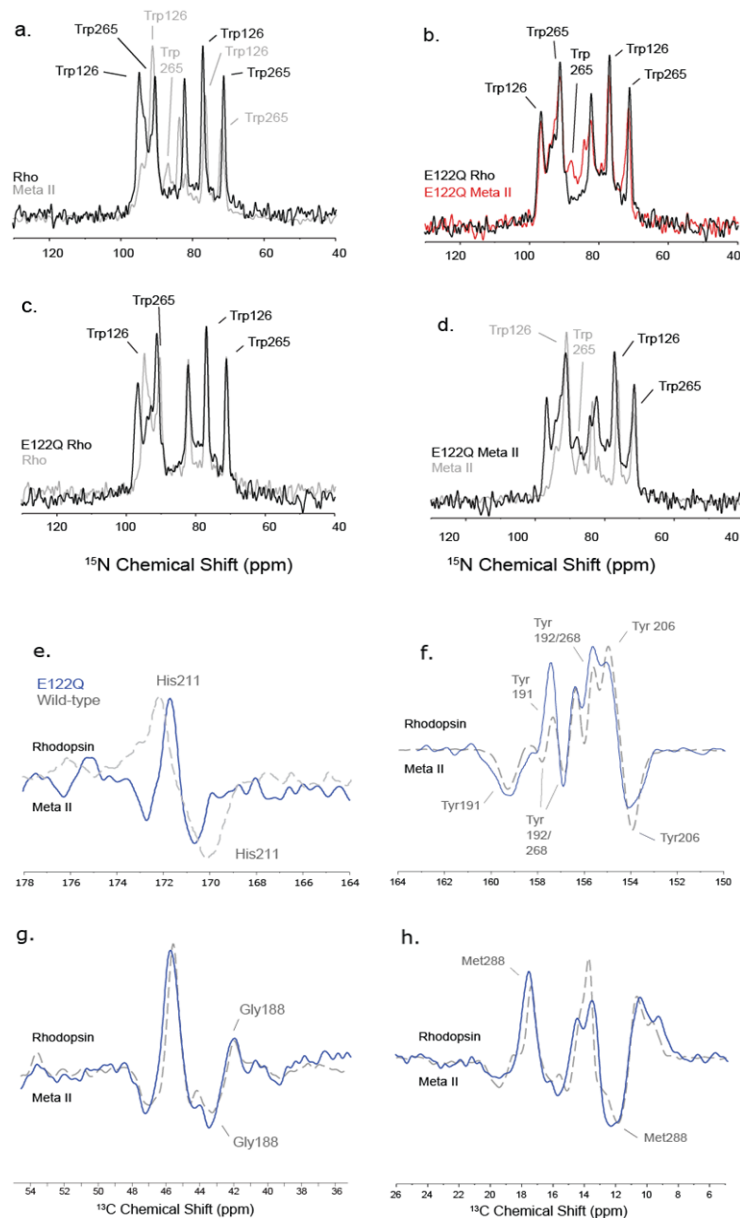


Figure 6.7 ^{15}N and ^{13}C spectra of NMR E122Q rhodopsin. Spectra were recorded using solid state magic angle spinning NMR of purified E122Q rhodopsin labelled with ^{15}N tryptophan and ^{13}C histidine, tyrosine, glycine and methionine. Panels a-h contain the following spectrum comparisons. a. WT rhodopsin and WT Metarhodopsin II (Meta II). b. E122Q rhodopsin and E122Q Meta II. c. E122Q rhodopsin and WT rhodopsin. d. E122Q Meta II and WT Meta II. e. 1- ^{13}C -histidine labelled E122Q and WT rhodopsin. f. 4- ^{13}C -tyrosine labelled E122Q and WT rhodopsin. g. 2- ^{13}C -glycine labelled E122Q and WT rhodopsin. h. 5- ^{13}C -methionine labelled E122Q and WT rhodopsin. Panels e.-h. show the difference spectra of rho/Meta II.

6.4 Discussion

E122 has been described as a functional determinant of opsin function (Imai *et al.*, 1997). Its role in the stabilisation of rhodopsin through the hydrogen bond network and close proximity to the ligand binding pocket have major influence on properties of opsins (Imai *et al.*, 1997; Ahuja *et al.*, 2009b; Hornak *et al.*, 2009). The variation of the residue at this position is seen between opsin types paired to high residue conservation within that opsin type. For example, differences between rhodopsin and cone opsins at this position are necessary as pigments with optimal molecular properties are required for vision in dim light versus bright light (Imai *et al.*, 1997, 2007).

In this present study the variation in Meta II half-life can be attributed to the functional roles of residues at position 122. Rhodopsin E122 mutants containing residues usually found in cone pigments have shorter half-lives compared to WT rhodopsin. The residues commonly seen in other opsin types also had much shorter Meta II half-lives. This might suggest these opsins are required to have photocycles similar to cones in that they decay fast after activation and also regenerate fast. Rhodopsin is adapted for vision in dim-light conditions where photons are scarce and therefore by prolonging the active form (Meta II) there is more time for a productive interaction with transducin to initiate the signalling cascade (Ingram *et al.*, 2016). Return of the receptor and photoreceptor cell to the resting (dark) state post-signalling needs to be timely to allow for further cycles of signalling as more photons are absorbed, the rate of which is different in dim-light and bright-light visual receptors (Ebrey and Koutalos, 2001; Fu, 2010).

The RP mutant E122G had a much longer Meta II half-life (2.5 times) but interestingly could only activate transducin at 10% of the rate of WT rhodopsin. In addition, ¹⁵N

NMR spectra revealed that in both the rhodopsin and Meta II state E122G resembles the WT Meta II, suggesting that switch one is 'on' in both the inactive and active state of rhodopsin. However, the slight difference in the Trp265 resonance suggests it is not completely locked into the Meta II formation consistent with the long Meta II half-life. This is in stark contrast with the ^{15}N NMR results for E122Q, known for its short Meta II half-life, here the Trp126 indole NH resonance is shifted downfield in comparison to E122G which can be attributed to an increase in the strength of hydrogen bonding, likely between the indole NH and the glutamine sidechain. Furthermore, upon illumination the only difference seen in the Meta II spectrum is the appearance of the Trp265 resonance suggesting that there is no change in the hydrogen bond network around Trp126-Gln122. Together, this suggests that in E122Q switch one is held in the 'off' position, here consistent with the fast decay of its Meta II conformation. This with previous work further shows the importance of residue 122 in the functioning of rhodopsin (and other opsins) gives a strong indication of how important E122 is in rhodopsin for its specific functioning (Imai *et al.*, 1997). While the Meta II half-life of rhodopsin is slower than that of cone opsins to ensure signalling under dim-light conditions, the E122G mutation which results in an even slower Meta II half-life is detrimental to its ability to activate transducin (Ebrey and Koutalos, 2001). A potential reason for this may be due to the effect on the hydrogen bond network in the active state which may prevent efficient binding of the G-protein to the receptor or catalytic turnover. Upon the reception of light by rhodopsin 11-*cis*-retinal isomerises which shifts the methyl group C20 towards EL2 and the β -ionone ring between residues 207 and 208 of helix 5 (Ahuja *et al.*, 2009b).

When WT rhodopsin transitions to Meta II there is an upfield shift in the Trp126 and Trp265 resonances (Figure 6.6, panel a.) which are associated with hydrogen bonding

loss. However, in E122G rhodopsin the Trp126 resonance suggests that the loss of hydrogen bonding is already present. There is a higher backbone flexibility in E122G rhodopsin which remains similar when it converts to Meta II (Figure 6.6, panel b.). The results of the ^{13}C NMR showed that E122G is able to become Meta II upon illumination. Resonances alike to that of WT were shown for Tyr191, Gly188 and Met288 which provided probes for Meta II conversion. The lack of the typical upfield shift of the Tyr206 resonance seen in WT upon illumination due to the weakening of its interaction with His211 suggests that in E122G this interaction is preserved in its Meta II conformation. Alongside this, the strong band in the Meta II of the methionine spectra which is not usually present, in combination these further suggest that E122G is less stable in the Meta II conformation than WT.

Molecular dynamics experiments have given an indication to how the active state of rhodopsin is stabilised. The movement of the β -ionone ring leads to the disruption of the hydrogen bond between the sidechain of E122 and the backbone carbonyl oxygen of H211 and stabilises helix 5's active position (Patel *et al.*, 2005; Bhattacharya *et al.*, 2008; Hornak *et al.*, 2009). E122 then forms a new bond with H211's δ nitrogen, and H211 also forms a water mediated hydrogen bond with W265 and an E122 to C167 hydrogen bond also forms stabilising the active state (Bhattacharya *et al.*, 2008). The stable active formation exposes some previously hidden residues to water and likely the G_α subunit of transducin (Bhattacharya *et al.*, 2008).

The role of the E122 position in rhodopsin structure and function has previously drawn attention. Our data is in agreement with previous findings that E122 is important for spectral tuning and active state (Meta II) stability. We further find that signal transduction properties of the mutant pigments can also be affected. This might imply that light induced structural changes in rhodopsin mutant E122G alter its interaction

with transducin. Another possibility is that there are differences in the way that this mutant interacts with other components of the signal transduction pathway (rhodopsin kinase and arrestin), or perhaps interacts with components of non-cognate signalling pathways (other G proteins, GRKs, arrestins) which could be detrimental to the health of photoreceptor cells.

7. Conclusion

7.1 PiggyBac transposon cell line construction and expression optimisation provide a rapid, easy and effective method for rhodopsin mutant expression at high levels.

Structural studies of membrane proteins often require milligram amounts of purified protein. Stable cell lines have proven useful but have previously been limited by the time needed (several months) and labour needed for their construction. Here we have shown that high expressing inducible stable cell pools can be made in an accelerated (several weeks) manner using the piggyBac transposon method. The plasmid (pB007NCO) constructed for transposon delivery of the expression/selection cassette was too large for reproducible mutagenesis, due to inefficiency of the Quikchange method when using plasmids of large sizes (Yang *et al.*, 2022). Here a stepwise approach was taken for construction of the expression plasmid. First, Site-directed mutagenesis was performed using pMT4 as the template. The *EcoRI-NotI* fragment from pMT4 was then cloned into pACMV TetO. From pACMV TetO the expression/selection cassette containing the CMV[TetO] promoter/gene target, along with neomycin resistance marker, was isolated by PCR and cloned into the piggyBac plasmid at the *NheI* site to form pB007NCO.

Despite the additional steps required at the cloning stage, this novel approach towards stable cell line pool generation removes the need for multiple transfections compared to transient methods, whilst decreasing the time taken to produce stable cell lines. This is owing to their transfection method, which leads to a higher transposon cargo copy number, removing the requirement for colonies to be isolated and grown individually. (Reeves *et al.*, 1996). The cloning procedure was recently further optimised so that

KpnI NotI fragments could be cloned directly into the piggyBac pB007 CMV-TetO/Neo expression module, further decreasing the time taken to produce stable cell lines.

In addition to the increased speed of stable cell line production achieved via this novel methodology, the expression levels of WT rhodopsin protein using either HEK293S or HEK293S (GnTI-) cell pools were very high and in line with the reported expression levels from traditional methods (Reeves et al., 2002a). Furthermore, this method of producing stable cell line pools can be optimised, via both time duration and temperature, in order to improve the efficiency of protein accumulation from specific rhodopsin mutants. For traditionally low expressing mutants (P23A, G106W) increased expression levels could be achieved through optimisation of the time provided for gene expression and rhodopsin accumulation, whilst for certain mutants (P23A, G101V, G106W), optimisation of receptor expression through lowering expression temperature was found to be highly effective, which is in agreement with previous studies (Lin *et al.*, 2015).

One explanation for this effect is that by reducing the length of the time of expression, cytotoxicity imparted by rhodopsin class two RP mutants is less severe. The reason for reduced expression of these mutants is that prolonged UPR activation can result in cell death (Athanasίου et al., 2017b). This observation gives argument that optimising the expression of each rhodopsin RP mutant individually is beneficial, especially if it has low expression levels under conventional expression conditions. As shown here, the conditions often used for expression of WT rhodopsin (37°C, 60-72 hours) is not the most effective method for production of certain mutants. Unlike for WT rhodopsin, expression of some RP mutants may not be cumulative due to cytotoxic effects resulting in cell death (Reeves et al., 2002a; Athanasίου et al., 2017b). These improvements for the construction of cell lines and tailored optimization of the

expression conditions for individual mutants could be greatly utilised in structure and function studies of rhodopsin RP mutants. Of equal importance is the observation that previous classification for RP rhodopsin mutants may not paint the complete picture. For example, P23A which was previously shown to misfold when expressed for 60-72 hours were found to fold and form pigment at much earlier time points. However, these pigments were not present at later times of cell harvest. This suggests that the originally formed rod opsins are unstable and are not able to generate pigment beyond these early time points.

7.2 LMNG provides a suitable alternative to DDM for studies of opsin function.

A further improvement for the study of rhodopsin RP mutants was through the use of the detergent LMNG as an alternative to DDM. By using LMNG it was shown that WT opsin and mutant opsin could be purified, and importantly the purified rod opsins were competent for pigment formation. This is in contrast to previous studies using DDM where rod opsin was found to convert rapidly to forms incapable of combining with 11-cis retinal to form pigment (Sakamoto and Khorana, 1995; Reeves *et al.*, 1999). When rhodopsin was purified in LMNG, Meta II and transducin activation assays were shown to continue to work effectively for analysis of the light activated rhodopsin pigment, albeit with slightly reduced activity levels which is in agreement with previous work using LMNG. An explanation for this observation is that the additional hydrogen bonding in the LMNG micelle reduces receptor flexibility (Lee *et al.*, 2020).

7.3 Rhodopsin RP mutants have vastly different phenotypic properties that hold the key to understanding the structure and activation of rhodopsin.

The role of the N-terminus and extracellular loops in rhodopsins ability to fold and bind its ligand have been well documented (Opefi *et al.*, 2013). The majority of rhodopsin RP mutants are grouped as class two, categorised by their misfolding, retention in the ER and overall instability. While the EL1 mutants likely fall into this category, the mutants E122G, R252P, S298D and K311E were selected for study due to preliminary work in the Reeves laboratory suggesting that they did not misfold and therefore would be likely to affect other aspects of rhodopsin function and/or signalling properties. Examination of such mutants was predicted to provide novel information as to how activation and functioning of rhodopsin occurs. A summary of the biochemistry data for the mutants is shown in Table 7.1.

R252P and K311E showed little to minor differences compared to WT rhodopsin in their expression and function as determined through analysis of their photobleaching, Meta II stability and transducin activation capabilities. While they currently remain enigmatic, further analysis of these mutants may reveal differences which may help categorise them more effectively and aid in understanding their role in RP. In the TM region of the rhodopsin protein class two mutations are the most common as the presence of bulky or charged residues are incompatible with normal receptor folding. Class three to seven mutations have also been found in this region (Athanasίου *et al.*, 2018). R252 has polar contacts to E232 of Intracellular Loop 3 (IL3) and K248, E249 and I256 of TM6 (see Figure 7.1). The close proximity of R252 to IL3, which is known to be involved in the binding and activation of proteins which interact with rhodopsin

on the cytoplasmic side, could suggest that these interactions may be altered when R252 is mutated (Deupi, 2013). R252P however has an observed frequency of $8.8E-5$ and listed to have uncertain significance which is in agreement with the results here. Potentially this mutant may not be pathogenic based on the results and the frequency at which the variant is observed.

K311E is located at the start of the C-terminal helix, just after the seventh TM helix. Many mutations in the C-terminus have been categorised as class one mutations whereas those in the seventh TM have been identified as class two or class six mutations (Athanasίου *et al.*, 2018). Therefore, experiments to show the trafficking of the K311E mutant or of transducin activation both in the dark and without retinal bound could be useful in categorising this mutant into either class one or class six.

S298D showed decreased stability of the Meta II intermediate alongside an abnormal photobleaching profile. This is reminiscent of the N-terminal mutants described previously and suggests that like those S298D may be a class two or four mutation (Opefi *et al.*, 2013; Athanasίου *et al.*, 2018). Further investigation of this mutant by NMR or by other structural methods is therefore warranted. A limitation here when looking at the impact of these mutations on the functioning of rhodopsin in the context of retinitis pigmentosa is the potential differences between human and bovine rhodopsin. Here bovine rhodopsin was used to study human mutations, for the all of the mutations but one, the residue in question was the same in the bovine as the human. S298D however would actually be A298D in human leading to potential differences. Throughout the entirety of rhodopsin there are several differences in the rhodopsin sequence, however previous studies have suggested that despite the differences there is a high level of similarity in rhodopsin structure and function between human and bovine (Kazmin *et al.*, 2015).

E122G (which has a GnomAD frequency of $3.8E-6$) proved particularly interesting with regards to its more than two-fold increased Meta II half-life, but its decreased ability to activate transducin. Based on these properties, it could be that E122G is a class three mutant owing to similarities to mutants at residue R135 which have also been placed in this group (Cideciyan *et al.*, 1998; Iannaccone *et al.*, 2006). Due to the known role of E122 in opsin as a functional determinant in rod and cone visual pigments, this mutant was selected for further examination of its Meta II half-life and transducin activation (Imai *et al.*, 1997). Rhodopsin mutants incorporating the various residues at position 122 found in various opsin types were thus constructed and examined side by side.

E122 of rhodopsin and its equivalents in other opsin types is known as a functional determinant (Imai *et al.*, 1997). The glutamic acid at this position is highly conserved in rhodopsin (94.4%, see Chapter 6). Isoleucine, leucine, cysteine, methionine are the next most common residues found in this position across all opsin types. Rhodopsin mutant E122Q has previously been extensively studied where it was found to have a greatly decreased Meta II half-life (Imai *et al.*, 2007), reminiscent of cone opsin properties (Imai *et al.*, 2007), reminiscent of cone opsin properties. Here, E122Q was also found to have a much shorter Meta II half-life (3.49 mins) and most of the opsin type mutants studied also exhibited these shorter half-lives (E122I 3.83 mins, E122L 7.56 mins and E122M 5.30 mins). E122C had a slightly longer Meta II half-life (16.75 mins compared to WT rhodopsin 15.65 mins). E122G remained the stand-out mutant with the longest Meta II half-life (38.41 mins). These vast differences reiterate the role of E122 not only in rod and cone pigments but across opsin types as a functional determinant, likely linked to its role in the activation and signalling properties rhodopsin (Imai *et al.*, 1997; Bhattacharya *et al.*, 2008; Ahuja *et al.*, 2009b; Hornak *et al.*, 2009).

This observation was motivation for the structural and activation studies by SSMA NMR for this mutant.

Meta II stability and transducin activation assays serve as important ways to study the biochemical properties of rhodopsin. However these cannot be compared directly to the activation of rhodopsin in the eye due to the lack of other system components needed in this context. For example, an extended Meta II stability, such as that seen in E122G may not be seen in vivo. This is due to the lack of rhodopsin kinase/arrestin in the assays used. In vivo rhodopsin kinase phosphorylates activated rhodopsin which allows the rhodopsin to bind arrestin which results in the termination of rhodopsin signalling (Gray-Keller *et al.*, 1997; Krupnick *et al.*, 1997; Vishnivetskiy *et al.*, 2007; Park, 2014). Here, there is no rhodopsin kinase or arrestin which means that rhodopsin signalling cannot be terminated by the usual means.

Table 7.1 Summary of WT and RP mutant biochemical data. Highlighted cells show differences to the WT. ND = no data.

		WT	G101V	V104F	G106W	E122G	R252P	S298D	K311E
λ_{\max} (nm)		500	499	499	494	482	500	500	500
Dark state acidification shift seen		Yes	ND	ND	ND	Yes	Yes	Yes	Yes
Photobleaching profile compared to WT		-	Staggered	Staggered	ND	As WT	As WT	Staggered	As WT
Photobleached acidification shift seen		Yes	Yes	Yes	Yes	Yes	Yes	Yes	Yes
Meta II	half-life (mins)	17.67	5.96	10.06	9.97	42.45	13.87	4.00	18.69
	S.D.	1.76	2.96	1.78	0.78	3.07	0.53	0.38	ND
	<i>n</i>	12	2	5	2	7	8	7	1
Transducin activation	Relative rate	-	0.35	0.64	0.18	0.45	0.85	0.30	0.76
	S.D.	0.0007	0.0002	0.0006	0.0002	0.0002	0.0005	0.0002	0.0003
	<i>n</i>	11	6	8	2	8	9	8	3
Potential mutant class		-	2	2	2	3	-	2 or 4	-

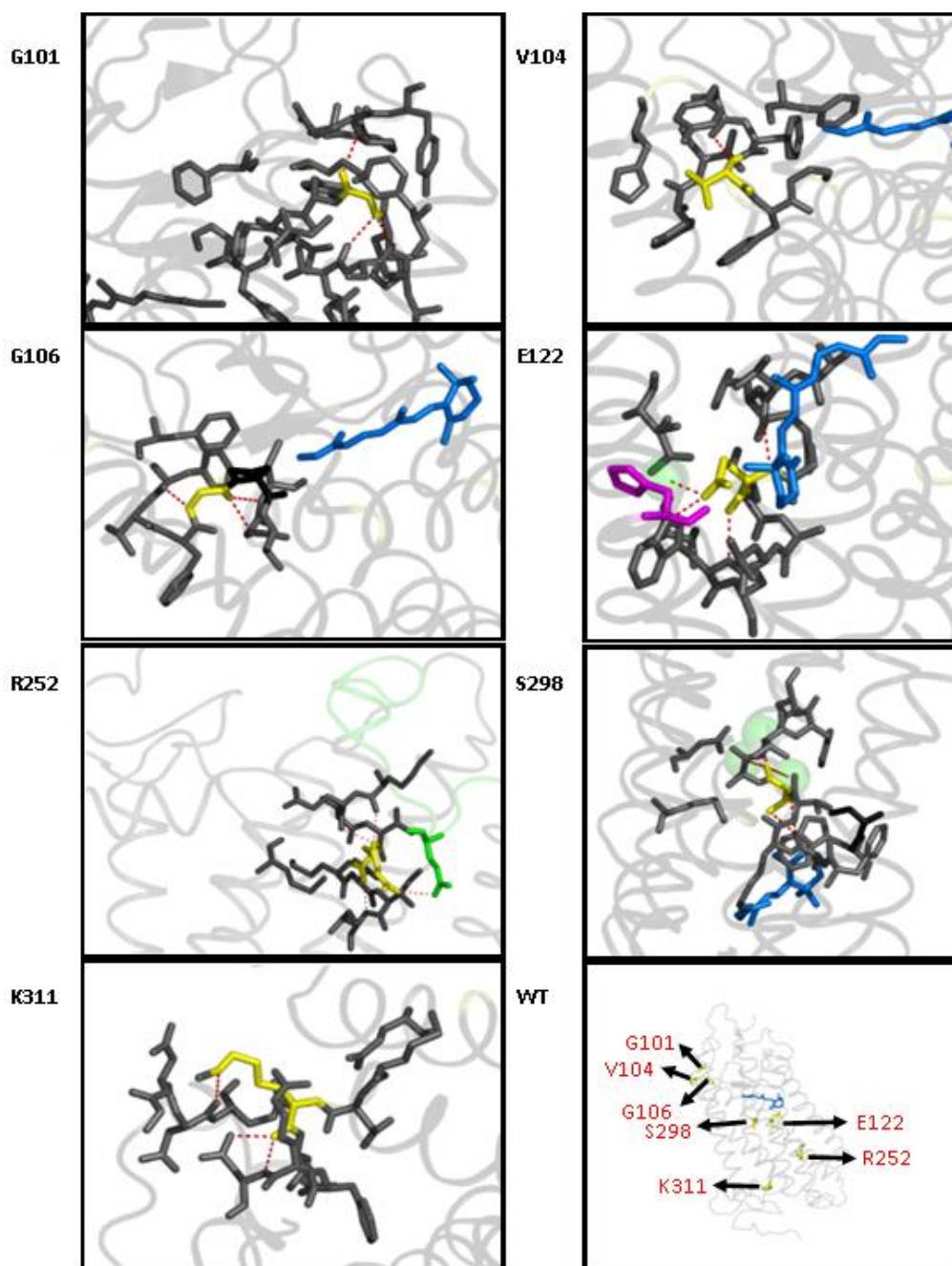


Figure 7.1 Polar contacts (red) made by the WT residues at the positions analysed through this work. In each panel, the relevant residue is shown as yellow sticks. E122 also shows H211 as magenta sticks and a zinc molecule (green), R252 has IL3 shown in green, S298 shows contacts to 3 O molecules (green). The WT panel shows the full rhodopsin structure and each of the mutants as yellow sticks. All residues within 5 Å of the relevant residue are shown as grey sticks. Grey cartoon shows the rest of the structure. Images were created using PyMOL and the rhodopsin structure PDB 1U19.

7.4 Concluding remarks.

Overall, this work has shown that the piggyBac expression system works efficiently for the expression of rhodopsin and its mutants and with further optimisation, this expression might be further increased to produce high levels of mutants and other GPCRs that are currently difficult to express. This fast, effective and relatively straightforward method proved to be invaluable for the construction of several (up to ten) rhodopsin mutant cell lines simultaneously, without the need for individual colony isolation and expansion. For these reasons it will likely aid in the study of the vast array of rhodopsin RP mutants, which have been identified but not yet categorised, as well as other GPCRs. This method which has been developed and refined over the course of this work, has enabled the construction of several cell lines expressing rhodopsin RP mutants and contributed to the structural analysis of RP mutant of rhodopsin, E122G, which through NMR studies has been shown to be pivotal in the activation of rhodopsin, a discovery which could aid in understanding how rhodopsin and other GPCRs activate.

8. References

Adelman, Z. N., Jasinskiene, N., Vally, K. J. M., Peek, C., Travanty, E. A., Olson, K. E., Brown, S. E., Stephens, J. L., Knudson, D. L., Coates, C. J. and James, A. A. (2004) 'Formation and loss of large, unstable tandem arrays of the piggyBac transposable element in the yellow fever mosquito, *Aedes aegypti*'.

Ahuja, S., Crocker, E., Eilers, M., Hornak, V., Hirshfeld, A., Ziliox, M., Syrett, N., Reeves, P. J., Gobind Khorana, H., Sheves, M. and Smith, S. O. (2009) 'Location of the Retinal Chromophore in the Activated State of Rhodopsin * \square S', *THE JOURNAL OF BIOLOGICAL CHEMISTRY*, 284(15), pp. 10190–10201. doi: 10.1074/jbc.M805725200.

Ahuja, S., Hornak, V., Yan, E. C. Y., Syrett, N., Goncalves, J. A., Hirshfeld, A., Ziliox, M., Sakmar, T. P., Sheves, M., Reeves, P. J., Smith, S. O. and Eilers, M. (2009) 'Helix Movement is Coupled to Displacement of the Second Extracellular Loop in Rhodopsin Activation', *Nature structural & molecular biology*, 16(2), p. 168. doi: 10.1038/NSMB.1549.

Andrés, A., Garriga, P. and Manyosa, J. (2003) 'Altered functionality in rhodopsin point mutants associated with retinitis pigmentosa', *Biochemical and Biophysical Research Communications*, 303(1), pp. 294–301. doi: 10.1016/S0006-291X(03)00328-0.

Athanasiou, D., Aguila, M., Opefi, C. A., *et al.* (2017) 'Rescue of mutant rhodopsin traffic by metformin-induced AMPK activation accelerates photoreceptor degeneration', *Human Molecular Genetics*, 26(2), pp. 305–319. doi: 10.1093/hmg/ddw387.

- Athanasίου, D., Aguila, M., Bellingham, J., Kanuga, N., Adamson, P. and Cheetham, M. E. (2017) 'The role of the ER stress-response protein PERK in rhodopsin retinitis pigmentosa', *Human Molecular Genetics*, 26(24), p. 4896. doi: 10.1093/HMG/DDX370.
- Athanasίου, D., Aguila, M., Bellingham, J., Li, W., McCulley, C., Reeves, P. J. and Cheetham, M. E. (2018) 'The molecular and cellular basis of rhodopsin retinitis pigmentosa reveals potential strategies for therapy', *Progress in Retinal and Eye Research*. Elsevier Ltd, pp. 1–23. doi: 10.1016/j.preteyeres.2017.10.002.
- Athanasίου, D., Aguilà, M., Bevilacqua, D., Novoselov, S. S., Parfitt, D. A. and Cheetham, M. E. (2013) 'The cell stress machinery and retinal degeneration', *FEBS Letters*, 587(13), pp. 2008–2017. doi: 10.1016/j.febslet.2013.05.020.
- Baeshen, M. N., Al-Hejin, A. M., Bora, R. S., Ahmed, M. M. M., Ramadan, H. A. I., Saini, K. S., Baeshen, N. A. and Redwan, E. M. (2015) 'Production of biopharmaceuticals in E. Coli: Current scenario and future perspectives', *Journal of Microbiology and Biotechnology*. Korean Society for Microbiolog and Biotechnology, pp. 953–962. doi: 10.4014/jmb.1412.12079.
- Basith, S., Cui, M., Macalino, S. J. Y., Park, J., Clavio, N. A. B., Kang, S. and Choi, S. (2018) 'Exploring G protein-coupled receptors (GPCRs) ligand space via cheminformatics approaches: Impact on rational drug design', *Frontiers in Pharmacology*, 9(MAR), p. 128. doi: 10.3389/FPHAR.2018.00128/BIBTEX.
- Bhattacharya, S., Hall, S. E. and Vaidehi, N. (2008) 'Agonist-Induced Conformational Changes in Bovine Rhodopsin: Insight into Activation of G-Protein-Coupled Receptors', *Journal of Molecular Biology*, 382(2), pp. 539–555. doi: 10.1016/j.jmb.2008.06.084.

- Blackshaw, S. and Snyder, S. H. (1999) 'Encephalopsin: A Novel Mammalian Extraretinal Opsin Discretely Localized in the Brain'.
- Bosch-Presegué, L., Ramon, E., Toledo, D., Cordoní, A. and Garriga, P. (2011) 'Alterations in the photoactivation pathway of rhodopsin mutants associated with retinitis pigmentosa', *FEBS Journal*, 278(9), pp. 1493–1505. doi: 10.1111/j.1742-4658.2011.08066.x.
- Breyton, C., Javed, W., Vermot, A., Arnaud, C. A., Hajjar, C., Dupuy, J., Petit-Hartlein, I., Le Roy, A., Martel, A., Thépaut, M., Orelle, C., Jault, J. M., Fieschi, F., Porcar, L. and Ebel, C. (2019) 'Assemblies of lauryl maltose neopentyl glycol (LMNG) and LMNG-solubilized membrane proteins', *Biochimica et Biophysica Acta - Biomembranes*, 1861(5), pp. 939–957. doi: 10.1016/J.BBAMEM.2019.02.003.
- Cakir, F., Tas, A. and Sobaci, G. (2011) 'Electroretinogram in Hereditary Retinal Disorders', in *Electroretinograms*. InTech. doi: 10.5772/21704.
- Campochiaro, P. A. and Mir, T. A. (2018) 'The mechanism of cone cell death in Retinitis Pigmentosa', *Progress in Retinal and Eye Research*, 62, pp. 24–37. doi: 10.1016/J.PRETEYERES.2017.08.004.
- Caro, L. N., Li, Z., Balo, A. R., Van Eps, N., Rini, J. M. and Ernst, O. P. (2015) 'Rapid and facile recombinant expression of bovine rhodopsin in HEK293S GnTI- cells using a piggyBac inducible system', in *Methods in Enzymology*. Academic Press Inc., pp. 307–330. doi: 10.1016/bs.mie.2015.01.005.
- Castiglione, G. M. and Chang, B. S. (2018) 'Functional trade-offs and environmental variation shaped ancient trajectories in the evolution of dim-light vision', *eLife*. doi: 10.7554/eLife.35957.001.

Chandler, B., Todd, L. and Smith, S. O. (2021) 'Magic angle spinning NMR of G protein-coupled receptors'. doi: 10.1016/j.pnmrs.2021.10.002.

Chaptal, V. *et al.* (2017) 'Quantification of Detergents Complexed with Membrane Proteins', *Scientific Reports* 2017 7:1, 7(1), pp. 1–12. doi: 10.1038/srep41751.

Chen, Yuanyuan, Chen, Yu, Jastrzebska, B., Golczak, M., Gulati, S., Tang, H., Seibel, W., Li, X., Jin, H., Han, Y., Gao, S., Zhang, J., Liu, X., Heidari-Torkabadi, H., Stewart, P. L., Harte, W. E., Tochtrop, G. P. and Palczewski, K. (2018) 'A novel small molecule chaperone of rod opsin and its potential therapy for retinal degeneration', *Nature Communications*, 9(1). doi: 10.1038/s41467-018-04261-1.

Cideciyan, A. V., Hood, D. C., Huang, Y., Banin, E., Li, Z. Y., Stone, E. M., Milam, A. H. and Jacobson, S. G. (1998) 'Disease sequence from mutant rhodopsin allele to rod and cone photoreceptor degeneration in man', *Proceedings of the National Academy of Sciences of the United States of America*, 95(12), p. 7103. doi: 10.1073/PNAS.95.12.7103.

Comander, J., Difranco, C. W., Sanderson, K., Place, E., Maher, M., Zampaglione, E., Zhao, Y., Huckfeldt, R. M., Bujakowska, K. M. and Pierce, E. (2023) 'C L I N I C A L M E D I C I N E Natural history of retinitis pigmentosa based on genotype, vitamin A/E supplementation, and an electroretinogram biomarker', *JCI Insight*, 8(13). doi: 10.1172/jci.

Comitato, A., Schirotti, D., Montanari, M. and Marigo, V. (2019) 'Calpain Activation Is the Major Cause of Cell Death in Photoreceptors Expressing a Rhodopsin Misfolding Mutation', *Molecular Neurobiology*. doi: 10.1007/s12035-019-01723-5.

Costanzi, S., Siegel, J., Tikhonova, I. G. and Jacobson, K. A. (2009) 'Rhodopsin and the others: a historical perspective on structural studies of G protein-coupled

receptors', *Current pharmaceutical design*, 15(35), p. 3994. doi: 10.2174/138161209789824795.

Daruwalla, A., Choi, E. H., Palczewski, K. and Kiser, P. D. (2018) 'Structural biology of 11-cis-retinaldehyde production in the classical visual cycle', *Biochemical Journal*. Portland Press Ltd, pp. 3171–3188. doi: 10.1042/BCJ20180193.

Deupi, X. (2013) 'Relevance of rhodopsin studies for GPCR activation ☆'. doi: 10.1016/j.bbabi.2013.09.002.

Dias, M. F., Joo, K., Kemp, J. A., Fialho, S. L., da Silva Cunha, A., Woo, S. J. and Kwon, Y. J. (2018) 'Molecular genetics and emerging therapies for retinitis pigmentosa: Basic research and clinical perspectives', *Progress in Retinal and Eye Research*. Elsevier Ltd, pp. 107–131. doi: 10.1016/j.preteyeres.2017.10.004.

Ding, S., Wu, X., Li, G., Han, M., Zhuang, Y. and Xu, T. (2005) 'Efficient transposition of the piggyBac (PB) transposon in mammalian cells and mice', *Cell*, 122(3), pp. 473–483. doi: 10.1016/j.cell.2005.07.013.

Dizhoor, A. M., Woodruff, M. L., Olshevskaya, E. V., Cilluffo, M. C., Cornwall, M. C., Sieving, P. A. and Fain, G. L. (2008) 'Night blindness and the mechanism of constitutive signaling of mutant G90D rhodopsin', *Journal of Neuroscience*, 28(45), pp. 11662–11672. doi: 10.1523/JNEUROSCI.4006-08.2008.

Doi, T., Molday, R. S. and Gobind Khorana, H. (1990) 'Role of the intradiscal domain in rhodopsin assembly and function.', *Proceedings of the National Academy of Sciences of the United States of America*, 87(13), p. 4991. doi: 10.1073/PNAS.87.13.4991.

- Dryja, T. P., McGee, T. L., Hahn, L. B., Cowley, G. S., Olsson, J. E., Reichel, E., Sandberg, M. A. and Berson, E. L. (1990) 'Mutations within the Rhodopsin Gene in Patients with Autosomal Dominant Retinitis Pigmentosa', *New England Journal of Medicine*, 323(19), pp. 1302–1307. doi: 10.1056/NEJM199011083231903.
- Duda, M., Domagalik, A., Orłowska-Feuer, P., Krzysztynska-Kuleta, O., Beldzik, E., Smyk, M. K., Stachurska, A., Oginska, H., Jeczmiem-Lazur, J. S., Fafrowicz, M., Marek, T., Lewandowski, M. H. and Sarna, T. (2020) 'Melanopsin: From a small molecule to brain functions', *Neuroscience & Biobehavioral Reviews*, 113, pp. 190–203. doi: 10.1016/J.NEUBIOREV.2020.03.012.
- Ebrey, T. and Koutalos, Y. (2001) 'Vertebrate Photoreceptors'.
- Eilers, M., Reeves, P. J., Ying, W., Khorana, H. G. and Smith, S. O. (1999) 'Magic angle spinning NMR of the protonated retinylidene Schiff base nitrogen in rhodopsin: Expression of ¹⁵N-lysine- and ¹³C-glycine-labeled opsin in a stable cell line', *Proceedings of the National Academy of Sciences of the United States of America*, 96(2), pp. 487–492. doi: 10.1073/pnas.96.2.487.
- Ernst, O. P. and Menon, A. K. (2015) 'Phospholipid scrambling by rhodopsin', *Photochemical and Photobiological Sciences*, 14(11), pp. 1922–1931. doi: 10.1039/c5pp00195a.
- Espósito, A. C. C., de Souza, N. P., Miot, L. D. B. and Miot, H. A. (2021) 'Expression of OPN3 in fibroblasts, melanocytes, and keratinocytes of skin with facial melasma in comparison with unaffected adjacent skin'. doi: 10.1016/j.abd.2020.05.016.
- Farrens, D. L. and Khorana, H. G. (1995) 'Structure and function in rhodopsin: Measurement of the rate of metarhodopsin II decay by fluorescence spectroscopy',

Journal of Biological Chemistry, 270(10), pp. 5073–5076. doi: 10.1074/jbc.270.10.5073.

Faurobert, E., Otto-Bruc, A., Chardin, P. and Chabre, M. (1993) 'Tryptophan W207 in transducin T α is the fluorescence sensor of the G protein activation switch and is involved in the effector binding', *EMBO Journal*, 12(11), pp. 4191–4198. doi: 10.1002/j.1460-2075.1993.tb06103.x.

Ferrari, S., Parmeggiani, F., S. Sorrentino, F., Ponzin, D., Barbaro, V. and Di Iorio, E. (2011) 'Retinitis Pigmentosa: Genes and Disease Mechanisms', *Current Genomics*, 12(4), pp. 238–249. doi: 10.2174/138920211795860107.

Fu, Y. (2010) 'Phototransduction in Rods and Cones', *Vertebrate Photoreceptors: Functional Molecular Bases*, pp. 23–45. doi: 10.1007/978-4-431-54880-5_2.

Gao, Y., Hu, H., Ramachandran, S., Erickson, J. W., Cerione, R. A. and Skiniotis, G. (2019) 'Structures of the Rhodopsin-Transducin Complex: Insights into G-Protein Activation', *Molecular Cell*, 75(4), pp. 781-790.e3. doi: 10.1016/j.molcel.2019.06.007.

Gleim, S., Stojanovic, A., Arehart, E., Byington, D. and Hwa, J. (2009) 'Conserved rhodopsin intradiscal structural motifs mediate stabilization; effects of zinc † NIH Public Access', *Biochemistry*, 48(8), pp. 1793–1800. doi: 10.1021/bi800968w.

Gossen, M. and Bujard, H. (1992) *Tight control of gene expression in mammalian cells by tetracycline-responsive promoters*, *Cell Biology*.

Gragg, M. and Park, P. S. H. (2018) 'Misfolded rhodopsin mutants display variable aggregation properties', *Biochimica et Biophysica Acta - Molecular Basis of Disease*, 1864(9), pp. 2938–2948. doi: 10.1016/j.bbadis.2018.06.004.

- Gray-Keller, M. P., Detwiler, P. B., Benovic, J. L. and Gurevich, V. V. (1997) 'Arrestin with a single amino acid substitution quenches light-activated rhodopsin in a phosphorylation-independent fashion', *Biochemistry*, 36(23), pp. 7058–7063. doi: 10.1021/bi963110k.
- Grime, R. L., Logan, R. T., Nestorow, S. A., Sridhar, P., Edwards, P. C., Tate, C. G., Klumperman, B., Dafforn, T. R., Poyner, D. R., Reeves, P. J. and Wheatley, M. (2021) 'Differences in SMA-like polymer architecture dictate the conformational changes exhibited by the membrane protein rhodopsin encapsulated in lipid nano-particles', *Nanoscale*, 13(31), pp. 13519–13528. doi: 10.1039/D1NR02419A.
- Gupta, S. K. and Shukla, P. (2016) 'Advanced technologies for improved expression of recombinant proteins in bacteria: perspectives and applications', *Crit Rev Biotechnol*, 36(6), pp. 1089–1098. doi: 10.3109/07388551.2015.1084264.
- Halford, S., Freedman, M. S., Bellingham, J., Inglis, S. L., Poopalasundaram, S., Soni, B. G., Foster, R. G. and Hunt, D. M. (2001) 'Characterization of a Novel Human Opsin Gene with Wide Tissue Expression and Identification of Embedded and Flanking Genes on Chromosome 1q43', *Genomics*, 72(2), pp. 203–208. doi: 10.1006/GENO.2001.6469.
- Hamel, C. (2006) 'Retinitis pigmentosa', *Orphanet Journal of Rare Diseases*, 1(1), p. 40. doi: 10.1186/1750-1172-1-40.
- Hargrave, P. A., Hamm, H. E. and Hofmann, K. P. (1993) 'Interaction of rhodopsin with the G-protein, transducin', *BioEssays*, pp. 43–50. doi: 10.1002/bies.950150107.
- Hartong, D. T., Berson, E. L. and Dryja, T. P. (2006) *Retinitis pigmentosa Prevalence and inheritance patterns*, www.thelancet.com. doi: 10.1016/S0140-6736(06)69740-7.

- Hofmann, K. P. (1999) 'Signalling states of photoactivated rhodopsin', *Novartis Foundation Symposium*, 224, pp. 158–180. doi: 10.1002/9780470515693.ch10.
- Hoon, M., Okawa, H., Della Santina, L. and Wong, R. O. L. (2014) 'Functional architecture of the retina: Development and disease', *Progress in Retinal and Eye Research*, 42, pp. 44–84. doi: 10.1016/j.preteyeres.2014.06.003.
- Hornak, V., Ahuja, S., Eilers, M., Goncalves, J. A., Sheves, M., Reeves, P. J. and Smith, S. O. (2009) 'Light activation of rhodopsin: insights from molecular dynamics simulations guided by solid-state NMR distance restraints'. doi: 10.1016/j.jmb.2009.12.003.
- Hoshino, A., Ratnapriya, R., Brooks, M. J., Chaitankar, V., Wilken, M. S., Zhang, C., Starostik, M. R., Gieser, L., La Torre, A., Nishio, M., Bates, O., Walton, A., Bermingham-McDonogh, O., Glass, I. A., Wong, R. O. L., Swaroop, A. and Reh, T. A. (2017) 'Molecular Anatomy of the Developing Human Retina', *Developmental Cell*, 43(6), pp. 763-779.e4. doi: 10.1016/j.devcel.2017.10.029.
- Iannaccone, A., Man, D., Waseem, N., Jennings, B. J., Ganapathiraju, M., Gallaher, K., Reese, E., Bhattacharya, S. S. and Klein-Seetharaman, J. (2006) 'Retinitis pigmentosa associated with rhodopsin mutations: Correlation between phenotypic variability and molecular effects', *Vision Research*, 46(27), pp. 4556–4567. doi: 10.1016/J.VISRES.2006.08.018.
- Imai, H., Kefalov, V., Sakurai, K., Chisaka, O., Ueda, Y., Onishi, A., Morizumi, T., Fu, Y., Ichikawa, K., Nakatani, K., Honda, Y., Chen, J., Yau, K. W. and Shichida, Y. (2007) 'Molecular properties of rhodopsin and rod function', *Journal of Biological Chemistry*, 282(9), pp. 6677–6684. doi: 10.1074/jbc.M610086200.

- Imai, H., Kojima, D., Oura, T., Tachibanaki, S., Terakita, A. and Shichida, Y. (1997) 'Single amino acid residue as a functional determinant of rod and cone visual pigments', *Proceedings of the National Academy of Sciences of the United States of America*, 94(6), pp. 2322–2326. doi: 10.1073/PNAS.94.6.2322/ASSET/9A641488-674A-49DE-93AF-DB54A4C4DF82/ASSETS/GRAPHIC/PQ0673876004.JPEG.
- Ingram, N. T., Sampath, A. P. and Fain, G. L. (2016) 'Why are rods more sensitive than cones?', *The Journal of Physiology*, 594(19), p. 5415. doi: 10.1113/JP272556.
- Isberg, V., Mordalski, S., Munk, C., Rataj, K., Harpsøe, K., Hauser, A. S., Vroling, B., Bojarski, A. J., Vriend, G. and Gloriam, D. E. (2016) 'GPCRdb: an information system for G protein-coupled receptors', *Nucleic Acids Research*, 44. doi: 10.1093/nar/gkv1178.
- Janz, J. M. and Farrens, D. L. (2004) 'Role of the retinal hydrogen bond network in rhodopsin Schiff base stability and hydrolysis', *Journal of Biological Chemistry*, 279(53), pp. 55886–55894. doi: 10.1074/jbc.M408766200.
- Janz, J. M., Fay, J. F. and Farrens, D. L. (2003) 'Stability of dark state rhodopsin is mediated by a conserved ion pair in intradiscal loop E-2', *Journal of Biological Chemistry*, 278(19), pp. 16982–16991. doi: 10.1074/jbc.M210567200.
- Kahlig, K. M., Saridey, S. K., Kaja, A., Daniels, M. A., George, A. L. and Wilson, M. H. (2010) 'Multiplexed transposon-mediated stable gene transfer in human cells', *Proceedings of the National Academy of Sciences of the United States of America*, 107(4), pp. 1343–1348. doi: 10.1073/pnas.0910383107.
- Kaštánková, I., Štach, M., Žižková, H., Ptáčková, P., Šmilauerová, K., Mucha, M., Šroller, V. and Otáhal, P. (2021) 'Enzymatically produced piggyBac transposon vectors for efficient non-viral manufacturing of CD19-specific CAR T cells', *Molecular*

Therapy. Methods & Clinical Development, 23, p. 119. doi: 10.1016/J.OMTM.2021.08.006.

Kaushal, S. and Khorana, H. G. (1994) 'Structure and Function in Rhodopsin. 7. Point Mutations Associated with Autosomal Dominant Retinitis Pigmentosa', *Biochemistry*, 33(20), pp. 6121–6128. doi: 10.1021/bi00186a011.

Kazmin, R., Rose, A., Szczepek, M., Elgeti, M., Ritter, E., Piechnick, R., Hofmann, K. P., Scheerer, P., Hildebrand, P. W. and Bartl, F. J. (2015) 'The activation pathway of human rhodopsin in comparison to bovine rhodopsin', *Journal of Biological Chemistry*, 290(33), pp. 20117–20127. doi: 10.1074/jbc.M115.652172.

Khorana, H. G. (1993) 'Two light-transducing membrane proteins: Bacteriorhodopsin and the mammalian rhodopsin', in *Proceedings of the National Academy of Sciences of the United States of America*, pp. 1166–1171. doi: 10.1073/pnas.90.4.1166.

Kimata, N., Pope, A., Eilers, M., Opefi, C. A., Ziliox, M., Hirshfeld, A., Zaitseva, E., Vogel, R., Sheves, M., Reeves, P. J. and Smith, S. O. (2016) 'Retinal orientation and interactions in rhodopsin reveal a two-stage trigger mechanism for activation'. doi: 10.1038/ncomms12683.

Kimata, N., Pope, A., Sanchez-Reyes, O. B., Eilers, M., Opefi, C. A., Ziliox, M., Reeves, P. J. and Smith, S. O. (2016) 'Free backbone carbonyls mediate rhodopsin activation', *Nature Publishing Group*. doi: 10.1038/nsmb.3257.

Kimata, N., Reeves, P. J. and Smith, S. O. (2015) 'Uncovering the triggers for GPCR activation using solid-state NMR spectroscopy', *Journal of Magnetic Resonance*, 253, pp. 111–118. doi: 10.1016/j.jmr.2014.12.014.

- Klein-Seetharaman, J., Getmanova, E. V., Loewen, M. C., Reeves, P. J. and Khorana, H. G. (1999) 'NMR spectroscopy in studies of light-induced structural changes in mammalian rhodopsin: Applicability of solution ^{19}F NMR', *Proceedings of the National Academy of Sciences of the United States of America*, 96(24), pp. 13744–13749. doi: 10.1073/pnas.96.24.13744.
- Kooistra, A. J., Mordalski, S., Gáspár Gáspár, G., Andy-Szekeres, P. ´, Esguerra, M., Mamyrbekov, A., Munk, C., Gy¨, G., Keser, G. M. and Gloriam, D. E. (2021) 'GPCRdb in 2021: integrating GPCR sequence, structure and function', *Nucleic Acids Research*, 49, pp. 335–343. doi: 10.1093/nar/gkaa1080.
- Kraus, J., Sarkar, S., Quinn, C. M. and Polenova, T. (2021) 'Solid-state NMR spectroscopy of microcrystalline proteins', *Annual Reports on NMR Spectroscopy*, 102, pp. 81–151. doi: 10.1016/BS.ARNMR.2020.10.002.
- Krebs, M. P., Holden, D. C., Joshi, P., Clark, C. L., Lee, A. H. and Kaushal, S. (2010) 'Molecular Mechanisms of Rhodopsin Retinitis Pigmentosa and the Efficacy of Pharmacological Rescue', *Journal of Molecular Biology*, 395(5), pp. 1063–1078. doi: 10.1016/j.jmb.2009.11.015.
- Krupnick, J. G., Gurevich, V. V. and Benovic, J. L. (1997) 'Mechanism of quenching of phototransduction: Binding competition between arrestin and transducin for phosphorhodopsin', *Journal of Biological Chemistry*, 272(29), pp. 18125–18131. doi: 10.1074/jbc.272.29.18125.
- Lee, S., Ghosh, S., Jana, S., Robertson, N., Tate, C. G. and Vaidehi, N. (2020) 'How Do Branched Detergents Stabilize GPCRs in Micelles?' doi: 10.1021/acs.biochem.0c00183.

- Leung, N. Y. and Montell, C. (2017) 'Unconventional roles of opsins'. doi: 10.1146/annurev-cellbio-100616-060432.
- Lewin, A. S., Rossmiller, B. and Mao, H. (2014) 'Gene augmentation for adRP mutations in RHO', *Cold Spring Harbor Perspectives in Medicine*, 4(9). doi: 10.1101/cshperspect.a017400.
- Li, T., Sandberg, M. A., Pawlyk, B. S., Rosner, B., Hayes, K. C., Dryja, T. P. and Berson, E. L. (1998) 'Effect of vitamin A supplementation on rhodopsin mutants threonine-17 → methionine and proline-347 → serine in transgenic mice and in cell cultures', *Proceedings of the National Academy of Sciences of the United States of America*, 95(20), pp. 11933–11938. doi: 10.1073/pnas.95.20.11933.
- Lin, C. Y., Huang, Z., Wen, W., Wu, A., Wang, C. and Niu, L. (2015) 'Enhancing Protein Expression in HEK-293 Cells by Lowering Culture Temperature', *PloS one*, 10(4). doi: 10.1371/JOURNAL.PONE.0123562.
- Lin, J. H., Li, H., Yasumura, D., Cohen, H. R., Zhang, C., Panning, B., Shokat, K. M., LaVail, M. M. and Walter, P. (2007) 'IRE1 signaling affects cell fate during the unfolded protein response', *Science*, 318(5852), pp. 944–949. doi: 10.1126/science.1146361.
- Liu, H. and Naismith, J. H. (2008) 'An efficient one-step site-directed deletion, insertion, single and multiple-site plasmid mutagenesis protocol', *BMC biotechnology*, 8, p. 91. doi: 10.1186/1472-6750-8-91.
- Lobanova, E. S., Finkelstein, S., Skiba, N. P. and Arshavsky, V. Y. (2013) 'Proteasome overload is a common stress factor in multiple forms of inherited retinal degeneration', *Proceedings of the National Academy of Sciences of the United States of America*, 110(24), pp. 9986–9991. doi: 10.1073/pnas.1305521110.

Madeira, F., Park, Y. M., Lee, J., Buso, N., Gur, T., Madhusoodanan, N., Basutkar, P., Tivey, A. R. N., Potter, S. C., Finn, R. D. and Lopez, R. (2019) 'The EMBL-EBI search and sequence analysis tools APIs in 2019.', *Nucleic acids research*, 47(W1), pp. W636–W641. doi: 10.1093/nar/gkz268.

Le Maire, M., Champeil, P. and Møller, J. V. (2000) 'Interaction of membrane proteins and lipids with solubilizing detergents', *Biochimica et Biophysica Acta (BBA) - Biomembranes*, 1508(1–2), pp. 86–111. doi: 10.1016/S0304-4157(00)00010-1.

Mao, H., Gorbatyuk, M. S., Rossmiller, B., Hauswirth, W. W. and Lewin, A. S. (2012) 'Long-Term Rescue of Retinal Structure and Function by Rhodopsin RNA Replacement with a Single Adeno-Associated Viral Vector in P23H RHO Transgenic Mice'. doi: 10.1089/hum.2011.213.

Matias-Florentino, M., Ayala-Ramirez, R., Graue-Wiechers, F. and Zenteno, J. C. (2009) 'Molecular Screening of Rhodopsin and Peripherin/RDS Genes in Mexican Families with Autosomal Dominant Retinitis Pigmentosa', <http://dx.doi.org/10.3109/02713680903283169>, 34(12), pp. 1050–1056. doi: 10.3109/02713680903283169.

Mckee, A. G., Kuntz, C. P., Ortega, J. T., Woods, H., Most, V., Roushar, F. J., Meiler, J., Jastrzebska, B. and Schleich, J. P. (2021) 'Systematic profiling of temperature- and retinal-sensitive rhodopsin variants by deep mutational scanning', *J. Biol. Chem*, (6), pp. 101359–101360. doi: 10.1016/j.jbc.2021.101359.

Mendes, H. F., Van Der Spuy, J., Chapple, J. P. and Cheetham, M. E. (2005) 'Mechanisms of cell death in rhodopsin retinitis pigmentosa: Implications for therapy', *Trends in Molecular Medicine*. Elsevier Ltd, pp. 177–185. doi: 10.1016/j.molmed.2005.02.007.

- Meng, E. C. and Bourne, H. R. (2001) 'Receptor activation: What does the rhodopsin structure tell us?', *Trends in Pharmacological Sciences*, pp. 587–593. doi: 10.1016/S0165-6147(00)01825-3.
- Milam, A. H., Li, Z.-Y. and Fariss, R. N. (1998) *Histopathology of the Human Retina in Retinitis Pigmentosa*.
- Mollaaghababa, R., Davidson, F. F., Kaiser, C. and Khorana, H. G. (1996) 'Structure and function in rhodopsin: Expression of functional mammalian opsin in *Saccharomyces cerevisiae*', *Proceedings of the National Academy of Sciences of the United States of America*, 93(21), pp. 11482–11486. doi: 10.1073/pnas.93.21.11482.
- Morshedian, A., Kaylor, J. J., Radu, R. A., Fain, G. L. and Travis Correspondence, G. H. (2019) 'Light-Driven Regeneration of Cone Visual Pigments through a Mechanism Involving RGR Opsin in Müller Glial Cells', *Neuron*, 102, pp. 1172–1183. doi: 10.1016/j.neuron.2019.04.004.
- Murray, A. R., Fliesler, S. J. and Al-Ubaidi, M. R. (2009) 'Rhodopsin: The Functional Significance of Asn-Linked Glycosylation and Other Post-Translational Modifications', *Ophthalmic Genetics*, 30(3), pp. 109–120. doi: 10.1080/13816810902962405.
- Nathans, J. (1992) 'Rhodopsin: structure, function, and genetics', *Biochemistry*, 31(21), pp. 4923–4931. doi: 10.1021/bi00136a001.
- Nathans, J., Thomas, D. and Hogness, D. S. (1986) 'Molecular genetics of human color vision: The genes encoding blue, green, and red pigments', *Science*, 232(4747), pp. 196–202. doi: 10.1126/SCIENCE.2937147.

- Natochin, M., Gasimov, K. G., Moussaif, M. and Artemyev, N. O. (2003) 'Rhodopsin determinants for transducin activation: A gain-of-function approach', *Journal of Biological Chemistry*, 278(39), pp. 37574–37581. doi: 10.1074/jbc.M305136200.
- Neaves, L. C. (2020) *Characterisation of Rhodopsin Retinitis Pigmentosa mutants located in Intradiscal Loop 1*.
- Noorwez, S. M., Kuksa, V., Imanishi, Y., Zhu, L., Filipek, S., Palczewski, K. and Kaushal, S. (2003) 'Pharmacological chaperone-mediated in vivo folding and stabilization of the P23H-opsin mutant associated with autosomal dominant retinitis pigmentosa', *Journal of Biological Chemistry*, 278(16), pp. 14442–14450. doi: 10.1074/jbc.M300087200.
- Noorwez, S. M., Malhotra, R., McDowell, J. H., Smith, K. A., Krebs, M. P. and Kaushal, S. (2004) 'Retinoids Assist the Cellular Folding of the Autosomal Dominant Retinitis Pigmentosa Opsin Mutant P23H', *Journal of Biological Chemistry*, 279(16), pp. 16278–16284. doi: 10.1074/jbc.M312101200.
- Opefi, C. (2011) *Restoring structure and function in rhodopsin autosomal dominant retinitis pigmentosa mutants*.
- Opefi, C. A., South, K., Reynolds, C. A., Smith, S. O. and Reeves, P. J. (2013) 'Retinitis pigmentosa mutants provide insight into the role of the N-terminal cap in rhodopsin folding, structure, and function', *Journal of Biological Chemistry*, 288(47), pp. 33912–33926. doi: 10.1074/jbc.M113.483032.
- Orlans, H. O., Merrill, J., Barnard, A. R., Issa, P. C., Peirson, S. N. and Maclaren, R. E. (2019) 'Filtration of short-wavelength light provides therapeutic benefit in retinitis pigmentosa caused by a common rhodopsin mutation', *Investigative Ophthalmology and Visual Science*, 60(7), pp. 2733–2742. doi: 10.1167/iovs.19-26964.

- Ortega, J. T., McKee, A. G., Roushar, F. J., Penn, W. D., Schleich, J. P. and Jastrzebska, B. (2022) 'Chromenone derivatives as novel pharmacological chaperones for retinitis pigmentosa-linked rod opsin mutants', *Human Molecular Genetics*, 31(20), pp. 3439–3457. doi: 10.1093/hmg/ddac125.
- Owczarek, B., Gerszberg, A. and Hnatuszko-Konka, K. (2019) 'A Brief Reminder of Systems of Production and Chromatography-Based Recovery of Recombinant Protein Biopharmaceuticals', *BioMed Research International*. Hindawi Limited. doi: 10.1155/2019/4216060.
- Owen, T. S., Salom, D., Sun, W. and Palczewski, K. (2018) 'Increasing the Stability of Recombinant Human Green Cone Pigment'. doi: 10.1021/acs.biochem.7b01118.
- Palczewski, K., Kumasaka, T., Hori, T., Behnke, C. A., Motoshima, H., Fox, B. A., Le Trong, I., Teller, D. C., Okada, T., Stenkamp, R. E., Yamamoto, M. and Miyano, M. (2000) 'Crystal structure of rhodopsin: A G protein-coupled receptor', *Science*, 289(5480), pp. 739–745. doi: 10.1126/science.289.5480.739.
- Parfitt, D. A., Aguila, M., McCulley, C. H., Bevilacqua, D., Mendes, H. F., Athanasiou, D., Novoselov, S. S., Kanuga, N., Munro, P. M., Coffey, P. J., Kalmar, B., Greensmith, L. and Cheetham, M. E. (2014) 'The heat-shock response co-inducer arimoclomol protects against retinal degeneration in rhodopsin retinitis pigmentosa.', *Cell death & disease*, 5. doi: 10.1038/cddis.2014.214.
- Parfitt, D. A. and Cheetham, M. E. (2016) 'Targeting the proteostasis network in rhodopsin retinitis pigmentosa', in *Advances in Experimental Medicine and Biology*. Springer New York LLC, pp. 479–484. doi: 10.1007/978-3-319-17121-0_64.

- Park, P. S. H. (2014) 'Constitutively Active Rhodopsin and Retinal Disease', in *Advances in Pharmacology*. Academic Press Inc., pp. 1–36. doi: 10.1016/B978-0-12-417197-8.00001-8.
- Patel, A. B., Crocker, E., Reeves, P. J., Getmanova, E. V, Eilers, M., Khorana, H. G. and Smith, S. O. (2005) 'Changes in Interhelical Hydrogen Bonding upon Rhodopsin Activation'. doi: 10.1016/j.jmb.2005.01.069.
- Pérez-González, A. and Caro, E. (2019) 'Benefits of using genomic insulators flanking transgenes to increase expression and avoid positional effects', *Scientific Reports*, 9(1). doi: 10.1038/s41598-019-44836-6.
- Phelan, J. K. and Bok, D. (2000) 'A brief review of retinitis pigmentosa and the identified retinitis pigmentosa genes', *Molecular Vision*, 6, pp. 116–124.
- Phillips, W. J. and Cerione, R. A. (1988) 'The intrinsic fluorescence of the alpha subunit of transducin. Measurement of receptor-dependent guanine nucleotide exchange.', *The Journal of biological chemistry*, 263(30), pp. 15498–505. Available at: <http://www.ncbi.nlm.nih.gov/pubmed/3049609> (Accessed: 25 March 2020).
- Ploier, B., Caro, L. N., Morizumi, T., Pandey, K., Pearing, J. N., Goren, M. A., Finnemann, S. C., Graumann, J., Arshavsky, V. Y., Dittman, J. S., Ernst, O. P. and Menon, A. K. (2016) 'Dimerization deficiency of enigmatic retinitis pigmentosa-linked rhodopsin mutants', *Nature Communications*, 7. doi: 10.1038/ncomms12832.
- Polans, A., Baehr, W. and Palczewski, K. (1996) 'Turned on by Ca²⁺! The physiology and pathology of Ca²⁺-binding proteins in the retina', *Trends in Neurosciences*. Trends Neurosci, pp. 547–554. doi: 10.1016/S0166-2236(96)10059-X.

Pope, A., Eilers, M., Reeves, P. J. and Smith, S. O. (2013) 'Amino acid conservation and interactions in rhodopsin: Probing receptor activation by NMR spectroscopy ☆'. doi: 10.1016/j.bbabbio.2013.10.007.

Provencio, I., Jiang, G., De Grip, W. J., Paär, W., Hayes, P. and Rollag, M. D. (1998) 'Melanopsin: An opsin in melanophores, brain, and eye', 95, pp. 340–345. Available at: www.pnas.org. (Accessed: 20 July 2023).

Rao, V. R., Cohen, G. B. and Oprian, D. D. (1994) 'Rhodopsin mutation G90D and a molecular mechanism for congenital night blindness', *Nature*, 367(6464), pp. 639–642. doi: 10.1038/367639a0.

Reeves, P. J., Callewaert, N., Contreras, R. and Khorana, H. G. (2002) 'Structure and function in rhodopsin: High-level expression of rhodopsin with restricted and homogeneous N-glycosylation by a tetracycline-inducible N-acetylglucosaminyltransferase I-negative HEK293S stable mammalian cell line', *Proceedings of the National Academy of Sciences of the United States of America*, 99(21), pp. 13419–13424. doi: 10.1073/pnas.212519299.

Reeves, P. J., Hwa, J. and Khorana, H. G. (1999) 'Structure and function in rhodopsin: Kinetic studies of retinal binding to purified opsin mutants in defined phospholipid-detergent mixtures serve as probes of the retinal binding pocket', *Biochemistry*, 96, pp. 1927–1931. Available at: www.pnas.org. (Accessed: 5 September 2023).

Reeves, P. J., Kim, J. M. and Khorana, H. G. (2002) 'Structure and function in rhodopsin: A tetracycline-inducible system in stable mammalian cell lines for high-level expression of opsin mutants', *Proceedings of the National Academy of Sciences of the United States of America*, 99(21), pp. 13413–13418. doi: 10.1073/pnas.212519199.

- Reeves, P. J., Thurmond, R. L. and Khorana, H. G. (1996) 'Structure and function in rhodopsin: High level expression of a synthetic bovine opsin gene and its mutants in stable mammalian cell lines', *Proceedings of the National Academy of Sciences of the United States of America*, 93(21), pp. 11487–11492. doi: 10.1073/pnas.93.21.11487.
- Ropelewski, P. and Imanishi, Y. (2019) 'Disrupted plasma membrane protein homeostasis in a xenopus laevis model of retinitis pigmentosa', *Journal of Neuroscience*, 39(28), pp. 5581–5593. doi: 10.1523/JNEUROSCI.3025-18.2019.
- Sakamoto, T. and Khorana, H. G. (1995) 'Structure and function in rhodopsin: the fate of opsin formed upon the decay of light-activated metarhodopsin II in vitro.', *Proceedings of the National Academy of Sciences of the United States of America*, 92(1), p. 249. doi: 10.1073/PNAS.92.1.249.
- Saliba, R. S., Munro, P. M. G., Luthert, P. J. and Cheetham, M. E. (2002) 'The cellular fate of mutant rhodopsin: Quality control, degradation and aggresome formation', *Journal of Cell Science*, 115(14), pp. 2907–2918.
- Salom, D., Lodowski, D. T., Stenkamp, R. E., Le Trong, I., Golczak, M., Jastrzebska, B., Harris, T., Ballesteros, J. A. and Palczewski, K. (2006) 'Crystal structure of a photoactivated deprotonated intermediate of rhodopsin', *Proceedings of the National Academy of Sciences of the United States of America*, 103(44), pp. 16123–16128. doi: 10.1073/pnas.0608022103.
- Sandoval-Villegas, N., Nurieva, W., Amberger, M. and Ivics, Z. (2021) 'Contemporary Transposon Tools: A Review and Guide through Mechanisms and Applications of Sleeping Beauty, piggyBac and Tol2 for Genome Engineering', *International journal of molecular sciences*, 22(10). doi: 10.3390/IJMS22105084.

- Sarkar, A., Atapattu, A., Belikoff, E. J., Heinrich, J. C., Li, X., Horn, C., Wimmer, E. A. and Scott, M. J. (2006) 'Insulated piggyBac vectors for insect transgenesis', *BMC Biotechnology*, 6. doi: 10.1186/1472-6750-6-27.
- Schulze-Bonsel, K., Feltgen, N., Burau, H., Hansen, L. and Bach, M. (2006) 'Visual Acuties "Hand Motion" and "Counting Fingers" Can Be Quantified with the Freiburg Visual Acuity Test', *Investigative Ophthalmology & Visual Science*, 47(3), pp. 1236–1240. doi: 10.1167/IOVS.05-0981.
- Scott, B. M., Chen, S. K., Bhattacharyya, N., Moalim, A. Y., Plotnikov, S. V., Heon, E., Peisajovich, S. G. and Chang, B. S. W. (2019) 'Coupling of Human Rhodopsin to a Yeast Signaling Pathway Enables Characterization of Mutations Associated with Retinal Disease', *Genetics*, 211(2), p. 597. doi: 10.1534/GENETICS.118.301733.
- Sharma, M., Benharouga, M., Hu, W. and Lukacs, G. L. (2000) 'Conformational and Temperature-sensitive Stability Defects of the F508 Cystic Fibrosis Transmembrane Conductance Regulator in Post-endoplasmic Reticulum Compartments*'. doi: 10.1074/jbc.M009172200.
- Shichida, Y. and Morizumi, T. (2006) 'Mechanism of G-protein Activation by Rhodopsin', *Photochemistry and Photobiology*, 83(1), pp. 70–75. doi: 10.1562/2006-03-22-IR-854.
- Shukla, S. and Tekwani, B. L. (2020) 'Histone Deacetylases Inhibitors in Neurodegenerative Diseases, Neuroprotection and Neuronal Differentiation', *Frontiers in Pharmacology*. Frontiers Media S.A., p. 537. doi: 10.3389/fphar.2020.00537.
- Sieving, P. A., Richards, J. E., Naarendorp, F., Bingham, E. L., Scorrt, K. and Alpern, M. (1995) 'Dark-light: Model for nightblindness from the human rhodopsin Gly-90 →

- Asp mutation', *Proceedings of the National Academy of Sciences of the United States of America*, 92(3), pp. 880–884. doi: 10.1073/pnas.92.3.880.
- Singh, S. K. and Sigworth, F. J. (2015) 'Cryo-EM: spinning the micelles away', *Structure (London, England : 1993)*, 23(9), p. 1561. doi: 10.1016/J.STR.2015.08.001.
- Sizova, O. S., Shinde, V. M., Lenox, A. R. and Gorbatyuk, M. S. (2014) 'Modulation of cellular signaling pathways in P23H rhodopsin photoreceptors', *Cellular Signalling*, 26(4), pp. 665–672. doi: 10.1016/j.cellsig.2013.12.008.
- Smith, S. O. (2010) 'Structure and Activation of the Visual Pigment Rhodopsin', *Annual Review of Biophysics*, 39, pp. 309–328. doi: 10.1146/annurev-biophys-101209-104901.
- Suh, S., Choi, E. H. and Atanaskova Mesinkovska, N. (2020) 'The expression of opsins in the human skin and its implications for photobiomodulation: A Systematic Review', *Photodermatology Photoimmunology and Photomedicine*, 36(5), pp. 329–338. doi: 10.1111/PHPP.12578.
- Sung, Ching Hwa, Davenport, C. M., Hennessey, J. C., Maumenee, I. H., Jacobson, S. G., Heckenlively, J. R., Nowakowski, R., Fishman, G., Gouras, P. and Nathans, J. (1991) 'Rhodopsin mutations in autosomal dominant retinitis pigmentosa', *Proceedings of the National Academy of Sciences of the United States of America*, 88(15), pp. 6481–6485. doi: 10.1073/PNAS.88.15.6481.
- Sung, C. H., Schneider, B. G., Agarwal, N., Papermaster, D. S. and Nathans, J. (1991) 'Functional heterogeneity of mutant rhodopsins responsible for autosomal dominant retinitis pigmentosa.', *Proceedings of the National Academy of Sciences of the United States of America*, 88(19), p. 8840. doi: 10.1073/PNAS.88.19.8840.

Tam, B. M. and Moritz, O. L. (2009) 'The Role of Rhodopsin Glycosylation in Protein Folding, Trafficking, and Light-Sensitive Retinal Degeneration'. doi: 10.1523/JNEUROSCI.4259-09.2009.

Tam, B. M., Xie, G., Oprian, D. D. and Moritz, O. L. (2006) 'Mislocalized rhodopsin does not require activation to cause retinal degeneration and neurite outgrowth in *Xenopus laevis*', *Journal of Neuroscience*, 26(1), pp. 203–209. doi: 10.1523/JNEUROSCI.3849-05.2006.

Tarttelin, E. E., Bellingham, J., Hankins, M. W., Foster, R. G. and Lucas, R. J. (2003) 'Neuroopsin (Opn5): A novel opsin identified in mammalian neural tissue', *FEBS Letters*, 554(3), pp. 410–416. doi: 10.1016/S0014-5793(03)01212-2.

Toledo, D., Ramon, E., Aguilà, M., Cordoní, A., Pérez, J. J., Mendes, H. F., Cheetham, M. E. and Garriga, P. (2011) 'Molecular mechanisms of disease for mutations at Gly-90 in rhodopsin', *Journal of Biological Chemistry*, 286(46), pp. 39993–40001. doi: 10.1074/jbc.M110.201517.

Tripathi, N. K. and Shrivastava, A. (2019) 'Recent Developments in Bioprocessing of Recombinant Proteins: Expression Hosts and Process Development', *Frontiers in Bioengineering and Biotechnology*. Frontiers Media S.A., p. 420. doi: 10.3389/fbioe.2019.00420.

Vats, A., Xi, Y., Feng, B., Clinger, O. D., St Leger, A. J., Liu, X., Ghosh, A., Dermond, C. D., Lathrop, K. L., Tochtrop, G. P., Picaud, S. and Chen, Y. (2022) 'Nonretinoid chaperones improve rhodopsin homeostasis in a mouse model of retinitis pigmentosa'. doi: 10.1172/jci.

Viringipurampeer, I. A., Metcalfe, A. L., Bashar, A. E., Sivak, O., Yanai, A., Mohammadi, Z., Moritz, O. L., Gregory-Evans, C. Y. and Gregory-Evans, K. (2016)

'NLRP3 inflammasome activation drives bystander cone photoreceptor cell death in a P23H rhodopsin model of retinal degeneration', *Human Molecular Genetics*, 25(8), pp. 1501–1516. doi: 10.1093/hmg/ddw029.

Vishnivetskiy, S. A., Raman, D., Wei, J., Kennedy, M. J., Hurley, J. B. and Gurevich, V. V. (2007) 'Regulation of arrestin binding by rhodopsin phosphorylation level', *Journal of Biological Chemistry*, 282(44), pp. 32075–32083. doi: 10.1074/jbc.M706057200.

Wald, G. (1968) 'The molecular basis of visual excitation', *Nature*, 219(5156), pp. 800–807. doi: 10.1038/219800a0.

Wan, A., Place, E., Pierce, E. A. and Comander, J. (2019) 'Characterizing variants of unknown significance in rhodopsin: a functional genomics approach', *Human Mutation*, p. humu.23762. doi: 10.1002/humu.23762.

Wang, J., Xu, D., Zhu, T., Zhou, Y., Chen, X., Wang, F., Zhang, Jieping, Tian, H., Gao, F., Zhang, Jingfa, Jin, C., Xu, J., Lu, L., Liu, Q. and Xu, G. T. (2019) 'Identification of two novel RHO mutations in Chinese retinitis pigmentosa patients', *Experimental Eye Research*, 188. doi: 10.1016/j.exer.2019.107726.

Wang, X., Koulov, A. V., Kellner, W. A., Riordan, J. R. and Balch, W. E. (2008) 'Chemical and Biological Folding Contribute to Temperature Sensitive Δ F508 CFTR Trafficking', *Traffic (Copenhagen, Denmark)*, 9(11), p. 1878. doi: 10.1111/J.1600-0854.2008.00806.X.

White, J. F., Noinaj, N., Shibata, Y., Love, J., Kloss, B., Xu, F., Gvozdenovic-Jeremic, J., Shah, P., Shiloach, J., Tate, C. G. and Grisshammer, R. (2012) 'Structure of the agonist-bound neurotensin receptor', *Nature*, 490(7421), pp. 508–513. doi: 10.1038/nature11558.

- Wilson, M. H., Coates, C. J. and George, A. L. (2007) 'PiggyBac transposon-mediated gene transfer in human cells', *Molecular Therapy*, 15(1), pp. 139–145. doi: 10.1038/sj.mt.6300028.
- Wiseman, D. N., Otchere, A., Patel, J. H., Uddin, R., Pollock, N. L., Routledge, S. J., Rothnie, A. J., Slack, C., Poyner, D. R., Bill, R. M. and Goddard, A. D. (2020) 'Expression and purification of recombinant G protein-coupled receptors: A review', *Protein Expression and Purification*, 167. doi: 10.1016/j.pep.2019.105524.
- Wu, Y., Guo, Y., Yi, J., Xu, H., Yuan, L., Yang, Z. and Deng, H. (2019) 'Heterozygous RHO p.R135W missense mutation in a large Han-Chinese family with retinitis pigmentosa and different refractive errors', *Bioscience Reports*. doi: 10.1042/BSR20182198.
- Xiao, J., Adil, M. Y., Chang, K., Yu, Z., Yang, L., Utheim, T. P., Chen, D. F. and Cho, K. S. (2019) 'Visual Contrast Sensitivity Correlates to the Retinal Degeneration in Rhodopsin Knockout Mice', *Investigative ophthalmology & visual science*, 60(13), pp. 4196–4204. doi: 10.1167/iovs.19-26966.
- Xiao, S., White, J. F., Betenbaugh, M. J., Grisshammer, R. and Shiloach, J. (2013) 'Transient and Stable Expression of the Neurotensin Receptor NTS1: A Comparison of the Baculovirus-Insect Cell and the T-REx-293 Expression Systems', *PLoS ONE*, 8(5). doi: 10.1371/journal.pone.0063679.
- Xie, G., Gross, A. K. and Oprian, D. D. (2003) 'An Opsin Mutant with Increased Thermal Stability †', *Biochemistry*, 42(7), pp. 1995–2001. doi: 10.1021/bi020611z.
- Yang, Z., Chen, Z. and Zhang, Y. (2022) 'A simple and economical site-directed mutagenesis method for large plasmids by direct transformation of two overlapping PCR fragments', *BioTechniques*, 73(5), pp. 239–245. doi: 10.2144/btn-2022-0085.

- Yao, F., Svensjö, T., Winkler, T., Lu, M., Eriksson, C. and Eriksson, E. (1998) 'Tetracycline repressor, tetR, rather than the tetR-mammalian cell transcription factor fusion derivatives, regulates inducible gene expression in mammalian cells', *Human Gene Therapy*, 9(13), pp. 1939–1950. doi: 10.1089/hum.1998.9.13-1939.
- Yao, J., Qiu, Y., Frontera, E., Jia, L., Khan, N. W., Klionsky, D. J., Ferguson, T. A., Thompson, D. A. and Zacks, D. N. (2018) 'Inhibiting autophagy reduces retinal degeneration caused by protein misfolding', *Autophagy*, 14(7), pp. 1226–1238. doi: 10.1080/15548627.2018.1463121.
- Yu, X. W., Sun, W. H., Wang, Y. Z. and Xu, Y. (2017) 'Identification of novel factors enhancing recombinant protein production in multi-copy *Komagataella phaffii* based on transcriptomic analysis of overexpression effects', *Scientific Reports*, 7(1), pp. 1–12. doi: 10.1038/s41598-017-16577-x.
- Yue, W. W. S., Silverman, D., Ren, X., Frederiksen, R., Sakai, K., Yamashita, T., Shichida, Y., Cornwall, M. C., Chen, J. and Yau, K. W. (2019) 'Elementary response triggered by transducin in retinal rods', *Proceedings of the National Academy of Sciences of the United States of America*, 116(11), pp. 5144–5153. doi: 10.1073/pnas.1817781116.
- Yusa, K. (2015) 'piggyBac Transposon', in *Mobile DNA III*. American Society of Microbiology, pp. 875–892. doi: 10.1128/microbiolspec.mdna3-0028-2014.
- Zeng, F., Zhang, S., Hao, Z., Duan, S., Meng, Y., Li, P., Dong, J. and Lin, Y. (2018) 'Efficient strategy for introducing large and multiple changes in plasmid DNA', *Scientific Reports* 2018 8:1, 8(1), pp. 1–12. doi: 10.1038/s41598-018-20169-8.
- Zerti, D., Dorgau, B., Felemban, M., Ghareeb, A. E., Yu, M., Ding, Y., Krasnogor, N. and Lako, M. (2019) 'Developing a simple method to enhance the generation of cone

and rod photoreceptors in pluripotent stem cell-derived retinal organoids', *STEM CELLS*. doi: 10.1002/stem.3082.

Zhang, J., Choi, E. H., Tworak, A., David Salom, X., Henri Leinonen, X., Christopher Sander, X. L., Hoang, T. V., Handa, J. T., Seth Blackshaw, X., Grazyna Palczewska, X., Philip Kiser, X. D. and Krzysztof Palczewski, X. (2019) 'Photoc generation of 11-cis-retinal in bovine retinal pigment epithelium'. doi: 10.1074/jbc.RA119.011169.

Zhao, S., Jiang, E., Chen, S., Gu, Y., Shanguan, A. J., Lv, T., Luo, L. and Yu, Z. (2016) 'PiggyBac transposon vectors: The tools of the human gene encoding', *Translational Lung Cancer Research*. AME Publishing Company, pp. 120–125. doi: 10.3978/j.issn.2218-6751.2016.01.05.

Zhou, Z., Gong, Q. and January, C. T. (1999) 'Correction of Defective Protein Trafficking of a Mutant HERG Potassium Channel in Human Long QT Syndrome: PHARMACOLOGICAL AND TEMPERATURE EFFECTS *', *Journal of Biological Chemistry*, 274(44), pp. 31123–31126. doi: 10.1074/JBC.274.44.31123.

9. Appendices

Appendix 1 Mutagenic primers

Table 1. Primer sequences used for site directed mutagenesis

Mutant	Primer sequence 5' to 3'
E122G F	gccaccctgggcggtggcattgcactgtgg
E122G R	gagaccacagtgcaatgccaccgcccaggg
R252P F	gagaaggaggtcacgccgatggttatcatc
R252P R	catgatgataaccatcggcgtgacctcctt
S298D F	ctttcttgccaagacggatgccgtctaca
S298D R	cgggtttagacggcatccgtcttgcaaa
K311E F	ctacatcatgatgaacgagcagttccggaa
K311E R	gcagttccggaactgctcgttcatcatgat
P23A F	ggcgtggtgcgagccacttcgaggctccgcag
P23A R	ctgaggagcctcgaagtggctgcgaccacgcc

For the EL1 mutants, pMT4-rho(mutants) made previously were used (Neaves, 2020).

Appendix 2 PCR and sequencing primers

Table 2. Primers used for PCR and Sequencing

Mutant	Primer sequence 5' to 3'	Used for
Neo CMV F	gaggaggctagcgcggagtgtatgatcttctaggatccagac	PCR
Neo CMV R	gaggaggctagccagcggccatcgatcgaccaattctcatg	PCR
SEQ1	caacaagacgggcgtggtgc	Sequencing
SEQF2	gtgtgcaagcccatgagcaac	Sequencing
SEQR2	gaacgactcattgttggtctcc	Sequencing
SEQ pB007NCO	gatagagatcgtcgacgagc	Sequencing

Appendix 3 Sequencing results

Sequencing results are presented here to show the relevant mutations aligned against a WT rhodopsin control. The mutation codon is highlighted for each, and where appropriate other regions of interest are also highlighted.

Chapter 4 – N-terminal/EL1 mutants

P23A

CCG to GCC change observed at the correct position.

Rho_WT	1	-----	0
7_F1	1	GTATTAAGCAGAGCTCTCCCTATCAGTGATAGAGATCTCCCTATCAGTGA	50
Rho_WT	1	-----	0
7_F1	51	TAGAGATCGTCGACGAGCTCGTTTAGTGAACCGTCAGATCTCTAGAAGCT	100
Rho_WT	1	-----ATGAACGGTACCGAAGGCCAAACTTCTACGTTTCCTTTC	39
7_F1	101	GGAATTCACCATGAACGGTACCGAAGGCCAAACTTCTACGTTTCCTTTC	150
Rho_WT	40	TCCAACAAGACGGGCGTGGTGCAGCCCGTTCGAGGCTCCGCAGTACTA	89
7_F1	151	TCCAACAAGACGGGCGTGGTGCAGCGCCGTTTCGAGGCTCCGCAGTACTA	200
Rho_WT	90	CCTGGCGGAGCCCTGGCAGTTCTCCATGCTGGCCGCCTACATGTTCTTGC	139
7_F1	201	CCTGGCGGAGCCCTGGCAGTTCTCCATGCTGGCCGCCTACATGTTCTTGC	250
Rho_WT	140	TGATCATGCTTGGCTTCCCGATCAACTTCCTCAGCTGTACGTACAGTC	189
7_F1	251	TGATCATGCTTGGCTTCCCGATCAACTTCCTCAGCTGTACGTACAGTC	300
Rho_WT	190	CAGCACAGAAGCTTCGCACACCGCTCAACTACATCCTGCTCAACCTGGC	239
7_F1	301	CAGCACAGAAGCTTCGCACACCGCTCAACTACATCCTGCTCAACCTGGC	350
Rho_WT	240	CGTGGCAGATCTCTTCATGGTCTTCGGTGGCTTACCACCACCCTCTACA	289
7_F1	351	CGTGGCAGATCTCTTCATGGTCTTCGGTGGCTTACCACCACCCTCTACA	400
Rho_WT	290	CCTCTCTCCATGGGTACTTCGTCTTTGGGCCGACGGGCTGCAACCTCGAG	339
7_F1	401	CCTCTCTCCATGGGTACTTCGTCTTTGGGCCGACGGGCTGCAACCTCGAG	450
Rho_WT	340	GGCTTCTTTGCCACCCTGGGCGGTGAAATTGCACTGTGGTCTCTGGTAGT	389
7_F1	451	GGCTTCTTTGCCACCCTGGGCGGTGAAATTGCACTGTGGTCTCTGGTAGT	500
Rho_WT	390	ACTGGCGATCGAGCGGTACGTGGTGGTGTGCAAGCCCATGAGCAACTTCC	439
7_F1	501	ACTGGCGATCGAGCGGTACGTGGTGGTGTGCAAGCCCATGAGCAACTTCC	550

Rho_WT	440	GCTTCGGTGAGAACCACGCCATCATGGGCGTCGCCTTCACCTGGGTCATG	489
7_F1	551	GCTTCGGTGAGAACCACGCCATCATGGGCGTCGCCTTCACCTGGGTCATG	600
Rho_WT	490	GCTCTGGCCTGTGCGGCCCCGCCGCTCGTCGGCTGGTCTAGATACATCCC	539
7_F1	601	GCTCTGGCCTGTGCGGCCCCGCCGCTCGTCGGCTGGTCTAGATACATCCC	650
Rho_WT	540	GGAGGGCATGCAGTGCCTGTCGCGGGATCGATTACTACACGCCGCACGAGG	589
7_F1	651	GGAGGGCATGCAGTGCCTGTCGCGGGATCGATTACTACACGCCGCACGAGG	700
Rho_WT	590	AGACCAACAATGAGTCGTTTCGTCATCTACATGTTTCGTGGTCCACTTCATC	639
7_F1	701	AGACCAACAATGAGTCGTTTCGTCATCTACATGTTTCGTGGTCCACTTCATC	750
Rho_WT	640	ATCCCGCTGATTGTCATCTTCTTCTGCTATGGCCAGCTGGTGTTCACCGT	689
7_F1	751	ATCCCGCTGATTGTCATCTTCTTCTGCTATGGCCAGCTGGTGTTCACCGT	800
Rho_WT	690	CAAGGAGGCTGCAGCCCAGCAGCAGGAGAGCGCCACCACTCAGAAGGCCG	739
7_F1	801	CAAGGAGGCTGCAGCCCAGCAGCAGGAGAGCGCCACCACTCAGAAGGCCG	850
Rho_WT	740	AGAAGGAGGTCACGCGTATGGTTATCATCATGGTCATCGCTTTCCTAATC	789
7_F1	851	AGAAGGAGGTCACGCGTATGGTTATCATCATGGTCATCGCTTTCCTAATC	900
Rho_WT	790	TGCTGGCTGCCATATGCTGGTGTGGCGTTCTACATCTTCACCCATCAGGG	839
7_F1	901	TGCTGGCTGCCATATGCTGGTGTGGCGTTCTACATCTTCACCCATCAGGG	950
Rho_WT	840	CTCTGACTTTGGGCCCATCTTTCATGACCATCCCGGCTTCTTTGCCAAGA	889
7_F1	951	CTCTGACTTTGGGCCCATCTTTCATGACCATCCCGGCTTCTTTGCCAAGA	1000
Rho_WT	890	CGTCTGCCGTCTACAACCCGGTCATCTACATCATGATG-AACAAGCAGTT	938
7_F1	1001	CGTCTGCCGTCTACAACCCGGTCATCTACATCATGATGAAACAAGCAGTT	1050
Rho_WT	939	CCGGAAGTGCATGGTCACCACTCTCTGCTGTGGCAAGAACCCGCTGGGTG	988
7_F1	1051	CCGGAAGTGCATGGGCACCA-----	1070
Rho_WT	989	ACGACGAGGCGTCGACCACCGTCTCCAAGACAGAGACCAGCCAAGTGGCG	1038

7_F1	1071	-----	1070
Rho_WT	1039	CCTGCCTAAGCGGCCGCAAATTCGGGGGGGGGGGGGGGGGGGG	1080

7_F1	1071	-----	1070

G101V

GGG to GTC change observed at the correct position.

Rho_WT	1	-----	0
11_F1	1	GAGCATATAGCAGAGCTCCCTATCAGTGATAGAGATCCCTATCAGT	50
Rho_WT	1	-----	0
11_F1	51	GATAGAGATCGTCGACGAGCTCGTTTAGTGAACCGTCAGATCTCTAGAAG	100
Rho_WT	1	-----ATGAACGGTACCGAAGGCCAAACTTCTACGTTCCCTT	37
11_F1	101	CTGGAATTCCACCATGAACGGTACCGAAGGCCAAACTTCTACGTTCCCTT	150
Rho_WT	38	TCTCCAACAAGACGGGCGTGGTGCAGCCCGTTCGAGGCTCCGCAGTAC	87
11_F1	151	TCTCCAACAAGACGGGCGTGGTGCAGCCCGTTCGAGGCTCCGCAGTAC	200
Rho_WT	88	TACCTGGCGGAGCCCTGGCAGTTCTCCATGCTGGCCGCCTACATGTTCCCT	137
11_F1	201	TACCTGGCGGAGCCCTGGCAGTTCTCCATGCTGGCCGCCTACATGTTCCCT	250
Rho_WT	138	GCTGATCATGCTTGGCTTCCCGATCAACTTCCTCACGCTGTACGTACAG	187
11_F1	251	GCTGATCATGCTTGGCTTCCCGATCAACTTCCTCACGCTGTACGTACAG	300
Rho_WT	188	TCCAGCACAAGAAGCTTCGCACACCGCTCAACTACATCCTGCTCAACCTG	237
11_F1	301	TCCAGCACAAGAAGCTTCGCACACCGCTCAACTACATCCTGCTCAACCTG	350
Rho_WT	238	GCCGTGGCAGATCTCTTCATGGTCTTCGGTGGCTTACCACCACCCTCTA	287
11_F1	351	GCCGTGGCAGATCTCTTCATGGTCTTCGGTGGCTTACCACCACCCTCTA	400
Rho_WT	288	CACCTCTCTCCATGGGTACTTTCGTTTGGGCCGACGGGCTGCAACCTCG	337
11_F1	401	CACCTCTCTCCATGTCGTTACTTTCGTTTGGGCCGACGGGCTGCAACCTCG	450
Rho_WT	338	AGGGCTTCTTTGCCACCCTGGGCGGTGAAATTGCACTGTGGTCTCTGGTA	387
11_F1	451	AGGGCTTCTTTGCCACCCTGGGCGGTGAAATTGCACTGTGGTCTCTGGTA	500
Rho_WT	388	GTACTGGCGATCGAGCGGTACGTGGTGGTGTGCAAGCCCATGAGCAACTT	437
11_F1	501	GTACTGGCGATCGAGCGGTACGTGGTGGTGTGCAAGCCCATGAGCAACTT	550
Rho_WT	438	CCGCTTCGGTGAGAACCACGCCATCATGGGCGTCGCCTTACCTGGGTCA	487
11_F1	551	CCGCTTCGGTGAGAACCACGCCATCATGGGCGTCGCCTTACCTGGGTCA	600
Rho_WT	488	TGGCTCTGGCCTGTGCGGCCCCGCCGCTCGTCGGCTGGTCTAGATACATC	537
11_F1	601	TGGCTCTGGCCTGTGCGGCCCCGCCGCTCGTCGGCTGGTCTAGATACATC	650
Rho_WT	538	CCGGAGGGCATGCAGTGCCTCGTGCGGGATCGATTACTACACGCCGCACGA	587
11_F1	651	CCGGAGGGCATGCAGTGCCTCGTGCGGGATCGATTACTACACGCCGCACGA	700
Rho_WT	588	GGAGACCAACAATGAGTCGTTTCGTCATCTACATGTTTCGTTGGTCCACTTCA	637
11_F1	701	GGAGACCAACAATGAGTCGTTTCGTCATCTACATGTTTCGTTGGTCCACTTCA	750

Rho_WT	638	TCATCCCCTGATTGTCATCTTCTTCTGCTATGGCCAGCTGGTGTTCACC	687
11_F1	751	TCATCCCCTGATTGTCATCTTCTTCTGCTATGGCCAGCTGGTGTTCACC	800
Rho_WT	688	GTCAAGGAGGCTGCAGCCCAGCAGCAGGAGAGCGCCACCACTCAGAAGGC	737
11_F1	801	GTCAAGGAGGCTGCAGCCCAGCAGCAGGAGAGCGCCACCACTCAGAAGGC	850
Rho_WT	738	CGAGAAGGAGGTCACGCGTATGGTTATCATCATGGTCATCGCTTTCCTAA	787
11_F1	851	CGAGAAGGAGGTCACGCGTATGGTTATCATCATGGTCATCGCTTTCCTAA	900
Rho_WT	788	TCTGCTGGCTGCCATATGCTGGTGTGGCGTTCTACATCTTCACCCATCAG	837
11_F1	901	TCTGCTGGCTGCCATATGCTGGTGTGGCGTTCTACATCTTCACCCATCAG	950
Rho_WT	838	GGCTCTGACTTTGGGCCATCTTCATGACCATCCCGGCTTCTTTGCCAA	887
11_F1	951	GGCTCTGACTTTGGGCCATCTTCATGACCATCCCGGCTTCTTTGCCAA	1000
Rho_WT	888	GACGTCTGCCGTCTACAACCCGGTCATCTACATCATGATGAACAAGCAGT	937
11_F1	1001	GACGTCTGCCGTCTACAACCCGGTCATCTACATCATGATGAACAAGCAGT	1050
Rho_WT	938	TCCGGAAGTGCATGGTCACCACTCTCTGCTGTGGCAAGAACCCGCTGGGT	987
11_F1	1051	TCCGGAAGTGCATGGTCACCACTCTCTGCTGTGGCAAGAACCCGCTGGGT	1100
Rho_WT	988	GACGACGAGGCGTCGACCACCGTCTCCAAGACAGAGACCAGCCAAGTGGC	1037
		.	
11_F1	1101	GACAA-----	1105
Rho_WT	1038	GCCTGCCTAAGCGGCCGC	1055
11_F1	1106	-----	1105

V104F

GTC to TTC change observed at the correct position.

Rho_WT	1	-----	0
13_F1	1	TAATAGCAGAGCTCTCCCTATCAGTGATAGAGATCTCCCTATCAGTGATA	50
Rho_WT	1	-----	0
13_F1	51	GAGATCGTCGACGAGCTCGTTTAGTGAACCGTCAGATCTCTAGAAGCTGG	100
Rho_WT	1	-----ATGAACGGTACCGAAGGCCAAACTTCTACGTTCCCTTTCTC	41
13_F1	101	AATTCCACCATGAACGGTACCGAAGGCCAAACTTCTACGTTCCCTTTCTC	150
Rho_WT	42	CAACAAGACGGGCGTGGTGCAGCCCGTTCGAGGCTCCGCAGTACTACC	91
13_F1	151	CAACAAGACGGGCGTGGTGCAGCCCGTTCGAGGCTCCGCAGTACTACC	200
Rho_WT	92	TGGCGGAGCCCTGGCAGTTCTCCATGCTGGCCGCCTACATGTTCTGCTG	141
13_F1	201	TGGCGGAGCCCTGGCAGTTCTCCATGCTGGCCGCCTACATGTTCTGCTG	250
Rho_WT	142	ATCATGCTTGGCTTCCCGATCAACTTCCTCAGCTGTACGTACAGTCCA	191
13_F1	251	ATCATGCTTGGCTTCCCGATCAACTTCCTCAGCTGTACGTACAGTCCA	300
Rho_WT	192	GCACAAGAAGCTTCGCACACCGCTCAACTACATCCTGCTCAACCTGGCCG	241
13_F1	301	GCACAAGAAGCTTCGCACACCGCTCAACTACATCCTGCTCAACCTGGCCG	350
Rho_WT	242	TGGCAGATCTCTTCATGGTCTTCGGTGGCTTACCACCACCCTCTACACC	291
13_F1	351	TGGCAGATCTCTTCATGGTCTTCGGTGGCTTACCACCACCCTCTACACC	400
Rho_WT	292	TCTCTCCATGGGTACTTCTGTTTGGGCCGACGGGCTGCAACCTCGAGGG	341
13_F1	401	TCTCTCCATGGGTACTTCTGTTTGGGCCGACGGGCTGCAACCTCGAGGG	450
Rho_WT	342	CTTCTTTGCCACCCTGGGCGGTGAAATTGCACTGTGGTCTCTGGTAGTAC	391
13_F1	451	CTTCTTTGCCACCCTGGGCGGTGAAATTGCACTGTGGTCTCTGGTAGTAC	500
Rho_WT	392	TGGCGATCGAGCGGTACGTGGTGGTGTGCAAGCCCATGAGCAACTCCGC	441
13_F1	501	TGGCGATCGAGCGGTACGTGGTGGTGTGCAAGCCCATGAGCAACTCCGC	550
Rho_WT	442	TTCCGGTGAAGAACCACGCCATCATGGGCGTCGCCTTACCTGGGTCATGGC	491
13_F1	551	TTCCGGTGAAGAACCACGCCATCATGGGCGTCGCCTTACCTGGGTCATGGC	600
Rho_WT	492	TCTGGCCTGTGCGGCCCGCCGCTCGTCGGCTGGTCTAGATACATCCCGG	541
13_F1	601	TCTGGCCTGTGCGGCCCGCCGCTCGTCGGCTGGTCTAGATACATCCCGG	650
Rho_WT	542	AGGGCATGCAGTGCTCGTGCGGGATCGATTACTACACGCCGCACGAGGAG	591
13_F1	651	AGGGCATGCAGTGCTCGTGCGGGATCGATTACTACACGCCGCACGAGGAG	700
Rho_WT	592	ACCAACAATGAGTCGTTTCGTCATCTACATGTTTCGTTCCACTTCATCAT	641
13_F1	701	ACCAACAATGAGTCGTTTCGTCATCTACATGTTTCGTTCCACTTCATCAT	750

Rho_WT	642	CCCCTGATTGTCATCTTCTTCTGCTATGGCCAGCTGGTGTTCACCGTCA	691
13_F1	751	CCCCTGATTGTCATCTTCTTCTGCTATGGCCAGCTGGTGTTCACCGTCA	800
Rho_WT	692	AGGAGGCTGCAGCCCAGCAGCAGGAGAGCGCCACCACTCAGAAGGCCGAG	741
13_F1	801	AGGAGGCTGCAGCCCAGCAGCAGGAGAGCGCCACCACTCAGAAGGCCGAG	850
Rho_WT	742	AAGGAGGTCACGCGTATGGTTATCATCATGGTCATCGCTTTCCTAATCTG	791
13_F1	851	AAGGAGGTCACGCGTATGGTTATCATCATGGTCATCGCTTTCCTAATCTG	900
Rho_WT	792	CTGGCTGCCATATGCTGGTGTGGCGTTCTACATCTTCACCCATCAGGGCT	841
13_F1	901	CTGGCTGCCATATGCTGGTGTGGCGTTCTACATCTTCACCCATCAGGGCT	950
Rho_WT	842	CTGACTTTGGGCCCATCTTCATGACCATCCCGGCTTCTTTGCCAAGACG	891
13_F1	951	CTGACTTTGGGCCCATCTTCATGACCATCCCGGCTTCTTTGCCAAGACG	1000
Rho_WT	892	TCTGCCGTCTACAACCCGGTCATCTACATCATGATGAACAAGCAGTCCG	941
13_F1	1001	TCTGCCGTCTACAACCCGGTCATCTACATCATGATGAACAAGCAGTCCG	1050
Rho_WT	942	GAACTGCATGGTCACCACTCTCTGCTGTGGCAAGAACCCGCTGGGTGACG	991
13_F1	1051	GAACTGCATGGTCACCACTCTCTGCTGTGGCAAGAACCCGCTGGGTGACG	1100
Rho_WT	992	ACGAGGCGTCGACCACCGTCTCCAAGACAGAGACCAGCCAAGTGGCGCCT	1041
13_F1	1101	ACGAGGCGTCGACCACCGTCTCCAAG-----	1126
Rho_WT	1042	GCCTAAGCGGCCGC	1055
13_F1	1127	-----	1126

G106W

GGG to TGG change observed at the correct position.

Rho_WT	1	-----	0
15_F1	1	GAGCATTAAGCAGAAGCTCTCCCTATCAGTGATAGAGATCTCCCTATCAG	50
Rho_WT	1	-----	0
15_F1	51	TGATAGAGATCGTTCGACGAGCTCGTTTAGTGAACCGTCAGATCTCTAGAA	100
Rho_WT	1	-----ATGAACGGTACCGAAGGCCAAACTTCTACGTTCCCT	36
15_F1	101	GCTGGAATTCACCATGAACGGTACCGAAGGCCAAACTTCTACGTTCCCT	150
Rho_WT	37	TTCTCCAACAAGACGGGCGTGGTGCGCAGCCCGTTCGAGGCTCCGCAGTA	86
15_F1	151	TTCTCCAACAAGACGGGCGTGGTGCGCAGCCCGTTCGAGGCTCCGCAGTA	200
Rho_WT	87	CTACCTGGCGGAGCCCTGGCAGTTCTCCATGCTGGCCGCTACATGTTCC	136
15_F1	201	CTACCTGGCGGAGCCCTGGCAGTTCTCCATGCTGGCCGCTACATGTTCC	250
Rho_WT	137	TGCTGATCATGCTTGGCTTCCCGATCAACTTCTCAGCTGTACGTCACA	186
15_F1	251	TGCTGATCATGCTTGGCTTCCCGATCAACTTCTCAGCTGTACGTCACA	300
Rho_WT	187	GTCCAGCACAAGAAGCTTCGCACACCGCTCAACTACATCCTGCTCAACCT	236
15_F1	301	GTCCAGCACAAGAAGCTTCGCACACCGCTCAACTACATCCTGCTCAACCT	350
Rho_WT	237	GGCCGTGGCAGATCTCTCATGGTCTTCGGTGGCTTCACCACCACCCTCT	286
15_F1	351	GGCCGTGGCAGATCTCTCATGGTCTTCGGTGGCTTCACCACCACCCTCT	400
Rho_WT	287	ACACCTCTCTCCATGGGTA	336
15_F1	401	ACACCTCTCTCCATGGGTA	450
Rho_WT	337	GAGGGCTTCTTTGCCACCCTGGGCGGTGAAATTGCACTGTGGTCTCTGGT	386
15_F1	451	GAGGGCTTCTTTGCCACCCTGGGCGGTGAAATTGCACTGTGGTCTCTGGT	500
Rho_WT	387	AGTACTGGCGATCGAGCGGTACGTGGTGGTGTGCAAGCCCATGAGCAACT	436
15_F1	501	AGTACTGGCGATCGAGCGGTACGTGGTGGTGTGCAAGCCCATGAGCAACT	550
Rho_WT	437	TCCGCTTCGGTGAGAACCACGCCATCATGGGCGTCGCCTTCACCTGGGTC	486
15_F1	551	TCCGCTTCGGTGAGAACCACGCCATCATGGGCGTCGCCTTCACCTGGGTC	600
Rho_WT	487	ATGGCTCTGGCCTGTGCGCCCCGCGCTCGTCGGCTGGTCTAGATACAT	536
15_F1	601	ATGGCTCTGGCCTGTGCGCCCCGCGCTCGTCGGCTGGTCTAGATACAT	650
Rho_WT	537	CCCGGAGGGCATGCAGTGCTCGTGCGGGATCGATTACTACACGCCGCACG	586
15_F1	651	CCCGGAGGGCATGCAGTGCTCGTGCGGGATCGATTACTACACGCCGCACG	700
Rho_WT	587	AGGAGACCAACAATGAGTCGTTTCGTATCTACATGTTTCGTGGTCCACTTC	636
15_F1	701	AGGAGACCAACAATGAGTCGTTTCGTATCTACATGTTTCGTGGTCCACTTC	750

Rho_WT	637	ATCATCCCGCTGATTGTCATCTTCTTCTGCTATGGCCAGCTGGTGTTCAC	686
15_F1	751	ATCATCCCGCTGATTGTCATCTTCTTCTGCTATGGCCAGCTGGTGTTCAC	800
Rho_WT	687	CGTCAAGGAGGCTGCAGCCCAGCAGCAGGAGAGCGCCACCACTCAGAAGG	736
15_F1	801	CGTCAAGGAGGCTGCAGCCCAGCAGCAGGAGAGCGCCACCACTCAGAAGG	850
Rho_WT	737	CCGAGAAGGAGGTCACGCGTATGGTTATCATCATGGTCATCGCTTTCCTA	786
15_F1	851	CCGAGAAGGAGGTCACGCGTATGGTTATCATCATGGTCATCGCTTTCCTA	900
Rho_WT	787	ATCTGCTGGCTGCCATATGCTGGTGTGGCGTTCTACATCTTCACCCATCA	836
15_F1	901	ATCTGCTGGCTGCCATATGCTGGTGTGGCGTTCTACATCTTCACCCATCA	950
Rho_WT	837	GGGCTCTGACTTTGGGCCATCTTCATGACCATCCCGGCTTCTTTGCCA	886
15_F1	951	GGGCTCTGACTTTGGGCCATCTTCATGACCATCCCGGCTTCTTTGCCA	1000
Rho_WT	887	AGACGTCTGCCGTCTACAACCCGGTCATCTACATCATGATGAACAAGCAG	936
15_F1	1001	AGACGTCTGCCGTCTACAACCCGGTCATCTACATCATGATGAACAAGCAG	1050
Rho_WT	937	TTCCGGAAGTGCATGGTCACCACTCTCTGCTGTGGCAAGAACCCGCTGGG	986
15_F1	1051	TTCCGGAAGTGCATGGTCACCACTCTCTGCTGTGGCAAGAACCCGCTGGG	1100
Rho_WT	987	TGACGACGAGGCGTCGACCACCGTCTCCAAGACAGAGACCAGCCAAGTGG	1036
15_F1	1101	TGACGA-----	1106
Rho_WT	1037	CGCCTGCCTAAGCGGCCGC	1055
15_F1	1107	-----	1106

Chapter 5 – RP mutants

E122G

GAA to GGC change observed at correct position. This plasmid was also used for the

E122G work in Chapter 6.

Rho	1	-----	0
1_F1	1	GCAATAAGCAGAGCTCTCCCTATCAGTGATAGAGATCTCCCTATCAGTGA	50
Rho	1	-----	0
1_F1	51	TAGAGATCGTCGACGAGCTCGTTTAGTGAACCGTCAGATCTCTAGAAGCT	100
Rho	1	-----ATGAACGGTACCGAAGGCCAAACTTCTACGTTTCCTTTC	39
1_F1	101	 GGAATTCCACCATGAACGGTACCGAAGGCCAAACTTCTACGTTTCCTTTC	150
Rho	40	TCCAACAAGACGGGCGTGGTGCGCAGCCGTTTCGAGGCTCCGCAGTACTA	89
1_F1	151	 TCCAACAAGACGGGCGTGGTGCGCAGCCGTTTCGAGGCTCCGCAGTACTA	200
Rho	90	CCTGGCGGAGCCCTGGCAGTTCTCCATGCTGGCCGCCTACATGTTCTCTGC	139
1_F1	201	 CCTGGCGGAGCCCTGGCAGTTCTCCATGCTGGCCGCCTACATGTTCTCTGC	250
Rho	140	TGATCATGCTTGGCTTCCCGATCAACTTCCTCACGCTGTACGTACAGTC	189
1_F1	251	 TGATCATGCTTGGCTTCCCGATCAACTTCCTCACGCTGTACGTACAGTC	300
Rho	190	CAGCACAAGAAGCTTCGCACACCGCTCAACTACATCCTGCTCAACCTGGC	239
1_F1	301	 CAGCACAAGAAGCTTCGCACACCGCTCAACTACATCCTGCTCAACCTGGC	350
Rho	240	CGTGGCAGATCTCTTCATGGTCTTCGGTGGCTTCACCACCACCCTCTACA	289
1_F1	351	 CGTGGCAGATCTCTTCATGGTCTTCGGTGGCTTCACCACCACCCTCTACA	400
Rho	290	CCTCTCTCCATGGGTACTTCGTCTTTGGGCCGACGGGCTGCAACCTCGAG	339
1_F1	401	 CCTCTCTCCATGGGTACTTCGTCTTTGGGCCGACGGGCTGCAACCTCGAG	450
Rho	340	GGCTTCTTTGCCACCCTGGGCGGTGAAATTGCACTGTGGTCTCTGGTAGT	389
1_F1	451	 GGCTTCTTTGCCACCCTGGGCGGTGGCATTGCACTGTGGTCTCTGGTAGT	500
Rho	390	ACTGGCGATCGAGCGGTACGTGGTGGTGTGCAAGCCCATGAGCAACTTCC	439
1_F1	501	 ACTGGCGATCGAGCGGTACGTGGTGGTGTGCAAGCCCATGAGCAACTTCC	550
Rho	440	GCTTCGGTGAGAACCACGCCATCATGGGCGTCGCCTTCACCTGGGTCATG	489
1_F1	551	 GCTTCGGTGAGAACCACGCCATCATGGGCGTCGCCTTCACCTGGGTCATG	600
Rho	490	GCTCTGGCCTGTGCGGCCCGCCGCTCGTCGGTGGTCTAGATACATCCC	539

1_F1	601	GCTCTGGCCTGTGCGGCCCGCCGCTCGTCGGCTGGTCTAGATACATCCC	650
Rho	540	GGAGGGCATGCAGTGCTCGTGCGGGATCGATTACTACACGCCGCACGAGG	589
1_F1	651	GGAGGGCATGCAGTGCTCGTGCGGGATCGATTACTACACGCCGCACGAGG	700
Rho	590	AGACCAACAATGAGTCGTTTCGTCATCTACATGTTTCGTGGTCCACTTCATC	639
1_F1	701	AGACCAACAATGAGTCGTTTCGTCATCTACATGTTTCGTGGTCCACTTCATC	750
Rho	640	ATCCCGCTGATTGTTCATCTTCTTCTGCTATGGCCAGCTGGTGTTCACCGT	689
1_F1	751	ATCCCGCTGATTGTTCATCTTCTTCTGCTATGGCCAGCTGGTGTTCACCGT	800
Rho	690	CAAGGAGGCTGCAGCCCAGCAGCAGGAGAGCGCCACCACTCAGAAGGCCG	739
1_F1	801	CAAGGAGGCTGCAGCCCAGCAGCAGGAGAGCGCCACCACTCAGAAGGCCG	850
Rho	740	AGAAGGAGGTCACGCGTATGGTTATCATCATGGTCATCGCTTTCCTAATC	789
1_F1	851	AGAAGGAGGTCACGCGTATGGTTATCATCATGGTCATCGCTTTCCTAATC	900
Rho	790	TGCTGGCTGCCATATGCTGGTGTGGCGTTCTACATCTTCACCCATCAGGG	839
1_F1	901	TGCTGGCTGCCATATGCTGGTGTGGCGTTCTACATCTTCACCCATCAGGG	950
Rho	840	CTCTGACTTTGGGCCCATCTTCATGACCATCCCGGCTTCTTTGCCAAGA	889
1_F1	951	CTCTGACTTTGGGCCCATCTTCATGACCATCCCGGCTTCTTTGCCAAGA	1000
Rho	890	CGTCTGCCGTCTACAACCCGGTTCATCTACATCATGATGAACAAGCAGTTC	939
1_F1	1001	CG-----	1002
Rho	940	CGGAACTGCATGGTCACCACTCTCTGCTGTGGCAAGAACCCGCTGGGTGA	989
1_F1	1003	-----	1002
Rho	990	CGACGAGGCGTCGACCACCGTCTCCAAGACAGAGACCAGCCAAGTGGCGC	1039
1_F1	1003	-----	1002
Rho	1040	CTGCCTAAGCGGCCGCAAATTCGGGGGGGGGGGGGGGGGGGG 1080	
1_F1	1003	----- 1002	

R252P

CGT to CCG change observed at the correct position.

Rho	1	-----	0
3_F1	1	GCATTAGCAGAGCTCTCCCTATCAGTGATAGAGATCTCCCTATCAGTGAT	50
Rho	1	-----	0
3_F1	51	AGAGATCGTCGACGAGCTCGTTTAGTGAACCGTCAGATCTCTAGAAGCTG	100
Rho	1	-----ATGAACGGTACCGAAGGCCAAACTTCTACGTTCTTTCT	40
3_F1	101	GAATTCCACCATGAACGGTACCGAAGGCCAAACTTCTACGTTCTTTCT	150
Rho	41	CCAACAAGACGGGCGTGGTGCGCAGCCCGTTCGAGGCTCCGCAGTACTAC	90
3_F1	151	CCAACAAGACGGGCGTGGTGCGCAGCCCGTTCGAGGCTCCGCAGTACTAC	200
Rho	91	CTGGCGGAGCCCTGGCAGTTCTCCATGCTGGCCGCTACATGTTCTGCT	140
3_F1	201	CTGGCGGAGCCCTGGCAGTTCTCCATGCTGGCCGCTACATGTTCTGCT	250
Rho	141	GATCATGCTTGGCTTCCCAGTCAACTTCCCTCAGCTGTACGTCACAGTCC	190
3_F1	251	GATCATGCTTGGCTTCCCAGTCAACTTCCCTCAGCTGTACGTCACAGTCC	300
Rho	191	AGCACAAGAAGCTTCGCACACCGCTCAACTACATCCTGCTCAACCTGGCC	240
3_F1	301	AGCACAAGAAGCTTCGCACACCGCTCAACTACATCCTGCTCAACCTGGCC	350
Rho	241	GTGGCAGATCTCTTCATGGTCTTCGGTGGCTTACCACCACCCTCTACAC	290
3_F1	351	GTGGCAGATCTCTTCATGGTCTTCGGTGGCTTACCACCACCCTCTACAC	400
Rho	291	CTCTCTCCATGGGTACTTCGTCTTTGGGCCGACGGGCTGCAACCTCGAGG	340
3_F1	401	CTCTCTCCATGGGTACTTCGTCTTTGGGCCGACGGGCTGCAACCTCGAGG	450
Rho	341	GCTTCTTTGCCACCCTGGGCGGTGAAATGCACTGTGGTCTCTGGTAGTA	390
3_F1	451	GCTTCTTTGCCACCCTGGGCGGTGAAATGCACTGTGGTCTCTGGTAGTA	500
Rho	391	CTGGCGATCGAGCGGTACGTGGTGGTGTGCAAGCCCATGAGCAACTCCG	440
3_F1	501	CTGGCGATCGAGCGGTACGTGGTGGTGTGCAAGCCCATGAGCAACTCCG	550
Rho	441	CTTCGGTGAGAACCACGCCATCATGGGCGTCGCCTTACCTGGGTCATGG	490
3_F1	551	CTTCGGTGAGAACCACGCCATCATGGGCGTCGCCTTACCTGGGTCATGG	600
Rho	491	CTCTGGCCTGTGCGGCCCGCGCTCGTCGGCTGGTCTAGATAACATCCCG	540
3_F1	601	CTCTGGCCTGTGCGGCCCGCGCTCGTCGGCTGGTCTAGATAACATCCCG	650
Rho	541	GAGGGCATGCAGTGCTCGTGCGGGATCGATTACTACACGCCGCACGAGGA	590
3_F1	651	GAGGGCATGCAGTGCTCGTGCGGGATCGATTACTACACGCCGCACGAGGA	700
Rho	591	GACCAACAATGAGTCGTTTCGTATCTACATGTTTCGTGGTCCACTTCATCA	640
3_F1	701	GACCAACAATGAGTCGTTTCGTATCTACATGTTTCGTGGTCCACTTCATCA	750

Rho	641	TCCCGCTGATTGTCATCTTCTTCTGCTATGGCCAGCTGGTGTTCACCGTC	690
3_F1	751	TCCCGCTGATTGTCATCTTCTTCTGCTATGGCCAGCTGGTGTTCACCGTC	800
Rho	691	AAGGAGGCTGCAGCCCAGCAGCAGGAGAGCGCCACCACTCAGAAGGCCGA	740
3_F1	801	AAGGAGGCTGCAGCCCAGCAGCAGGAGAGCGCCACCACTCAGAAGGCCGA	850
Rho	741	GAAGGAGGTCACGCGTATGGTTATCATCATGGTCATCGCTTTCCTAATCT	790
3_F1	851	GAAGGAGGTCACGCCGATGGTTATCATCATGGTCATCGCTTTCCTAATCT	900
Rho	791	GCTGGCTGCCATATGCT-GGTGTGGCGTTCTACATCTTCACCCATCAGGG	839
3_F1	901	GCTGGCTGCCATATGCTGGGTGTGGCGTTCTACATCTTCACCCATCAGGG	950
Rho	840	CTCTGACTTTGGGCCCATCTTCATGACCATCCCGGCTTTCCTTGCCAAGA	889
3_F1	951	CTCTGACTTTGGGCCCATCTTCATGACCATC-----	981
Rho	890	CGTCTGCCGTCTACAACCCGGTCATCTACATCATGATGAACAAGCAGTTC	939
3_F1	982	-----	981
Rho	940	CGGAACTGCATGGTCACCACTCTCTGCTGTGGCAAGAACCCGCTGGGTGA	989
3_F1	982	-----	981
Rho	990	CGACGAGGCGTCGACCACCGTCTCCAAGACAGAGACCAGCCAAGTGGCGC	1039
3_F1	982	-----	981
Rho	1040	CTGCCTAAGCGGCCGCAAATTCCGGGGGGGGGGGGGGGGGGGG 1080	
3_F1	982	-----	981

S298D

TCT to GAT change observed at the correct position.

Rho	1	-----	0
5_F1	1	GCAAATAGCAGAGCTCTCCCTATCAGTGATAGAGATCTCCCTATCAGTGA	50
Rho	1	-----	0
5_F1	51	TAGAGATCGTCGACGAGCTCGTTTAGTGAACCGTCAGATCTCTAGAAGCT	100
Rho	1	-----ATGAACGGTACCGAAGGCCAAACTTCTACGTTCCCTTC	39
5_F1	101	 GGAATTCACCATGAACGGTACCGAAGGCCAAACTTCTACGTTCCCTTC	150
Rho	40	TCCAACAAGACGGGCGTGGTGCGCAGCCGTTTCGAGGCTCCGCAGTACTA	89
5_F1	151	 TCCAACAAGACGGGCGTGGTGCGCAGCCGTTTCGAGGCTCCGCAGTACTA	200
Rho	90	CCTGGCGGAGCCCTGGCAGTTCTCCATGCTGGCCGCCTACATGTTCCCTGC	139
5_F1	201	 CCTGGCGGAGCCCTGGCAGTTCTCCATGCTGGCCGCCTACATGTTCCCTGC	250
Rho	140	TGATCATGCTTGGCTTCCCGATCAACTTCCTCAGCTGTACGTACAGTC	189
5_F1	251	 TGATCATGCTTGGCTTCCCGATCAACTTCCTCAGCTGTACGTACAGTC	300
Rho	190	CAGCACAAGAAGCTTCGCACACCGCTCAACTACATCCTGCTCAACCTGGC	239
5_F1	301	 CAGCACAAGAAGCTTCGCACACCGCTCAACTACATCCTGCTCAACCTGGC	350
Rho	240	CGTGGCAGATCTCTTCATGGTCTTCGGTGGCTTACCACCACCCTCTACA	289
5_F1	351	 CGTGGCAGATCTCTTCATGGTCTTCGGTGGCTTACCACCACCCTCTACA	400
Rho	290	CCTCTCTCCATGGGTACTTCGTCTTTGGGCCGACGGGCTGCAACCTCGAG	339
5_F1	401	 CCTCTCTCCATGGGTACTTCGTCTTTGGGCCGACGGGCTGCAACCTCGAG	450
Rho	340	GGCTTCTTTGCCACCCTGGGCGGTGAAATGCACTGTGGTCTCTGGTAGT	389
5_F1	451	 GGCTTCTTTGCCACCCTGGGCGGTGAAATGCACTGTGGTCTCTGGTAGT	500
Rho	390	ACTGGCGATCGAGCGGTACGTGGTGGTGTGCAAGCCCATGAGCAACTTCC	439
5_F1	501	 ACTGGCGATCGAGCGGTACGTGGTGGTGTGCAAGCCCATGAGCAACTTCC	550
Rho	440	GCTTCGGTGAGAACCACGCCATCATGGGCGTCGCCTTCACCTGGGTCATG	489
5_F1	551	 GCTTCGGTGAGAACCACGCCATCATGGGCGTCGCCTTCACCTGGGTCATG	600
Rho	490	GCTCTGGCCTGTGCGGCCCGCCGCTCGTCGGCTGGTCTAGATACATCCC	539
5_F1	601	 GCTCTGGCCTGTGCGGCCCGCCGCTCGTCGGCTGGTCTAGATACATCCC	650
Rho	540	GGAGGGCATGCAGTGCTCGTGCGGGATCGATTACTACACGCCGCACGAGG	589
5_F1	651	 GGAGGGCATGCAGTGCTCGTGCGGGATCGATTACTACACGCCGCACGAGG	700
Rho	590	AGACCAACAATGAGTCGTTTCGTCATCTACATGTTTCGTGGTCCACTTCATC	639
5_F1	701	 AGACCAACAATGAGTCGTTTCGTCATCTACATGTTTCGTGGTCCACTTCATC	750

Rho	640	ATCCCGCTGATTGTCATCTTCTTCTGCTATGGCCAGCTGGTGTTCACCGT	689
5_F1	751		800
Rho	690	CAAGGAGGCTGCAGCCCAGCAGCAGGAGAGCGCCACCACTCAGAAGGCCG	739
5_F1	801		850
Rho	740	AGAAGGAGGTCACGCGTATGGTTATCATCATGGTCATCGCTTTCCTAATC	789
5_F1	851		900
Rho	790	TGCTGGCTGCCATATGCTGGTGTGGCGTTCTACATCTTCACCCATCAGGG	839
5_F1	901		950
Rho	840	CTCTGACTTTGGGCCCATCTTCATGACCATCCCGGCTTCTTTGCCAAGA	889
5_F1	951		1000
Rho	890	CGTCTGCCGTCTACAACCCGGTCATCTACATCATGATGAACAAGCAGTTC	939
5_F1	1001	CG-----	1002
Rho	940	CGGAACTGCATGGTCACCACTCTCTGCTGTGGCAAGAACCCGCTGGGTGA	989
5_F1	1003	-----	1002
Rho	990	CGACGAGGCGTCGACCACCGTCTCCAAGACAGAGACCAGCCAAGTGGCGC	1039
5_F1	1003	-----	1002
Rho	1040	CTGCCTAAGCGGCCGCAAATTCCGGGGGGGGGGGGGGGGGGGG 1080	
5_F1	1003	----- 1002	
Rho	1	ATGAACGGTACCGAAGGCCAAACTTCTACGTTCTTTCTCCAACAAGAC	50
5_F2	1	-----	0
Rho	51	GGGCGTGGTGCGCAGCCCGTTTCGAGGCTCCGCAGTACTACCTGGCGGAGC	100
5_F2	1	-----	0
Rho	101	CCTGGCAGTTCTCCATGCTGGCCGCCTACATGTTCTTGCTGATCATGCTT	150
5_F2	1	-----	0
Rho	151	GGCTTCCCGATCAACTTCCTCACGCTGTACGTACAGTCCAGCACAAGAA	200
5_F2	1	-----	0
Rho	201	GCTTCGCACACCGCTCAACTACATCCTGCTCAACCTGGCCGTGGCAGATC	250
5_F2	1	-----	0

Rho	251	TCTTCATGGTCTTCGGTGGCTTCACCACCACCCTCTACACCTCTCTCCAT	300
5_F2	1	-----	0
Rho	301	GGGTACTTCGTCTTTGGGCCGACGGGCTGCAACCTCGAGGGCTTCTTTGC	350
5_F2	1	-----	0
Rho	351	CACCCCTGGGCGGTGAAATTGCACTGTGGTCTCTGGTAGTACTGGCGATCG	400
5_F2	1	-----	0
Rho	401	AGCGGTACGTGGTGGTGTGCAAGCCCATGAGCAACTTCCGCTTCGGTGAG	450
5_F2	1	-----CGG---G	4
Rho	451	AACCACGCCATCATGGGCGTCGCCTTACCTGGGTCATGGCTCTGGCCTG	500
5_F2	5	AAAC-CGCCATCATGGGCGTCGCCTTACCTGGGTCATGGCTCTGGCCTG	53
Rho	501	TGCGGCCCGCCGCTCGTCGGCTGGTCTAGATACATCCCGGAGGGCATGC	550
5_F2	54	TGCGGCCCGCCGCTCGTCGGCTGGTCTAGATACATCCCGGAGGGCATGC	103
Rho	551	AGTGCTCGTGCGGGATCGATTACTACACGCCGCACGAGGAGACCAACAAT	600
5_F2	104	AGTGCTCGTGCGGGATCGATTACTACACGCCGCACGAGGAGACCAACAAT	153
Rho	601	GAGTCGTTCGTTCATCTACATGTTTCGTGGTCCACTTCATCATCCCGCTGAT	650
5_F2	154	GAGTCGTTCGTTCATCTACATGTTTCGTGGTCCACTTCATCATCCCGCTGAT	203
Rho	651	TGTCATCTTCTTCTGCTATGGCCAGCTGGTGTTCACCGTCAAGGAGGCTG	700
5_F2	204	TGTCATCTTCTTCTGCTATGGCCAGCTGGTGTTCACCGTCAAGGAGGCTG	253
Rho	701	CAGCCCAGCAGCAGGAGAGCGCCACCACTCAGAAGGCCGAGAAGGAGGTC	750
5_F2	254	CAGCCCAGCAGCAGGAGAGCGCCACCACTCAGAAGGCCGAGAAGGAGGTC	303
Rho	751	ACGCGTATGGTTATCATCATGGTCATCGCTTTCCTAATCTGCTGGCTGCC	800
5_F2	304	ACGCGTATGGTTATCATCATGGTCATCGCTTTCCTAATCTGCTGGCTGCC	353
Rho	801	ATATGCTGGTGTGGCGTTCTACATCTTCAACCATCAGGGCTCTGACTTTG	850
5_F2	354	ATATGCTGGTGTGGCGTTCTACATCTTCAACCATCAGGGCTCTGACTTTG	403
Rho	851	GGCCCATCTTCATGACCATCCCGGCTTCTTTGCCAAGACG TCT GCCGTC	900
5_F2	404	GGCCCATCTTCATGACCATCCCGGCTTCTTTGCCAAGACG GAT GCCGTC	453
Rho	901	TACAACCCGGTCATCTACATCATGATGAACAAGCAGTTCGGAACTGCAT	950
5_F2	454	TACAACCCGGTCATCTACATCATGATGAACAAGCAGTTCGGAACTGCAT	503
Rho	951	GGTCACCACTCTCTGCTGTGGCAAGAACCCGCTGGGTGACGACGAGGCGT	1000
5_F2	504	GGTCACCACTCTCTGCTGTGGCAAGAACCCGCTGGGTGACGACGAGGCGT	553
Rho	1001	CGACCACCGTCTCCAAGACAGAGACCAGCCAAGTGGCGCCTGCCTAAGCG	1050

5_F2	554	CGACCACCGTCTCCAAGACAGAGACCAGCCAAGTGGCGCCTGCCTAAGCG	603
Rho	1051	GCCGCAAATTCGGGGGGGGGGGGGGGGGGGG-----	1080
		
5_F2	604	GCCGC----TC--GAGGCCGGCAAGGCCGGATCCGACGTAACTTGTTTA	647
Rho	1081	-----	1080
5_F2	648	TTGCAGCTTATAATGGTTACAAATAAAGCAATAGCATCACAAATTTTACA	697
Rho	1081	-----	1080
5_F2	698	AATAAAGCATTTTTTTTCACTGCATTCTAGTTGTGGTTTGTCCAAACTCAT	747
Rho	1081	-----	1080
5_F2	748	CAATGTATCTTATCATGTCTGGATCTACTAGTTCTAGCTAGAAGACTCTA	797
Rho	1081	-----	1080
5_F2	798	GGGTGTGACTTCTGAAGAGAAGAAGGAAGAGGAAGGGTGGAGGTTAGGAA	847
Rho	1081	-----	1080
5_F2	848	ACAGTGAGTCGGGCTTGTGGGTCTCTCCTGGTGATCTGACAGCTTCTGGG	897
Rho	1081	-----	1080
5_F2	898	TCAGAACTCGGAGTCACCACGACAAACTGCTCTCTGTCTGCAGCACAGGG	947
Rho	1081	-----	1080
5_F2	948	TTCAGGCAAAGTCTTGGTTGCCAGGCGGTG	977

K311E

AAG to GAG change observed the correct position.

Rho_WT	1	ATGAACGGTACCGAAGGCCAAACTTCTACGTTCTTTCTCCAACAAGAC	50
17_F2	1	-----	0
Rho_WT	51	GGGCGTGGTGCGCAGCCGTTTCGAGGCTCCGCAGTACTACCTGGCGGAGC	100
17_F2	1	-----	0
Rho_WT	101	CCTGGCAGTTCTCCATGCTGGCCGCCTACATGTTCTGCTGATCATGCTT	150
17_F2	1	-----	0
Rho_WT	151	GGCTTCCCGATCAACTTCCTCACGCTGTACGTACAGTCCAGCACAAGAA	200
17_F2	1	-----	0
Rho_WT	201	GCTTCGCACACCGCTCAACTACATCCTGCTCAACCTGGCCGTGGCAGATC	250
17_F2	1	-----	0
Rho_WT	251	TCTTCATGGTCTTCGGTGGCTTCACCACCACCCTCTACACCTCTCTCCAT	300
17_F2	1	-----	0
Rho_WT	301	GGTACTTCGTCTTTGGGCCGACGGGCTGCAACCTCGAGGGCTTCTTTGC	350
17_F2	1	-----	0
Rho_WT	351	CACCCCTGGGCGGTGAAATTGCACTGTGGTCTCTGGTAGTACTGGCGATCG	400
17_F2	1	-----	0
Rho_WT	401	AGCGGTACGTGGTGGTGTGCAAGCCCATGAGCAACTTCCGCTTCGGTGAG	450
17_F2	1	-----CG---G	3
Rho_WT	451	AACCACGCCATCAT-GGGCGTCGCCTTCACCTGGGTCATGGCTCTGGCCT	499
17_F2	4	AAACACGCCATCATGGGCGTCGCCTTCACCTGGGTCATGGCTCTGGCCT	53
Rho_WT	500	GTGCGGCCCGCCGCTCGTCGGCTGGTCTAGATAACATCCCGGAGGGCATG	549
17_F2	54	GTGCGGCCCGCCGCTCGTCGGCTGGTCTAGATAACATCCCGGAGGGCATG	103
Rho_WT	550	CAGTGCCTCGTGCGGGATCGATTACTACACGCCGCACGAGGAGACCAACAA	599
17_F2	104	CAGTGCCTCGTGCGGGATCGATTACTACACGCCGCACGAGGAGACCAACAA	153
Rho_WT	600	TGAGTCGTTTCGTTCATCTACATGTTTCGTGGTCCACTTCATCATCCCGCTGA	649
17_F2	154	TGAGTCGTTTCGTTCATCTACATGTTTCGTGGTCCACTTCATCATCCCGCTGA	203
Rho_WT	650	TTGTCATCTTCTTCTGCTATGGCCAGCTGGTGTTCACCGTCAAGGAGGCT	699
17_F2	204	TTGTCATCTTCTTCTGCTATGGCCAGCTGGTGTTCACCGTCAAGGAGGCT	253
Rho_WT	700	GCAGCCCAGCAGCAGGAGAGCGCCACCCTCAGAAGGCCGAGAAGGAGGT	749
17_F2	254	GCAGCCCAGCAGCAGGAGAGCGCCACCCTCAGAAGGCCGAGAAGGAGGT	303

Rho_WT	750	CACGCGTATGGTTATCATCATGGTCATCGCTTTCCTAATCTGCTGGCTGC	799
17_F2	304	CACGCGTATGGTTATCATCATGGTCATCGCTTTCCTAATCTGCTGGCTGC	353
Rho_WT	800	CATATGCTGGTGTGGCGTTCTACATCTTCACCCATCAGGGCTCTGACTTT	849
17_F2	354	CATATGCTGGTGTGGCGTTCTACATCTTCACCCATCAGGGCTCTGACTTT	403
Rho_WT	850	GGGCCCATCTTCATGACCATCCCGGCTTCTTTGCCAAGACGTCTGCCGT	899
17_F2	404	GGGCCCATCTTCATGACCATCCCGGCTTCTTTGCCAAGACGTCTGCCGT	453
Rho_WT	900	CTACAACCCGGTCATCTACATCATGATGAACAAGCAGTTCCGGAAGTCA	949
		.	
17_F2	454	CTACAACCCGGTCATCTACATCATGATGAACGAGCAGTTCCGGAAGTCA	503
Rho_WT	950	TGGTCACCACTCTCTGCTGTGGCAAGAACCCGCTGGGTGACGACGAGGCG	999
17_F2	504	TGGTCACCACTCTCTGCTGTGGCAAGAACCCGCTGGGTGACGACGAGGCG	553
Rho_WT	1000	TCGACCACCGTCTCCAAGACAGAGACCAGCCAAGTGGCGCCTGCCTAAGC	1049
17_F2	554	TCGACCACCGTCTCCAAGACAGAGACCAGCCAAGTGGCGCCTGCCTAAGC	603
Rho_WT	1050	GGCCGC-----	1055
17_F2	604	GGCCGCTCGAGGCCGGCAAGGCCGGATCCGACGTTAACTTGTATTGCA	653
Rho_WT	1056	-----	1055
17_F2	654	GCTTATAATGGTTACAAATAAAGCAATAGCATCACAAATTCACAAATAA	703
Rho_WT	1056	-----	1055
17_F2	704	AGCATTTTTTTTCACTGCATTCTAGTTGTGGTTTGTCCAACTCATCAATG	753
Rho_WT	1056	-----	1055
17_F2	754	TATCTTATCATGTCTGGATCTACTAGTTCTAGCTAGAAGACTCTAGGGTG	803
Rho_WT	1056	-----	1055
17_F2	804	TGACTTCTGAAGAGAAGAAGGAAGAGGAAGGGTGGAGGTAGGAAACAGT	853
Rho_WT	1056	-----	1055
17_F2	854	GAGTCGGGCTTGTGGTCTCTCCTGGTATCTGACAGCTTCTGGGTCAGA	903
Rho_WT	1056	-----	1055
17_F2	904	ACTCGGAGTCACCACGACAAACTGCTCTCTGTCTGCAGCACAGGGTTCAG	953
Rho_WT	1056	-----	1055
17_F2	954	GCAAAGTCTTGGTTGCCAGGCGGTGAGGTCAGGGGTGGGGAAGCCAGGG	1003
Rho_WT	1056	-----	1055
17_F2	1004	CTGGGGATTCCCATCTCCTCAGTTTCACTTCTGCACCTAACCTGGGTCA	1053
Rho_WT	1056	-----	1055

17_F2 1054 GGTCCCTTCTGCCGGGACACTGATGACGCGCTGGCAGGTCTCACTATCATT 1103
Rho_WT 1056 ----- 1055
17_F2 1104 GGGTGGCGAG 1113

Chapter 6 – E122 mutants

E122C

GAA to TGC change observed at the correct position.

pMT4	1	-----	0
1.6_SeqF1-TS0	1	CGGAGTGGAGGAATGAAATCAACTTTGCCTTTCTCTCCACAAGTGTCCAC	50
pMT4	1	-----GGTACCCACCATGAACGGCACCGAAGGCCCAA	32
1.6_SeqF1-TS0	51	TCCCAGGTCCAAGGTACCCACCATGAACGGCACCAAAGGCCCAA	100
pMT4	33	ACTTCTACGTTCTTTCTCCAACAAGACGGGCGTGGTGCAGCCCGTTC	82
1.6_SeqF1-TS0	101	ACTTCTACGTTCTTTCTCCAACAAGACGGGCGTGGTGCAGCCCGTTC	150
pMT4	83	GAGGCTCCGCAGTACTACCTGGCGGAGCCCTGGCAGTTCTCCATGCTGGC	132
1.6_SeqF1-TS0	151	GAGGCTCCGCAGTACTACCTGGCGGAGCCCTGGCAGTTCTCCATGCTGGC	200
pMT4	133	CGCCTACATGTTCTTGCTGATCATGCTTGGCTTCCCGATCAACTTCTTCA	182
1.6_SeqF1-TS0	201	CGCCTACATGTTCTTGCTGATCATGCTTGGCTTCCCGATCAACTTCTTCA	250
pMT4	183	CGCTGTACGTCACAGTCCAGCACAAGAAGCTTCGCACACCGCTCAACTAC	232
1.6_SeqF1-TS0	251	CGCTGTACGTCACAGTCCAGCACAAGAAGCTTCGCACACCGCTCAACTAC	300
pMT4	233	ATCCTGCTCAACCTGGCCGTGGCAGATCTTTCATGGTCTTCGGTGGCTT	282
1.6_SeqF1-TS0	301	ATCCTGCTCAACCTGGCCGTGGCAGATCTTTCATGGTCTTCGGTGGCTT	350
pMT4	283	CACCACCACCTCTACACCTCTCTCCATGGGTACTTCGTCTTTGGGCCGA	332
1.6_SeqF1-TS0	351	CACCACCACCTCTACACCTCTCTCCATGGGTACTTCATCTTTGGGCCGA	400
pMT4	333	CGGGCTGCAACCTCGAGGGCTTCTTTGCCACCCTGGGCGGTGAAATTGCA	382
1.6_SeqF1-TS0	401	CGGGCTGCAACCTCGAGGGCTTCTTTGCCACCCTGGGCGGTGCAATTGCA	450
pMT4	383	CTGTGGTCTCTGGTAGTACTGGCGATCGAGCGGTACGTGGTGGTGTGCAA	432
1.6_SeqF1-TS0	451	CTGTGGTCTCTGGTAGTACTGGCGATCGAGCGGTACGTGGTGGTGTGCAA	500
pMT4	433	GCCCATGAGCAACTTCCGCTTCGGTGAGAACCACGCCATCATGGGCGTCG	482
1.6_SeqF1-TS0	501	GCCCATGAGCAACTTCCGCTTCGGTGAGAACCACGCCATCATGGGCGTCG	550
pMT4	483	CCTTCACCTGGGTTCATGGCTCTGGCCTGTGCGGCCCCGCGCTCGTCGGC	532
1.6_SeqF1-TS0	551	CCTTCACCTGGGTTCATGGCTCTGGCCTGTGCGGCCCCGCGCTCGTCGGC	600
pMT4	533	TGGTCTAGATACATCCCGAGGGCATGCAGTGCTCGTGCGGGATCGATTA	582
1.6_SeqF1-TS0	601	TGGTCTAAATACATCCCGAGGGCATGCAGTGCTCGTGCGGGATCGATTA	650
pMT4	583	CTACACGCCGCACGAGGAGACCAACAATGAGTCGTTTCGTCTACATGT	632
1.6_SeqF1-TS0	651	CTACACGCCGCACGAGGAGACCAACAATGAGTCGTTTCGTCTACATGT	700
pMT4	633	TCGTGGTCCACTTCATCATCCCGCTGATTGTCATCTTCTTCTGCTATGGC	682

1.6_SeqF1-TS0	701	TCGTGGTCCACTTCATCATCCCGCTGATTGTCATCTTCTTCTGCTATGGC	750
pMT4	683	CAGCTGGTGTTCACCGTCAAGGAGGCTGCAGCCCAGCAGCAGGAGAGCGC	732
1.6_SeqF1-TS0	751	CAGCTGGTGTTCACCGTCAAAGAGGCTGCAGCCCAACAACAGGAGAGCGC	800
pMT4	733	CACCACTCAGAAGGCCGAGAAGGAGGTCACGCGTATGGTTATCATCATGG	782
1.6_SeqF1-TS0	801	CACCACTCA-AAGGCCGAGAAGGAGGTCACGCGTATGGTTATCATCATGG	849
pMT4	783	TCATCGCTTTCCTAATCTGCTGGCTGCCATATGCTGGTGTGGCGTTCTAC	832
1.6_SeqF1-TS0	850	TCATCGCTTTCCTAATCTGCTGGCTGCAATATGCTGGTGTGGCGTTCTAC	899
pMT4	833	ATCTTCACCCATCAGGGCTCTGACTTTGGGCCATCTTCATGACCATCCC	882
1.6_SeqF1-TS0	900	ATCTTCACCCATCAGGGCTCTGACTTTGGGCCATCTTCATGACCATCCC	949
pMT4	883	-GGCTTCTTTGCCAAGACGTCTGCCGTCTACAACCCGGTCATCTACATC	931
1.6_SeqF1-TS0	950	GGGCTTTC-TTGCCAAAACGTCTGCCGTCTACAACCCGGTCATCTACATC	998
pMT4	932	ATGATGAACAAGCAGTTCGGAACTGCATGGTCACCACT-CTCTGCT-GT	979
1.6_SeqF1-TS0	999	ATGATGAACAAGCAGTTCGGG-ACTGCATGGTCACCACTCCTCTGCTGGT	1047
pMT4	980	GGCAAGAACCCGCT-GGGTGCAGACGAGGCGTCG-ACCACCG-TCTCCAA	1026
1.6_SeqF1-TS0	1048	GGCAAGAACCCGCTGGGGTGCAGACGA-GCGTCGAACCACCGTTCTCAA	1096
pMT4	1027	GACAG-AGACCAGCCAAGTGGCGCCTGCCTAAGC-GGCCGCAA-----	1068
1.6_SeqF1-TS0	1097	AAAAGAAAAACAGCCAA-TGGCGCTG-CTAAACGGGCCGCAAATTCGT	1144
pMT4	1069	-----	1068
1.6_SeqF1-TS0	1145	AAGGTGTGGAACACTGCCTCAAGGCTCGACATTCGCGCCCAACCTGGACA	1194
pMT4	1069	-----	1068
1.6_SeqF1-TS0	1195	GCAATCTAACCTGATGGCGTGGTAGGATTTATACCCGGCTGCAATCAGGT	1244
pMT4	1069	-----	1068
1.6_SeqF1-TS0	1245	AATCGAACAACTATGAAAACATGCAG	1270

E122G

See appendix 3.2, the same plasmid used for the work in Chapter 5 was used here.

E122I

GAA to ATC change observed at the correct position.

Rho	1	-----	0
E122I	1	TGGGGGGGAGGCTTTATAAGCAGAGCTCTCCCTATCAGTGATAGAGATC	50
Rho	1	-----	0
E122I	51	TCCCTATCAGTGATAGAGATCGTCGACGAGCTCGTTTAGTGAACCGTCAG	100
Rho	1	-----CATGAACGGCACCGAAGGCCAAACTT	27
E122I	101	ATCTCTAGAAGCTGGGTACCCACCATGAACGGCACCGAAGGCCAAACTT	150
Rho	28	CTACGTTCCCTTTCTCCAACAAGACGGGCGTGGTGCGCAGCCCGTTCGAGG	77
E122I	151	CTACGTTCCCTTTCTCCAACAAGACGGGCGTGGTGCGCAGCCCGTTCGAGG	200
Rho	78	CTCCGCAGTACTACCTGGCGGAGCCCTGGCAGTTCTCCATGCTGGCCGCC	127
E122I	201	CTCCGCAGTACTACCTGGCGGAGCCCTGGCAGTTCTCCATGCTGGCCGCC	250
Rho	128	TACATGTTCCCTGCTGATCATGCTTGGCTTCCCGATCAACTTCCCTCACGCT	177
E122I	251	TACATGTTCCCTGCTGATCATGCTTGGCTTCCCGATCAACTTCCCTCACGCT	300
Rho	178	GTACGTCACAGTCCAGCACAAGAAGCTTCGCACACCGCTCAACTACATCC	227
E122I	301	GTACGTCACAGTCCAGCACAAGAAGCTTCGCACACCGCTCAACTACATCC	350
Rho	228	TGCTCAACCTGGCCGTGGCAGATCTCTTCATGGTCTTCGGTGGCTTACC	277
E122I	351	TGCTCAACCTGGCCGTGGCAGATCTCTTCATGGTCTTCGGTGGCTTACC	400
Rho	278	ACCACCCTCTACACCTCTCTCCATGGGTACTTCGTCTTTGGGCCGACGGG	327
E122I	401	ACCACCCTCTACACCTCTCTCCATGGGTACTTCGTCTTTGGGCCGACGGG	450
Rho	328	CTGCAACCTCGAGGGCTTCTTTGCCACCCTGGGCGGTGAAATTGCACTGT	377
E122I	451	CTGCAACCTCGAGGGCTTCTTTGCCACCCTGGGCGGTATCATTGCACTGT	500
Rho	378	GGTCTCTGGTAGTACTGGCGATCGAGCGGTACGTGGTGGTGTGCAAGCCC	427
E122I	501	GGTCTCTGGTAGTACTGGCGATCGAGCGGTACGTGGTGGTGTGCAAGCCC	550
Rho	428	ATGAGCAACTTCCGCTTCGGTGAGAACCACGCCATCATGGGCGTCGCCTT	477
E122I	551	ATGAGCAACTTCCGCTTCGGTGAGAACCACGCCATCATGGGCGTCGCCTT	600
Rho	478	CACCTGGGTCATGGCTCTGGCCTGTGCGGCCCGCCGCTCGTCGGCTGGT	527
E122I	601	CACCTGGGTCATGGCTCTGGCCTGTGCGGCCCGCCGCTCGTCGGCTGGT	650

E122L

GAA to CTG change observed at the correct position.

pMT4	1	-----	0
3.1_E122L	1	TAGCGGAGCTCTCCGTATCAGGTGATAGAGATCTCCCTATCAGGTGATAG	50
pMT4	1	-----GG	2
3.1_E122L	51	AGATCGTCGACGAGCTCGTTTAGTGAACCGTCGGATCTCTAGAAGCTGGG	100
pMT4	3	TACCCACCATGAACGGCACC GAAGGCCCAAAC TTCTACGTTCC TTTCTCC	52
3.1_E122L	101	TACCCACCATGAACGGCACC GAAGGCCCAAAC TTCTACGTTCC TTTCTCC	150
pMT4	53	AACAAGACGGGCGTGGTGC GCAGCCCGTTCGAGGCTCCGCAGTACTACCT	102
3.1_E122L	151	AACAAGACGGGCGTGGTGC GCAGCCCGTTCGAGGCTCCGCAGTACTACCT	200
pMT4	103	GGCGGAGCCCTGGCAGTTCTCCATGCTGGCCGCCTACATGTTCCCTGTGTA	152
3.1_E122L	201	GGCGGAGCCCTGGCAGTTCTCCATGCTGGCCGCCTACATGTTCCCTGTGTA	250
pMT4	153	TCATGCTTGGCTTCCCGATCAACTTCCTCACGCTGTACGTCACAGTCCAG	202
3.1_E122L	251	TCATGCTTGGCTTCCCGATCAACTTCCTCACGCTGTACGTCACAGTCCAG	300
pMT4	203	CACAAGAAGCTTCGCACACCGCTCAACTACATCCTGCTCAACCTGGCCGT	252
3.1_E122L	301	CACAAGAAGCTTCGCACACCGCTCAACTACATCCTGCTCAACCTGGCCGT	350
pMT4	253	GGCAGATCTCTTCATGGTCTTCGGTGGCTTCACCACCACCCTCTACACCT	302
3.1_E122L	351	GGCAGATCTCTTCATGGTCTTCGGTGGCTTCACCACCACCCTCTACACCT	400
pMT4	303	CTCTCCATGGGTACTTCGTCTTTGGGCCGACGGGCTGCAACCTCGAGGGC	352
3.1_E122L	401	CTCTCCATGGGTACTTCGTCTTTGGGCCGACGGGCTGCAACCTCGAGGGC	450
pMT4	353	TTCTTTGCCACCCTGGGCGGTGAAATTGCACTGTGGTCTCTGGTAGTACT	402
3.1_E122L	451	TTCTTTGCCACCCTGGGCGGTCTGATTGCACTGTGGTCTCTGGTAGTACT	500
pMT4	403	GGCGATCGAGCGGTACGTGGTGGTGTGCAAGCCCATGAGCAACTTCCGCT	452
3.1_E122L	501	GGCGATCGAGCGGTACGTGGTGGTGTGCAAGCCCATGAGCAACTTCCGCT	550
pMT4	453	TCGGTGAGAACCACGCCATCATGGGCGTCGCCTTCACCTGGGTCATGGCT	502
3.1_E122L	551	TCGGTGAGAACCACGCCATCATGGGCGTCGCCTTCACCTGGGTCATGGCT	600
pMT4	503	CTGGCCTGTGCGGCCCCGCGCTCGTCGGCTGGTCTAGATACATCCCGGA	552
3.1_E122L	601	CTGGCCTGTGCGGCCCCGCGCTCGTCGGCTGGTCTAGATACATCCCGGA	650
pMT4	553	GGGCATGCAGTGCTCGTGCGGGATCGATTACTACACGCCGCACGAGGAGA	602
3.1_E122L	651	GGGCATGCAGTGCTCGTGCGGGATCGATTACTACACGCCGCACGAGGAGA	700
pMT4	603	CCAACAATGAGTCGTTTCGTATCTACATGTTTCGTGGTCCACTTCATCATC	652
3.1_E122L	701	CCAACAATGAGTCGTTTCGTATCTACATGTTTCGTGGTCCACTTCATCATC	750

pMT4	653	CCGCTGATTGTCATCTTCTTCTGCTATGGCCAGCTGGTGTTCACCGTCAA	702
3.1_E122L	751	CCGCTGATTGTCATCTTCTTCTGCTATGGCCAGCTGGTGTTCACCGTCAA	800
pMT4	703	GGAGGCTGCAGCCCAGCAGCAGGAGAGCGCCACCACTCAGAAGCCGAGA	752
3.1_E122L	801	GGAGGCTGCAGCCCAGCAGCAGGAGAGCGCCACCACTCAGAAGCCGAGA	850
pMT4	753	AGGAGGTCACGCGTATGGTTATCATCATGGTCATCGCTTTCCTAATCTGC	802
3.1_E122L	851	AGGAGGTCACGCGTATGGTTATCATCATGGTCATCGCTTTCCTAATCTGC	900
pMT4	803	TGGCTGCCATATGCTGGTGTGGCGTTCTACATCTTCACCCATCAGGGCTC	852
3.1_E122L	901	TGGCTGCCATATGCTGGTGTGGCGTTCTACATCTTCACCCATCAGGGCTC	950
pMT4	853	TGACTTTGGGCCCATCTTCATGACCATCCCGGCTTCTTTGCCAAGACGT	902
3.1_E122L	951	TGACTTTGGGCCCATCTTCATGACCATCCCGGCTTCTTTGCCAAGACGT	1000
pMT4	903	CTGCCGTCTACAACCCGGTCATCTACATCATGATGAACAAGCAGTTCCGG	952
3.1_E122L	1001	CTGCCGTCTACAACCCGGTCATCTACATCATGATGAACAAGCAGTTCCGG	1050
pMT4	953	AACTGCATGGTCACCACTCTCTGCTGTGGCAAGAACCCGCTGGGTGACGA	1002
3.1_E122L	1051	AACTGCATGGTCACCACTCTCTGCTGTGGCAAGAACCCGCTGGGTGACAA	1100
pMT4	1003	CGAGGCGTCGACCACCGTCTCCAAGACAGAGACCAGCCAAGTGGCGCCTG	1052
3.1_E122L	1101	CGAGGCGTCAACCACCGTCTCCAAGA-----	1126
pMT4	1053	CCTAAGCGCCGC	1065
3.1_E122L	1127	-----	1126

E122M

GAA to ATG change observed at the correct position.

pMT4	1	-----	0
5.1_E122M	1	GAATGAACATCCACTTTGCCTTTCTCTCACAGGTGTCCACTCCCAGGTCC	50
pMT4	1	-----GGTACCCACCATGAACGGCACCGAAGGCCAAACTTCTACGT	42
5.1_E122M	51	AACTGCAAGGTACCCACCATGAACGGCACCGAAGGCCAAACTTCTACGT	100
pMT4	43	TCCTTTCTCCAACAAGACGGGCGTGGTGCAGCCCGTTCGAGGCTCCGC	92
5.1_E122M	101	TCCTTTCTCCAACAAGACGGGCGTGGTGCAGCCCGTTCGAGGCTCCGC	150
pMT4	93	AGTACTACCTGGCGGAGCCCTGGCAGTTCTCCATGCTGGCCGCTACATG	142
5.1_E122M	151	AGTACTACCTGGCGGAGCCCTGGCAGTTCTCCATGCTGGCCGCTACATG	200
pMT4	143	TTCTGCTGATCATGCTTGGCTTCCCGATCAACTTCCTCACGCTGTACGT	192
5.1_E122M	201	TTCTGCTGATCATGCTTGGCTTCCCGATCAACTTCCTCACGCTGTACGT	250
pMT4	193	CACAGTCCAGCACAAGAAGCTTCGCACACCGCTCAACTACATCCTGCTCA	242
5.1_E122M	251	CACAGTCCAGCACAAGAAGCTTCGCACACCGCTCAACTACATCCTGCTCA	300
pMT4	243	ACCTGGCCGTGGCAGATCTTTCATGGTCTTCGGTGGCTTCACCACCACC	292
5.1_E122M	301	ACCTGGCCGTGGCAGATCTTTCATGGTCTTCGGTGGCTTCACCACCACC	350
pMT4	293	CTCTACACCTCTCTCCATGGGTACTIONTCGCTTTGGGCCGACGGGCTGCAA	342
5.1_E122M	351	CTCTACACCTCTCTCCATGGGTACTIONTCGCTTTGGGCCGACGGGCTGCAA	400
pMT4	343	CCTCGAGGGCTTCTTTGCCACCCTGGGCGGTGAAATTGCACTGTGGTCTC	392
5.1_E122M	401	CCTCGAGGGCTTCTTTGCCACCCTGGGCGGTATGATTGCACTGTGGTCTC	450
pMT4	393	TGGTAGTACTGGCGATCGAGCGGTACGTGGTGGTGTGCAAGCCCATGAGC	442
5.1_E122M	451	TGGTAGTACTGGCGATCGAGCGGTACGTGGTGGTGTGCAAGCCCATGAGC	500
pMT4	443	AACTTCCGCTTCGGTGAGAACCACGCCATCATGGGCGTCGCCTTCACCTG	492
5.1_E122M	501	AACTTCCGCTTCGGTGAGAACCACGCCATCATGGGCGTCGCCTTCACCTG	550
pMT4	493	GGTCATGGCTCTGGCCTGTGCGGCCCGCCGCTCGTCGGCTGGTCTAGAT	542
5.1_E122M	551	GGTCATGGCTCTGGCCTGTGCGGCCCGCCGCTCGTCGGCTGGTCTAGAT	600
pMT4	543	ACATCCCGGAGGGCATGCAGTGCTCGTGCGGGATCGATTACTACACGCCG	592
5.1_E122M	601	ACATCCCGGAGGGCATGCAGTGCTCGTGCGGGATCGATTACTACACGCCG	650
pMT4	593	CACGAGGAGACCAACAATGAGTCGTTTCGTCATCTACATGTTTCGTGGTCCA	642
5.1_E122M	651	CACGAGGAGACCAACAATGAGTCGTTTCGTCATCTACATGTTTCGTGGTCCA	700
pMT4	643	CTTCATCATCCCCTGATTGTTCATCTTCTTCTGCTATGGCCAGCTGGTGT	692
5.1_E122M	701	CTTCATCATCCCCTGATTGTTCATCTTCTTCTGCTATGGCCAGCTGGTGT	750
pMT4	693	TCACCGTCAAGGAGGCTGCAGCCAGCAGCAGGAGAGCGCCACCACTCAG	742

5.1_E122M	751	TCACCGTCAAGGAGGCTGCAGCCCAGCAGCAGGAGAGCGCCACCACTCAG	800
pMT4	743	AAGGCCGAGAAGGAGGTACGCGTATGGTTATCATCATGGTCATCGCTTT	792
5.1_E122M	801	AAGGCCGAGAAGGAGGTACGCGTATGGTTATCATCATGGTCATCGCTTT	850
pMT4	793	CCTAATCTGCTGGCTGCCATATGCTGGTGTGGCGTTCTACATCTTCACCC	842
5.1_E122M	851	CCTAATCTGCTGGCTGCCATATGCTGGTGTGGCGTTCTACATCTTCACCC	900
pMT4	843	ATCAGGGCTCTGACTTTGGGCCCATCTTCATGACCATCCCGGCTTTCTTT	892
5.1_E122M	901	ATCAGGGCTCTGACTTTGGGCCCATCTTCATGACCATCCCGGCTTTCTTT	950
pMT4	893	GCCAAGACGTCTGCCGTCTACAACCCGGTCATCTACATCATGATGAACAA	942
5.1_E122M	951	GCCAAGACGTCTGCCGTCTACAACCCGGTCATCTACATCATGATGAACAA	1000
pMT4	943	GCAGTCCGGAAGTGCATGGTCAACCACTCTCTGCTGTGGCAAGAACCCGC	992
5.1_E122M	1001	GCAGTCCGGAAGTGCATGGTCAACCACTCTCTGCTGTGGCAAGAACCCGC	1050
pMT4	993	TGGGTGACGACGAGGCGTCGACCACCGTCTCCAAGACAGAGACCAGCCAA	1042
5.1_E122M	1051	TGGGTGACGACGAGGCGTCGACCACCGTCTCCAAGACAGAGACCAGCCAA	1100
pMT4	1043	GTGGCGCCTGCCTAAGCGCCGCAAA-----	1068
5.1_E122M	1101	GTGGCGCCTGCCTAAGCGCCGCAAAATCCGGGGGGGGGGGGGGGAA	1150
pMT4	1069	-- 1068	
5.1_E122M	1151	AG 1152	

E122Q

GAA to CAA change observed at the correct position.

Rho	1	-----	0
E122Q	1	GGGGGTGAAGTTAATAGCAGAGCTCTCCCTATCAGTGATAGAGATCTCC	50
Rho	1	-----	0
E122Q	51	CTATCAGTGATAGAGATCGTCGACGAGCTCGTTTAGTGAACCGTCAGATC	100
Rho	1	-----CATGAACGGCACCGAAGGCCAAACTTCTA	30
E122Q	101	TCTAGAAGCTGGGTACCCACCATGAACGGCACCGAAGGCCAAACTTCTA	150
Rho	31	CGTTCCTTTCTCCAACAAGACGGGCGTGGTGCGCAGCCCGTTTCGAGGCTC	80
E122Q	151	CGTTCCTTTCTCCAACAAGACGGGCGTGGTGCGCAGCCCGTTTCGAGGCTC	200
Rho	81	CGCAGTACTACCTGGCGGAGCCCTGGCAGTTCTCCATGCTGGCCGCTAC	130
E122Q	201	CGCAGTACTACCTGGCGGAGCCCTGGCAGTTCTCCATGCTGGCCGCTAC	250
Rho	131	ATGTTCTGCTGATCATGCTTGGCTTCCCGATCAACTTCCTCACGCTGTA	180
E122Q	251	ATGTTCTGCTGATCATGCTTGGCTTCCCGATCAACTTCCTCACGCTGTA	300
Rho	181	CGTCACAGTCCAGCACAAGAAGCTTCGCACACCGCTCAACTACATCCTGC	230
E122Q	301	CGTCACAGTCCAGCACAAGAAGCTTCGCACACCGCTCAACTACATCCTGC	350
Rho	231	TCAACCTGGCCGTGGCAGATCTTTCATGGTCTTCGGTGGCTTCACCACC	280
E122Q	351	TCAACCTGGCCGTGGCAGATCTTTCATGGTCTTCGGTGGCTTCACCACC	400
Rho	281	ACCCTCTACACCTCTCTCCATGGGTACTTCGTCTTTGGGCCGACGGGCTG	330
E122Q	401	ACCCTCTACACCTCTCTCCATGGGTACTTCGTCTTTGGGCCGACGGGCTG	450
Rho	331	CAACCTCGAGGGCTTCTTTGCCACCCTGGGCGGTGAAATTGCACTGTGGT	380
E122Q	451	CAACCTCGAGGGCTTCTTTGCCACCCTGGGCGGTCAAATTGCACTGTGGT	500
Rho	381	CTCTGGTAGTACTGGCGATCGAGCGGTACGTGGTGGTGTGCAAGCCCATG	430
E122Q	501	CTCTGGTAGTACTGGCGATCGAGCGGTACGTGGTGGTGTGCAAGCCCATG	550
Rho	431	AGCAACTTCCGCTTCGGTGAGAACCACGCCATCATGGGCGTCGCCTTCAC	480
E122Q	551	AGCAACTTCCGCTTCGGTGAGAACCACGCCATCATGGGCGTCGCCTTCAC	600
Rho	481	CTGGGTCATGGCTCTGGCCTGTGCGGCCCGCCGCTCGTCGGCTGGTCTA	530
E122Q	601	CTGGGTCATGGCTCTGGCCTGTGCGGCCCGCCGCTCGTCGGCTGGTCTA	650
Rho	531	GATACATCCCGAGGGCATGCAGTGCTCGTGCGGGATCGATTACTACACG	580
E122Q	651	GATACATCCCGAGGGCATGCAGTGCTCGTGCGGGATCGATTACTACACG	700
Rho	581	CCGCACGAGGAGACCAACAATGAGTCGTTTCGTCATCTACATGTTTCGTGGT	630
E122Q	701	CCGCACGAGGAGACCAACAATGAGTCGTTTCGTCATCTACATGTTTCGTGGT	750
Rho	631	CCACTTCATCATCCCGCTGATTGTCATCTTCTTCTGCTATGGCCAGCTGG	680

E122Q	751	CCACTTCATCATCCCGCTGATTGTCATCTTCTTCTGCTATGGCCAGCTGG	800
Rho	681	TGTTCCACCGTCAAGGAGGCTGCAGCCCAGCAGCAGGAGAGCGCCACCACT	730
E122Q	801	TGTTCCACCGTCAAGGAGGCTGCAGCCCAGCAGCA-GAGAGCGCCACCACT	849
Rho	731	CAGAAGGCCGAGAAGGAGGTCACGCGTATGGTTATCATCATGGTCATCGC	780
E122Q	850	CAGAAAGCCGAGAAGGAGGTCACGCGTATGGTTATCATCATGGTCATCGC	899
Rho	781	TTTCCTAATCTGCTGGCTGCCATATGCTGGTGTGGCGTTCTACATCTTCA	830
E122Q	900	TTTCCTAATCTGCTGGCTGCCATATGCTGGTGTGGCGTTCTACATCTTCA	949
Rho	831	CCCATCAGGGCTCTGACTTTGGGCCATCTTCATGACCATCCCGGCTTTC	880
E122Q	950	CCCATCA-GGCTCTGACTTTGGGCCATCTTCATGACCAT-CCGGCTTTC	997
Rho	881	TTTGCCAAGACGTCTGCCGTCTACAACCCGGTCATCTACATCATGATGAA	930
E122Q	998	TTTGCCAAGACGTCTGCCGTCTACGACCCGGTCATCTACATCATGATG-A	1046
Rho	931	CAAGCAGTTCGGAAGTGCATGGTCACCACTCTCTGCTGTGGCAAGAACC	980
E122Q	1047	CAAGCAGTTC--GGACTGCAT-GTCACCACTCTCTGCTGGTGCAGGA--C	1091
Rho	981	CGCTGGGTGACGACGAGGCGTCGACCACCGTCTC---CAAGACAGAGA--	1025
E122Q	1092	CGCTGGGTGACGACGA-GCGTCGAC--ACGTCTCAGACGAGACAGCGAGG	1138
Rho	1026	-CCAGC-----CAAGTGCGCCTGCCTA-----	1047
E122Q	1139	CCCTGCTAGCGCGCTCAAGGCGCAAGCCGATCGACTAACTTGTATTATGCA	1188
Rho	1048	-----	1047
E122Q	1189	CTAATGTCAATAGCCAGCTCCAATCGCAACTGAGACGTTTATCAAGACA	1238
Rho	1048	----- 1047	
E122Q	1239	ACTCGA 1244	

E122G N2C D282C

AAC to TGC (N2C), GAC to TGC (D282C) and GAA to GGC (E122G) changes all observed at the correct positions.

```

Rho      1 ----- 0
2_F1    1 AGCATTAGCAGAGCTCTCCCTATCAGTGATAGAGATCTCCCTATCAGTGA 50
Rho      1 ----- 0
2_F1    51 TAGAGATCGTCGACGAGCTCGTTTAGTGAACCGTCAGATCTCTAGAAGCT 100
Rho      1 -----ATGAACGGTACCGAAGGCCAAACTTCTACGTTTCCTTTC 39
          |||.|||
2_F1    101 GGAATTCACCATGTGCGGTACCGAAGGCCAAACTTCTACGTTTCCTTTC 150
Rho      40 TCCAACAAGACGGGCGTGGTGCAGCCCGTTCGAGGCTCCGCAGTACTA 89
          |||
2_F1    151 TCCAACAAGACGGGCGTGGTGCAGCCCGTTCGAGGCTCCGCAGTACTA 200
Rho      90 CCTGGCGGAGCCCTGGCAGTTCTCCATGCTGGCCGCCTACATGTTCCCTGC 139
          |||
2_F1    201 CCTGGCGGAGCCCTGGCAGTTCTCCATGCTGGCCGCCTACATGTTCCCTGC 250
Rho     140 TGATCATGCTTGGCTTCCCGATCAACTTCCTCACGCTGTACGTACAGTC 189
          |||
2_F1    251 TGATCATGCTTGGCTTCCCGATCAACTTCCTCACGCTGTACGTACAGTC 300
Rho     190 CAGCACAGAAGCTTCGCACACCGCTCAACTACATCCTGCTCAACCTGGC 239
          |||
2_F1    301 CAGCACAGAAGCTTCGCACACCGCTCAACTACATCCTGCTCAACCTGGC 350
Rho     240 CGTGGCAGATCTCTTCATGGTCTTCGGTGGCTTCACCACCACCCTCTACA 289
          |||
2_F1    351 CGTGGCAGATCTCTTCATGGTCTTCGGTGGCTTCACCACCACCCTCTACA 400
Rho     290 CCTCTCTCCATGGGTACTTCGTCTTTGGGCCGACGGGCTGCAACCTCGAG 339
          |||
2_F1    401 CCTCTCTCCATGGGTACTTCGTCTTTGGGCCGACGGGCTGCAACCTCGAG 450
Rho     340 GGCTTCTTTGCCACCCTGGGCGGTGAAATTGCACTGTGGTCTCTGGTAGT 389
          |||.|||
2_F1    451 GGCTTCTTTGCCACCCTGGGCGGTGGCATTGCACTGTGGTCTCTGGTAGT 500
Rho     390 ACTGGCGATCGAGCGGTACGTGGTGGTGTGCAAGCCCATGAGCAACTTCC 439
          |||
2_F1    501 ACTGGCGATCGAGCGGTACGTGGTGGTGTGCAAGCCCATGAGCAACTTCC 550
Rho     440 GCTTCGGTGAGAACCACGCCATCATGGGCGTCGCCTTCACCTGGGTTCATG 489
          |||
2_F1    551 GCTTCGGTGAGAACCACGCCATCATGGGCGTCGCCTTCACCTGGGTTCATG 600
Rho     490 GCTCTGGCCTGTGCGGCCCGCCGCTCGTCGGCTGGTCTAGATACATCCC 539
          |||
2_F1    601 GCTCTGGCCTGTGCGGCCCGCCGCTCGTCGGCTGGTCTAGATACATCCC 650
Rho     540 GGAGGGCATGCAGTGCTCGTGCGGGATCGATTACTACACGCCGCACGAGG 589

```

2_F1	651	 GGAGGGCATGCAGTGCCTCGTGC GGGATCGATTACTACACGCCGCACGAGG	700
Rho	590	AGACCAACAATGAGTCGTTTCGTCATCTACATGTTTCGTTGGTCCACTTCATC	639
2_F1	701	 AGACCAACAATGAGTCGTTTCGTCATCTACATGTTTCGTTGGTCCACTTCATC	750
Rho	640	ATCCCGCTGATTGTCATCTTCTTCTGCTATGGCCAGCTGGTGTTCACCGT	689
2_F1	751	 ATCCCGCTGATTGTCATCTTCTTCTGCTATGGCCAGCTGGTGTTCACCGT	800
Rho	690	CAAGGAGGCTGCAGCCCAGCAGCAGGAGAGCGCCACCACTCAGAAGGCCG	739
2_F1	801	 CAAGGAGGCTGCAGCCCAGCAGCAGGAGAGCGCCACCACTCAGAAGGCCG	850
Rho	740	AGAAGGAGGTCACGCGTATGGTTATCATCATGGTCATCGCTTTCCTAATC	789
2_F1	851	 AGAAGGAGGTCACGCGTATGGTTATCATCATGGTCATCGCTTTCCTAATC	900
Rho	790	TGCTGGCTGCCATATGCTGGTGTGGCGTTCTACATCTTCACCCATCAGGG	839
2_F1	901	 TGCTGGCTGCCATATGCTGGTGTGGCGTTCTACATCTTCA-CCATCAGGG	949
Rho	840	CTCTGAC TTTGGGCCATCTTCATGACCATCCCGGCTTCTTTGCCAAGA	889
2_F1	950	 CTCTTGC TTTGGG-CCATCTTCATGACCATCCCGGC-TTCTTTGCC-AGA	996
Rho	890	CGTCTGCCGTCTACAACCCGGTCATCTACATCATGATGAACAAGCAGTTC	939
2_F1	997	 CGT-----	999
Rho	940	CGGAACTGCATGGTCACCACTCTCTGCTGTGGCAAGAACCCGCTGGGTGA	989
2_F1	1000	-----	999
Rho	990	CGACGAGGCGTCGACCACCGTCTCCAAGACAGAGACCAGCCAAGTGGCGC	1039
2_F1	1000	-----	999
Rho	1040	CTGCCTAAGCGGCCGCAAATTCGGGGGGGGGGGGGGGGGGGG 1080	
2_F1	1000	----- 999	

E122Q N2C D282C

GAA to CAA change observed at the correct position. When aligned to a N2C D282C sequence both TGC codons can be seen for N2C and D282C.

RhoN2CD282C	1	-----CATGTGC GG	9
E122QN2CD282C	1	CGTTTAGTGAACCGTCAGATCTCTAGAAGCTGGGTACCCACCATGTGC GG	50
RhoN2CD282C	10	CACCGAAGGCCCAAACCTTCTACGTTCCCTTCTCCAACAAGACGGGCGTGG	59
E122QN2CD282C	51	CACCGAAGGCCCAAACCTTCTACGTTCCCTTCTCCAACAAGACGGGCGTGG	100
RhoN2CD282C	60	TGCGCAGCCCGTTTCGAGGCTCCGCAGTACTACCTGGCGGAGCCCTGGCAG	109
E122QN2CD282C	101	TGCGCAGCCCGTTTCGAGGCTCCGCAGTACTACCTGGCGGAGCCCTGGCAG	150
RhoN2CD282C	110	TTCTCCATGCTGGCCGCCTACATGTTCCCTGCTGATCATGCTTGGCTTCCC	159
E122QN2CD282C	151	TTCTCCATGCTGGCCGCCTACATGTTCCCTGCTGATCATGCTTGGCTTCCC	200
RhoN2CD282C	160	GATCAACTTCCTCACGCTGTACGTCACAGTCCAGCACAGAAGCTTCGCA	209
E122QN2CD282C	201	GATCAACTTCCTCACGCTGTACGTCACAGTCCAGCACAGAAGCTTCGCA	250
RhoN2CD282C	210	CACCGTCAACTACATCCTGCTCAACCTGGCCGTGGCAGATCTCTTCATG	259
E122QN2CD282C	251	CACCGTCAACTACATCCTGCTCAACCTGGCCGTGGCAGATCTCTTCATG	300
RhoN2CD282C	260	GTCTTCGGTGGCTTCACCACCACCTCTACACCTCTCTCCATGGGTACTT	309
E122QN2CD282C	301	GTCTTCGGTGGCTTCACCACCACCTCTACACCTCTCTCCATGGGTACTT	350
RhoN2CD282C	310	CGTCTTTGGGCCGACGGGCTGCAACCTCGAGGGCTTCTTTGCCACCCTGG	359
E122QN2CD282C	351	CGTCTTTGGGCCGACGGGCTGCAACCTCGAGGGCTTCTTTGCCACCCTGG	400
RhoN2CD282C	360	GCGGTGAAATTGCACTGTGGTCTCTGGTAGTACTGGCGATCGAGCGGTAC	409
E122QN2CD282C	401	GCGGTCAAATTGCACTGTGGTCTCTGGTAGTACTGGCGATCGAGCGGTAC	450
RhoN2CD282C	410	GTGGTGGTGTGCAAGCCCATGAGCAACTTCGGCTTCGGTGAGAACCACGC	459
E122QN2CD282C	451	GTGGTGGTGTGCAAGCCCATGAGCAACTTCGGCTTCGGTGAGAACCACGC	500
RhoN2CD282C	460	CATCATGGGCGTCGCCTTACCTGGGTCATGGCTCTGGCCTGTGCGGCC	509
E122QN2CD282C	501	CATCATGGGCGTCGCCTTACCTGGGTCATGGCTCTGGCCTGTGCGGCC	550
RhoN2CD282C	510	CGCCGCTCGTCGGCTGGTCTAGATACATCCCGGAGGGCATGCAGTGCTCG	559
E122QN2CD282C	551	CGCCGCTCGTCGGCTGGTCTAGATACATCCCGGAGAGCATGCAGTGCTCG	600
RhoN2CD282C	560	TGCGGGATCGATTACTACACGCCGCACGAGGAGACCAACAATGAGTCGTT	609
E122QN2CD282C	601	TGCGGGATCGATTACTACACGCCGCACGAGGAGACCAACAATGAGTCGTT	650
RhoN2CD282C	610	CGTCATCTACATGTTTCGTGGTCCACTTCATCATCCCGCTGATTGTCATCT	659
E122QN2CD282C	651	CGTCATCTACATGTTTCGTGGTCCACTTCATCATCCCGCTGATTGTCATCT	700
RhoN2CD282C	660	TCTTCTGCTATGGCCAGCTGGTGTTCACCGTCAAGGAGGCTGCAGCCAG	709
E122QN2CD282C	701	TCTTCTGCTATGGCCAGCTGGTGTTCACCGTCAAGGAGGCTGCAGCCAA	750

RhoN2CD282C	710	CAGCAGGAGAGCGCCACCACTCAGAAGGCCGAGAAGGAGGTCACGCGTAT	759
E122QN2CD282C	751	.	798
RhoN2CD282C	760	GGTTATCATCATGGTCATCGCTTTCCTAATCTGCTGGCTGCCATATGCTG	809
E122QN2CD282C	799	GGTTATCATCATGGTCATCGCTTTCCTAATCTGCTGGCTGCCATATGCTG	848
RhoN2CD282C	810	G-TGTGGCGTTCTACATCTTCACCCATCAGGGCT-CTTGC TTTGGGCC-	856
E122QN2CD282C	849	.	897
RhoN2CD282C	857	ATCTTCATGACCATCCC-GGCTTTCCTTGGCAAGACGCTGCCGTCTACA	905
E122QN2CD282C	898	947
RhoN2CD282C	906	ACCCGGTCATCTACATCATGATGAACAAGCAG-TTCCGGAAGTGCATGGT	954
E122QN2CD282C	948	. .	997
RhoN2CD282C	955	CACCACT-CTCTGCTGTGGCAAGAACCCGCTGGGTG--ACGACGAGG-CG	1000
E122QN2CD282C	998	1047
RhoN2CD282C	1001	TCGACCACCGTCTCCAAGACAG-AGACCAGCCAAGTGGCGCCTGCCTAAG	1049
E122QN2CD282C	1048	1097
RhoN2CD282C	1050	C-----	1050
E122QN2CD282C	1098	 CCGGCCGCCGAGCAGGCAAAGGCCGATTCCGACAGTTACGTTGTCTAAT	1147
RhoN2CD282C	1051	-----	1050
E122QN2CD282C	1148	GCAGCTTAAATGTTTCAAATAAGGCTAGCGCACTCCACACGATATCAGCG	1197
RhoN2CD282C	1051	----- 1050	
E122QN2CD282C	1198	CACGATTACCAGTACGATG 1216	

Appendix 4 Protein sequences/species used for the alignment of transmembrane helix 3.

Table 3. Protein sequences used in the transmembrane alignment of helix 3.

Sequence	Number of sequences						
	OPN1SW	OPN1W	OPN1LW	OPN2	OPN3	OPN4	OPN5
Acheilognathus melanogaster	-	-	-	3	-	-	-
Aesculapian false coral snake	1	-	1	1	-	-	-
African clawed frog	1	-	1	1	-	-	1
African elephant	1	-	-	1	2	1	2
African puff adder	1	-	1	1	-	-	-
Agassiz's desert tortoise	1	-	-	1	1	1	1
Alaska plaice	-	-	-	1	-	-	-
Alpaca	1	-	-	1	1	1	1
American alligator	-	-	1	1	1	2	1
American black bear	-	-	-	1	-	1	1
American bullfrog	-	-	-	1	-	-	-
American plaice	-	-	-	1	-	-	-
Amphisbaena alba	1	-	1	1	-	-	-
Amphisbaena sp. BFS-2-15	1	-	1	1	-	-	-
Annular seabream	-	-	-	1	-	-	-
Antillean ghost-faced bat	-	-	1	1	-	-	-
Aquila chrysaetos chrysaetos	2	-	-	1	1	3	2
Arctic flounder	-	-	-	1	-	-	-
Arrowtooth flounder	-	-	-	2	-	-	-
Arulius barb	-	-	-	1	-	-	-
Aruma histrio	-	-	-	1	-	-	-
Asian grass lizard	1	-	1	1	-	-	-
Atlantic bottle-nosed dolphin	1	-	1	1	1	2	1
Atlantic halibut	-	-	-	1	-	-	-
Atlantic salmon	-	-	-	1	-	1	-
Atractus badius	1	-	1	1	-	-	-
Atractus flammigerus	1	-	1	1	-	-	-
Atractus reticulatus	1	-	1	1	-	-	-
Austrofundulus limnaeus	2	-	-	1	1	-	1
Azemiops kharini	1	-	1	1	-	-	-
Bachia flavescens	1	-	1	1	-	-	-
Baikal sculpin	-	-	-	1	-	-	-

Sequence	Number of sequences						
	OPN1SW	OPN1W	OPN1LW	OPN2	OPN3	OPN4	OPN5
Baikal yellowfin	-	-	-	1	-	-	-
Baikalian deep-water sculpin	-	-	-	1	-	-	-
Ball python	-	-	-	1	-	-	-
banded cat-eyed snake	1	-	1	1	-	-	-
Barba amarilla	1	-	1	1	-	-	-
Barbodes aff. banksi BOLD:AAU3665	-	-	-	1	-	-	-
Bare-tailed woolly opossum	-	-	-	1	-	-	-
Barfin flounder	-	-	-	1	-	-	-
Barramundi	-	-	-	1	1	3	-
Barred danio	-	-	-	1	-	-	-
beaked dace	-	-	-	1	-	-	-
beauty snake	1	-	1	1	-	-	-
Beira killifish	-	-	-	1	-	-	-
Beluga whale	1	-	1	1	1	2	1
Bengalese finch	-	-	-	1	1	-	-
Berthold's worm lizard	1	-	1	1	-	-	-
bigmouth buffalo	-	-	-	1	-	-	-
Big-scale sand smelt	-	-	-	1	-	-	-
Bigscale soldierfish	-	-	-	1	-	-	-
bigspot barb	-	-	-	1	-	-	-
Black goby	-	-	-	1	-	-	-
Black myotis	1	-	1	1	-	-	-
black redhorse	-	-	-	1	-	-	-
black rockcod	-	-	-	1	-	1	-
black ruby barb	-	-	-	1	-	-	-
Black snub-nosed monkey	1	-	-	1	1	2	1
Black-bearded tomb bat	-	-	-	1	-	-	-
blackfin flounder	-	-	-	1	-	-	-
Blackmouth catshark	-	-	-	1	-	-	-
blackspot barb	-	-	-	1	-	-	-
blackstripe livebearer	-	-	-	1	-	-	-
blackstripe rasbora	-	-	-	1	-	-	-
Blind cave fish	1	-	1	1	-	-	-
Blood fluke	-	-	-	1	-	1	-
Blue lined squirrelfish	-	-	-	1	-	-	-
blue-crowned manakin	-	-	-	1	1	1	1
bluefin notho	-	-	-	1	-	-	-
Bogota fruit-eating bat	1	-	1	1	-	-	-
Boiga forsteni	-	-	1	1	-	-	-
Bolivian squirrel monkey	1	-	-	1	-	2	2

Sequence	Number of sequences						
	OPN1SW	OPN1W	OPN1LW	OPN2	OPN3	OPN4	OPN5
Bombay earth snake	1	-	1	1	-	-	-
Bovine	1	-	1	1	-	1	1
Brazilian free-tailed bat	2	-	1	1	-	-	-
Brevibora cf. cheeya BOLD:AAW7115	-	-	-	1	-	-	-
brilliant rasbora	-	-	-	1	-	-	-
Brongersma's worm snake	-	-	-	1	-	-	-
Brown greater galago	-	-	-	1	-	-	-
Brown-capped capuchin	2	-	-	1	1	2	1
buff striped keelback	1	-	1	1	-	-	-
Burrowing owl	-	-	-	1	-	1	1
butter sole	-	-	-	1	-	-	-
Cajun dwarf crayfish	-	-	-	1	-	-	-
California flounder	-	-	-	1	-	-	-
California kingsnake	1	-	1	1	-	-	-
California sealion	1	-	-	1	5	2	1
Canada lynx	1	-	-	1	1	1	1
Cane toad	-	-	-	1	-	-	-
Cape dune mole rat	-	-	-	1	-	-	-
Cape golden mole	1	-	-	1	-	1	1
Captains wood snake	1	-	1	1	-	-	-
Caribbean manatee	-	-	-	1	-	-	-
Carpet viper	1	-	1	1	-	-	-
Cat	1	-	1	1	1	1	2
Cebus capucinus imitator	1	-	-	1	1	2	2
celestial pearl danio	-	-	-	1	-	-	-
central bearded dragon	1	-	-	1	1	1	-
Ceylonese tree viper	1	-	1	1	-	-	-
chalak barb	-	-	-	1	-	-	-
Channel catfish	-	-	-	1	1	1	-
channel darter	-	-	-	2	-	-	-
checkered barb	-	-	-	1	-	-	-
Checkered keelback	1	-	1	1	-	-	-
Cheetah	1	-	-	1	1	1	1
cherry barb	-	-	-	1	-	-	-
Chestnut long-tongued bat	-	-	1	1	-	-	-
Chicken	1	1	1	1	1	1	1
Chimpanzee	1	-	1	1	1	3	2
Chinese alligator	-	-	1	1	-	1	1
Chinese barb	-	-	-	1	-	-	-
Chinese hamster	-	1	-	1	-	-	-

Sequence	Number of sequences						
	OPN1SW	OPN1W	OPN1LW	OPN2	OPN3	OPN4	OPN5
Chinese liver fluke	-	-	-	3	-	-	-
Chinese softshell turtle	-	-	-	1	-	1	1
Chironius bicarinatus	1	-	1	1	-	-	-
Chironius fuscus	1	-	1	1	-	-	-
Chondrostoma nasus	-	-	-	1	-	-	-
Chrysopelea ornata	1	-	1	1	-	-	-
Chub	-	-	-	3	-	-	-
Clariidae sp. BMNH 2--8.9.17.1-2	-	-	-	1	-	-	-
Clearfin squirrelfish	-	-	-	1	-	-	-
Cloudy snail-eating snake	1	-	1	1	-	-	-
C-O sole	-	-	-	1	-	-	-
coastrange sculpin	-	-	-	2	-	-	-
Coelacanth	-	-	-	1	-	1	1
Collared blind snake	-	-	-	1	-	-	-
Collared flycatcher	1	-	-	1	1	1	1
Comephorus dybowskii	-	-	-	1	-	-	-
Commerson's glassy perchlet	-	-	-	1	-	-	-
Common carp	-	-	-	1	-	-	-
Common cuttlefish	-	-	-	1	-	-	-
Common dab	-	-	-	1	-	-	-
common dace	-	-	-	1	-	-	-
Common European adder	1	-	1	1	-	-	-
Common pheasant	-	-	-	1	1	1	1
Common sole	-	-	-	1	-	-	-
Common two-banded seabream	-	-	-	1	-	-	-
Common wombat	1	-	-	1	-	1	2
Copperhead	1	-	1	1	-	-	-
Coquerel's sifaka	1	-	-	1	1	1	2
Corn snake	1	-	1	1	-	-	-
Cortez flounder	-	-	-	1	-	-	-
Crab-eating macaque	-	-	-	1	1	2	2
Crayfish	-	-	-	2	-	-	-
cresthead flounder	-	-	-	1	-	-	-
crossed-fork back golden-line fish	-	-	-	1	-	-	-
Crown squirrelfish	-	-	-	1	-	-	-
Cuban fig-eating bat	2	-	1	1	-	-	-
Cuban funnel-eared bat	-	-	1	1	-	-	-
curlfin sole	-	-	-	1	-	-	-
dadio	-	-	-	1	-	-	-
Damaraland mole rat	-	-	-	1	-	-	-

Sequence	Number of sequences						
	OPN1SW	OPN1W	OPN1LW	OPN2	OPN3	OPN4	OPN5
Danio aesculapii	-	-	-	1	-	-	-
Danio aff. choprai BOLD:AAU2157	-	-	-	1	-	-	-
Danio aff. dangila BOLD:AAU2158	-	-	-	1	-	-	-
Danio aff. dangila BOLD:AAU2159	-	-	-	1	-	-	-
Danio aff. kyathit BOLD:AAJ4326	-	-	-	1	-	-	-
Danio cf. dangila BOLD:AAV9219	-	-	-	1	-	-	-
Danio cf. kerri BOLD:AAU2162	-	-	-	1	-	-	-
Danio cf. rerio RCYY5-1-11	-	-	-	1	-	-	-
Danio choprai	-	-	-	2	-	-	-
Danio kyathit	-	-	-	1	-	-	-
Danio meghalayensis	-	-	-	1	-	-	-
Danio rerio x Danio aff. kyathit RC-455	-	-	-	1	-	-	-
Danio roseus	-	-	-	1	-	-	-
Dasypeltis scabra	1	-	1	1	-	-	-
Dawkinsia tambraparniei	-	-	-	1	-	-	-
Day's glassy perchlet	-	-	-	1	-	-	-
Denison barb	-	-	-	2	-	-	-
Desmopuntius cf. hexazona BOLD:AAU3668	-	-	-	1	-	-	-
Desmopuntius pentazona	-	-	-	1	-	-	-
Desmopuntius rhomboocellatus	-	-	-	1	-	-	-
Devario cf. acuticephala BOLD:AAV9172	-	-	-	1	-	-	-
Devario cf. browni BOLD:AAU-873	-	-	-	2	-	-	-
Devario cf. chrysotaeniatus BOLD:AAU3723	-	-	-	1	-	-	-
Devario cf. devario BOLD:AAU2862	-	-	-	1	-	-	-
Devario sondhii	-	-	-	1	-	-	-
Devario sp. 'purple cypris'	-	-	-	1	-	-	-
Devario sp. undet1RAC	-	-	-	1	-	-	-
Devario sp. undet2RAC	-	-	-	1	-	-	-
Dianchi golden-line fish	1	-	-	1	-	-	-
Dipsas catesbyi	1	-	1	1	-	-	-
Dipsas indica	1	-	1	1	-	-	-
Dipsas indica petersi	1	-	1	1	-	-	-
Dipsas mikanii	1	-	1	1	-	-	-
Dipsas neuwiedi	1	-	1	1	-	-	-
Dog	1	-	1	1	1	1	1
Dover sole	-	-	-	1	-	-	-
Drill	1	-	-	1	-	2	2
Duckbill platypus	-	-	1	1	-	-	1
dusky sole	-	-	-	1	-	-	-
dwarf danio	-	-	-	2	-	-	-

Sequence	Number of sequences						
	OPN1SW	OPN1W	OPN1LW	OPN2	OPN3	OPN4	OPN5
Dwarf little fruit bat	1	-	1	1	-	-	-
Eastern brown snake	1	-	1	1	3	-	1
Eastern buffy flower bat	-	-	1	1	-	-	-
Eastern tiger salamander	-	-	-	1	-	-	-
Echinanthera cephalostriata	1	-	1	1	-	-	-
Echinanthera undulata	1	-	1	1	-	-	-
Elacatinus atronasus	-	-	-	1	-	-	-
Elacatinus digueti	-	-	-	1	-	-	-
Elacatinus figaro	-	-	-	1	-	-	-
Elacatinus genie	-	-	-	1	-	-	-
Elacatinus horsti	-	-	-	5	-	-	-
Elacatinus illecebrosus	-	-	-	1	-	-	-
Elacatinus louisae	-	-	-	1	-	-	-
Elacatinus prochilos	-	-	-	2	-	-	-
Elacatinus puncticulatus	-	-	-	3	-	-	-
Elacatinus randalli	-	-	-	1	-	-	-
Elacatinus xanthiprora	-	-	-	1	-	-	-
Electric eel	-	-	-	1	2	-	1
Elegant rasbora	-	-	-	1	-	-	-
elongate glass-perchlet	-	-	-	1	-	-	-
Embassichthys bathybius	-	-	-	1	-	-	-
English sole	-	-	-	1	-	-	-
Enhydris innominata	1	-	1	1	-	-	-
Eurasian minnow	-	-	-	1	-	-	-
European cat snake	1	-	1	1	-	-	-
European catfish	-	-	-	1	-	-	-
European common frog	-	-	-	1	-	-	-
European domestic ferret	1	-	-	1	-	1	1
European flounder	-	-	-	1	-	-	-
European pilchard	-	-	-	1	-	-	-
European plaice	-	-	-	1	-	-	-
European seabass	-	-	-	1	-	-	-
European toad	-	-	-	1	-	-	-
Eyesh palm pitviper	1	-	1	1	-	-	-
eyeless golden-line fish	-	-	-	2	-	-	-
eyespot rasbora	-	-	-	2	-	-	-
False coral snake	1	-	1	1	-	-	-
Far Eastern smooth flounder	-	-	-	1	-	-	-
Fat sculpin	-	-	-	1	-	-	-
Fat-tailed dunnart	-	-	-	1	-	1	-

Sequence	Number of sequences						
	OPN1SW	OPN1W	OPN1LW	OPN2	OPN3	OPN4	OPN5
Feylinia sp. BFS-2-15	1	-	1	1	-	-	-
Fischer's little fruit bat	1	-	1	1	-	-	-
flat wolf snake	1	-	1	1	-	-	-
Flat-faced fruit-eating bat	1	-	1	1	-	-	-
flathead flounder	-	-	-	1	-	-	-
Flathead mullet	-	-	-	1	-	-	-
flathead sole	-	-	-	3	-	-	-
Florida carpenter ant	-	-	-	1	-	-	-
Florida kingsnake	1	-	1	1	-	-	-
Forest marsh snake	1	-	1	1	-	-	-
Fraternal fruit-eating bat	1	-	1	1	-	-	-
Freckled crayfish	-	-	-	1	-	-	-
Frogmouth	1	-	-	1	1	-	-
Fruit eating bat	-	-	1	1	-	-	-
Geoffroy's tailless bat	1	-	1	1	-	-	-
Ghost shark	-	-	-	1	1	2	2
ghost shiner	-	-	-	2	-	-	-
Giant danio	-	-	-	1	-	-	-
Giant panda	1	-	-	1	1	1	1
Gilthead sea bream	1	-	-	1	1	-	2
Ginsburgellus novemlineatus	-	-	-	1	-	-	-
giraffe devario	-	-	-	2	-	-	-
Glossy snake	1	-	1	1	-	-	-
Goat	1	-	1	1	-	3	1
gold ring danio	-	-	-	1	-	-	-
golden barb	-	-	-	2	-	-	-
Golden grey mullet	-	-	-	1	-	-	-
Golden hamster	-	1	-	3	1	2	-
Golden snub-nosed monkey	1	-	-	1	-	2	1
Goldfish	1	-	1	1	-	-	-
Gonionotophis sp	1	-	1	1	-	-	-
gopher snake	1	-	1	1	-	-	-
Grass carp	-	-	-	2	-	-	-
Grass goby	-	-	-	1	-	-	-
Gray short-tailed opossum	1	-	2	1	1	2	2
Great stripe-faced bat	1	-	1	1	-	-	-
Greater Antillean long-tongued bat	-	-	1	1	-	-	-
Greater bulldog bat	-	-	1	1	-	-	-
Greater cane rat	-	-	-	1	-	-	-
Greater horseshoe bat	-	-	-	2	1	1	2

Sequence	Number of sequences						
	OPN1SW	OPN1W	OPN1LW	OPN2	OPN3	OPN4	OPN5
Greater spear-nosed bat	2	-	1	1	-	-	-
Greater white-lined bat	2	-	1	1	-	-	-
Green anole	1	-	1	1	1	1	1
Green monkey	1	-	-	1	1	1	1
Greenish naked-backed fruit bat	-	-	-	1	-	-	-
Greenland flounder	-	-	-	1	-	-	-
greenstripe barb	-	-	-	1	-	-	-
Guinea pig	1	1	-	1	1	2	1
Guppy	-	-	-	1	-	-	-
Hairy big-eyed bat	1	-	1	1	-	-	-
Harbor seal	-	-	-	1	-	-	-
Harlequin rasbora	-	-	-	1	-	-	-
Harp seal	-	-	-	1	-	-	-
Hasarius adansoni	-	-	-	1	-	-	-
Hawaiian monk seal	1	-	-	1	1	3	1
Hawaiian squirrelfish	-	-	-	1	-	-	-
Heterodon nasicus	1	-	1	1	-	-	-
highfin glassy perchlet	-	-	-	2	-	-	-
Highland yellow-shouldered bat	-	-	1	1	-	-	-
Hikari danio	-	-	-	1	-	-	-
Hipposideros larvatus	-	-	-	1	-	-	-
Honeybee	1	-	-	1	-	-	-
honeycomb toby	-	-	-	2	-	-	-
Horned desert viper	1	-	1	1	-	-	-
hornyhead turbot	-	-	-	1	-	-	-
Horse	1	-	1	1	1	1	1
Horseshoe whip snake	1	-	1	1	-	-	-
huchen	1	-	-	1	-	2	-
Human	1	1	1	1	1	1	1
Hybrid cattle	2	-	1	1	-	2	1
Hypsiglena jani	1	-	1	1	-	-	-
Hypsopsetta guttulata	-	-	-	1	-	-	-
Iconisemion striatum	-	-	-	2	-	-	-
ide	-	-	-	1	-	-	-
Imantodes lentiferus	1	-	1	1	-	-	-
Indian glass barb	-	-	-	1	-	-	-
Indian glassy fish	-	-	-	1	-	-	-
Indian wolf snake	1	-	1	1	-	-	-
Indoreonectes cf. evezardi ND-2-17	-	-	-	5	-	-	-
Indoreonectes evezardi	-	-	-	1	-	-	-

Sequence	Number of sequences						
	OPN1SW	OPN1W	OPN1LW	OPN2	OPN3	OPN4	OPN5
Inlecypriis auropurpleus	-	-	-	1	-	-	-
Jamaican fruit-eating bat	4	-	1	2	-	-	-
Japanese flying squid	-	-	-	1	-	-	-
Japanese lamprey	-	-	-	1	-	-	-
Japanese long-fingered bat	-	-	-	1	-	-	-
Japanese pufferfish	-	-	-	1	1	-	2
Japanese rat snake	1	-	1	1	-	-	-
Japanese rice fish	1	1	1	1	2	-	-
Jararaca	1	-	1	1	-	-	-
Javaen barb	-	-	-	1	-	-	-
Javan wart snake	1	-	1	1	-	-	-
Jerdon's carp	-	-	-	1	-	-	-
Jewelled blenny	1	-	-	1	1	1	-
John Dory	-	-	-	1	-	-	-
Kakapo	1	-	-	1	1	2	2
Kamchatka flounder	-	-	-	1	-	-	-
Kessler's sculpin	-	-	-	1	-	-	-
Khavli barb	-	-	-	1	-	-	-
King cobra	-	-	-	1	-	1	2
Lattice soldierfish	-	-	-	1	-	-	-
Leaping mullet	-	-	-	1	-	-	-
Least horseshoe bat	-	-	-	1	-	-	-
lemon sole	-	-	-	1	-	-	-
Lerma livebearer	-	-	-	12	-	-	-
Leschenault's rousette	-	-	-	1	-	-	-
Lesser dawn bat	-	-	-	1	-	-	-
Lesser false vampire bat	-	-	-	1	-	-	-
Lesser sac-winged bat	1	-	1	1	-	-	-
Lesser short-nosed fruit bat	-	-	-	1	-	-	-
Lesser spear-nosed bat	1	-	1	1	-	-	-
Limnocottus bergianus	-	-	-	1	-	-	-
Limnocottus pallidus	-	-	-	1	-	-	-
Linesnout goby	-	-	-	2	-	-	-
Liopsetta putnami	-	-	-	1	-	-	-
Liotyphlops beui	-	-	-	1	-	-	-
Little brown bat	1	-	-	1	-	1	1
Little skate	-	-	-	1	-	-	-
littlemouth flounder	-	-	-	2	-	-	-
Live sharksucker	-	-	-	1	1	-	-
logperch	-	-	-	1	-	-	-

Sequence	Number of sequences						
	OPN1SW	OPN1W	OPN1LW	OPN2	OPN3	OPN4	OPN5
Longfin Baikal sculpin	-	-	-	1	-	-	-
Long-finned pilot whale	-	-	-	1	-	-	-
longhead dab	-	-	-	1	-	-	-
Long-nosed tree snake	1	-	1	1	-	-	-
Long-spined sea scorpion	-	-	-	1	-	-	-
MacConnell's bat	1	-	1	1	-	-	-
Machete savane snake	1	-	1	1	-	-	-
Mahecola barb	-	-	-	2	-	-	-
mainland tiger snake	1	-	1	2	1	1	1
Malabar danio	-	-	-	1	-	-	-
Malabar glassy perchlet	-	-	-	1	-	-	-
Mantis	-	-	-	1	-	-	-
marbled flounder	-	-	-	2	-	-	-
Ma's night monkey	1	-	-	1	1	-	2
Medium ground-finch	1	-	-	1	-	-	1
Meerkat	1	-	-	1	2	1	1
Melanophidium khairi	-	-	-	1	-	-	-
Melanoseps occidentalis	1	-	1	1	-	-	-
Melon barb	-	-	-	2	-	-	-
Miami cave crayfish	-	-	-	1	-	-	-
Microdevario kubotai	-	-	-	2	-	-	-
Microdevario nana	-	-	-	1	-	-	-
Microrasbora cf. rubescens BOLD:AAU1781	-	-	-	1	-	-	-
Microrasbora erythromicron	-	-	-	1	-	-	-
Microrasbora rubescens	-	-	-	2	-	-	-
Microstomus shuntovi	-	-	-	1	-	-	-
Milkfish	-	-	-	1	1	-	1
Moller's lantern shark	-	-	-	1	-	-	-
Monocled cobra	1	-	1	1	-	-	-
Mouse	1	1	-	1	1	1	1
Moustached danio	-	-	-	1	-	-	-
Naked goby	-	-	-	1	-	-	-
Naked mole rat	-	-	-	1	-	-	-
neon goby	-	-	-	3	-	-	-
Nile tilapia	1	-	-	1	1	-	-
North Pacific giant octopus	-	-	-	1	-	-	-
North Pacific minke whale	1	-	1	1	1	1	1
Northern fur seal	-	-	-	1	1	2	1
Northern leopard frog	-	-	-	1	-	-	-
Northern mallard	-	-	-	1	-	-	3

Sequence	Number of sequences						
	OPN1SW	OPN1W	OPN1LW	OPN2	OPN3	OPN4	OPN5
Northern pike	-	-	-	2	-	-	-
northern rock sole	-	-	-	2	-	-	-
Northern white-cheeked gibbon	1	1	-	1	-	2	2
Nothobranchius kadleci	-	-	-	1	-	-	-
Nothobranchius pienaari	-	-	-	1	-	-	-
Ocellated saw-scaled viper	1	-	1	1	-	-	-
Odocoileus virginianus texanus	1	-	-	1	-	2	1
Olive baboon	1	-	1	1	1	2	2
Olive house snake	1	-	1	1	-	-	-
Olive keelback	1	-	1	1	-	-	-
Opheodrys aestivus	1	-	1	1	-	-	-
Ophiodes striatus	1	-	1	1	-	-	-
orbiculate cardinalfish	-	-	-	1	1	1	-
Ord's kangaroo rat	1	-	-	1	1	1	1
Oxyrhopus melanogenys	1	-	1	1	-	-	-
Pacific halibut	-	-	-	1	-	-	-
Pacific sand sole	-	-	-	1	-	-	-
Pacific walrus	1	-	1	1	1	1	1
Paedocypris cf. carbunculus BOLD:AAV-81-	-	-	-	1	-	-	-
Painted devil crayfish	-	-	-	1	-	-	-
pale rasbora	-	-	-	1	-	-	-
pale spear-nosed bat	2	-	-	1	1	1	1
Pallas' long-tongued bat	2	-	1	1	-	-	-
Pallas' mastiff bat	1	-	1	1	-	-	-
Pallas' tube nosed bat	-	-	-	1	-	-	-
Pareas monticola	-	-	-	1	-	-	-
Patagioenas fasciata monilis	-	-	-	1	1	1	-
Peacock blenny	-	-	-	1	-	-	-
pearl danio	-	-	-	1	-	-	-
Peters' Angolan colobus	1	-	-	1	1	2	2
Pethia aff. gelius BOLD:AAU2--7	-	-	-	1	-	-	-
Pethia erythromycter	-	-	-	1	-	-	-
Pethia manipurensis	-	-	-	1	-	-	-
Pethia padamyia	-	-	-	1	-	-	-
Pethia shalynius	-	-	-	1	-	-	-
Pethia stoliczkana	-	-	-	1	-	-	-
Pethia tiantian	-	-	-	1	-	-	-
Petrale sole	-	-	-	1	-	-	-
Philippine tarsier	3	-	1	1	-	2	1
Phoxinus csikii	-	-	-	1	-	-	-

Sequence	Number of sequences						
	OPN1SW	OPN1W	OPN1LW	OPN2	OPN3	OPN4	OPN5
Phoxinus karsticus	-	-	-	1	-	-	-
Phoxinus lumaireul	-	-	-	1	-	-	-
Phoxinus marsilii	-	-	-	1	-	-	-
Phoxinus septimaniae	-	-	-	1	-	-	-
Phoxinus sp. 1 AP-2-17	-	-	-	1	-	-	-
Phoxinus sp. 2 AP-2-17	-	-	-	1	-	-	-
Phoxinus sp. 3 AP-2-17	-	-	-	1	-	-	-
Phoxinus sp. 6 AP-2-17	-	-	-	1	-	-	-
Phoxinus sp. CER12	-	-	-	1	-	-	-
Phoxinus sp. CER4	-	-	-	1	-	-	-
Phoxinus sp. CH9	-	-	-	1	-	-	-
Phoxinus sp. GRS1	-	-	-	1	-	-	-
Phoxinus sp. GRS5	-	-	-	1	-	-	-
Phoxinus sp. KOL4	-	-	-	1	-	-	-
Phoxinus sp. LOZ5	-	-	-	1	-	-	-
Phoxinus sp. LUN2	-	-	-	1	-	-	-
Phoxinus sp. LUN4	-	-	-	1	-	-	-
Phoxinus sp. MRE1	-	-	-	1	-	-	-
Phoxinus sp. PTU5	-	-	-	1	-	-	-
Phoxinus sp. RAD5	-	-	-	1	-	-	-
Phoxinus sp. RAD6	-	-	-	1	-	-	-
Phoxinus sp. RAT5	-	-	-	1	-	-	-
Phoxinus sp. SCA3	-	-	-	1	-	-	-
Phoxinus sp. SCA4	-	-	-	1	-	-	-
Phoxinus sp. SVR2	-	-	-	1	-	-	-
Phoxinus sp. VAL11	-	-	-	1	-	-	-
Phoxinus sp. ZRM1	-	-	-	1	-	-	-
Phoxinus sp. ZRM4	-	-	-	1	-	-	-
Phyllonycteris poeyi	-	-	1	1	-	-	-
Pig	2	-	-	1	-	2	3
Pig-tailed macaque	1	-	-	1	1	3	2
Pimelodidae sp. RC-374	-	-	-	1	-	-	-
pinecone soldierfish	1	-	-	2	1	2	-
Pleuronichthys lighti	-	-	-	1	-	-	-
Polar bear	3	-	-	1	-	2	2
Polemon collaris	1	-	1	1	-	-	-
Prairie deer mouse	-	-	1	1	1	1	1
Pratt's roundleaf bat	-	-	-	1	-	-	-
Pseudoboa coronata	1	-	1	1	-	-	-
Pseudopleuronectes obscurus	-	-	-	1	-	-	-

Sequence	Number of sequences						
	OPN1SW	OPN1W	OPN1LW	OPN2	OPN3	OPN4	OPN5
Pteronotus pusillus	4	-	2	1	-	-	-
puffing snake	1	-	1	1	-	-	-
Puntius cf. sophore BOLD:AAV2874	-	-	-	1	-	-	-
Puntius sp. hybrid BOLD:AAU2-29	-	-	-	1	-	-	-
Pygmy chimpanzee	1	-	-	1	2	2	1
Rabbit	1	1	1	1	1	1	2
Rasbora aprotaenia	-	-	-	1	-	-	-
Rasbora tornieri	-	-	-	1	-	-	-
Rat	1	1	-	1	1	1	1
Red fox	1	-	-	1	1	1	1
Red pipe snake	-	-	-	1	-	-	-
Red sculpin	-	-	-	1	-	-	-
Red shiner	-	-	-	2	-	-	-
Red swamp crayfish	-	-	-	1	-	-	-
redside shiner	-	-	-	1	-	-	-
red-stripped rasbora	-	-	-	1	-	-	-
Rex sole	-	-	-	1	-	-	-
Rhesus macaque	1	-	1	1	2	1	1
Rhinoceros adder	1	-	1	1	-	-	-
Rhombic night adder	1	-	-	1	-	-	-
Rickett's big-footed bat	1	-	-	1	-	-	-
Ridged-eye flounder	-	-	-	1	-	-	-
Rikuzen flounder	-	-	-	2	-	-	-
Ringless green snake	-	-	1	1	-	-	-
river darter	-	-	-	1	-	-	-
Roach	-	-	-	1	-	1	-
rock sole	-	-	-	1	-	-	-
Rope fish	-	-	-	1	-	-	-
Rosy barb	-	-	-	2	-	-	-
roughscale sole	-	-	-	1	-	-	-
Rough-scaled sand boa	1	-	1	1	-	-	-
royal ground snake	1	-	1	1	-	-	-
Sabre squirrelfish	-	-	-	1	-	-	-
Saharan silver ant	-	-	-	1	-	-	-
Sakhalin sole	-	-	-	1	-	-	-
Salem cave crayfish	-	-	-	1	-	-	-
Salema	-	-	-	1	-	-	-
sand flounder	-	-	-	2	-	-	-
Sand goby	-	-	-	1	-	-	-
scale-eye plaice	-	-	-	1	-	-	-

Sequence	Number of sequences						
	OPN1SW	OPN1W	OPN1LW	OPN2	OPN3	OPN4	OPN5
Sea lamprey	-	-	-	1	-	-	-
Seba's short-tailed bat	2	-	1	1	-	-	-
Senegal bichir	-	-	-	1	-	-	-
Sharknose goby	-	-	-	1	-	-	-
Sheep	1	-	1	1	-	-	1
Short-beaked common dolphin	-	-	-	1	-	-	-
Short-eared elephant shrew	-	-	-	1	-	-	-
Short-headed sculpin	-	-	-	1	-	-	-
shortstripe goby	-	-	-	2	-	-	-
shotted halibut	-	-	-	1	-	-	-
Siberian sturgeon	-	-	-	1	-	-	-
Silky short-tailed bat	1	-	1	1	-	-	-
Silver carp	-	-	-	4	-	-	-
silver chub	-	-	-	2	-	-	-
silver rasbora	-	-	-	2	-	-	-
Silvery mole rat	-	-	-	1	-	-	-
Sinocyclocheilus angularis	-	-	-	2	-	-	-
Sinocyclocheilus angustiporus	-	-	-	2	-	-	-
Sinocyclocheilus anshuiensis	2	-	-	1	-	-	-
Sinocyclocheilus lateristriatus	-	-	-	1	-	-	-
Sinocyclocheilus qiubeiensis	-	-	-	1	-	-	-
Sinocyclocheilus tileihornes	-	-	-	2	-	-	-
slender sole	-	-	-	1	-	-	-
slime flounder	-	-	-	4	-	-	-
small eye golden-line fish	-	-	-	2	-	-	-
Small-eared galago	-	-	-	1	1	1	1
Smallmouth squirrelfish	-	-	-	1	-	-	-
Small-spotted catshark	-	-	-	1	-	-	-
sohachi	-	-	-	1	-	-	-
Sonora goby	-	-	-	1	-	-	-
Sooty mangabey	1	-	-	1	1	2	2
Sooty mustached bat	2	-	1	1	-	-	-
South American water snake	2	-	2	2	-	-	-
Southern cave crayfish	-	-	-	1	-	-	-
Sowerby's beaked whale	-	-	-	1	-	-	-
Spalerosophis diadema	1	-	1	1	-	-	-
speckled dace	-	-	-	1	-	-	-
speckled flounder	-	-	-	1	-	-	-
Speckled squirrelfish	-	-	-	1	-	-	-
Sperm whale	1	-	-	1	-	2	1

Sequence	Number of sequences						
	OPN1SW	OPN1W	OPN1LW	OPN2	OPN3	OPN4	OPN5
spinner barb	-	-	-	2	-	-	-
Spiny-headed seasnake	1	-	1	1	-	-	-
spiralin	-	-	-	1	-	-	-
Spotfin squirrelfish	-	-	-	1	-	-	-
Spotted flounder	-	-	-	1	-	-	-
Spotted green pufferfish	-	-	-	1	-	-	-
Spotted hyena	1	-	-	1	-	-	-
spotted sharpnosed puffer	-	-	-	2	-	-	-
spotted turbot	-	-	-	1	-	-	-
Squalius laietanus	-	-	-	3	-	-	-
Squalius sp. BOLD:AAD8346	-	-	-	1	-	-	-
Squalius sp. BOLD:AAE3493	-	-	-	1	-	-	-
Squid	-	-	-	1	-	-	-
Starry flounder	-	-	-	2	-	-	-
Stone flounder	-	-	-	1	-	-	-
Stone sculpin	-	-	-	1	-	-	-
striped barb	-	-	-	1	-	-	-
Striped bass	-	-	-	2	-	-	-
striped flying barb	-	-	-	1	-	-	-
Striped hairy-nosed bat	1	-	1	1	-	-	-
Striped red mullet	-	-	-	1	-	-	-
Striped seabream	-	-	-	1	-	-	-
striped shiner	-	-	-	1	-	-	-
stripe-headed round-eared bat	1	-	1	1	-	-	-
Sumatra barb	-	-	-	1	-	-	-
Sumatran orangutan	1	-	-	1	1	1	1
Sunbeam snake	-	-	-	1	-	-	-
Sundadanio axelrodi 'green'	-	-	-	1	-	-	-
Sundadanio cf. axelrodi BOLD:AAH9912	-	-	-	1	-	-	-
Sundadanio cf. axelrodi BOLD:AAU2681	-	-	-	1	-	-	-
Systemus cf. sarana RCYY-56-11	-	-	-	1	-	-	-
Systemus foerschi	-	-	-	1	-	-	-
Taeniophallus persimilis	1	-	1	1	-	-	-
Tanaka's snailfish	-	-	-	1	-	-	-
Tasmanian devil	1	-	-	1	1	1	1
Tent-making bat	1	-	1	1	-	-	-
Thamnodynastes hypoconia	1	-	1	1	-	-	-
Thamnodynastes pallidus	1	-	1	1	-	-	-
Thamnophis sirtalis	1	-	1	2	-	-	-
Thicklip grey mullet	-	-	-	1	-	-	-

Sequence	Number of sequences						
	OPN1SW	OPN1W	OPN1LW	OPN2	OPN3	OPN4	OPN5
Thirteen-lined ground squirrel	1	-	-	1	1	1	2
Three-toed box turtle	1	-	-	1	1	1	2
Ticto barb	-	-	-	1	-	-	-
tiger goby	-	-	-	1	-	-	-
Tiger tail seahorse	-	-	-	6	-	-	-
Tigrigobius dilepis	-	-	-	1	-	-	-
Tigrigobius inornatus	-	-	-	2	-	-	-
Tigrigobius janssi	-	-	-	1	-	-	-
Tigrigobius limbaughi	-	-	-	1	-	-	-
Tigrigobius multifasciatus	-	-	-	2	-	-	-
Tigrigobius nesiotetes	-	-	-	1	-	-	-
Tigrigobius pallens	-	-	-	2	-	-	-
Tigrigobius saucrus	-	-	-	1	-	-	-
Tilda's yellow-shouldered bat	1	-	1	1	-	-	-
Tomodon dorsatus	1	-	1	1	-	-	-
torrent sculpin	-	-	-	1	-	-	-
Trans-pecos rat snake	1	-	1	1	-	-	-
Trigonostigma cf. heteromorpha BOLD:AAJ8936	-	-	-	1	-	-	-
Trinidad blind snake	-	-	-	1	-	-	-
Tropical ratsnake	1	-	1	1	-	-	-
tropical rattlesnake	1	-	1	1	-	-	-
Tropidophis feicki	1	-	1	1	-	-	-
Tufted duck	1	-	-	1	1	1	-
Turquoise killifish	-	-	-	2	-	-	1
tusked goby	-	-	-	2	-	-	-
Ursus arctos horribilis	2	-	-	1	-	2	1
Vampire bat	-	-	1	1	-	-	-
Veined squid	-	-	-	1	-	-	-
Viperine snake	1	-	1	1	-	-	-
Virile crayfish	-	-	-	1	-	-	-
Wall lizard	1	-	-	1	1	1	1
Water snake	1	-	1	1	-	-	-
Waterhouse's leaf-nosed bat	-	-	1	1	-	-	-
Weddell seal	-	-	-	1	-	-	1
Western clawed frog	1	-	1	1	-	4	1
Western European hedgehog	1	-	1	1	-	1	1
Western Ghat glassy perchlet	-	-	-	1	-	-	-
Western lowland gorilla	1	-	-	1	-	2	2
Western mosquitofish	-	-	-	1	-	-	-
White perch	-	-	-	1	-	-	-

Sequence	Number of sequences						
	OPN1SW	OPN1W	OPN1LW	OPN2	OPN3	OPN4	OPN5
White-lipped pit viper	1	-	1	1	-	-	-
Wild turkey	-	-	-	1	-	4	1
willow flounder	-	-	-	1	-	-	-
Winter flounder	-	-	-	1	-	-	-
Wire-tailed manakin	1	-	-	1	1	1	-
Witch	-	-	-	1	-	-	-
wrinkle-lipped free-tailed bat	-	-	-	1	-	-	-
Xenopholis scalaris	1	-	1	1	-	-	-
Xystreureys liolepis	-	-	-	1	-	-	-
Yangtze finless porpoise	1	-	1	1	1	1	1
Yangtze river dolphin	1	-	1	1	1	2	1
yellow rasbora	-	-	-	3	-	-	-
yellowfin sole	-	-	-	1	-	-	-
Yellowstriped squirrelfish	-	-	-	1	-	-	-
Yellowtail flounder	-	-	-	1	-	-	-
Yoma danio	-	-	-	1	-	-	-
Zebra finch	-	-	-	1	1	2	1
Zebrafish	-	-	-	1	1	1	2
Bovine 1f88	-	-	-	1	-	-	-
Bovine 1gzm	-	-	-	1	-	-	-
Bovine 1hzx	-	-	-	1	-	-	-
Bovine 1l9h	-	-	-	1	-	-	-
Bovine 1u19	-	-	-	1	-	-	-
Bovine 2g87	-	-	-	1	-	-	-
Bovine 2hpy	-	-	-	1	-	-	-
Bovine 2i35	-	-	-	1	-	-	-
Bovine 2i36	-	-	-	1	-	-	-
Bovine 2i37	-	-	-	1	-	-	-
Bovine 2j4y	-	-	-	1	-	-	-
Bovine 2ped	-	-	-	1	-	-	-
Bovine 2x72	-	-	-	1	-	-	-
Bovine 3c9l	-	-	-	1	-	-	-
Bovine 3c9m	-	-	-	1	-	-	-
Bovine 3cap	-	-	-	1	-	-	-
Bovine 3dqb	-	-	-	1	-	-	-
Bovine 3oax	-	-	-	1	-	-	-
Bovine 3pqr	-	-	-	1	-	-	-
Bovine 3pxo	-	-	-	1	-	-	-
Bovine 4a4m	-	-	-	1	-	-	-
Bovine 4bey	-	-	-	1	-	-	-

Sequence	Number of sequences						
	OPN1SW	OPN1W	OPN1LW	OPN2	OPN3	OPN4	OPN5
Bovine 4bez	-	-	-	1	-	-	-
Bovine 4j4q	-	-	-	1	-	-	-
Bovine 4pxf	-	-	-	1	-	-	-
Bovine 4x1h	-	-	-	1	-	-	-
Bovine 5dys	-	-	-	1	-	-	-
Bovine 5en-	-	-	-	1	-	-	-
Bovine 5te3	-	-	-	1	-	-	-
Bovine 5te5	-	-	-	1	-	-	-
Bovine 5wkt	-	-	-	1	-	-	-
Bovine 6fk6	-	-	-	1	-	-	-
Bovine 6fk7	-	-	-	1	-	-	-
Bovine 6fk8	-	-	-	1	-	-	-
Bovine 6fk9	-	-	-	1	-	-	-
Bovine 6fka	-	-	-	1	-	-	-
Bovine 6fkb	-	-	-	1	-	-	-
Bovine 6fkc	-	-	-	1	-	-	-
Bovine 6fkd	-	-	-	1	-	-	-
Bovine 6fuf	-	-	-	1	-	-	-
Bovine 6nwe	-	-	-	1	-	-	-
Bovine 6ofj	-	-	-	1	-	-	-
Bovine 6oy9	-	-	-	1	-	-	-
Bovine 6oya	-	-	-	1	-	-	-
Bovine 6pel	-	-	-	1	-	-	-
Bovine 6pgs	-	-	-	1	-	-	-
Bovine 6ph7	-	-	-	1	-	-	-
Bovine 6qno	-	-	-	1	-	-	-
Bovine 7mt8	-	-	-	1	-	-	-
Bovine 7mt9	-	-	-	1	-	-	-
Bovine 7mta	-	-	-	1	-	-	-
Bovine 7mtb	-	-	-	1	-	-	-
Hasarius adansoni 6i9k	-	-	-	1	-	-	-
Human 4zwj	-	-	-	1	-	-	-
Human 5dgy	-	-	-	1	-	-	-
Human 5w-p	-	-	-	1	-	-	-
Human 6cmo	-	-	-	1	-	-	-
Japanese flying squid 2z73	-	-	-	1	-	-	-
Japanese flying squid 2ziy	-	-	-	1	-	-	-
Japanese flying squid 3aym	-	-	-	1	-	-	-
Japanese flying squid 3ayn	-	-	-	1	-	-	-
Japanese flying squid 4ww3	-	-	-	1	-	-	-